One dimensional bosons: From condensed matter systems to ultracold gases

M. A. Cazalilla

Centro de Fisica de Materiales, Paseo Manuel de Lardizabal, 5. E-20018 San Sebastian, Spain and Donostia International Physics Center, Paseo Manuel de Lardizabal, 4. E-20018 San Sebastian, Spain

R. Citro

Dipartimento di Fisica "E. R. Caianiello," Università di Salerno, and Spin-CNR, Via Ponte don Melillo, I-84084 Fisciano (Sa), Italy

T. Giamarchi

DPMC-MaNEP, University of Geneva, CH1211 Geneva, Switzerland

E. Orignac

Laboratoire de Physique, CNRS UMR5672 and École Normale Supérieure de Lyon, F-69364 Lyon Cedex 7, France

M. Rigol

Department of Physics, Georgetown University, Washington, D.C. 20057, USA

(published 1 December 2011)

The physics of one-dimensional interacting bosonic systems is reviewed. Beginning with results from exactly solvable models and computational approaches, the concept of bosonic Tomonaga-Luttinger liquids relevant for one-dimensional Bose fluids is introduced, and compared with Bose-Einstein condensates existing in dimensions higher than one. The effects of various perturbations on the Tomonaga-Luttinger liquid state are discussed as well as extensions to multicomponent and out of equilibrium situations. Finally, the experimental systems that can be described in terms of models of interacting bosons in one dimension are discussed.

DOI: 10.1103/RevModPhys.83.1405 PACS numbers: 67.85.−d, 75.10.Pq, 71.10.Pm, 74.78.−w

CONTENTS

I. INTRODUCTION

While still holding many surprises, one-dimensional (1D) quantum many-body systems have fascinated physicists and mathematicians alike for nearly a century. Indeed, shortly after the inception of quantum mechanics, Bethe (1931) found an exact solution to the 1D Heisenberg model using an *ansatz* for the wave function that now bears his name. This early exact solution of a spin-$\frac{1}{2}$ chain was to be followed by a multitude of exact solutions to other 1D models. Other simple 1D models, which could not be solved exactly, were thoroughly studied by powerful methods especially suited for 1D. Many researchers regarded these solutions as mere mathematical curiosities that were, in general, of rather limited interest for the real three-dimensional (3D) world. Subsequent technological developments in the 20th and 21st centuries led to the discovery, chemical synthesis, and more recently fabrication of a wide range of (quasi-)1D materials and physical systems. Interestingly enough, the properties of these systems are sometimes fairly well captured by the ''toy models'' of the past. In this article, we review the physics of some of these models as well as their experimental realizations. However, unlike earlier reviews which have mainly focused on 1D systems of fermions (Gogolin *et al.*, 1999; Giamarchi, 2004), we mainly deal with 1D systems where the constituent particles (or the relevant excitations) obey Bose statistics.

Compared to higher dimensions, the quantum statistics of the constituents plays a much less determinant role in 1D. Nevertheless, when computing physical properties, quantum statistics dictates the type of observables that may be experimentally accessible. Thus, because of the long standing interest in the electronic properties of quasi-1D materials and nanostructures, physicists have mainly focused their attention on 1D electron systems. Much less attention has been given to 1D bosons, with the important exception of spin systems. We show in Sec. II.D that spin-$\frac{1}{2}$ systems are mathematically equivalent to lattice hard-core bosons, and thus are also reviewed in this article. In fact, many quasi-1D materials exhibit (Mott-)insulating phases whose magnetic properties can be modeled by assuming that they consist of weakly coupled spin chains, similar to those analyzed by Bethe in his ground breaking work.

Besides the spin chains, interest in other bosonic systems is rather recent and was initially spurred by the fabrication of long 1D arrays of Josephson junctions. In these systems, Cooper pairs (which, to a first approximation, behave like bosons) can hop around in 1D. Even more recently, further experimental stimulus has come from the studies of the behavior at low temperatures of liquid ^{4}He confined in elongated mesoscopic pores, as well as from the availability of ultracold atomic gases loaded in highly anisotropic traps and optical lattices. Indeed, the strong confinement that can be achieved in these systems has made it possible to realize *tunable* low-dimensional quantum gases in the strongly correlated regime.

As often happens in physics, the availability of new experimental systems and methods has created an outburst of theoretical activity, thus leading to a fascinating interplay between theory and experiment. In this article, we attempt to survey the developments concerning 1D systems of interacting bosons. Even with this constraint, it is certainly impossible to provide a comprehensive review of all aspects of this rapidly evolving field.

The outline of this article is as follows. In Sec. II the basic models are derived starting from the most general Hamiltonian of bosons interacting through a two-body potential in the presence of an arbitrary external potential. Models both in the continuum and on the lattice are discussed. This section also introduces some important mappings allowing one to establish the mathematical relationship of some of these boson models to other models describing $S=\frac{1}{2}$ spins or spinless fermions on 1D lattices. In Sec. III, exact solutions of integrable models along with results on their correlation functions are reviewed. Some of these results are important by themselves and not just merely academic models, as there currently exist fairly faithful experimental realizations of them. In Sec. IV, we describe some of the computational approaches that can be used to tackle both integrable and nonintegrable models. We also discuss their application to some 1D models of much current interest. Section V reviews the basic field-theoretic tools that describe the universal low-energy phenomena in a broad class of 1D interacting boson models, the so-called Tomonaga-Luttinger liquid (TLL) phase. For these systems, the method of bosonization and its relationship to the hydrodynamic description of superfluids (SF) (which is briefly reviewed in Sec. II) are described.

The classification of phases and phase transitions exhibited by the models introduced in Sec. II is presented in Sec. VI, where besides the Mott transition between the TLL phase and the Mott-insulating phase, other kinds of instabilities arising when the bosons move in the presence of a disorder potential will be described. The low-energy picture is often unable to provide the quantitative details that other methods such as exact solutions (Sec. III) or computational approaches (IV) do. Thus, when results from any (or both) of the latter methods are available, they complement the picture provided by bosonization. Further extensions are considered in Sec. VII, where studies of multicomponent (binary mixtures of bosons or bosons and fermions) and coupled 1D systems, as well as the nonequilibrium dynamics of isolated quantum systems, are reviewed. Next, we turn to the experimental realizations of systems of interacting bosons in 1D, which include spin ladders, superconducting wires, Josephson junctions, as well as the most recent ultracold atomic systems. Finally, in Sec. IX we shall provide a brief outlook for the field.

II. MODELS FOR INTERACTING BOSONS

In this section, we introduce the basic models that describe interacting bosons in 1D, both in the continuum and on a lattice. These models will be analyzed using various techniques in the rest of the review. However, before embarking on the study of 1D physics *per se*, we recall the main general results for bosons in dimensions higher than one. This will serve as a reference with which we can compare the results in 1D.

A. Bosons in dimensions higher than one

As Einstein discovered shortly after Bose introduced a new type of quantum statistics, when the temperature of a system of N noninteracting bosons is lowered, a phase transition occurs. Below the transition temperature, the occupation (N_0) of the lowest available energy state becomes macroscopic, i.e., N_0/N tends to a constant for N large. The transition was therefore named "Bose-Einstein condensation," and the macroscopically occupied quantum state, "Bose-Einstein condensate." The acronym BEC is used indistinctly for both concepts. Mathematically, a BEC can be described by a coherent state of matter, i.e., an eigenstate of the boson field operator: $\hat{\Psi}(\mathbf{r})|\psi_0(\tau)\rangle = \Psi_0(\mathbf{r},\tau)|\psi_0(\tau)\rangle$, hence $|\psi_0(\tau)\rangle = e^{\hat{a}_0^\dagger(\tau)}|0\rangle$, where $|0\rangle$ is the zero-particle state, $\hat{a}_0(\tau) = \int d\mathbf{r}\Psi_0^*(\mathbf{r},\tau)\hat{\Psi}(\mathbf{r})$, and $\Psi_0(\mathbf{r},\tau)$ is a complex function of space ($\mathbf{r}$) and time (τ).

The above definition implies that the $U(1)$ symmetry group related to particle conservation must be spontaneously broken. However, this is sometimes problematic (Leggett, 2001; 2006) because the use of coherent states for massive particles violates the superselection rule forbidding the quantum superposition of states with different particle numbers. The definition of BEC according to Yang (1962) circumvents this problem by relating the existence of a BEC to the case in which the one-particle density matrix of the system, $g_1(\mathbf{r},\mathbf{r}',\tau) = \langle\hat{\Psi}^\dagger(\mathbf{r},\tau)\hat{\Psi}(\mathbf{r}',\tau)\rangle$, behaves as $g_1(\mathbf{r},\mathbf{r}',\tau) \to \Psi_0^*(\mathbf{r},\tau)\Psi_0(\mathbf{r}',\tau)$ [$\Psi_0(\mathbf{r},\tau) \neq 0$] for $|\mathbf{r}-\mathbf{r}'| \to +\infty$. This behavior is referred to as off-diagonal long-range order and $\Psi_0(\mathbf{r},\tau)$ is called the order parameter of the BEC phase.

However, Yang's definition is not applicable to finite systems. Following Penrose and Onsager (1956), a more general criterion is obtained by diagonalizing the one-particle density matrix[1] as $g_1(\mathbf{r},\mathbf{r}',\tau) = \sum_\alpha N_\alpha(\tau)\phi_\alpha^*(\mathbf{r},\tau)\phi_\alpha(\mathbf{r}',\tau)$, where the natural orbitals ϕ_α are normalized such that $\int d\mathbf{r}|\phi_\alpha(\mathbf{r},\tau)|^2 = 1$. The existence of a BEC depends on the magnitude of the N_α compared to N. When there is only one eigenvalue of $O(N)$ [say, $N_0 \sim O(N)$], the system is a BEC described by $\Psi_0(\mathbf{r},\tau) = \sqrt{N_0(\tau)}\phi_0(\mathbf{r},\tau)$. When there are several such eigenvalues, one speaks of a "fragmented" BEC (see Mueller *et al.*, 2006, and references therein). Furthermore, provided the depletion of the BEC is small, that is, for $N - N_0 \ll N$ [indeed $N_0(T) \to N$ as $T \to 0$ for the noninteracting gas], it is possible to describe the state of the system using $|\psi_0^N(\tau)\rangle = (1/\sqrt{N!})[\hat{a}_0^\dagger(\tau)]^N|0\rangle$. Note that contrary to the coherent state $|\Psi_0(\tau)\rangle$, $|\psi_0^N(\tau)\rangle$ has a well-defined particle number and can be obtained from $|\psi_0(\tau)\rangle$ by projecting it onto a state with total particle number equal to N.

The definitions of BEC according to Yang, Penrose, and Onsager are equivalent in the thermodynamic limit and also apply to interacting systems. In general, the ratio N_0/N is called the condensate fraction. It is important not to confuse the condensate fraction, which for a BEC is finite, with the superfluid fraction. The latter is a thermodynamic property that is physically related to the fraction of the system mass that is not dragged along by the walls of the container when the latter rotates at constant angular frequency. In charged systems, it is related to Meissner effect, i.e., the expulsion of an externally applied magnetic field. Mathematically, the superfluid fraction can be obtained as the thermodynamic response to a change in the boundary conditions of the system (see Sec. V for a discussion concerning 1D systems). Indeed, the noninteracting Bose gas below the condensation temperature is the canonical example of a BEC that is not a superfluid. On the other hand, the 1D models discussed here do not exhibit BEC (even at $T = 0$).

The above discussion does not provide any insights into how to compute the BEC wave function $\Psi_0(\mathbf{r},\tau)$ for a general system of mass m bosons interacting through a potential $V_{\rm int}(\mathbf{r})$ and moving in an external potential $V_{\rm ext}(\mathbf{r},\tau)$, which is described by the Hamiltonian

$$\hat{H} = \int d\mathbf{r}\hat{\Psi}^\dagger(\mathbf{r})\left[-\frac{\hbar^2}{2m}\nabla^2 + V_{\rm ext}(\mathbf{r},\tau)\right]\hat{\Psi}(\mathbf{r}) + \int d\mathbf{r}d\mathbf{r}'\hat{\Psi}^\dagger(\mathbf{r})\hat{\Psi}^\dagger(\mathbf{r}')V_{\rm int}(\mathbf{r}'-\mathbf{r})\hat{\Psi}(\mathbf{r})\hat{\Psi}(\mathbf{r}'). \quad (1)$$

For such a system, in the spirit of a mean-field theory Pitaevskii (1961) and Gross (1963) independently derived an equation for the condensate wave function by approximating $\hat{\Psi}(\mathbf{r})$ in the equation of motion, $i\hbar\partial_\tau\hat{\Psi}(\mathbf{r},\tau) = [\hat{\Psi}(\mathbf{r},\tau), \hat{H} - \mu\hat{N}]$, by its expectation value $\langle\hat{\Psi}(\mathbf{r},\tau)\rangle = \Psi_0(\mathbf{r},\tau)$ over a coherent state, where μ is the chemical potential and $\hat{N}$ is the number operator. The Gross-Pitaevskii (GP) equation reads

$$i\hbar\partial_\tau\Psi_0(\mathbf{r},\tau) = \left[-\frac{\hbar^2}{2m}\nabla^2 - \mu + V_{\rm ext}(\mathbf{r},\tau) + \int d\mathbf{r}'V_{\rm int}(\mathbf{r}-\mathbf{r}')|\Psi_0(\mathbf{r}',\tau)|^2\right]\Psi_0(\mathbf{r},\tau). \quad (2)$$

For an alternative derivation, which does not assume the spontaneous breakdown of the $U(1)$ symmetry, one can look for the extrema of the functional $\langle\psi(\tau)|i\hbar\partial_\tau - (\hat{H} - \mu\hat{N})|\psi(\tau)\rangle$, using the (time-dependent Hartree) ansatz $|\psi(\tau)\rangle = (1/\sqrt{N_0!})[\hat{a}_0^\dagger(\tau)]^{N_0}|0\rangle$, where $\hat{a}_0(\tau) = \int d\mathbf{r}\Psi_0^*(\mathbf{r},\tau)\hat{\Psi}(\mathbf{r})|0\rangle$ and μ is a Lagrange multiplier to ensure that $\int d\mathbf{r}|\Psi_0(\mathbf{r},\tau)|^2 = N_0$.

The use of the Gross-Pitaevskii equation (2) to describe the interacting boson system assumes a small BEC depletion, i.e., $N_0 \simeq N$. This is a good approximation in the absence of

[1]This is mathematically always possible because $g_1(\mathbf{r},\mathbf{r}',\tau) = \langle\hat{\Psi}^\dagger(\mathbf{r},\tau)\hat{\Psi}(\mathbf{r}',\tau)\rangle$ is a positive-definite Hermitian matrix provided $\mathbf{r}$, $\mathbf{r}'$ are regarded as matrix indices.

strong correlations and at low temperatures. Thus, it is particularly suitable for dilute ultracold gases (Pitaevskii and Stringari, 1991; 2003; Leggett, 2001), for which the interparticle potential range is much smaller than the interparticle distance d. In these systems, interactions are well described by the Lee-Huang-Yang pseudopotential (Huang and Yang, 1957; Lee *et al.*, 1957; Lee and Yang, 1957) $V(\mathbf{r}) \simeq (4\pi\hbar^2 a_s/m)\delta(\mathbf{r})\partial_r(r\cdot)$, where a_s is the s-wave scattering length. Typically, $a_s \ll d$, except near a s-wave Feshbach resonance (Pitaevskii and Stringari, 2003; Leggett, 2006). For trapped gases, it has been rigorously established that in the limit of $N \to \infty$ and Na_s fixed, the Gross-Pitaevskii approximation becomes exact for the ground-state energy and particle density (Lieb *et al.*, 2000). Furthermore, in this limit, the gas is both 100% Bose condensed (Lieb and Seiringer, 2002) and 100% superfluid (Lieb *et al.*, 2002).

In a uniform system, the above definitions of BEC imply that the momentum distribution

$$n(\mathbf{k}) = \int d\mathbf{r} e^{-i\mathbf{k}\cdot\mathbf{r}} g_1(\mathbf{r}) = N_0\delta(\mathbf{k}) + \tilde{n}(\mathbf{k}), \tag{3}$$

where $\tilde{n}(\mathbf{k})$ is a regular function of $\mathbf{k}$. The Dirac delta function is the hallmark of the BEC in condensed matter systems such as liquid ^{4}He below the λ transition. On top of the condensate, interacting boson systems support excitations with a dispersion that strongly deviates from the free-particle dispersion $\epsilon_0(\mathbf{k}) = \hbar^2\mathbf{k}^2/2m$. A way to compute the excitation spectrum is to regard the GP equation as a time-dependent Hartree equation. Thus, its linearized form describes the condensate excitations, which, for a uniform dilute gas, have a dispersion of the form $\epsilon(\mathbf{k}) = \sqrt{\epsilon_0(\mathbf{k})[\epsilon_0(\mathbf{k}) + 2g\rho_0]}$, where $\rho_0 = N/V$, and g is the strength of the interaction. This was first obtained by Bogoliubov, who proceeded differently by deriving a quadratic Hamiltonian from (1) in terms of $\delta\hat{\Psi}(\mathbf{r}) = \hat{\Psi}(\mathbf{r}) - \sqrt{N_0}$ and $\delta\hat{\Psi}^\dagger(\mathbf{r}) = \hat{\Psi}^\dagger(\mathbf{r}) - \sqrt{N_0}$ and keeping only the (leading) terms up to $O(N_0)$. Note that, in the $|\mathbf{k}| \to 0$ limit, the excitations above the BEC state are linearly dispersing phonons: $\epsilon(\mathbf{k}) \simeq \hbar v_s|\mathbf{k}|$, where $v_s = \sqrt{g\rho_0/2m}$. From the point of view of the spontaneous breakdown of the $U(1)$ symmetry, the phonons are the Goldstone modes of the broken-symmetry phase.

We conclude this section by reviewing the hydrodynamic approach. Although we derive it from the GP equation for a dilute gas, its validity extends beyond the assumptions of this theory to arbitrarily interacting superfluid systems in any dimension. We begin by setting $\Psi_0(\mathbf{r}, \tau) = \sqrt{\rho(\mathbf{r}, \tau)}e^{i\theta(\mathbf{r},\tau)}$ in Eq. (2). Hence,

$$\partial_\tau\rho + \frac{\hbar}{m}\nabla\cdot(\rho\nabla\theta) = 0, \tag{4}$$

$$\partial_\tau\theta + \left(\frac{\hbar(\nabla\theta)^2}{2m} + \frac{1}{\hbar}[V_{\text{ext}} + g\rho] - \frac{\hbar}{2m}\frac{\nabla^2\sqrt{\rho}}{\sqrt{\rho}}\right) = 0. \tag{5}$$

Equation (4) is the just continuity equation where the particle current $\mathbf{j}(\mathbf{r}, \tau) = \rho(\mathbf{r}, \tau)\mathbf{v}(\mathbf{r}, \tau) = (\hbar/m)\rho(\mathbf{r}, \tau)\nabla\theta(\mathbf{r}, \tau)$. The second equation describes a potential flow with velocity potential $(\hbar/m)\theta(\mathbf{r}, \tau)$. The last term in Eq. (5) is called the quantum pressure. If we call ℓ the typical distance characterizing the density variations, the quantum pressure term scales as $\sim\hbar^2/m\ell^2$ and therefore it is negligible compared to the classical pressure term $g\rho$ when $\ell \gg \xi = \hbar/\sqrt{m\rho g}$ (ξ is known as the healing length). In the limit of a slowly varying density profile, the quantum pressure term in Eq. (5) can be dropped and the equations can be written as

$$\partial_\tau\rho + \nabla\cdot(\rho\mathbf{v}) = 0, \tag{6}$$

$$\partial_\tau\mathbf{v} + \nabla\left(\frac{V_{\text{ext}}}{m} + \frac{1}{2}\mathbf{v}^2\right) = -\frac{\nabla P}{\rho m}. \tag{7}$$

These equations coincide with the classical Euler equation describing the flow of a nonviscous fluid with an equation of state where $P(\rho) = g\rho^2/2$. This result is in agreement with simple thermodynamic considerations from which the classical fluid of Eq. (6) has, at zero temperature, an energy per unit volume $e(\rho) = g\rho^2/2$ and chemical potential $\mu(\rho) = g\rho$. In the literature on ultracold gases, this approximation is known as the Thomas-Fermi approximation. In the static case ($\mathbf{v} = 0$ and $\partial_\tau\rho = 0$), it leads to $\nabla[V_{\text{ext}}(\mathbf{r}) + P(\rho(\mathbf{r}))] = 0$, which allows one to determine the BEC density profile $\rho(\mathbf{r})$ for a given trapping potential $V_{\text{ext}}(\mathbf{r})$.

As mentioned, the validity of the hydrodynamic equations is very general and applies to strongly interacting bosons as well as fermion superfluids, for which the dependence of the chemical potential on the density is very different. However, in 1D the assumptions that underlie GP (and Bogoliubov) theory break down. Quantum and thermal fluctuations are strong enough to prevent the existence of BEC, or equivalently the spontaneous breakdown of the $U(1)$ symmetry in the thermodynamic limit. This result is a consequence of the Mermin-Wagner-Hohenberg (MWH) theorem (Hohenberg, 1967; Mermin and Wagner, 1966; 1968), which states that, at finite temperature, there cannot be a spontaneous breakdown of continuous symmetry groups [like $U(1)$] in two-dimensional (2D) classical systems with short-range interactions. Indeed, at $T = 0$, a 1D quantum system with a spectrum of long-wavelength excitations with linear dispersion can be mapped, using functional integral methods, to a 2D classical system (see Sec. II.D for an example). Therefore, the MWH theorem also rules out the existence of a BEC in those 1D systems. For the 1D noninteracting Bose gas, the excitations have a quadratic dispersion, and thus the mapping and the theorem do not apply. However, a direct proof of the absence of BEC in this case is straightforward (see, e.g., Pitaevskii and Stringari, 2003).

In the absence of a BEC, the assumptions of the GP theory and the closely related Bogoliubov method break down. When applied to 1D interacting boson systems in the thermodynamic limit, these methods are plagued by infrared divergences. The latter are a manifestation of the dominant effect of long-wavelength thermal and quantum fluctuations, as described by the MWH theorem. By decoupling the density and phase fluctuations, Popov (1972 and 1987) was able to deal with these infrared divergences within the functional integral formalism. However, Popov's method relies on integrating the short-wavelength fluctuations perturbatively, which is a controlled approximation only for a weakly interacting system. For arbitrary interaction strength, it is

necessary to resort to a different set of tools to tackle the 1D world. Before going into their discussion, we first need to define the various models that we use to describe interacting bosons in 1D, and whose solutions are reviewed in the following sections.

B. Bosons in the continuum in 1D

We first consider the case of bosons moving in the continuum along one direction (henceforth denoted by x). Thus, we assume that a very strong confinement is applied in the transverse directions [denoted $\mathbf{r}_\perp = (y, z)$] so that only the lowest energy transverse quantum state $\phi_0(\mathbf{r}_\perp)$ needs to be considered. Hence, the many-body wave function reads

$$\psi_B(\mathbf{r}_1, \ldots, \mathbf{r}_N) = \psi_B(x_1, \ldots, x_N) \prod_{i=1}^{N} \phi_0(\mathbf{r}_{i\perp}). \tag{8}$$

In what follows, we focus on the degrees of freedom described by $\psi_B(x_1, \ldots, x_N)$. The most general Hamiltonian for a system of N bosons interacting through a two-body potential $V_{\rm int}(x)$ while moving in an external potential $V_{\rm ext}(x)$ reads

$$\hat{H} = \sum_{i=1}^{N} \left[\frac{\hat{p}_i^2}{2m} + V_{\rm ext}(\hat{x}_i) \right] + \sum_{i<j=1}^{N} V_{\rm int}(\hat{x}_i - \hat{x}_j), \tag{9}$$

where m is the atom mass and $\hat{p}_i = -i\hbar(\partial/\partial x_i)$ the ith particle momentum operator ($[\hat{x}_i, \hat{p}_j] = i\hbar\delta_{ij}$).

The simplest nontrivial model of interacting bosons in the continuum is the one introduced by Lieb (1963) and Lieb and Liniger (1963), which is obtained from Eq. (9) upon setting $V_{\rm ext}(x) = 0$ and considering a Dirac delta interaction $V_{\rm int}(x) = g\delta(x)$. When a transverse external confinement is considered, an effective one-dimensional model with Dirac delta interaction can still be obtained within a pseudopotential approximation by properly summing over the virtual excitations of the high-energy transverse modes (Olshanii, 1998) (cf. Sec. IV.A.2). For the Lieb-Liniger model, the Hamiltonian reads

$$\hat{H} = -\frac{\hbar^2}{2m} \sum_{i=1}^{N} \frac{\partial^2}{\partial x_i^2} + g \sum_{i<j=1}^{N} \delta(x_i - x_j). \tag{10}$$

It is convenient to parametrize the interaction strength in this model using the parameter $c = mg/\hbar^2$, which has the dimension of an inverse length. Thus, $c = 0$ corresponds to free bosons while $c \to +\infty$ is the hard-core or Tonks-Girardeau limit (Girardeau, 1960). As shown in Sec. III.A, in this limit the model can be solved exactly by mapping it onto a system of noninteracting fermions. Moreover, as shown by Lieb and Liniger, the model can be solved for all values of c using the Bethe ansatz. This solution is reviewed in Sec. III.B. Gurarie (2006) studied a generalization of the Lieb-Liniger model with Feshbach resonant interactions, which can be approximately solved by the Bethe ansatz. However, we shall not review this solution here and refer the interested reader to Gurarie (2006).

The Lieb-Liniger model is not the only interacting boson model that can be solved exactly. The following model,

$$\hat{H} = -\frac{\hbar^2}{2m} \sum_{i=1}^{N} \frac{\partial^2}{\partial x_i^2} + \sum_{i<j=1}^{N} \frac{g}{(x_i - x_j)^2}, \tag{11}$$

which was introduced by Calogero (1969) also has this property. Moreover, Calogero showed that the model is also solvable when a harmonic potential, i.e., for $\sum_{i=1}^{N} V_{\rm ext}(\hat{x}_i) = \frac{1}{2} m\omega^2 \sum_{i=1}^{L} x_i^2$, is added to Eq. (11). The interaction strength in the model (11) is characterized by the dimensionless parameter λ, where $\lambda(\lambda - 1) = 2mg/\hbar^2$. Note that the interaction potential in this model is singular for $x_i = x_j$. To deal with this behavior, we must require that the many-body wave function vanishes when $x_i = x_j$, that is, the model describes a system of hard-core bosons with $1/x^2$ interactions. For $\lambda = 0, 1$, one recovers the Tonks-Girardeau (TG) gas. This model will be further discussed in Sec. III.E.

Furthermore, besides the two types of interactions leading to the exactly solvable models of Lieb, Liniger, and Calogero, it is also possible to consider other kinds of interactions that are experimentally relevant. Among them, three types of interactions play an especially important role: (i) $V_{\rm int}(x) \sim 1/|x|^3$ describes a system of (polarized) dipoles in 1D. This interaction is relevant for systems of dipolar ultracold atoms (Griesmaier *et al.*, 2005) or bosonic molecules. Note that, contrary to 3D, the integral of this potential $\int_{-x}^{+x} dx' V_{\rm int}(x')$ converges for large x [i.e., the Fourier transform $V_{\rm int}(q)$ is finite as $q \to 0$] and thus it is essentially not different from a short but finite range interaction potential. (ii) The unscreened Coulomb potential $V_{\rm int}(x) \propto 1/|x|$ is relevant for charged systems such as superconducting wires, Josephson junction arrays, and trapped ion systems. $V_{\rm int}(q \to 0)$ is singular even in 1D and this leads to some modifications of the properties of the system at long wavelengths compared to the case of short-range interactions.

Furthermore, other models that are worth studying deal with the effect of different kinds of external potentials such as periodic, disorder, or trapping potentials. The effect of a weak periodic potential will be considered in Sec. VI.A, whereas the effect of a strong periodic potential is best discussed by using the lattice models that will be introduced in the following section. In both cases, the potential leads to the existence of bosonic Mott insulators. Disorder potentials are another type of external potentials that are relevant for both condensed matter systems, where it appears naturally, and currently for ultracold atomic systems, where it is introduced artificially to study its effects in a more controlled way. In 1D Bose systems, as discussed in Sec. VI.B, it can lead to glassy phases. In addition, in ultracold atomic systems the atoms are in the gaseous phase and therefore need to be contained. As described in Sec. VIII.D, the confining potential can be made using either laser light or (time-dependent) magnetic fields, and for small gas clouds, it can be well approximated by a harmonic potential $V_{\rm ext}(x) = \frac{1}{2} m\omega^2 x^2$. Such a potential makes the system intrinsically inhomogeneous, and thus can lead to phase separated coexistence of different phases. The effect of the trap will be discussed below.

C. Bosons on the lattice in 1D

In the previous section, we have introduced several models of interacting bosons in the continuum. However, when the bosons move in the presence of a deep periodic potential, e.g., for $V_{\rm ext}(x) = V_0 \cos(Gx)$, where V_0 is the largest energy scale in the problem, a more convenient starting point is to project

the Bose field operator on the basis of Wannier orbitals $w_0(x)$ belonging to the lowest Bloch band of $V_{\rm ext}(x)$. Thus,

$$\Psi(x) \simeq \sum_{i=1}^{L} w_0(x - ia)\hat{b}_i, \tag{12}$$

where $a = 2\pi/G$ is the lattice parameter. In doing the above approximation, we have neglected the projection of $\Psi(x)$ on higher bands. Thus, if V_0 is decreased, taking into account the Wannier orbitals of higher bands may become necessary. Upon inserting Eq. (12) into the second quantized version of Eq. (9), the following Hamiltonian is obtained:

$$\hat{H} = \sum_{i,j=1}^{L}\Big[-t_{ij}\hat{b}_i^\dagger\hat{b}_j + \sum_{k,l=1}^{L} V_{ik,jl}^{\rm int}\hat{b}_i^\dagger\hat{b}_k^\dagger\hat{b}_j\hat{b}_l\Big], \tag{13}$$

where $t_{ij} = -\int dx w_0^*(x - ia)\hat{H}_0(x)w_0(x - ja)$, $\hat{H}_0 = (\hbar^2/2m)\partial_x^2 + V_{\rm ext}(x)$, and $V_{ik,jl}^{\rm int} = \int dx dx' w_0^*(x - ia)w^*(x' - ka)V_{\rm int}(x - x')w_0(x' - ja)w_0(x - la)$. When the boundary conditions are periodic, we must further require that $\hat{b}_{L+1}^\dagger = \hat{b}_1^\dagger$ and $\hat{b}_{L+1} = \hat{b}_1$. For a deep lattice potential, it is possible to further simplify this model because in this limit the orbitals $w_0(x - ia)$ are strongly localized about $x = ia$ and it is sufficient to retain only the diagonal as well as nearest-neighbor terms, which leads to the extended Hubbard model:

$$\hat{H}_{\rm EBHM} = \sum_{i=1}^{L}\Big[-t(\hat{b}_i^\dagger\hat{b}_{i+1} + \text{H.c.}) - \mu\hat{n}_i + \frac{U}{2}\hat{b}_i^\dagger\hat{b}_i^\dagger\hat{b}_i\hat{b}_i + V\hat{n}_i\hat{n}_{i+1}\Big], \tag{14}$$

where $\hat{n}_i = \hat{b}_i^\dagger\hat{b}_i$ is the site occupation operator and μ is the chemical potential. We discuss this model in Sec. VI.A. The first term is the kinetic energy of the bosons in the tight-binding approximation, while the last two terms describe an on-site interaction of strength U and a nearest-neighbor interaction of strength V.

When the range of the interaction is small compared to the lattice parameter a, it is possible to further neglect the nearest-neighbor interaction compared to the on-site interaction U because the overlap of the Wannier orbitals in a deep lattice potential makes V small. The resulting model is known as the Bose-Hubbard model:

$$\hat{H}_{\rm BHM} = \sum_{i=1}^{L}\Big[-t(\hat{b}_i^\dagger\hat{b}_{i+1} + \text{H.c.}) - \mu\hat{n}_i + \frac{U}{2}\hat{b}_i^\dagger\hat{b}_i^\dagger\hat{b}_i\hat{b}_i\Big]. \tag{15}$$

In condensed matter systems, such as Josephson junction arrays, it is usually difficult to compute t and U from first principles. However, in cold atomic systems the forms of the external potential and the atom-atom interaction are accurately known so that it is possible to compute t and U from first principles (Bloch *et al.*, 2008).

For finite values of U/t, the Bose-Hubbard model is not exactly solvable. However, for $U/t \to +\infty$, the sectors of the Hilbert space where $n_i = 0$, 1 and $n_i > 1$ decouple and the model describes a gas of hard-core bosons, which is the lattice analogue of the TG gas. For this system, the Hamiltonian reduces to the kinetic energy

$$\hat{H}_{\rm LTG} = \sum_{i=1}^{L}\Big[-t(\hat{b}_i^\dagger\hat{b}_{i+1} + \text{H.c.}) - \mu\hat{n}_i\Big], \tag{16}$$

supplemented with the constraint that $(\hat{b}_i^\dagger)^2|\Psi_{\rm phys}\rangle = (\hat{b}_i)^2|\Psi_{\rm phys}\rangle = 0$ on all physical states $|\Psi_{\rm phys}\rangle$. Moreover, as in the continuum case, the model remains exactly solvable when an external potential of the form $\hat{V}_{\rm ext} = \sum_i v_{\rm ext}(i)\hat{n}_i$ is added to the Hamiltonian. The properties of the lattice hard-core bosons both for $\hat{V}_{\rm ext} = 0$ and for the experimentally relevant case of a harmonic trap are discussed in Sec. III.A.2. We note that in dimensions higher than 1, the lattice gas of hard-core bosons on a hypercubic lattice is known rigorously to possess a BEC condensed ground state (Kennedy *et al.*, 1988).

When the interactions are long range, such as for Cooper pairs in Josephson junction arrays, which interact via the Coulomb interaction, or for dipolar ultracold atoms and molecules, the nearest-neighbor interaction $V\sum_i\hat{n}_i\hat{n}_{i+1}$ in Eq. (14) cannot be neglected. If U is sufficiently large in the system, so that the $U \to +\infty$ limit is a reasonable approximation, the extended Bose-Hubbard model [Eq. (14)] reduces to the so-called t-V model, whose Hamiltonian reads

$$\hat{H}_{t\text{-}V} = \sum_{i=1}^{L}[-t(\hat{b}_i^\dagger\hat{b}_{i+1} + \text{H.c.}) - \mu\hat{n}_i + V\hat{n}_i\hat{n}_{i+1}]. \tag{17}$$

This model is Bethe-ansatz solvable and is sometimes also called the quantum lattice gas model (Yang and Yang, 1966a; 1966b; 1966c). As we will see in the next section, this model is equivalent to an anisotropic spin-$\frac{1}{2}$ model called the XXZ chain (Orbach, 1958; Walker, 1959) and to the 6 vertex model of statistical mechanics (Lieb, 1967). It is convenient to introduce the dimensionless parameter $\Delta = V/(2t)$ to measure the strength of the interaction in units of the hopping.

D. Mappings and various relationships

In 1D, several transformations allow the various models introduced above to be related to each other as well as to other models. We explore them in this section. The first mapping relates a system of hard-core bosons to a spin-$\frac{1}{2}$ chain (Holstein and Primakoff, 1940; Matsubara and Matsuda, 1956; Fisher, 1967). The latter is described by the set of Pauli matrices $\{\hat{\sigma}_j^x, \hat{\sigma}_j^y, \hat{\sigma}_j^z\}_{j=1}^L$ (below we use $\hat{\sigma}_j^\pm = \hat{\sigma}_j^x \pm i\hat{\sigma}_j^y$), where j is the site index. The transformation due to Holstein and Primakoff (1940) reads[2]

$$\hat{\sigma}_j^+ = \hat{b}_j^\dagger\sqrt{1 - \hat{n}_j}, \quad \hat{\sigma}_j^- = \sqrt{1 - \hat{n}_j}\hat{b}_j, \quad \hat{\sigma}_j^z = \hat{n}_j - 1/2. \tag{18}$$

Hence, Eq. (16) maps onto the XX spin-chain model

$$\hat{H}_0 = \sum_{j=1}^{L}[-2t(\hat{\sigma}_j^x\hat{\sigma}_{j+1}^x + \hat{\sigma}_j^y\hat{\sigma}_{j+1}^y) - \mu(\hat{\sigma}_j^z + \tfrac{1}{2})] \tag{19}$$

Furthermore, the nearest-neighbor interaction in the t-V model [cf. Eq. (17)] becomes an Ising interaction

[2]The Holstein-Primakoff transformation is actually more general as it can be used for higher S spins and in any dimension.

$$\hat{H}_{\rm int} = V\sum_{j=1}^{L}(\hat{\sigma}_j^z + \tfrac{1}{2})(\hat{\sigma}_{j+1}^z + \tfrac{1}{2}). \tag{20}$$

Therefore, the t-V model maps onto the XXZ or Heisenberg-Ising spin-chain model in a magnetic field. Alternatively, spin systems can be seen as faithful representations of hard-core boson systems.

Another useful transformation relates $S = \frac{1}{2}$ spins (and hence hard-core bosons) to spinless fermions. This is a fairly convenient way of circumventing the hard-core constraint by means of the Pauli principle. Following Jordan and Wigner (1928), we introduce the transformation by relating fermions to spins (Jordan and Wigner, 1928; Lieb *et al.*, 1961; Katsura, 1962; Niemeijer, 1967):

$$\hat{\sigma}_j^+ = \hat{c}_j^\dagger e^{-i\pi\sum_{m<j}\hat{c}_m^\dagger\hat{c}_m}, \qquad \hat{\sigma}_j^- = e^{i\pi\sum_{m<j}\hat{c}_m^\dagger\hat{c}_m}\hat{c}_j, \qquad \hat{\sigma}_j^z = \hat{c}_j^\dagger\hat{c}_j - 1/2, \tag{21}$$

where $\{\hat{c}_i, \hat{c}_j^\dagger\} = \delta_{ij}$, and otherwise anticommute, as corresponds to fermions. By combining the transformations (21) and (18), Eq. (16) is mapped onto a noninteracting fermion Hamiltonian

$$\hat{H}_0 = \sum_{j=1}^{L}[-t(\hat{c}_j^\dagger\hat{c}_{j+1} + \text{H.c.}) - \mu\hat{c}_j^\dagger\hat{c}_j]. \tag{22}$$

Nevertheless, as given above, the mapping assumes open boundary conditions. For periodic boundary conditions

$$\hat{b}_1^\dagger\hat{b}_L = -\hat{c}_1^\dagger\hat{c}_L e^{i\pi\sum_{j=1}^{L}\hat{c}_j^\dagger\hat{c}_j}, \tag{23}$$

which means that when the total number of particles in the chain $N = \langle\hat{N}\rangle$ (where $\hat{N} = \sum_{m=1}^{L}\hat{c}_m^\dagger\hat{c}_m$ commutes with $\hat{H}$) is odd, the fermions obey periodic boundary conditions, while if N is even, they obey antiperiodic boundary conditions.

A consequence of the mappings between the Fermi gas and the TG in the continuum and the lattice is that the spectra and thermodynamics of the TG gas and the noninteracting fermion model (22) are identical. In particular, the low-energy excitations of the TG gas have linear dispersion, which contribute a term linear in the temperature T to the specific heat at low T (see Sec. III for an extended discussion). In addition, on the lattice it is also possible to show (see, e.g., the Appendix in Cazalilla, 2004a) the equivalence of the Jordan-Wigner approximation and Girardeau's Bose-Fermi mapping, which applies to the many-body wave functions of both models and is reviewed in Sec. III.A.

At low lattice filling, that is, when the number of particles N is very small compared to the number of lattice sites L, single-particle dispersion of the lattice model is well approximated by a parabola, i.e., $\epsilon(k) = -2t\cos ka \simeq -2t + \hbar^2k^2/2m^*$ where $m^* = \hbar^2/(2a^2t)$ is the lattice effective mass. The TG gas of hard-core bosons in the continuum is thus recovered. Indeed, by carefully taking the low-filling limit of the Bose-Hubbard model (15), it is also possible to recover the Lieb-Liniger model (10) and hence, in the limit $U/t \gg 1$, the leading corrections of $O(t/U)$ to the lattice TG Hamiltonian. These corrections can then be used to compute various thermodynamic quantities of the lattice and continuum TG gases (Cazalilla, 2003). In the low-filling limit, the corrections yield an attractive interaction between the Jordan-Wigner fermions (Sen, 1999; 2003), which is a particular case of the mapping found by Cheon and Shigehara (1999) between the Lieb-Liniger model and a model of spinless fermions with (momentum-dependent) attractive interactions.

In the opposite limit of large lattice filling (i.e., $n_0 = N/L \gg 1$), the representation

$$\hat{b}_j^\dagger = \sqrt{\hat{n}_j}e^{-i\hat{\theta}_j} \quad \text{and} \quad \hat{b}_j = e^{i\hat{\theta}_j}\sqrt{\hat{n}_j}, \tag{24}$$

in terms of the on-site particle number ($\hat{n}_j$) and phase ($\hat{\theta}_j$) operators becomes useful. The phase operator $\hat{\theta}_j$ is defined as the canonical conjugate of $\hat{n}_j$, that is, we assume that $[\hat{n}_j, \hat{\theta}_j] = i\delta_{ij}$. Hence, $\hat{n}_j = i\partial/\partial\theta_j$ and the many-body wave functions become functions of the set of angles $\{\theta_j\}_{j=1}^L$, where $\theta_i \in [0, 2\pi)$. The angle nature of the θ_j stems from the discreteness of the eigenvalues of $\hat{n}_j$. The operator $e^{i\hat{\theta}_j}$ decreases the eigenvalue of $\hat{n}_j$ by one, just as $\hat{b}_j$ does, but if repeatedly applied to an eigenstate with small eigenvalue, it will yield unphysical states with negative eigenvalues of $\hat{n}_j$. Indeed, this is one of the problems usually encountered when working with $\hat{\theta}_j$. However, when the mean lattice filling $\langle\hat{n}_j\rangle = n_0 \gg 1$ these problems become less serious.

Using Eq. (24), the kinetic energy term in the Bose-Hubbard model (15) becomes $-t\sum_j(\sqrt{\hat{n}_{j+1}}e^{i(\hat{\theta}_j - \hat{\theta}_{j+1})}\sqrt{\hat{n}_j} + \text{H.c.})$. In addition, the interaction energy and chemical potential can be written as $\sum_j[(U/2)\hat{b}_j^\dagger\hat{b}_j^\dagger\hat{b}_j\hat{b}_j - \mu\hat{n}_j] = \sum_j[(U/2)\hat{N}_j^2 - \delta\mu\hat{N}_j]$, where $\hat{N}_j = \hat{n}_j - \langle\hat{n}_j\rangle = \hat{n}_j - n_0 = i\partial/\partial\theta_j$ and $\delta\mu$ is the deviation of the chemical potential from the value for which $\langle\hat{n}_j\rangle = n_0$. If the fluctuations of $\hat{N}_j$ are small, which is the case provided $U \gg tn_0$, $\hat{n}_j$ can be replaced by n_0 and thus the phase model is obtained:

$$\hat{H} = \sum_{j=1}^{L}\left[-E_J\cos(\hat{\theta}_j - \hat{\theta}_{j+1}) + \frac{E_C}{2}\hat{N}_j^2 - \delta\mu\hat{N}_j\right], \tag{25}$$

where $E_J = 2n_0t$, $E_C = U$. In the case of arrays of Josephson junctions (cf. Sec. VIII), the interaction is the long-range Coulomb potential, and a more realistic model is obtained by replacing $E_C/2\sum_j\hat{N}_j^2$ by $\sum_{ij}V_{ij}\hat{N}_i\hat{N}_j$, where V_{ij} is a function of $|i-j|$.

Interestingly, when formulated in the language of the Feynman path integral, the model in Eq. (25) with $\delta\mu = 0$ provides a particular example of a general relationship between some models of quantum bosons in 1D and some classical systems in 2D. As pointed out by Feynman (1972), the partition function $Z = \text{Tr}e^{-\beta\hat{H}}$ ($\beta = 1/k_BT$, with k_B the Boltzmann constant) of a quantum system can be written as a sum over all system configurations weighted by e^{-S}, where S is the analytic continuation of the classical action to imaginary time τ_E. For the model in Eq. (25), $Z = \int\prod_{j=1}^{L}[d\theta_j]e^{-S[\theta_j]}$, where $[d\theta_j]$ is the integration measure over all possible configurations of the angle θ_j, and $S[\theta_j]$ is given by

$$S[\theta_j] = \sum_{j=1}^{L}\int_0^{\hbar\beta}d\tau_E\left[\frac{\hbar\dot{\theta}_j^2}{2E_C} - \frac{E_J}{\hbar}\cos(\theta_{j+1} - \theta_j)\right], \tag{26}$$

where $\theta_j = d\theta_j/d\tau_E$. The term proportional to $\dot{\theta}_j^2$ in Eq. (26) plays the role of the kinetic energy, and stems from the operator $E_C\hat{N}_j^2/2$ in the Hamiltonian, where $\hat{N}_j = i\partial/\partial\theta_j$

plays the role of the momentum. Indeed, in certain applications, such as, e.g., the computational methods discussed in Sec. IV, it is sometimes useful to discretize the integral over τ. A convenient discretization of the term $\propto \sum_j \dot{\theta}_j^2/2$ is provided by $-\sum_{j,\tau_E} \cos(\theta_{j,\tau_E+\Delta\tau_E} - \theta_{j,\tau_E})$. By suitably choosing the units of the "lattice parameter" $\Delta\tau_E$, the partition function corresponding to Eq. (26) can be related to that of the classical XY model. The latter describes a set of planar classical spins $\mathbf{S_r} = (\cos\theta_\mathbf{r}, \sin\theta_\mathbf{r})$ interacting ferromagnetically on a square lattice and its classical Hamiltonian reads:

$$H_{XY} = -\bar{J} \sum_{\langle \mathbf{r},\mathbf{r}' \rangle} \mathbf{S_r} \cdot \mathbf{S_{r'}} = -\bar{J} \sum_{\langle \mathbf{r},\mathbf{r}' \rangle} \cos(\theta_\mathbf{r} - \theta_{\mathbf{r}'}), \tag{27}$$

where $\mathbf{r} = (j, \tau_E/\Delta\tau_E)$, and $\langle \mathbf{r}, \mathbf{r}' \rangle$ means that the sum runs over nearest-neighbor sites only. Assuming that $\theta_\mathbf{r}$ varies slowly with $\mathbf{r}$, we may be tempted to take a continuum limit of the XY model, where $-\cos(\theta_\mathbf{r} - \theta_{\mathbf{r}'})$ is replaced by $\frac{1}{2}\sum_{\langle \mathbf{r},\mathbf{r}' \rangle}(\theta_\mathbf{r} - \theta_{\mathbf{r}'})^2 = \frac{1}{2}\int d\mathbf{r}(\nabla_\mathbf{r}\theta)^2$. Indeed, this procedure seems to imply that this model [and the equivalent quantum model of Eq. (26)] are always superfluids with linearly dispersing excitations in the quantum case. However, this conclusion is incorrect as the continuum limit neglects the existence of nonsmooth configurations of $\theta_\mathbf{r}$, which are topological excitations corresponding to vortices of the classical XY model and to quantum phase slips in 1D quantum models. The correct way of taking the continuum limit of models such as Eq. (25) or its ancestor, the Bose-Hubbard model, will be described in Sec. V, where the bosonization method is reviewed.

To sum up, we have seen that, equipped with the knowledge about a handful of 1D models, it is possible to analyze a wide range of phenomena, which extend even beyond 1D to 2D classical statistical mechanics. In the following, we begin our tour of 1D systems by studying the exactly solvable models, for which a rather comprehensive picture can be obtained.

III. EXACT SOLUTIONS

A. The Tonks-Girardeau (hard-core boson) gas

We first consider the Tonks-Girardeau model corresponding to the limit $c \to +\infty$ of Eq. (10). In this limit, the exact ground-state energy was first obtained by Bijl (1937) and explicitly derived by Nagamiya (1940). The infinitely strong contact repulsion between the bosons imposes a constraint in the form that any many-body wave function of the TG gas must vanish every time two particles meet at the same point. As first pointed out by Girardeau (1960), this constraint can be implemented by writing the wave function $\psi_B(x_1, \ldots)$ as follows:

$$\psi_B(x_1, \ldots, x_N) = S(x_1, \ldots, x_N)\psi_F(x_1, \ldots, x_N), \tag{28}$$

where $S(x_1, \ldots, x_N) = \prod_{i>j=1}^N \mathrm{sign}(x_i - x_j)$ and $\psi_F(x_1, \ldots)$ is the many-body wave function of a (fictitious) gas of spinless fermions. Note that the function $S(x_1, \ldots)$ compensates the sign change of $\psi_F(x_1, \ldots)$ when any two particles are exchanged and thus yields a wave function obeying Bose statistics. Furthermore, eigenstates must satisfy the noninteracting Schrödinger equation when all N coordinates are different. Hence, in the absence of an external potential, and on a ring of circumference L with periodic boundary conditions [i.e., $\psi_B(x_1, \ldots, x_j + L, \ldots, x_N) = \psi_B(x_1, \ldots, x_j, \ldots, x_N)$], the (unnormalized) ground-state wave function has the Bijl-Jastrow form

$$\psi_B^0(x_1, \ldots, x_N) \propto \prod_{i<j} \sin\frac{\pi}{L}|x_i - x_j|. \tag{29}$$

This form of the ground-state wave function is generic of various 1D models in the limit of infinitely strong repulsion and of the Calogero-Sutherland model as we will see later. The ground-state energy of the TG gas is then $E = \hbar^2(\pi\rho_0)^2/6\pi m$, where $\rho_0 = N/L$ is the mean particle density; and the energy of the lowest excited state is $E(q) \sim \hbar^2\pi\rho_0/m|q|$ for $|q| \ll \pi\rho_0$ suggesting a linear phonon spectrum. As with the free Fermi gas, the TG gas has a finite compressibility at $T = 0$ and a specific heat linear in temperature. As we will see in Sec. V, these properties are not limited to the case of infinite contact repulsion but are generic features of interacting 1D bosons.

1. Correlation functions in the continuum

Besides thermodynamic properties, the mapping of Eq. (28) also allows the calculation of the correlation functions of the TG gas. Since Eq. (28) implies that the probability of finding particles at given positions is the same in the TG and in the free spinless Fermi gases, the density correlation functions of both gases are identical. In particular, the pair-correlation function $D_2(x) = \langle \rho(x)\rho(0) \rangle / \rho_0^2$ is given by

$$D_2(x) = 1 - \left[\frac{\sin(\pi\rho_0 x)}{\pi\rho_0 x}\right]^2. \tag{30}$$

However, computing the one-particle density matrix,

$$g_1(x, y) = \int \prod_{i=2}^N dx_i \psi_B^*(x, \ldots x_N)\psi_B(y, \ldots x_N), \tag{31}$$

is considerably more involved. Upon inserting Eq. (28) into Eq. (31), we see that the sign functions do not cancel out and therefore the bosonic and fermionic correlations are not identical anymore.

Nevertheless, it can be shown (Schultz, 1963) that $g_1(x, y)$ can be expressed as the Fredholm determinant of a linear integral equation (Tricomi, 1985). Another representation (Lenard, 1964) of $g_1(x, y)$ is in terms of a Toeplitz determinant. Such determinants have been thoroughly studied in relation to the 2D Ising model (Szego, 1952; Wu, 1966). The asymptotic long-distance behavior of the Toeplitz determinant can be obtained (Ovchinnikov, 2009) from the Fisher-Hartwig theorem (Fisher and Hartwig, 1968), which yields

$$g_1(x) = \rho_0 G^4(3/2)\left[\frac{1}{2\rho_0 L|\sin(\pi x/L)|}\right]^{1/2}, \tag{32}$$

where $G(z)$ is Barnes' G function; $G(3/2) = A^{-3/2}\pi^{1/4}e^{1/8}2^{1/24}$; $A = 1.282\,427\,12\ldots$ is Glaisher's constant. Thus, $G^4(3/2) = 1.306\,991\ldots$. In the thermodynamic limit, a more complete asymptotic expression is available (Vaidya and Tracy, 1979a; 1979b; Gangardt, 2004):

$$g_1(x) = \frac{\rho_\infty}{|\pi\rho_0 x|^{1/2}}\Big[1 - \frac{1}{8}\Big(\cos(2\pi\rho_0 x) + \frac{1}{4}\Big)\frac{1}{(\pi\rho_0 x)^2} - \frac{3}{16}\frac{\sin(2\pi\rho_0 x)}{(\pi\rho_0 x)^3} + \frac{33}{2048}\frac{1}{(\pi\rho_0 x)^4} + \frac{93}{256}\frac{\cos(2\pi\rho_0 x)}{256(\pi\rho_0 x)^4} + \ldots\Big], \tag{33}$$

where $\rho_\infty = G(3/2)^4/\sqrt{2} = \pi e^{1/2} 2^{-1/3} A^{-6}$. The leading term of Eq. (33) agrees with Eq. (32) for $L \to \infty$. The slow power-law decay of $g_1(x)$ at long distances leads to a divergence in the momentum distribution: $n(k) \sim |k|^{-1/2}$ for $k \to 0$. The lack of a delta function at $k = 0$ in $n(k)$ implies the absence of BEC. However, the $\sim k^{-1/2}$ divergence can be viewed as a remnant of the tendency of the system to form a BEC. The power-law behavior of $g_1(x)$ as $|x| \to \infty$ [or $n(k)$ as $k \to 0$] is often referred to as *quasilong-range* order.

Alternative ways of deriving the $g_1(x)$ follow from the analogy (Lenard, 1964) between the ground-state wave function of the TG gas and the distribution of eigenvalues of random matrices (Mehta, 2004) from the circular unitary ensemble. It is also possible to show (Jimbo *et al.*, 1980; Forrester *et al.*, 2003a) that the density matrix of the TG gas satisfies the Painlevé V nonlinear second order differential equation (Ince, 1956). Furthermore, the Fredholm determinant representation can be generalized to finite temperature (Lenard, 1966).

The asymptotic expansion of the one-particle density-matrix function at finite temperature in the grand-canonical ensemble has been derived (Its *et al.*, 1991). Asymptotically with distance, it decays exponentially, and, for $\mu > 0$, the dominant term reads

$$g_1(x, 0, \beta) \sim \frac{\sqrt{2m\beta^{-1}}}{\pi\hbar}\rho_\infty e^{-2|x|/r_c} F(\beta\mu), \tag{34}$$

where $\beta^{-1} = k_B T$ and ρ_∞ is the same constant as in Eq. (33), the correlation radius r_c is given by

$$r_c^{-1} = \frac{\sqrt{2m\beta^{-1}}}{2\pi\hbar}\int_{-\infty}^{\infty} d\lambda \ln\left|\frac{e^{\lambda^2-\beta\mu}+1}{e^{\lambda^2-\beta\mu}-1}\right|, \tag{35}$$

whereas $F(u)$ is a regular function of $u = \beta\mu$ given by

$$F(u) = \exp\Big[-\frac{1}{2}\int_u^\infty d\sigma\Big(\frac{dc}{d\sigma}\Big)^2\Big], \qquad c(\sigma) = \frac{1}{\pi}\int_{-\infty}^{\infty} d\lambda \ln\left|\frac{e^{\lambda^2-\sigma}+1}{e^{\lambda^2-\sigma}-1}\right|. \tag{36}$$

Two regimes can be distinguished: For $0 < \beta\mu \ll 1$, the correlation length r_c is just proportional to the de Broglie thermal length $\sqrt{2m\beta^{-1}}/\hbar$. For $1 \ll \beta\mu$, the integral in Eq. (35) is dominated by λ in the vicinity of $\pm\sqrt{\beta\mu}$. By linearizing λ^2 in the vicinity of these points, the integral can be shown to be proportional to $(\beta\mu)^{-1/2}$. As a result, one obtains $r_c \sim \hbar v_F \beta$ (where $v_F = \hbar\pi\rho_0/m$ is the Fermi velocity) for a degenerate TG gas. For the one-particle Green's function $G_B^<(x, \tau; \beta) = \langle\hat{\Psi}^\dagger(x, \tau)\hat{\Psi}(0, 0)\rangle$, Korepin *et al.* (1993) showed that

$$G_B^<(x, \tau; \beta) \propto \exp\Big[\int_{-\infty}^{\infty}\frac{dk}{2\pi}\left|x + t\frac{\hbar k}{m}\right| \times \ln\left|\frac{e^{\beta(\hbar^2k^2/2m)-\beta\mu}-1}{e^{\beta(\hbar^2k^2/2m)-\beta\mu}+1}\right|\Big]. \tag{37}$$

For $1 \ll \beta\mu$, one can use the previous expansion of the integrand around the points $k = \pm k_F = \pm\sqrt{2m\mu}/\hbar$, which gives $G_B^<(x, \tau; \beta) \propto \exp[-(\pi/4\beta\hbar v_F)(|x - v_F\tau| + |x + v_F\tau|)]$. These results can also be recovered by using the field-theoretic approach reviewed in Sec. V.

So far we have dealt with the homogeneous TG gas, which can be relevant for condensed matter systems. However, ultracold atomic gases are confined by inhomogeneous potentials. Fortunately, the TG gas remains solvable even in the presence of an external potential.

The Bose-Fermi mapping, Eq. (28), is still valid in the presence of any external confining potential $V_{\rm ext}(x)$. However, the eigenstates are constructed from the Slater determinants

$$\psi_F(x_1, \ldots, x_N) = \frac{1}{\sqrt{N!}}\det_{n=0,j=1}^{n=N-1,j=N}\varphi_n(x_j), \tag{38}$$

where $\varphi_n(x_j)$ are the eigenfunctions of the noninteracting Schrödinger equation in the presence of $V_{\rm ext}(x)$. Considerable simplification results from the fact that the confining potential in experiments is, to a good approximation, harmonic: $V_{\rm ext}(x) = \frac{1}{2}m\omega^2x^2$. Using Eqs. (38) and (28), the eigenfunctions of many-body Hamiltonian are constructed from the harmonic-oscillator orbitals: $\varphi_n(x) = [\mathcal{H}_n(x/\ell_{\rm HO})/\sqrt{2^n n!\ell_{\rm HO}\sqrt{\pi}}]e^{-x^2/2\ell_{\rm HO}^2}$, where $\mathcal{H}_n(z)$ are the Hermite polynomials and $\ell_{\rm HO} = \sqrt{\hbar/(m\omega)}$ is the oscillator length (in what follows and unless otherwise stated, all lengths are measured in units where $\ell_{\rm HO} = 1$), which yields the following ground-state wave function:

$$\psi_B^0(x_1, \ldots, x_N) = C_N^{-1/2}\prod_{k=1}^N e^{-x_k^2/2}\prod_{i>j=1}^N |x_i - x_j|, \tag{39}$$

where $C_N = N!\prod_{n=0}^{N-1} 2^{-n}\sqrt{\pi}n!$. Also in this case, the special form of the mapping (28) implies that the density profile and density correlations of the harmonically trapped TG gas are identical to those of a harmonically trapped gas of noninteracting spinless fermions. The latter have been studied in detail (Vignolo *et al.*, 2000; Brack and van Zyl, 2001) and will not be review here. Instead, we focus on the off-diagonal correlations and the momentum distribution which, as in the homogeneous case, are different for the Fermi and TG gases.

The one-particle density matrix $g_1(x, y)$ can be obtained evaluating the $(N-1)$-dimensional integral in Eq. (31) using Eq. (39). From this result, we can obtain the natural orbitals (cf. Sec. II.A), which obey $\int dy g_1(x, y)\phi_\alpha(y) = N_\alpha\phi_\alpha(x)$, as well as the momentum distribution: $n(k) = 1/2\pi\int dxdy g_1(x, y)e^{ik(x-y)}$. In the ground state, N_0 is the largest eigenvalue, followed by N_1, etc. As discussed in Sec. II.A, when the system exhibits BEC, N_0 is of $O(N)$ (Penrose and Onsager, 1956; Leggett, 2001). Furthermore, note that, because the trapped system is not translationally invariant, N_α and $n(k)$ are not proportional to each other. In other words, the natural orbitals $\phi_\alpha(x)$ are not plane waves.

For harmonically trapped systems with a few particles $N \leq 10$, $g_1(x, y)$ was first computed by Girardeau *et al.* (2001) and Lapeyre *et al.* (2002). To obtain the thermodynamic limit scaling of $n(k = 0)$ and N_0 with N, Papenbrock (2003) studied $g_1(x, y)$ for larger systems by writing the integrals in Eq. (31) in terms of an integration measure that is identical to the joint probability density for eigenvalues of $(N - 1)$-dimensional random matrices from the Gaussian unitary ensemble (GUE), and expressed the measure in terms of harmonic-oscillator orbitals. This enabled the computation of $g_1(x, y)$ in terms of determinants of the $(N - 1)$-dimensional matrices:

$$g_1(x, y) = \frac{2^{N-1} e^{-(x^2+y^2)/2}}{\sqrt{\pi}(N-1)!} \det_{m,n=0}^{m,n=N-2} [B_{m,n}(x, y)],$$
$$B_{m,n}(x, y) = \int_{-\infty}^{\infty} dz |z - x||z - y| \varphi_m(z)\varphi_n(z). \tag{40}$$

The form of $g_1(x, y)$ above and its relation to the GUE had earlier been discussed by Forrester *et al.* (2003a). Equation (40) allowed Papenbrock (2003) to study $g_1(x, y)$ and $n(k)$ for up to $N = 160$. The leading N behavior of $n(k = 0)$ was found to be $n(k = 0) \propto N$. The behavior of λ_0 was then inferred from the result for $n(k = 0)$ and a scaling argument, which resulted in $N_0 \propto \sqrt{N}$.

A detailed study of the lowest natural orbitals and their occupations N_α in a harmonic trap was given by Forrester *et al.* (2003b). Using a numerical approach based on an expression similar to Eq. (40), they computed $g_1(x, y)$ and obtained the natural orbitals by a quadrature method up to $N = 30$. By fitting the results of the two lowest natural orbitals ($\alpha = 0, 1$) to a law $N_\alpha = aN^p + b + cN^{-q}$, they found that

$$N_0 = 1.43\sqrt{N} - 0.56 + 0.12N^{-2/3}$$
$$N_1 = 0.61\sqrt{N} - 0.56 + 0.12N^{-4/3}. \tag{41}$$

Furthermore, a mapping to a classical Coulomb gas allowed Forrester *et al.* (2003b) to obtain an asymptotic expression for $g_1(x, y)$ of the harmonically trapped TG gas in the limit of large N. Their result reads

$$g_1(x, y) = N^{1/2} \frac{G^4(3/2)}{\pi} \frac{(1 - x^2)^{1/8}(1 - y^2)^{1/8}}{|x - y|^{1/2}}. \tag{42}$$

This expression shows that $g_1(x, y)$ in the trap exhibits a power-law decay similar to the one found in homogeneous systems. Using a scaling argument, the behavior of $N_{\alpha=0,1}$ can be obtained from Eq. (42), which reproduces the leading behavior obtained numerically [Eq. (41)]. In addition, the one-particle density matrix in harmonic traps was also studied by Gangardt (2004) using a modification of the replica trick. The leading order in N obtained by Gangardt agrees with Eq. (42), and his method further allows one to obtain the finite-size corrections to Eq. (42). Indeed, the leading corrections in the trap and homogeneous systems [cf. Eq. (33)] are identical.

Another quantity of interest is the momentum distribution $n(k)$. Whereas the small k behavior can be obtained from the asymptotic formula (42), the large k asymptotics gives information about short-distance one-particle correlations not captured by Eq. (42). For two hard-core bosons in a harmonic trap, Minguzzi *et al.* (2002) found that $n(k \to +\infty) \sim k^{-4}$. Since the singularities arising in the integrals involved also appear in the many-body case, this behavior was believed to hold for arbitrary N. Similar results were obtained numerically for up to eight particles in harmonic traps (Lapeyre *et al.*, 2002) and analytically, using asymptotic expansions, for homogeneous systems (Forrester *et al.*, 2003b).

Olshanii and Dunjko (2003) showed that the tail $\sim k^{-4}$ is a generic feature of delta-function interactions, i.e., it applies to the Lieb-Liniger model at all values of the dimensionless parameter $\gamma = c/\rho_0$. The behavior can be traced back to the kink in the first derivative of the exact eigenstates at the point where two particles meet. For homogeneous systems (Olshanii and Dunjko, 2003)

$$n(k \to \infty) = \frac{1}{\hbar\rho_0} \frac{\gamma^2 e'(\gamma)}{2\pi} \left(\frac{\hbar\rho_0}{k}\right)^4, \tag{43}$$

where the calculation of $e(\gamma)$ is discussed in Sec. III.B, and $n(k)$ is normalized so that $\int dk n(k) = 1$. Results for harmonically trapped systems can be obtained by means of the local density approximation (LDA). In those systems, $n(k \to \infty) \sim \Omega_{\rm HO}(\hbar\rho_0^0)^3/k^4$, where $\Omega_{\rm HO}$ is a dimensionless quantity and $\rho_0(x = 0)$ is the density at the trap center. Numerical results for $\Omega_{\rm HO}$ for different values of γ_0 (where γ_0 is the γ parameter in the center of the trap) are shown in Fig. 1. Based on the observed behavior of $\Omega_{\rm HO}$, Olshanii and Dunjko (2003) proposed that measuring the high-k tail of $n(k)$ allows one to identify the transition between the weakly interacting Thomas-Fermi and the strongly interacting Tonks-Girardeau regimes.

A straightforward and efficient approach to computing the one-particle density matrix of hard-core bosons in generic potentials in and out of equilibrium was introduced by Pezer and Buljan (2007). Indeed, $g_1(x, y, \tau) = \langle \Psi^\dagger(x, \tau)\Psi(y, \tau)\rangle$ (notice the addition of the dependence on time τ) can be written in terms of the solutions $[\varphi_i(x, \tau)]$ of the single-particle time-dependent Schördinger equation relevant to the problem

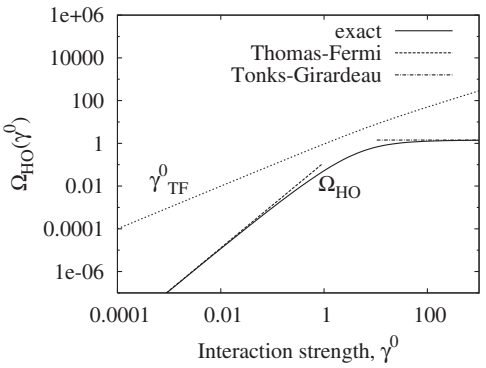

FIG. 1. Dimensionless coefficient $\Omega_{\rm HO}(\gamma^0)$ (see text) as a function of the interaction strength γ^0 at the center of the trap. The dotted line shows the Thomas-Fermi estimate $\gamma^0_{\rm TF} = (8/3^{2/3}) \times (Nma^2_{\rm 1D}\omega/\hbar)^{-2/3}$ for the interaction strength in the center of the system as a function of γ^0. The numerical results are compared with the asymptotic expressions in the Thomas-Fermi and Tonks-Girardeau regimes. From Olshanii and Dunjko, 2003.

$$g_1(x,y,\tau)=\sum_{i,j=0}^{N-1}\varphi_i^*(x,\tau)A_{ij}(x,y,\tau)\varphi_j(y,\tau), \tag{44}$$

where, from the general definition of the many-body Tonks-Girardeau wave function [Eq. (38)] and of the one-particle density matrix [Eq. (31)], one can write

$$\mathbf{A}(x,y,\tau)=(\det\mathbf{M})(\mathbf{M}^{-1})^T, \tag{45}$$

where $M_{ij}(x,y,\tau)=\delta_{ij}-2\int_x^y dx'\varphi_i^*(x',\tau)\varphi_j(x',\tau)$ (for $x<y$ without loss of generality). This approach has allowed the study of hard-core boson systems out of equilibrium (Buljan *et al.*, 2007; Pezer and Buljan, 2007) and was generalized to study hard-core anyons by del Campo (2008).

2. Correlation functions on the lattice

As mentioned in Sec. II.D, for hard-core bosons on the lattice, the Jordan-Wigner transformation, Eq. (21), plays the role of Girardeau's Bose-Fermi mapping (28). Thus, as in the continuum case, the spectrum, thermodynamic functions, and the correlation function of the operator $\hat{n}_j$ are identical to those of the noninteracting spinless lattice Fermi gas. However, the calculation of the one-particle density matrix is still a nontrivial problem requiring similar methods to those reviewed in Sec. III.A.1.

Using the Holstein-Primakoff transformation (18), the one-particle density matrix $g_1(m-n)=\langle\hat{b}_m^\dagger\hat{b}_n\rangle$ can be expressed in terms of spin correlation functions (Barouch *et al.*, 1970; Barouch and McCoy, 1971a; 1971b; Johnson and McCoy, 1971; McCoy *et al.*, 1971; Ovchinnikov, 2002; Ovchinnikov, 2004): $g_1(m-n)=\langle\hat{\sigma}_m^+\hat{\sigma}_n^-\rangle=\langle\hat{\sigma}_m^x\hat{\sigma}_n^x\rangle+\langle\hat{\sigma}_m^y\hat{\sigma}_n^y\rangle=2\langle\hat{\sigma}_m^x\hat{\sigma}_n^x\rangle$ [note that $\langle\hat{\sigma}_n^x\hat{\sigma}_m^y\rangle=0$ and $\langle\hat{\sigma}_n^x\hat{\sigma}_m^x\rangle=\langle\hat{\sigma}_n^y\hat{\sigma}_m^y\rangle$ by the $U(1)$ symmetry of the XX model]. Thus, consider the following set of correlation functions: $S_{\nu\nu}(n-m,\tau)=\langle\hat{\sigma}_m^\nu(\tau)\hat{\sigma}_n^\nu(\tau)\rangle$ where $\nu=x,y,z$. We first note that (Lieb *et al.*, 1961)

$$e^{i\pi\hat{c}_m^\dagger\hat{c}_m}=1-2\hat{c}_m^\dagger\hat{c}_m=\hat{A}_m\hat{B}_m, \tag{46}$$

where $\hat{A}_m=\hat{c}_m^\dagger+\hat{c}_m$ and $\hat{B}_m=\hat{c}_m^\dagger-\hat{c}_m$. Hence,

$$\begin{aligned}
S_{xx}(l-m)&=\tfrac{1}{4}\langle\hat{B}_l\hat{A}_{l+1}\hat{B}_{l+1}\ldots\hat{A}_{m-1}\hat{B}_{m-1}\hat{A}_m\rangle,\\
S_{yy}(l-m)&=\tfrac{1}{4}(-1)^{l-m}\langle\hat{A}_l\hat{B}_{l+1}\hat{A}_{l+1}\ldots\hat{B}_{m-1}\hat{A}_{m-1}\hat{B}_m\rangle,\\
S_{zz}(l-m)&=\tfrac{1}{4}\langle\hat{A}_l\hat{B}_l\hat{A}_m\hat{B}_m\rangle.
\end{aligned} \tag{47}$$

Using Wick's theorem (Caianiello and Fubini, 1952; Barouch and McCoy, 1971a), these expectation values are reduced to Pfaffians (Itzykson and Zuber, 1980). At zero temperature, the correlators over the partially filled Fermi sea have the form $\langle\Psi_F|\hat{A}_l\hat{A}_m|\Psi_F\rangle=0$, $\langle\Psi_F|\hat{B}_l\hat{B}_m|\Psi_F\rangle=0$ ($l\neq m$), and $\langle\Psi_F|\hat{B}_l\hat{A}_m|\Psi_F\rangle=2G_0(l-m)$, where $G_0(R)=\langle\Psi_F|\hat{c}_{m+R}^\dagger\hat{c}_m|\Psi_F\rangle$ is the free-fermion one-particle correlation function on a finite chain. The Pfaffians in Eq. (47) then reduce to the Toeplitz determinant (Lieb *et al.*, 1961) of a $R\times R$ matrix: $G(R)=\det_{lm}[2G_0(l-m-1)]$, $l,m=1,\ldots,R$. Thus,

$$S_{xx}(R)=\frac{1}{4}\begin{vmatrix} G_{-1} & G_{-2} & \ldots & G_{-R}\\ G_0 & G_{-1} & \ldots & G_{-R+1}\\ \cdot & \cdot & \cdots & \cdot\\ \cdot & \cdot & \cdots & \cdot\\ \cdot & \cdot & \cdots & \cdot\\ G_{R-2} & G_{R-3} & .. & G_{-1}\end{vmatrix}. \tag{48}$$

By taking the continuum limit of Eq. (48) as explained in Sec. II.C, the Toeplitz determinant representation of the continuum TG gas is recovered. For a half-filled lattice with an even number of sites L and a number of particles $N=L/2$ odd (Ovchinnikov, 2004), the free-fermion density-matrix $G_0(l)=\sin(\pi l/2)/L\sin(\pi l/L)$, so that $G_0(l)=0$ for even l, and the Toeplitz determinant (48) can be further simplified to yield $S_{xx}(R)=\frac{1}{2}(C_{N/2})^2$ (for even R), $S_{xx}(R)=-\frac{1}{2}C_{(R-1)/2}G_{(R+1)/2}$ (for odd N), where C_R is the determinant of the $R\times R$ matrix: $C_R=\det_{lm}[(-1)^{l-m}G_0(2l-2m-1)]$, $l,m=1,\ldots,R$.

On a finite chain and for odd N, C_R is a Cauchy determinant, shown by Ovchinnikov (2002) to yield

$$C_R=\left(\frac{2}{\pi}\right)^R\prod_{k=1}^{R-1}\left[\frac{\sin[\pi(2k)/L]^2}{\sin[\pi(2k+1)/L]\sin[\pi(2k-1)/L]}\right]^{R-k}. \tag{49}$$

In the thermodynamic limit, Eq. (49) reduces to

$$C_R=(2/\pi)^R\prod_{k=1}^{R-1}\left(\frac{4k^2}{4k^2-1}\right)^{R-k}, \tag{50}$$

and hence the one-body density matrix,

$$g_1(R)=2S_{xx}(R)\sim\frac{2C_0}{\sqrt{\pi}}\left(\frac{1}{R^{1/2}}-\frac{(-1)^R}{8R^{5/2}}\right) \tag{51}$$

for large R, where $2C_0/\sqrt{\pi}=0.588\,352\ldots$ can be expressed in terms of Glaisher's constant (Wu, 1966; McCoy, 1968; Ovchinnikov, 2004). Thus, also in this case, the one-particle density matrix of the bosons decays as a power law, indicating the absence of a BEC at $T=0$. At nonzero temperature, the power-law behavior is replaced by an exponential decay (Its *et al.*, 1993).

Next, we turn to the dynamical correlations $G_{\nu\nu}^<(R,\tau)=\langle e^{i\hbar H\tau/\hbar}\hat{\sigma}_m^\nu e^{-i\hat{H}\tau/\hbar}\hat{\sigma}_{m+R}^\nu\rangle$, $\nu=x,y$. To obtain these objects, it is convenient to consider the four spin correlator (McCoy *et al.*, 1971; Vaidya and Tracy, 1978)

$$C_{\nu\nu}(R,\tau,N)=\langle\hat{\sigma}_{1+(N/2)}^\nu(\tau)\hat{\sigma}_{1-R+N}^\nu(\tau)\hat{\sigma}_1^\nu(0)\hat{\sigma}_{1-R+(N/2)}^\nu(0)\rangle, \tag{52}$$

which is obtained by evaluating a Pfaffian (Lieb *et al.*, 1961; McCoy *et al.*, 1971). From the cluster property,

$$\lim_{N\to\infty}C_{\nu\nu}(R,\tau,N)=[G_{\nu\nu}^<(R,\tau)]^2. \tag{53}$$

$G_{\nu\nu}^<(R,\tau)$ can be obtained. The long-time behavior of the one-particle Green's function $G_B^<(R,\tau)=\langle\hat{b}_{n+R}^\dagger(\tau)\hat{b}_n(0)\rangle$ was computed by Müller and Shrock (1983; 1984) for $R=0$ following a method due to McCoy *et al.* (1983a; 1983b). They found that $G_B^<(0,\tau)\sim(i\tau)^{-1/2}$. When comparing this result with Eq. (51), we see that the leading asymptotic behavior is controlled by the same exponent ($=\frac{1}{2}$) in

both space and time. This is a consequence of the conformal invariance of the underlying field theory [see Sec. V and Gogolin *et al.* (1999); Giamarchi (2004) for an extended discussion].

At finite temperature, the asymptotic behavior of the Green's function has been obtained by Its *et al.* (1993)

$$G_B^<(R,\tau) \sim \exp\left[|R| \int_{-\pi}^{\pi} \frac{dk}{2\pi} \ln|\tanh\beta(\mu - 2t\cos k)|\right], \tag{54}$$

in the spacelike regime (for $|R| > 4\tau t/\hbar$, $\beta = 1/k_B T$), and

$$G_B^<(R,\tau) \sim \tau^{2(\nu_+^2+\nu_-^2)} \exp\left[\int_{-\pi}^{\pi} \frac{dk}{2\pi} |R - 4\tau \sin k| \times \ln|\tanh\beta(\mu - 2t\cos k)|\right], \tag{55}$$

in the timelike regime (for $|R| < 4\tau t/\hbar$), where

$$\nu_\pm = \frac{1}{2\pi} \ln|\tanh\beta(-\mu \mp 2\cos p_0)|, \tag{56}$$

where p_0 is defined by $\sin p_0 = |R|\hbar/4\tau t$. For $\beta\mu \gg 1$ and $|\mu/t| < 2$, one can expand in the vicinity of $\pm k_F = \pi n_0$ such that $\mu = 2t\cos k_F$, and obtain that the correlation functions (54) and (55) decay exponentially with x on a length scale $\pi/4\beta\hbar v_F$, as found previously in the continuum case. For infinite temperature, the correlation functions are local and Gaussian (Sur *et al.*, 1975).

Finally, we consider the effects of a trapping potential. As discussed in Sec. VIII, the use of a periodic potential generated by a deep optical lattice allows experimentalists to reach the strongly correlated regime where the system behaves essentially as a lattice TG gas in the presence of a trap (Paredes *et al.*, 2004).

As in the continuum case, the lattice TG gas remains exactly solvable when an external potential $\hat{V}_{\rm ext}$ is added to $\hat{H}_{\rm LTG}$ [Eq. (16)]. For the experimentally relevant harmonic potential, the Jordan-Wigner transformation maps the model described by $\hat{H}_{\rm LTG} + \hat{V}_{\rm ext}$ to the following fermionic Hamiltonian:

$$\hat{H}_F = \sum_j [-t(\hat{c}_j^\dagger \hat{c}_{j+1} + \text{H.c.}) + (Vx_j^2 - \mu)\hat{n}_j], \tag{57}$$

where $x_j = ja$, a is the lattice parameter, and V is the strength of the trapping potential. The above Hamiltonian can be easily diagonalized since it is quadratic. Using the single-particle eigenstates of Eq. (57), the momentum distribution $n(k)$ can be computed using Toeplitz determinants (Paredes *et al.*, 2004), as explained. In addition, an alternative and computationally more efficient way of calculating one-particle correlations in the lattice, for arbitrary external potentials, was introduced by Rigol and Muramatsu (2004 and 2005c). We note that the one-particle density matrix can be expressed in term of spin operators as $g_1(i,j) = \langle \hat{b}_i^\dagger \hat{b}_j \rangle = \langle \hat{\sigma}_i^+ \hat{\sigma}_j^- \rangle = \delta_{ij} + (-1)^{\delta_{ij}} \langle \hat{\sigma}_j^- \hat{\sigma}_j^+ \rangle$. Hence, in order to determine $g_1(i,j)$ it suffices to calculate

$$\begin{aligned} G(i,j) &= \langle \hat{\sigma}_i^- \hat{\sigma}_j^+ \rangle \\ &= \langle \Psi_F | \prod_{\beta=1}^{i-1} e^{i\pi \hat{c}_\beta^\dagger \hat{c}_\beta} \hat{c}_i \hat{c}_j^\dagger \prod_{\gamma=1}^{j-1} e^{-i\pi \hat{c}_\gamma^\dagger \hat{c}_\gamma} | \Psi_F \rangle \\ &= \det[(\mathbf{P}^i)^\dagger \mathbf{P}^j], \end{aligned} \tag{58}$$

where $|\Psi_F\rangle = \prod_{\kappa=1}^N \sum_{\varrho=1}^L P_{\varrho\kappa} \hat{c}_\varrho^\dagger |0\rangle$ is the Slater determinant corresponding to the fermion ground state in the trap, and $(\mathbf{P}^\alpha)_{L,N+1}$, with $\alpha = i, j$ is obtained using properties of Slater determinants and written as

$$P_{\varrho\kappa}^\alpha = \begin{cases} -P_{\varrho\kappa} & \text{for } \varrho < \alpha, \kappa = 1,\ldots,N \\ P_{\varrho\kappa} & \text{for } \varrho \geq \alpha, \kappa = 1,\ldots,N. \\ \delta_{\alpha\varrho} & \text{for } \kappa = N+1 \end{cases} \tag{59}$$

From Eq. (58), $G(i,j)$ and hence $g_1(i,j)$ are computed numerically. This method has the additional advantage that it can be easily generalized to study off-diagonal correlations in systems out of equilibrium (Rigol and Muramatsu, 2005b). It has also been generalized to study hard-core anyons by Hao *et al.* (2009).

To discuss the properties of the trapped gas, it is convenient to define a length scale determined by the confining potential in Eq. (57): $\zeta = (V/t)^{-1/2}$. We also define the "characteristic" density $\tilde{\rho} = Na/\zeta$, which is a dimensionless quantity that plays a similar role to the mean filling n_0 in homogeneous systems (Rigol and Muramatsu, 2004; 2005c). For $\tilde{\rho} > 2.68$, an incompressible plateau with $n_0 = 1$ is always present at the trap center.

A detailed study of $g_1(i,j)$, the lowest natural orbitals and their occupations, and the scaled momentum distribution function revealed that, in the regions where $n_i < 1$, their behavior is very similar to the one observed in the continuum trapped case (Rigol and Muramatsu, 2004; 2005c). One-particle correlations were found to decay as a power law, $g_1(i,j) \sim |i-j|^{-1/2}$, at long distances (see the main panel in Fig. 2), with a weak dependence on the density (discussed in

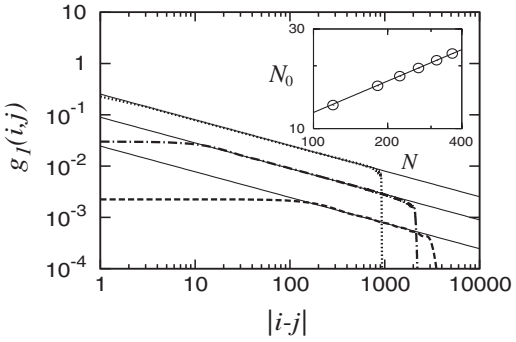

FIG. 2. One-particle density matrix of trapped hard-core bosons vs $|i-j|$ (i located in the center of the trap) for systems with $N = 1000$, $\tilde{\rho} = 2.0$, $n_0 = 0.75$ (dotted line), $N = 100$, $\tilde{\rho} = 4.47 \times 10^{-3}$, $n_0 = 0.03$ (dash-dotted line), and $N = 11$, $\tilde{\rho} = 2.46 \times 10^{-5}$, $n_0 = 2.3 \times 10^{-3}$ (dashed line), where n_0 is the filling of the central cite. The abrupt reduction of $g_1(i,j)$ occurs when $n_j \to 0$. Thin continuous lines correspond to power laws $|i-j|^{-1/2}$. The inset shows N_0 vs N for systems with $\tilde{\rho} = 1.0$ (○). The straight line exhibits $\sqrt{N}$ behavior. From Rigol and Muramatsu, 2005c.

Sec. IV.B.3). As a consequence of that power-law decay, the leading N behavior of N_0 and $n'_k = 0$ was found, both numerically and by scaling arguments, to be $N_0 \propto \sqrt{N}$ (see the inset in Fig. 2) and $n'_{k=0} \propto \sqrt{N}$, with proportionality constants that are only functions of $\tilde{\rho}$. On the other hand, the high-α and high-k asymptotics of the occupation of the natural orbitals and of the momentum distribution function, respectively, are not universal for arbitrary fillings. However, at very low filling, universal power-law decays $N_\alpha \propto \alpha^{-4}$ and $n'(k) \propto k^{-4}$ emerge in the lattice TG (Rigol and Muramatsu, 2004), in agreement with what was discussed for the TG gas in the continuum.

Finite temperatures in experiments have dramatic effects in the long-distance behavior of correlations in 1D systems. For the trapped TG gas in a lattice, exact results for $g_1(i, j)$, the natural orbitals and their occupations, as well as the momentum distribution function, can be obtained in the grand-canonical ensemble (Rigol, 2005). As in the homogeneous case, the power-law behavior displayed in Fig. 2 is replaced by an exponential decay, which implies that $n(k = 0) \sim O(1)$ and $N_0 \sim O(1)$ at finite T. As a result, the behavior of $n(k)$ at low momenta is very sensitive to the value of T. Hence, it can be used as a sensitive probe for thermometry (Rigol, 2005). Other studies of the momentum distribution of the trapped lattice TG gas at finite T have suggested that it can be well approximated by a Lévy distribution (Ponomarev *et al.*, 2010).

B. The Lieb-Liniger model

We now turn to the more general Lieb-Liniger model, Eq. (10). The model is integrable (Lieb, 1963; Lieb and Liniger, 1963) by the Bethe ansatz, i.e., its eigenfunctions are of the form

$$\psi_B(x_1, \ldots, x_N) = \sum_P A(P) e^{i \sum_n k_{P(n)} x_n}, \tag{60}$$

for $x_1 < x_2 < \ldots < x_N$ where the P's are the $N!$ possible permutations of the set $\{1, \ldots, N\}$. The value of the wave function $\psi_B(x_1, \ldots)$ when the condition $x_1 < x_2 < \cdots < x_N$ is not satisfied, is obtained from the symmetry of the wave function under permutation of the particle coordinates. The physical interpretation of the Bethe ansatz wave function is the following. When the particle coordinates are all distinct, the interaction energy term in Eq. (10) vanishes, and the Hamiltonian reduces to that of a system of noninteracting particles. Thus, the eigenstates of the Hamiltonian can be written as a linear combination of products of single-particle plane waves. If we now consider a case with two particles n and m of respective momenta k_n and k_m having the same coordinate, a collision between these two particles occurs. Because of the 1D nature of the system, the energy and momentum conservation laws imply that a particle can only emerge out of the collision carrying the same momenta or exchanging it with the other particle. Considering all possible sequences of two-body collisions starting from a particular set of momenta $k_1, \ldots, k_N$ leads to the form of the wave function (60). When the permutations P and P' only differ by the transposition of 1 and 2, the coefficients $A(P)$ and $A(P')$ are related by $A(P) = [(k_1 - k_2 + ic)/(k_1 - k_2 + ic)]A(P')$ so that the coefficients $A(P)$ are fully determined by two-body collisions. Considering three-body collisions then leads to a compatibility condition known as Yang-Baxter equation which amounts to require that any three-body collision can be decomposed into sequences of three successive two-body collisions. The Bethe ansatz wave function can be seen as a generalization of the Girardeau wave function (28), where the requirement of a vanishing wave function for two particles meeting at the same point has been replaced by a more complicated boundary condition. As in the case of the TG gas, the total energy of the state (60) is a function of the k_n by

$$E = \sum_n \frac{\hbar^2 k_n^2}{2m}. \tag{61}$$

However, the (pseudo-)momenta k_n are determined by requiring that the wave function (10) obeys periodic boundary conditions, i.e.,

$$e^{ik_n L} = \prod_{\substack{m=1 \\ m \neq n}}^{N} \frac{k_n - k_m + ic}{k_n - k_m - ic}, \tag{62}$$

for each $1 \leq n \leq N$. Taking the logarithm, it is seen that the eigenstates are labeled by a set of integers $\{I_n\}$, with

$$k_n = \frac{2\pi I_n}{L} + \frac{1}{L} \sum_m \log\left(\frac{k_n - k_m + ic}{k_n - k_m - ic}\right). \tag{63}$$

The ground state is obtained by filling the pseudo-Fermi sea of the I_n variables. In the continuum limit, the N equations (62) determining the k_n pseudomomenta as a function of the I_n quantum numbers reduce to an integral equation for the density $\rho(k_n) = 1/L(k_{n+1} - k_n)$ of pseudomomenta that reads (for zero ground-state total momentum)

$$2\pi\rho(k) = 1 + 2\int_{-q_0}^{q_0} \frac{c\rho(k')}{(k - k')^2 + c^2}, \tag{64}$$

with $\rho(k) = 0$ for $|k| > q_0$, while the ground-state energy per unit length and the density become

$$\frac{E}{L} = \int_{-q_0}^{q_0} dk \frac{\hbar^2 k^2}{2m} \rho(k), \quad \text{and} \quad \rho_0 = \int_{-q_0}^{q_0} dk \rho(k). \tag{65}$$

By working with dimensionless variables and functions,

$$g(u) = \rho_0(qu), \qquad \lambda = \frac{c}{q_0}, \qquad \gamma = \frac{c}{\rho_0}, \tag{66}$$

the integral equation can be recast as

$$2\pi g(u) = 1 + 2\lambda \int_{-1}^{1} \frac{g(u')du'}{\lambda^2 + (u - u')^2}, \tag{67}$$

where $g(u)$ is normalized such that $\gamma \int_{-1}^{1} g(u)du = \lambda$.

In the limit $c \to \infty$, $\lambda/(u^2 + \lambda^2) \to 0$ so that $g(u) = 1/(2\pi)$. Using Eq. (67), one finds that $\lambda/\gamma \to 1/\pi$, i.e., $q_0 = \pi\rho_0$. Thus, in this limit, the function $\rho(k) = \theta(\pi\rho_0 - |k|)/(2\pi)$ and the ground-state energy becomes that of the TG gas. In the general case, the integral equations have to be solved numerically. The function $g(u)$ being fixed by the ratio $\lambda = c/q_0$ and γ being also fixed by λ, the physical properties of the Lieb-Liniger gas depend only on the dimensionless ratio $\gamma = c/\rho_0$. An important consequence is that, in the

Lieb-Liniger model, low density corresponds to strong interaction, and high density corresponds to weak interaction, which is the reverse of the 3D case. As a consequence of the above mentioned scaling property, the energy per unit length is $E/L = \hbar^2\rho_0^3/2me(\gamma)$. The Bogoliubov approximation gives a fair agreement with $e(\gamma)$ for $0 < \gamma < 2$. The TG regime [defined by $e(\gamma) = \pi^2/3$ with less than 10% accuracy] is reached for $\gamma > 37$. Expansions of the ground-state energy to order $1/\gamma^3$ have been obtained (Guan and Batchelor, 2011) recently, and are very accurate for $\gamma > 3$, allowing one to describe the crossover.

Until now, we have only considered the ground-state energy with zero momentum. However, by considering Eq. (63), it is seen that if we shift all the I_n quantum numbers by the same integer r and at the same time we shift all the k_n pseudomomenta by the quantity $2\pi r/L$, we obtain another solution of Eq. (63). For such a solution, the wave function (60) is multiplied by a factor $e^{i(2\pi r/L)\sum_n x_n}$ indicating a shift of the total momentum $P = 2\hbar\pi rN/L$. At the same time, the ground-state energy is shifted by a quantity equal to $P^2/2Nm$, in agreement with the Galilean invariance of Eq. (10). The compressibility and the sound velocity can be derived from the expression of the energy per unit length. Remarkably, the sound velocity obtained from the Bogoliubov approximation agrees with the exact sound velocity derived from the Lieb-Liniger solution for $0 < \gamma < 10$ even though, as we have just seen, the range of agreement for the energy densities is much narrower. For $\lambda \gg 1$, one can obtain an approximate solution of the integral equations (67) by replacing the kernel by $2/\lambda$. Then, one finds (Lieb and Liniger, 1963) $g(u) \simeq \lambda/(2\pi\lambda - 2)$, which leads to $\pi\lambda = (2+\gamma)$ and $E = (\hbar^2\pi^2\rho_0^3/6m)[\gamma/(\gamma+2)]^2$. This expression of the energy is accurate to 1% for $\gamma > 10$. A systematic expansion of thermodynamic quantities in powers of $1/\gamma$ can be found in Iida and Wadati (2005). For the noninteracting limit, $\lambda \to 0$, the kernel of the integral equation (67) becomes $2\pi\delta(u-u')$ and the solutions become singular in that limit. This is an indication that 1D interacting bosons are not adiabatically connected with noninteracting bosons and present nongeneric physics.

Besides the ground-state properties, the Bethe-ansatz solution of the Lieb-Liniger model also allows the study of excited states (Lieb, 1963). Two types of excitations (that we call type I and type II) are found. Type I excitations are obtained by adding one particle of momentum $q > q_0$ to the $[N-1]$ particle ground state. Because of the interaction, the $N-1$ pseudomomenta k_n' $(1 \le n \le N-1)$ are shifted with respect to the ground-state pseudomomenta k_n by $k_n' = k_n + \omega_n/L$, while the pseudomomentum $k_N = q$. Taking the continuum limit of Eq. (63), one finds the integral equation (Lieb, 1963)

$$2\pi J(k) = 2c\int_{-q_0}^{q_0} \frac{J(k')}{c^2+(k-k')^2} - \pi + 2\tan^{-1}\left(\frac{q-k}{c}\right), \tag{68}$$

where $J(k) = \rho(k)\omega(k)$. The momentum and energy of type I excitations are obtained as a function of q and $J(k)$ as

$$P = q + \int_{-q_0}^{q_0} J(k)dk, \quad \epsilon_{\rm I} = -\mu + q^2 + 2\int_{-q_0}^{q_0} kJ(k)dk. \tag{69}$$

The type I excitations are gapless, with a linear dispersion for $P \to 0$ and a velocity equal to the thermodynamic velocity of sound. For weak coupling, they reduce to the Bogoliubov excitations. In the TG limit, they correspond to transferring one particle at the Fermi energy to a higher energy. Type II excitations are obtained by removing one particle of momentum $0 < k_h = q < q_0$ from the $[N+1]$ particle ground state. As in the case of type I excitations, the interaction of the hole with the particles creates a shift of the pseudomomenta, with this time $k_n' = k_n + \omega_n/L$ for $n \le h$ and $k_n' = k_{n+1} + \omega_n/L$ for $n > h$. The corresponding integral equation is (Lieb, 1963)

$$2\pi J(k) = 2c\int_{-q_0}^{q_0} \frac{J(k')}{c^2+(k-k')^2} + \pi - 2\tan^{-1}\left(\frac{q-k}{c}\right), \tag{70}$$

with the same definition for $J(k)$. The momentum and energy of the type II excitation are

$$P = -q + \int_{-q_0}^{q_0} J(k)dk, \quad \epsilon_{\rm II} = \mu - q^2 + 2\int_{-q_0}^{q_0} kJ(k)dk. \tag{71}$$

For $P = \pi\rho$, $\epsilon_{\rm II}$ is maximum, while for $q = K$, $P = 0$, and $\epsilon_{\rm II} = 0$. For $P \to 0$, the dispersion of type II excitation vanishes linearly with P, with the same velocity as the type I excitations. Type II excitations have no equivalent in the Bogoliubov theory. Type II and type I excitations are not independent from each other (Lieb, 1963): a type II excitation can be built from many type I excitations of vanishing momentum. The Lieb-Liniger thermodynamic functions can be obtained using the thermodynamic Bethe ansatz (Yang and Yang, 1969).

C. The t-V model

Results similar to those above can be obtained for the t-V model defined in Sec. II.C. Its Bethe-ansatz wave function, in second quantized form, reads

$$|\Psi_B\rangle = \sum_{1\le n_1<\cdots<n_N\le L} \sum_P e^{i\sum_{j=1}^N k_{P(j)}n_j} A(P)\hat{b}_{n_N}^\dagger \cdots \hat{b}_{n_1}^\dagger |0\rangle, \tag{72}$$

where $|0\rangle$ is the vacuum state of the bosons, and P is a permutation. By imposing periodic boundary conditions, the following set of equations for the pseudomomenta k_n is obtained:

$$e^{ik_jL} = (-)^{N-1}\prod_{\substack{l=1\\ l\ne j}}^N \frac{1-2\Delta e^{ik_j}+e^{i(k_j+k_l)}}{1-2\Delta e^{ik_l}+e^{i(k_j+k_l)}}. \tag{73}$$

By the same method as in the Lieb-Liniger gas, Eq. (73) can be turned into an integral equation for the density of pseudomomenta. The energy of the eigenstates is given by

$$E = -2t\sum_{j=1}^N \cos k_j. \tag{74}$$

For half-filling, solving Eq. (73) shows that the quantum lattice gas model has a period 2 density-wave ground state

(with gapped excitations) for $V > 2t$. This state corresponds to the more general Mott phenomenon to be examined in Sec. VI.A. For $V < -2t$, the system has a collapsed ground state. Using the mappings described in Sec. II.D, in the spin language the collapsed state becomes a ferromagnetic ground state, while the charge-density wave state becomes an Ising-like antiferromagnetic ground state. For $|V| < 2t$, the ground state has a uniform density and the excitations above the ground state are gapless. For incommensurate filling, no density-wave phase is obtained.

The Bethe-ansatz equations also allow the determination of the dispersion of excitations. In the half-filled case, for $|V| < 2t$, a continuum is obtained where the excitation energy $\hbar\omega$ obeys

$$\frac{\pi t}{2}\frac{\sqrt{1-(V/2t)^2}}{\arccos(V/2t)}|\sin(qa)| \le \hbar\omega \le \pi t\frac{\sqrt{1-(V/2t)^2}}{\arccos(V/2t)}|\sin(qa/2)|. \tag{75}$$

For small momentum, the upper and lower bounds of the continuum merge, yielding a linearly dispersion branch $\hbar\omega(q) = [\pi t\sqrt{1-(V/2t)^2}/\arccos(V/2t)]|qa|$. In the case of attractive interactions ($-2t < V < 0$) there are also bound states above the continuum with dispersion

$$\hbar\omega_n(q) = \pi t\frac{\sqrt{1-(V/2t)^2}}{\arccos(V/2t)}|\sin(qa/2)| \times\frac{\sqrt{1-\cos^2 y_n\cos^2 q/2}}{\sin y_n}, \tag{76}$$

where

$$y_n = \frac{n\pi}{2}\left[\frac{\pi}{\arccos(V/2t)} - 1\right], \tag{77}$$

and $y_n < \pi/2$. For $V > 2t$ and at half-filling, a density-wave state is formed. The transition between the liquid and the density wave was reviewed by Shankar (1990). The gap in the density-wave state is

$$E_G = -t\ln\left[2e^{-\lambda/2}\prod_1^\infty\left(\frac{1+e^{-4m\lambda}}{1+e^{-(4m-2)\lambda}}\right)^2\right], \tag{78}$$

where $\cosh\lambda = V/2t$. For $V \to 2t$, the gap behaves as $E_G \sim 4t\exp[-\pi^2/\sqrt{8(1-V/2t)}]$. The expectation value of the particle number on site n is $\langle\hat{b}_n^\dagger\hat{b}_n\rangle = [1+(-)^n P]$ where

$$P = \prod_1^\infty\left(\frac{1-e^{-2m\lambda}}{1+e^{-2m\lambda}}\right)^2. \tag{79}$$

The order parameter P of the density wave for $V - 2t \to 0^+$ vanishes as $P \sim (\pi\sqrt{2}/\sqrt{V/2t-1})\times\exp[-\pi^2/\sqrt{32(V/2t-1)}]$ and goes to 1 for $V \gg 2$.

Besides the t-V model, other integrable models of interacting lattice bosons have been constructed. These models are reviewed by Amico and Korepin (2004). They include correlated hopping and interactions beyond next nearest neighbor, finely tuned in order to produce integrability. In the continuum limit, they reduce to the Lieb-Liniger model.

D. Correlation functions of integrable models

Recent progress in the theory of integrable systems has found that the form factors (i.e., the matrix elements between two Bethe-ansatz eigenstates) of a given operator can be obtained by computing a determinant. These methods have been applied to the Lieb-Liniger and t-V models by Caux, *et al.* (2005, 2007), Caux and Maillet (2005), Caux and Calabrese (2006).

For the Lieb-Liniger model, Caux, and Calabrese (2006) and Caux, *et al.* (2007) computed the dynamic structure factor $S(q,\omega) = \int dxd\tau e^{i(\omega\tau-qx)}\langle\hat{\rho}(x,\tau)\hat{\rho}(0,0)\rangle$ and the single-particle Green's function $G^<(k,\omega) = \int dxd\tau e^{i(\omega\tau-kx)}\langle\hat{\Psi}^\dagger(x,\tau)\hat{\Psi}(0,0)\rangle$. For $S(q,\omega)$, the matrix elements of $\hat{\rho}(k) = \int dx e^{-iqx}\hat{\rho}(q)$ were calculated for up to $N = 150$ particles. It was checked that the f-sum rule, $\int d\omega\omega S(q,\omega) = 2\pi\rho_0 q^2$, was fulfilled to a few percent accuracy. Results for $S(q,\omega)$ are shown in Fig. 3. There, one can see that for $\gamma < 1$, most of spectral weight of $S(k,\omega)$ is found for $\hbar\omega$ in the vicinity of the dispersion of the type I excitation $\epsilon_I(k)$ (cf. discussion in Sec. III.B) so that $S(q,\omega) \simeq \frac{Nk^2}{L\epsilon_I(q)}\delta(\hbar\omega - \epsilon_I(q))$, i.e., Bogoliubov's theory provides a good approximation for the dynamic structure factor. For larger γ, the most spectral weight of $S(q,\omega)$ is found when $\epsilon_{II}(q) < \hbar\omega < \epsilon_I(q)$. Finally, at very large γ, the dynamical structure factor of the TG gas, with its characteristic particle-hole excitation spectrum becomes essentially identical to that of the free Fermi gas. For arbitrary γ, the exponents of the singularities of $S(q,\omega)$ for $\hbar\omega$ near $\epsilon_I(q)$ and $\epsilon_{II}(q)$ have been nonperturbatively computed by Imambekov and Glazman (2008). An interpolation formula for the structure factor encompassing these properties was proposed by Cherny and Brand (2009).

In the case of the one-particle correlation functions, Fig. 4, similar results were obtained. For small γ, the spectral weight of the single-particle correlation function peaks in the vicinity of the type I dispersion, in agreement with the Bogoliubov picture. For larger γ, the support of the spectral weight broadened, with the type II dispersion forming the lower threshold. For the t-V model, similar calculations have been carried out by J.-S. Caux, *et al.* (2005) and Caux and Maillet (2005).

In addition, local correlations of the form $g_n(\gamma,T) = \langle[\hat{\Psi}^\dagger(x)]^n[\hat{\Psi}(x)]^n\rangle$ have also been investigated for the Lieb-Liniger model by relying on its integrability. Indeed, $g_2(\gamma,T)$ follows, by virtue of the Hellman-Feynman theorem, from the free energy, which can be computed using the thermodynamic Bethe ansatz (Kheruntsyan *et al.*, 2005). For $n > 2$, one needs to resort to more sophisticated methods. Gangardt and Shlyapnikov (2003) obtained the asymptotic behavior of g_3 at large and small γ for $T = 0$. Later, Cheianov *et al.* (2006) computed g_3 for all γ at $T = 0$ by relating it to the ground-state expectation value of a conserved current of the Lieb-Liniger model. More recently, Kormos *et al.* (2009) and (2010) obtained general expressions for $g_n(\gamma,T)$ for arbitrary n, γ, and T by matching the scattering matrices of the Lieb-Liniger model and (the nonrelativistic limit of) the sinh-Gordon model, and then using the form factors of the latter field theory along with the thermodynamic Bethe-ansatz solution at finite T and chemical potential. In Sec. VIII, some of these results are reviewed in connection with the experiments.

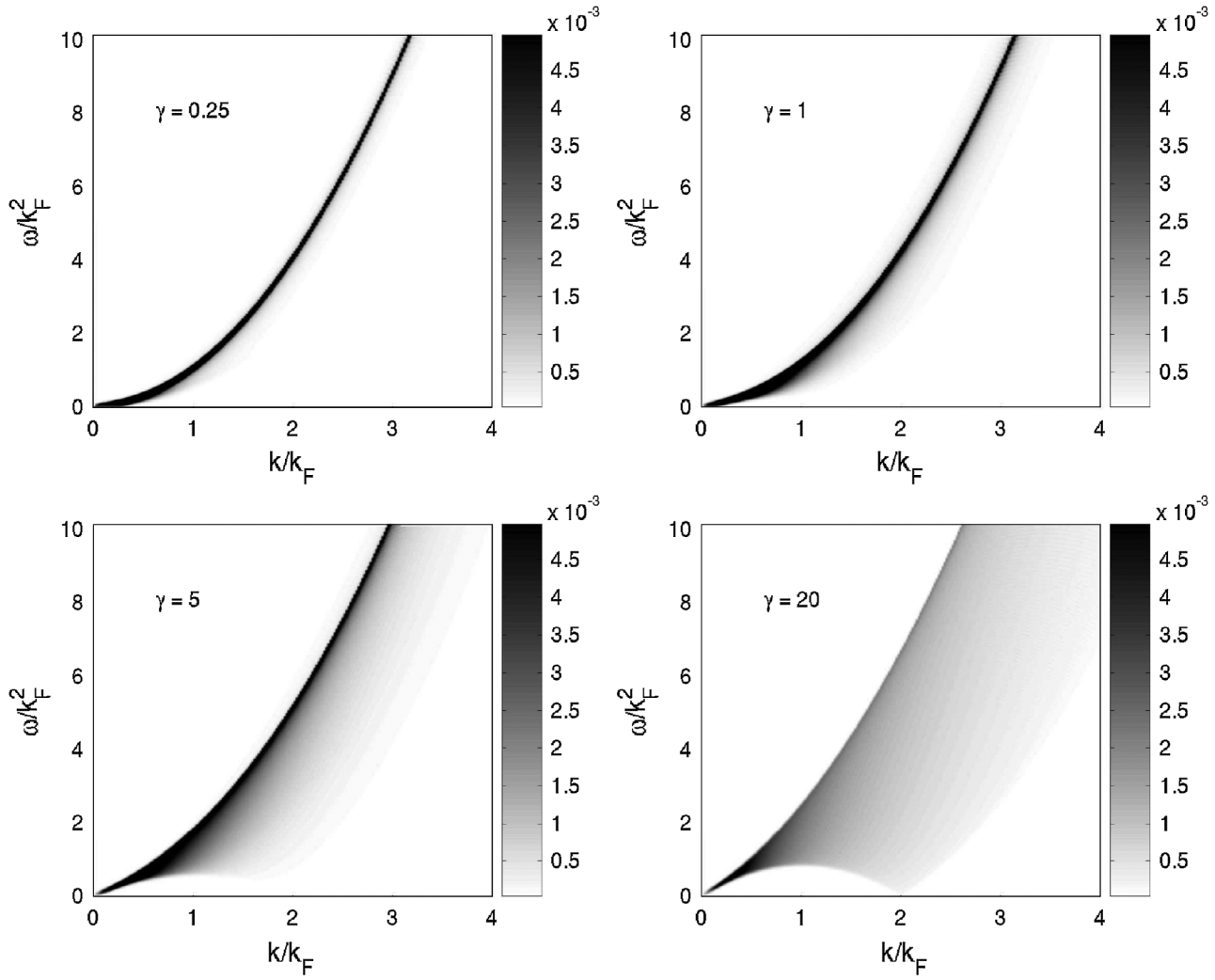

FIG. 3. Intensity plots of the dynamical structure factor $[S(q, \omega)]$. Data obtained from systems of length $L = 100$ at unit density, and $\gamma = 0.25$, 1, 5, and 20. From Caux, and Calabrese, 2006.

E. The Calogero-Sutherland model

We finish our tour of integrable models with the Calogero model introduced in Sec. II. This model has the advantage of leading to relatively simple expressions for its correlation functions. Moreover, the ground-state wave function of this model (11) in the presence of a harmonic confinement potential $\frac{1}{2}m\omega^2\sum_n x_n^2$ is exactly known (Sutherland, 1971a). It takes the form

$$\psi_B^0(x_1, \ldots, x_N) \propto e^{-(m\omega/2\hbar)\sum_{k=1}^{N} x_k^2} \prod_{j>i=1}^{N} |x_i - x_j|^{\lambda},$$

where λ is related to the dimensionless interaction parameter via $\lambda(\lambda - 1) = mg/\hbar^2$. For $\lambda = 1/2$, 1, 2, the probability density of the particle coordinates $|\psi_B(x_1, \ldots, x_N)|^2$ can be related to the joint probability density function of the eigenvalues of random matrices. More precisely, $\lambda = 1/2$ corresponds to the Gaussian orthogonal ensemble, $\lambda = 1$ to the Gaussian unitary ensemble (GUE), and $\lambda = 2$ to the Gaussian symplectic ensemble. Many results for the random matrices in the Gaussian ensembles are available (Mehta, 2004), and translate into exact results for the correlation functions of the Calogero-Sutherland models in the presence of a harmonic confinement. In particular, the one-particle density is known to be exactly ($R^2 = 2N\hbar\lambda/m\omega$)

$$\rho_0(x) = \frac{2N}{\pi R^2}\theta(R^2 - x^2)\sqrt{R^2 - x^2}. \tag{80}$$

In the homogeneous case with periodic boundary conditions, $\psi_B(x_1, \ldots, x_n + L, \ldots, x_N) = \psi_B(x_1, \ldots, x_n, \ldots, x_N)$, the Hamiltonian reads

$$\hat{H} = -\frac{\hbar^2}{2m}\sum_{i=1}^{N}\frac{\partial^2}{\partial x_i^2} + \sum_{i>j=1}^{N}\frac{g\pi^2}{L^2\sin^2[\frac{\pi(x_i - x_j)}{L}]}, \tag{81}$$

and the ground state is (Sutherland, 1971b)

$$\psi_B^0(x_1, \ldots, x_n) \propto \prod_{n<m}\sin\left|\frac{\pi(x_n - x_m)}{L}\right|^{\lambda}. \tag{82}$$

The energy per unit length $E/L = \pi^2\lambda^2\rho_0^3/3$ (Sutherland, 1971b). For $\lambda = 1$ (i.e., $g = 0$), Eq. (82) reduces to the TG gas wave function (29) thus illustrating that the Bijl-Jastrow product form is generic of the ground state of various 1D interacting models in the infinitely strong interaction limit.

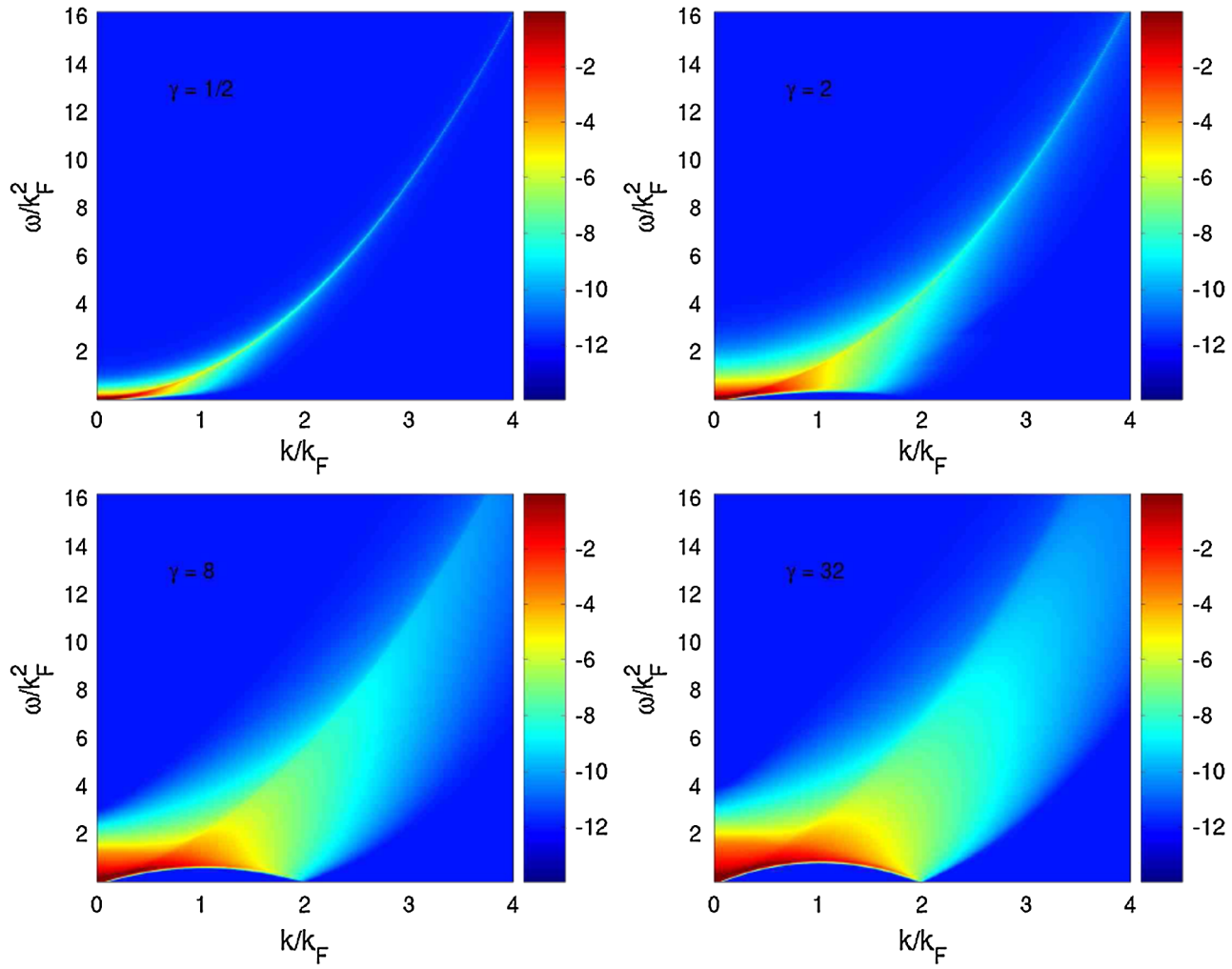

FIG. 4 (color online). Intensity plots of the logarithm of the dynamical one-particle correlation function of the Lieb-Liniger gas. Data obtained from systems of length $L = 150$ at unit density, and $\gamma = 0.5$, 2, 8, and 32. From J.-S. Caux, *et al.* (2007).

For $\lambda = 1/2$ and $\lambda = 2$, the results for the circular orthogonal ensemble and circular symplectic ensemble random matrices, respectively, can be used (Mehta, 2004). In particular, for $\lambda = 2$, the one-particle density matrix is $g_1(x) = \mathrm{Si}(2\pi\rho_0 x)/2\pi x$, where Si is the sine-integral function (Abramowitz and Stegun, 1972). Hence, the momentum distribution is $n(k) = \theta(4\pi^2\rho_0^2 - k^2)\ln(2\pi\rho_0/|k|)/4\pi$. These results show that long-range repulsive interactions (the case for $\lambda = 2$) further weaken the singularity at $k = 0$ in the momentum distribution with respect to hard-core repulsion. The above results can also be used to obtain the static structure factor $S(k) = \int dx\langle\hat{\rho}(x)\hat{\rho}(0)\rangle$ (Sutherland, 1971b; Mucciolo *et al.*, 1994):

$$S(k) = \frac{|k|}{\pi\rho_0}\left[1 - \frac{1}{2}\ln\left(1 + \frac{|k|}{\pi\rho_0}\right)\right] \quad (|k| < 2\pi\rho_0),$$
$$S(k) = 2 - \frac{|k|}{2\pi\rho_0}\ln\left|\frac{|k| + \pi\rho_0}{|k| - \pi\rho_0}\right| \quad (|k| > 2\pi\rho_0), \tag{83}$$

for $\lambda = 1/2$,

$$S(k) = \frac{|k|}{2\pi\rho_0} \quad (|k| < 2\pi\rho_0),$$
$$S(k) = 1 \quad (|k| > 2\pi\rho_0), \tag{84}$$

for $\lambda = 1$, and

$$S(k) = \frac{|k|}{4\pi\rho_0}\left[1 - \frac{1}{2}\ln\left(1 - \frac{|k|}{2\pi\rho_0}\right)\right] \quad (|k| < 2\pi\rho_0),$$
$$S(k) = 1 \quad (|k| > 2\pi\rho_0), \tag{85}$$

for $\lambda = 2$. The Fourier transform of the density-density response function was also obtained (Mucciolo *et al.*, 1994). It was shown that for $\lambda = 2$, the support of $S(q, \omega)$ touched the axis $\omega = 0$ for $q = 0, 2\pi\rho_0$, and $q = 4\pi\rho_0$. The general case of rational λ can be treated using Jack polynomial techniques (Ha, 1994; 1995). The dynamical structure factor $S(k, \omega)$ is nonvanishing only for $\omega_-(k) < \omega < \omega_+(k)$, where $\omega_\pm(k) = (\hbar\pi\lambda\rho_0/m)|k| \pm \hbar\lambda k^2/2m$ for $|k| < 2\pi\rho_0$ [$\omega_-(k)$ is a periodic function of $|k|$ with period $2\pi\rho_0$]. Near the edges (Pustilnik, 2006), $S(k, \omega \to \omega_-(k)) \propto [\omega - \omega_-(k)]^{1/\lambda - 1}$ and $S(k, \omega \to \omega_+(k)) \propto [\omega_+(k) - \omega]^{\lambda - 1}$. For $\lambda > 1$ (repulsive interactions), this implies a power-law divergence of the structure factor for $\omega \to \omega_-(k)$ and a structure factor vanishing as a power law for $\omega \to \omega_+(k)$. For $\lambda < 1$ (attraction), the behavior is reversed, with a power-law divergence only for $\omega \to \omega_+$ reminiscent of the results of Caux and Calabrese (2006) for the Lieb-Liniger model near the type I excitation. Using replica methods (Gangardt and

Kamenev, 2001), the long-distance behavior of the pair-correlation function is obtained as

$$D_2(x) = 1 - \frac{1}{2\pi^2\lambda(\rho_0 x)^2} + \sum_{m=1}^{\infty} \frac{2d_m(\lambda)^2 \cos(2\pi\rho_0 m x),}{(2\pi\rho_0|x|)^{2m^2/\lambda}}, \tag{86}$$

where

$$d_l(\lambda) = \frac{\prod_{a=1}^{l}\Gamma(1+a/\lambda)}{\prod_{a=1}^{l-1}\Gamma(1-a/\lambda)}. \tag{87}$$

For $\lambda = p/q$ rational, the coefficients d_l vanish for $l > p$. Equation (86) then reduces to the one derived (Ha, 1995) for rational λ. The replica method can be generalized to time-dependent correlations (Gangardt and Kamenev, 2001). For long distances, the one-body density matrix behaves as (Astrakharchik *et al.*, 2006)

$$g_1(x) = \rho_0 \frac{A^2(\lambda)}{(2\pi\rho_0|x|)^{\lambda/2}}\left[1 + \sum_{m=1}^{\infty}(-)^m \frac{D_m^2(\lambda)\cos(2\pi\rho_0 x)}{(2\pi\rho_0|x|)^{2m^2/\lambda}}\right], \tag{88}$$

where

$$A(\lambda) = \frac{\Gamma(1+\lambda)^{1/2}}{\Gamma(1+\lambda/2)} \times \exp\left[\int_0^{\infty}\frac{dt}{t}e^{-t}\left(\frac{\lambda}{4} - \frac{2[\cosh(t/2)-1]}{(1-e^{-t})(e^{t/\lambda}-1)}\right)\right],$$
$$D_m(\lambda) = \prod_{a=1}^{k}\frac{\Gamma(1/2+a/\lambda)}{\Gamma[1/2+(1-a)/\lambda]}. \tag{89}$$

The asymptotic form (88) is similar to the one derived for the TG gas, Eq. (33) differing only by the (nonuniversal) coefficients $D_m(\lambda)$.

IV. COMPUTATIONAL APPROACHES

The exactly solvable models discussed in the previous section allow one to obtain rather unique insights into the physics of 1D systems. However, exact solutions are restricted to integrable models, and it is difficult to ascertain how generic the physics of these models is. Besides, as we saw in the previous section, it is still extremely difficult to extract correlation functions. One thus needs to tackle the various models in Sec. II by generic methods that do not rely on integrability. One such approach is to focus on the low-energy properties as discussed in Sec. V. In order to go beyond low energies, one can use computational approaches. We thus present in this section various computational techniques that are used for 1D interacting quantum problems, and discuss some of the physical applications.

A. Bosons in the continuum

1. Methods

Several methods have been used to tackle boson systems in the continuum. We examine them before moving to the physical applications.

a. Variational Monte Carlo (VMC): Within this approach a variational trial wave function $\psi_T(\mathbf{R}, \alpha, \beta, \ldots)$ is introduced, where $\mathbf{R} \equiv (\mathbf{r}_1, \ldots, \mathbf{r}_N)$ are the particle coordinates, and $\alpha, \beta, \ldots$ are variational parameters. The form of ψ_T depends on the problem to be solved. One then minimizes the energy

$$E_{\mathrm{VMC}} = \frac{\int d\mathbf{r}_1 \ldots d\mathbf{r}_N \psi_T^*(\mathbf{R})\hat{H}\psi_T(\mathbf{R})}{\int d\mathbf{r}_1 \ldots d\mathbf{r}_N \psi_T^*(\mathbf{R})\psi_T(\mathbf{R})} \tag{90}$$

with respect to the variational parameters, using the Metropolis Monte Carlo method of integration (Umrigar, 1999). E_{VMC} is an upper bound to the exact ground-state energy. Unfortunately, the observables computed within this approach are always biased by the selection of ψ_T, so the method is only as good as the variational trial wave function itself.

b. Diffusion Monte Carlo: This is an exact method, within statistical errors, for computing ground-state properties of quantum systems (Kalos *et al.*, 1974; Ceperley and Kalos, 1979; Reynolds *et al.*, 1982). The starting point here is the many-body time-dependent Schrödinger equation written in imaginary time τ_E

$$[\hat{H}(\mathbf{R}) - \epsilon]\psi(\mathbf{R}, \tau_E) = -\hbar\frac{\partial\psi(\mathbf{R}, \tau_E)}{\partial\tau_E}, \tag{91}$$

where $\hat{H} = -\hbar^2/2m\sum_{i=1}^{N}\nabla_i^2 + \hat{V}_{\mathrm{int}}(\mathbf{R}) + \hat{V}_{\mathrm{ext}}(\mathbf{R})$. Upon expanding $\psi(\mathbf{R}, \tau_E)$ in terms of a complete set of eigenstates of the Hamiltonian $\psi(\mathbf{R}, \tau_E) = \sum_n c_n \exp[-(\epsilon_n - \epsilon)\tau_E/\hbar]\times\psi^n(\mathbf{R})$. Hence, for $\tau_E \to +\infty$, the steady-state solution of Eq. (91) for ϵ close to the ground-state energy is the ground state $\psi^0(\mathbf{R})$. The observables are then computed from averages over $\psi(\mathbf{R}, \tau_E \to +\infty)$.

The term diffusion Monte Carlo stems from the similarity of Eq. (91) and the diffusion equation. A direct simulation of (91) leads to large statistical fluctuations and a trial function $\psi_T(\mathbf{R})$ is required to guide the Metropolis walk, i.e., $\psi(\mathbf{R}, \tau_E) \to \psi(\mathbf{R}, \tau_E)\psi_T(\mathbf{R})$. $\psi_T(\mathbf{R})$ is usually obtained using variational Monte Carlo. $\psi_T(\mathbf{R})$ can introduce a bias into the calculation of observables that do not commute with $\hat{H}$, and corrective measures may need to be taken (Kalos *et al.*, 1974).

c. Fixed-node diffusion Monte Carlo: The diffusion Monte Carlo method above cannot be used to compute excited states because $\psi(\mathbf{R}, \tau_E)\psi_T(\mathbf{R})$ is not always positive and cannot be interpreted as a probability density. A solution to this problem is provided by the fixed-node diffusion Monte Carlo approach in which one enforces the positive definiteness of $\psi(\mathbf{R}, \tau_E)\psi_T(\mathbf{R})$ by imposing a nodal constraint so that $\psi(\mathbf{R}, \tau_E)$ and $\psi_T(\mathbf{R}, \tau_E)$ change sign together. The trial wave function $\psi_T(\mathbf{R})$ is used for that purpose and the constraint is fixed throughout the calculation. The calculation of $\psi(\mathbf{R}, \tau_E)$ then very much follows the approach used for the ground state. Here one just needs to keep in mind that the asymptotic value of $\psi_B(\mathbf{R}, \tau_E \to +\infty)$ is only an approximation to the exact excited state, and depends strongly on the parametrization of the nodal surface (Reynolds *et al.*, 1982).

2. The Lieb-Liniger gas

We next discuss the application of the above methods to the Lieb-Liniger model, Eq. (10). As mentioned in Sec II.B

(see also Sec. VIII for a brief description of the experimental methods), in order to realize such a system, a strong transverse confinement must be applied to an ultracold atomic gas. Olshanii (1998) pointed out that doing so modifies the interaction potential between the atoms, from the Lee-Huang-Yang pseudopotential (cf. Sec. II.A) that describes their interactions in the 3D gas in terms of the s-wave scattering length a_s, to a delta-function interaction described by the Lieb-Liniger model. The strength of the latter is given by the coupling g, which is related to a_s and the frequency of the transverse confinement $\omega_\perp$ by means of (Olshanii, 1998)

$$g = \frac{2\hbar^2 a_s}{m a_\perp^2} \frac{1}{1 - C a_s/a_\perp}, \tag{92}$$

where $a_\perp = \sqrt{\hbar/m\omega_\perp}$, $C = |\zeta(1/2)|/\sqrt{2} = 1.0326$, and $\zeta(\cdots)$ is the Riemann zeta function. The coupling g can also be expressed in terms of an effective 1D scattering length a_{1D}, $g = -2\hbar^2/m a_{1D}$, where $a_{1D} = -a_\perp(a_\perp/a_s - C)$. Hence, g increases as $\omega_\perp$ increases and the bosonic density profiles will start resembling those of noninteracting fermions as correlations between bosons are enhanced and the 1D Tonks-Girardeau regime is approached. These changes occur through a crossover that was studied theoretically, by means of diffusion Monte Carlo simulations (Astrakharchik and Giorgini, 2002; Blume, 2002).

In order to simulate the crossover from the 3D to 1D gas, two different models for the interatomic potential $\hat{V}_{\rm int} = \sum_{i<j} v(r_{ij})$ ($r_{ij} = |\mathbf{r}_i - \mathbf{r}_j|$) in the Hamiltonian ($\hat{H}$) of Eq. (91) were considered in the numerical studies: (i) a hard-core potential $v(r_{ij}) = \infty$ for $r_{ij} < a_s$ and $v(r_{ij}) = 0$ otherwise, where a_s corresponds to the 3D s-wave scattering length, a quantity that is experimentally measurable; and (ii) a soft-core potential $v(r_{ij}) = V_0$ for $r_{ij} < R$ and $v(r_{ij}) = 0$ otherwise, where R and a_s are related by $a_s = R[1 - \tanh(K_0 R)/K_0 R]$, with $K_0^2 = V_0 m/\hbar^2$ and $V_0 > 0$ [note that for $V_0 \to \infty$, the potential (ii) $\to$ (i)]. The external potential, whose shape drives the 3D to 1D crossover, was taken to be $V_{\rm ext}(\mathbf{r}) = m(\omega_\perp^2 \mathbf{r}_\perp^2 + \omega^2 x^2)/2$ to closely resemble actual experimental traps.

For the Monte Carlo sampling, $\Psi_T(\mathbf{R})$ was chosen to have a Bijl-Jastrow form (Bijl, 1940; Jastrow, 1955)

$$\Psi_T(\mathbf{R}) = \prod_{i=1}^{N} \varphi(\mathbf{r}_i) \prod_{j<k,j=1}^{N} f(r_{jk}), \tag{93}$$

which had been successfully used in a variational Monte Carlo study of the trapped bosonic gas in 3D (DuBois and Glyde, 2001). In Eq. (93), the single-particle orbital $\varphi(\mathbf{r})$ accounts for the effect of the external potential and was taken to be $\varphi(\mathbf{r}) = \exp(-\alpha_\perp r_\perp^2 - \alpha x^2)$, which is a harmonic-oscillator ground-state wave function with two variational parameters $\alpha_\perp$ and α. These parameters were optimized using variational Monte Carlo simulations. The two-particle function $f(r_{jk})$ was selected to be the exact solution of the Schrödinger equation for two particles interacting via corresponding two-body interatomic potential.

By changing the aspect ratio $\lambda = \omega/\omega_\perp$, the numerical simulations revealed the expected crossover between the mean-field Gross-Pitaevskii regime (Sec. II.A) and the strongly interacting Tonks-Girardeau limit (Sec. III.A.1), both for the ground-state energy and for the density profiles (Astrakharchik and Giorgini, 2002; Blume, 2002). For large anisotropies ($\lambda \ll 1$), a comparison of the full 3D simulation with the Lieb-Liniger theory (Sec. III.B) was also presented. The agreement between them was remarkable and validated the analytical expressions for a_{1D} and g in terms of a_s and $\omega_\perp$ (Astrakharchik and Giorgini, 2002).

The ground-state one-particle, and two-particle correlation functions of the Lieb-Liniger model, for which no closed analytic expressions are known, were calculated using the diffusion Monte Carlo method by Astrakharchik and Giorgini (2003 and 2006). For $x \to \infty$, the one-particle correlations were found to exhibit the power-law decay predicted by the Tomonaga-Luttinger liquid theory described in Sec. V, while two-particle correlations were seen to fermionize as the TG limit was approached. Local (Kheruntsyan *et al.*, 2003; 2005) and nonlocal (Sykes *et al.*, 2008; Deuar *et al.*, 2009) two-particle correlations, as well as density profiles, have been studied at finite temperatures by exact analytical methods and perturbation theory in some limits, and numerical calculations using the stochastic gauge method (Drummond *et al.*, 2004).

3. The super-Tonks-Girardeau gas

For negative values of g, the low-energy eigenstates of the Hamiltonian (10) are clusterlike bound states (McGuire, 1964) and their energy is not proportional to N (Lieb and Liniger, 1963). In order to access $g < 0$ starting from a 3D gas, Astrakharchik *et al.* (2004a; 2004b) considered a short-range two-body potential of the form $v(r_{ij}) = -V_0/\cosh^2(r_{ij}/r_0)$, where r_0 was fixed to be much smaller than $a_\perp$, and V_0 was varied. The inset in Fig. 5 shows how a_s changes with V_0 as a resonance is crossed. Following the effective theory of Olshanii (1998), g and a_{1D} vs a_s are depicted in Fig. 5. Figure 5 shows that there is a value of a_s, a_s^c, at which $a_{1D} = 0$ and $|g| \to \infty$. This is known as a confinement-induced resonance. The Lieb-Liniger regime ($g > 0$) is only accessible for $0 < a_s < a_s^c$, where $a_{1D} < 0$. On the other hand, $g < 0$ occurs for $a_s < 0$ and $a_s > a_s^c$, where $a_{1D} > 0$. It is also important to note that, at the 3D

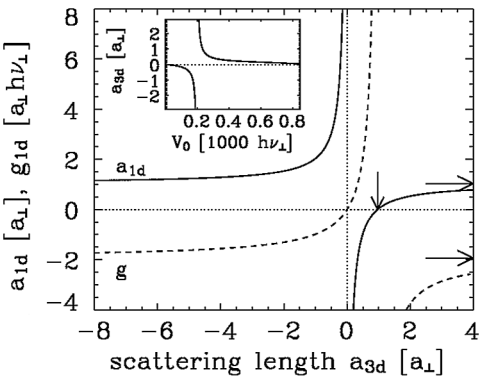

FIG. 5. g [dashed line, Eq. (92)] and a_{1D} (solid line) as a function of $a_{3d} = a_s$. The vertical arrow indicates the value of the s-wave scattering length a_s where g diverges, $a_s^c/a_\perp = 0.9684$. Horizontal arrows indicate the asymptotic values of g and a_{1D}, respectively, as $a_s \to \pm\infty$ ($g = -1.9368 a_\perp \hbar\omega_\perp$ and $a_{1D} = 1.0326 a_\perp$). Inset: a_s as a function of the well depth V_0. From Astrakharchik *et al.*, 2004b.

resonance $a_s \to \infty$, g, and a_{1D} reach an asymptotic value and become independent of the specific value of a_s.

Experimentally, for $g < 0$, one is in general interested in the lowest energy solution without bound states (a gaslike solution). This solution describes a highly excited state of the system. A computational study of this gaslike solution was done by Astrakharchik *et al.* (2004a, 2004b) using fixed-node diffusion Monte Carlo simulations for both 3D and effective 1D systems. In that study, the result of the exact diagonalization of two particles was used to construct the many-body nodal surface (expected to be a good approximation in the dilute limit). The many-body energy was then found to be remarkably similar for the highly anisotropic 3D case and the effective 1D theory using g from Eq. (92). A variational Monte Carlo analysis of the stability of such a solution suggested that it is stable if $\sqrt{N\lambda}a_{1D}/a_\perp \lesssim 0.78$, i.e., the stability can be improved by reducing the anisotropic parameter λ.

For small values of the gas parameter $\rho_0 a_{1D}$ ($0 < \rho_0 a_{1D} \lesssim 0.2$), the energy of the gaslike solution is well described by a gas of hard rods, i.e., particles interacting with the two-body potential $v(r_{ij}) = \infty$ for $r_{ij} < a_{1D}$ and $V(r_{ij}) = 0$ otherwise (Astrakharchik *et al.*, 2005; Girardeau and Astrakharchik, 2010). One- and two-particle correlation functions for $g < 0$ display unique behavior. They were computed both for the Hamiltonian (10) and for the hard-rod model, and were shown to behave similarly. The one-particle correlations decay faster than in the hard-core limit (Sec. III.A), for that reason, in this regime, the gas was called the "super-Tonks-Girardeau" gas. The structure factor (the Fourier transform of the two-particle correlation matrix) exhibits a peak at $\pi\rho_0$,[3] and, with increasing $\rho_0 a_{1D}$, the speed of sound was shown to increase beyond the TG result (Astrakharchik *et al.*, 2005; Mazzanti *et al.*, 2008). Analytically, it can be seen that for $g \to \infty$ Eq. (29) for the homogeneous gas and Eq. (39) for the trapped gas describes the ground state of the system. For negative values of g, those states can be obtained as highly excited states of the model with attractive interactions (Batchelor *et al.*, 2005a; Girardeau and Astrakharchik, 2010), which warrant their stability and suggest how to realize gaslike states when $g < 0$ in experiments (see discussion in Sec. VIII.D.3). As in the repulsive case, one possible method of detection may rely upon the measurement of the local correlations. Kormos *et al.* (2010) obtained the exact expression of the local correlators $g_n = \langle[\Psi^\dagger(0)]^n \times [\Psi(0)]\rangle$ of the super-Tonks gas at finite temperature and at any value of the coupling using the same method employed for Lieb-Liniger gas (Kormos *et al.*, 2009, 2011).

B. Bosons on a lattice

1. Methods

For lattice systems, in addition to the standard techniques valid in all dimensions, some specific and very powerful techniques are applicable in 1D.

[3]In the Tonks-Girardeau regime, for which the structure factor is identical to the one of noninteracting fermions, only a kink is observed at k_F.

a. Exact diagonalization and density-matrix renormalization group: A natural way to gain insight into the properties of a quantum system using a computer is by means of exact diagonalization. This approach is straightforward since one only needs to write the Hamiltonian for a finite system in a convenient basis and diagonalize it. Once the eigenvalues and eigenvectors are computed, any physical quantity can be calculated from them. A convenient basis to perform such diagonalizations for generic lattice Hamiltonians, which may lack translational symmetry, is the site basis $\{|\alpha\rangle\}$. The number of states in the site basis depends on the model, e.g., two states for hard-core bosons ($|0\rangle$ and $|1\rangle$) and infinite states for soft-core bosons.

Given the site basis, one can immediately generate the basis states for a finite lattice with N sites as

$$|m\rangle \equiv |\alpha\rangle_1 \otimes |\alpha\rangle_2 \otimes \cdots \otimes |\alpha\rangle_N, \tag{94}$$

from which the Hamiltonian matrix can be simply determined. Equation (94) reveals the main limitation of exact diagonalization, namely, the size of the basis (the Hilbert space) increases exponentially with the number of sites. If the site basis contains n states, then the matrix that one needs to diagonalize contains $n^N \times n^N$ elements.

Two general paths are usually followed to diagonalize those matrices: (i) full diagonalization using standard dense matrix diagonalization approaches (Press *et al.*, 1988), which allow one to compute all eigenvalues and eigenvectors required to study finite temperature properties and the exact time evolution of the system; and (ii) iterative diagonalization techniques such as the Lanczos algorithm (Cullum and Willoughby, 1985), which gives access the ground-state and low-energy excited states. The latter enable the study of larger system sizes, but they are still restricted to a few tens of lattice sites.

An alternative to such a brute force approach and an extremely accurate and efficient algorithm to study 1D lattice systems is the density-matrix renormalization group (DMRG) proposed by White (1992, 1993). This approach is similar in spirit to the numerical renormalization group (NRG) proposed by Wilson (1975) to study the single-impurity Kondo and Anderson problems. The NRG is an iterative nonperturbative approach that allows one to deal with the wide range of energy scales involved in those impurity problems by studying a sequence of finite systems with varying size, where degrees of freedom are integrated out by properly modifying the original Hamiltonian. However, it was early found by White and Noack (1992) that the NRG approach breaks down when solving lattice problems, even for the very simple noninteracting tight-binding chain, a finding that motivated the development of DMRG.

There are several reviews dedicated to the DMRG for studying equilibrium and nonequilibrium 1D systems (Hallberg, 2003; Manmana *et al.*, 2005; Noack and Manmana, 2005; Schollwöck, 2005; Chiara *et al.*, 2008), in which one can also find various justifications of the specific truncation procedure prescribed by DMRG. A basic understanding of it can be gained using the Schmidt decomposition. Suppose we are interested in studying the ground-state (or an excited-state) properties of a given Hamiltonian. Such a state $|\Psi\rangle$, with density matrix $\hat{\rho} = |\Psi\rangle\langle\Psi|$, can in principle be

divided into two parts M and N with reduced density matrices $\hat{\rho}_M = \mathrm{Tr}_N[\hat{\rho}]$ and $\hat{\rho}_N = \mathrm{Tr}_M[\hat{\rho}]$, where $\mathrm{Tr}_M[\cdot]$ and $\mathrm{Tr}_N[\cdot]$ mean tracing out the degrees of freedom of M and N, respectively. Remarkably, using the Schmidt decomposition (Schmidt, 1907) one can write $|\Psi\rangle$ in terms of the eigenstates and eigenvalues of the reduced density matrices of each part

$$|\Psi\rangle = \sum_\alpha \sqrt{w_\alpha}\,|m_\alpha\rangle|n_\alpha\rangle, \tag{95}$$

where $\hat{\rho}_M|m_\alpha\rangle = w_\alpha|m_\alpha\rangle$ and $\hat{\rho}_N|n_\alpha\rangle = w_\alpha|n_\alpha\rangle$, and the sum runs over the nonzero eigenvalues w_α, which can be proven to be identical for both parts. Hence, a convenient approximation to $|\Psi\rangle$ can be obtained by truncating the sum above to the first l eigenvalues, where l can be much smaller than the dimension of the smallest of the Hilbert spaces of M and N provided the w_α's decay sufficiently fast. This approximation was shown to be optimal to minimize the difference between the exact $|\Psi\rangle$ and the approximated one (White, 1993).

The DMRG is a numerical implementation of the above truncation. We stress that the DMRG is variational and that two variants are usually used: (i) the infinite-system DMRG, and (ii) the finite-system DMRG. We will explain them for the calculation of the ground state, but they can also be used to study excited states.

In the infinite-system DMRG, the idea is to start with the Hamiltonian $\mathbf{H}_L$ of a lattice with L sites, which can be diagonalized, and then (1) use an iterative approach to compute the ground state $|\Psi\rangle$ of $\mathbf{H}_L$ (Hamiltonian of the superblock), and its energy. (2) Compute the reduced density matrix of one half of the superblock (the "system" block). For definiteness, we assume that the system block is the left half of the superblock. (3) Use a dense matrix diagonalization approach to compute the eigenvectors with the l largest eigenvalues of the reduced density matrix from point 2. (4) Transform the Hamiltonian (and all other operators of interest) of the system block to the reduced density-matrix eigenbasis, i.e., $\mathbf{H}'_{L/2} = \mathbf{R}^\dagger \mathbf{H}_{L/2}\mathbf{R}$, where $\mathbf{R}$ is the rectangular matrix whose columns are the l eigenvectors of the reduced density matrix from point 3. (5) Construct a new system block from $\mathbf{H}'_{L/2}$ by adding a site to the right, $\mathbf{H}'_{L/2+1}$. Construct an "environment" block using the system block and an added site to its left, $\mathbf{H}''_{L/2+1}$. Connect $\mathbf{H}'_{L/2+1}$ and $\mathbf{H}''_{L/2+1}$ to form the Hamiltonian of the new superblock $\mathbf{H}_{L+2}$. (The same is done for all operators of interest.) Here we note that (i) we have assumed the original Hamiltonian is reflection symmetric, (ii) the superblock has open boundary conditions, and (iii) the superblock Hamiltonian (and any other superblock operator) will have dimension $2(l+n)$ (n is the number basis states for a site) at most, as opposed to the actual lattice Hamiltonian (or any other exact operator), which will have a dimension that scales exponentially with L. At this point, all steps starting from 1 are repeated with $L \to L+2$. When convergence for the energy (for the ground-state expectation value of all operators of interest) has been reached at point 1, the iterative process is stopped.

There are many problems for which the infinite-size algorithm exhibits poor convergence or no convergence at all. The finite-system DMRG provides the means for studying such systems. The basic idea within the latter approach is to reach convergence for the properties of interest in a finite-size chain. Results for the thermodynamic limit can then be obtained by extrapolation or using scaling theory in the vicinity of a phase transition. The finite-system DMRG utilizes the infinite-system DMRG in its first steps, namely, for building the finite-size chain with the desired length. Once the chain with the desired length has been constructed, one needs to perform sweeps across the chain by (i) increasing the system block size to the expense of the environment block size, up to a convenient minimum size for the latter, and then (ii) reversing the process by increasing the environment block size to the expense of the system block size, again up to a convenient minimum size for the latter. Those sweeps are repeated until convergence is reached. In general, this approach yields excellent results for the ground state and low-lying excited states properties. However, care should always be taken to check that the system is not trapped in some metastable state. Problems with incommensurate fillings and disordered potentials are particularly challenging in this respect. For the estimation of the errors as well as extensions of DMRG to deal with systems with periodic boundary conditions, higher dimensions, finite temperatures, and nonequilibrium dynamics, see the reviews previously mentioned.

b. Worldline quantum Monte Carlo: Quantum Monte Carlo (QMC) approaches provide a different way of dealing with many-body systems. They can be used to efficiently solve problems in one and higher dimensions. However, for fermionic and spin systems, QMC algorithms can be severely limited by the sign problem (Loh *et al.*, 1990; Troyer and Wiese, 2005).

One of the early QMC algorithms devised to deal with lattice problems is the discrete-time worldline algorithm, introduced by Hirsch *et al.* (1982). It is based in the path integral formulation of the partition function in imaginary time. The goal is to compute observables within the canonical ensemble $\langle\hat{O}\rangle = \mathrm{Tr}\{\hat{O}e^{-\beta\hat{H}}\}/Z$, where $Z = \mathrm{Tr}\{e^{-\beta\hat{H}}\}$ is the partition function. For example, for a 1D Hamiltonian that only couples nearest-neighbor sites, i.e., $\hat{H} = \sum_{i=1}^{L}\hat{H}_{i,i+1}$ and $[\hat{H}_{i,i+1}, \hat{H}_{j,j+1}] = 0$ if $j \geq i+2$, the Hamiltonian can then be split as the sum of two terms $\hat{H} = \hat{H}_{\mathrm{odd}} + \hat{H}_{\mathrm{even}}$, where $\hat{H}_{\mathrm{odd(even)}} = \sum_{i\,\mathrm{odd(even)}}\hat{H}_{i,i+1}$. Since $\hat{H}_{\mathrm{odd}}$ and $\hat{H}_{\mathrm{even}}$ do not commute, one can use the Trotter-Suzuki (TS) decomposition (Trotter, 1959; Suzuki, 1976) to write

$$e^{-\Delta\tau(\hat{H}_{\mathrm{odd}}+\hat{H}_{\mathrm{even}})} = e^{-\Delta\tau\hat{H}_{\mathrm{odd}}}e^{-\Delta\tau\hat{H}_{\mathrm{even}}} + O[(\Delta\tau)^2], \tag{96}$$

and Z is approximated by Z_{TS}:

$$\begin{aligned} Z_{\mathrm{TS}} &= \mathrm{Tr}\left\{\prod_{m=1}^{L} e^{-\Delta\tau\hat{H}_{\mathrm{odd}}}e^{-\Delta\tau\hat{H}_{\mathrm{even}}}\right\} \\ &= \sum_{m_1\cdots m_{2L}} \langle m_1|e^{-\Delta\tau\hat{H}_{\mathrm{odd}}}|m_{2L}\rangle\langle m_{2L}|e^{-\Delta\tau\hat{H}_{\mathrm{even}}}|m_{2L-1}\rangle\cdots \\ &\quad \times\langle m_3|e^{-\Delta\tau\hat{H}_{\mathrm{odd}}}|m_2\rangle\langle m_2|e^{-\Delta\tau\hat{H}_{\mathrm{even}}}|m_1\rangle, \end{aligned} \tag{97}$$

where $L\Delta\tau = \beta$, and $\{|m_\ell\rangle\}$ are complete sets of states introduced at each imaginary time slice. Since $\hat{H}_{\mathrm{odd}}$ and $\hat{H}_{\mathrm{even}}$ consist of a sum of mutually commuting pieces, the matrix elements in Eq. (97) can be reduced to products of the matrix elements of $e^{-\Delta\tau\hat{H}_{i,i+1}}$. A graphical representation of each term of the sum in Eq. (97) leads to a checkerboard

picture of space-time, where particles "move" along the so-called worldlines (the particle number must be the same at each τ, and periodic boundary conditions are applied to the imaginary time axis). The systematic error introduced by the Trotter-Suzuki decomposition can be proven to be $O((\Delta\tau)^2)$ for the partition function and also for Hermitian observables (Fye, 1986; Assaad, 2002).

The formulation above has been succeeded by a continuous time one with no discretization error (Prokof'ev *et al.*, 1996; Prokof'ev and Svistunov, 1998). The starting point for the latter is the operator identity

$$e^{-\beta\hat{H}} = e^{-\beta\hat{H}_{\rm d}} e^{-\int_0^\beta d\tau \hat{H}_{\rm od}(\tau)}, \tag{98}$$

where the Hamiltonian $\hat{H}$ has been split as the sum of its diagonal $\hat{H}_{\rm d}$, which now can contain a term $-\mu\hat{N}$ so that one can work in the grand-canonical ensemble, and off-diagonal $\hat{H}_{\rm od}$ terms in the site basis $\{|\alpha\rangle\}$ introduced with Eq. (94). In addition, $\hat{H}_{\rm od}(\tau) = e^{\tau\hat{H}_{\rm d}}\hat{H}_{\rm od}e^{-\tau\hat{H}_{\rm d}}$ and

$$e^{-\int_0^\beta d\tau \hat{H}_{\rm od}(\tau)} = 1 - \int_0^\beta d\tau \hat{H}_{\rm od}(\tau) + \cdots + (-1)^n \int_0^\beta d\tau_n \cdots \times \int_0^{\tau_2} d\tau_1 \hat{H}_{\rm od}(\tau_n)\cdots\hat{H}_{\rm od}(\tau_1) + \cdots \tag{99}$$

Once again, each term in the expansion of $e^{-\beta\hat{H}}$ has a graphical representation in terms of worldlines and the partition function $Z = \mathrm{Tr}\{e^{-\beta\hat{H}}\}$ can be written as a sum over all possible paths of these worldlines.

The Monte Carlo technique is then used to avoid the exponential sum over all the possible worldline configurations by sampling them in such a way that accurate results for physical quantities of interest are obtained in polynomial time. The challenge is then to develop efficient update schemes to perform such a sampling.

The updates within the discrete-time formulation are based on local deformations of the worldlines (Hirsch *et al.*, 1982). Observables that are diagonal in the occupation number (such as the density and the density-density correlations), as well as observables that conserve the number of particles in two contiguous sites (such as the kinetic energy and the current operator), can be easily computed while other observables that do not conserve the particle number locally, such as the one-particle density matrix $g_1(i,j) = \langle \hat{b}_i \hat{b}_j^\dagger \rangle$, are almost impossible to calculate (Scalettar, 1999). This local update scheme may lead to long autocorrelation times (Kawashima *et al.*, 1994) in a way similar to classical simulations with local updates. However, those times can be reduced by global moves in cluster (loop) algorithms, as proposed by Swendsen and Wang(1987) for the classical Ising model, and extended to quantum systems by Evertz *et al.* (1993), Kawashima *et al.* (1994), and Evertz (2003). In addition, other problems with this worldline formulation were removed by the loop algorithm, which works in the grand-canonical ensemble, and for which the time continuum limit $\Delta\tau \to 0$ in the Trotter-Suzuki decomposition was also implemented (Beard and Wiese, 1996).

Loop algorithms also have their limitations since they are difficult to construct for many Hamiltonians of interest and may suffer from "freezing" when there is a high probability of a single cluster occupying the entire system (Evertz *et al.*, 1993; Kawashima *et al.*, 1994; Evertz, 2003). These drawbacks can be overcome by the continuous-time worldline approach with worm updates, which works in an extended configuration space with open loops and for which all updates are local (Prokof'ev *et al.*, 1996; Prokof'ev and Svistunov, 1998; 2009) and by the stochastic series expansion (SSE) algorithm with nonlocal updates (Sandvik, 1992; 1999).

c. Stochastic series expansions: The SSE algorithm is based on the power series expansion of the partition function

$$Z = \mathrm{Tr}\{e^{-\beta\hat{H}}\} = \sum_m \sum_{n=0}^\infty \frac{(-\beta)^n}{n!}\langle m|\hat{H}^n|m\rangle, \tag{100}$$

where $\{|m\rangle\}$ is a convenient basis [such as the one in Eq. (94)]. It is useful to write the Hamiltonian as the sum of symmetric bond operators $\hat{H}_{a_i,b_i}$, where a_i denotes the operator type in the bond, $b_i \in \{1,\ldots L_b\}$ the bond index, and L_b the number of bonds. For example, if the basis in Eq. (94) is used, then the operator types in the bonds could be selected to be (i) diagonal, i.e., containing terms related to the density; and (ii) off-diagonal, i.e., containing the hopping related terms.

The partition function can then be written as

$$Z = \sum_m \sum_{n=0}^\infty \sum_{S_n} \frac{(-\beta)^n}{n!}\langle m|\prod_{i=1}^n \hat{H}_{a_i,b_i}|m\rangle, \tag{101}$$

where S_n is the set of all concatenations of n bond operators. The average expansion order can be shown to be $\langle n\rangle \sim L\beta$, and the width is proportional to $\sqrt{\langle n\rangle}$, so that one can truncate the sum over n at a finite cutoff $n_{\rm max}$ without introducing systematic errors ($n_{\rm max}$ can be adjusted during the warm up phase of the simulation) (Sandvik, 1999). By inserting $n_{\rm max} - n$ unit operators $\hat{H}_{0,0} = 1$ one can rewrite Z as

$$Z = \sum_m \sum_{S_{n_{\rm max}}} \frac{(-\beta)^n (n_{\rm max}-n)!}{n_{\rm max}!}\langle m|\prod_{i=1}^{n_{\rm max}} \hat{H}_{a_i,b_i}|m\rangle, \tag{102}$$

where now n is the number of nonunit operators in $S_{n_{\rm max}}$. This last expression simplifies the Monte Carlo sampling, which once again is used to avoid summing over an exponentially large number of terms. Various update schemes have been implemented within the SSE approach, such as the "operator loop updates" (Sandvik, 1999) and the "directed loops" (Syljuåsen and Sandvik, 2002; Alet *et al.*, 2005).

In general, the SSE as well as the continuous-time worldline formulation with worm updates have been found to be very efficient when dealing with both spin and boson systems. We note that within these two approaches (i) the superfluid density ρ_s is calculated through the fluctuations of the winding number W in the worldline configurations generated during the simulations $\rho_s = \langle W^2\rangle L/(2\beta t)$ (Pollock and Ceperley, 1987), where W is the net number of times that the worldlines wound around the periodic system; and (ii) the one-particle Green's function can also be efficiently computed (Dorneich and Troyer, 2001; Prokof'ev and Svistunov, 2009).

2. The Bose-Hubbard model and its phase diagram

We now analyze the Bose-Hubbard model (15). As discussed in Sec. VIII, this model is relevant in a wide variety of

contexts such as ^{4}He in various confined geometries (such as in porous media or between surfaces), granular superconductors, Josephson arrays, and ultracold gases in optical lattices. As with several other models on a lattice, and as discussed in Sec. VI.A, this model contains the necessary ingredients to describe a quantum phase transition between a superfluid and an insulator. This transition, which takes place only at integer fillings and is driven by quantum fluctuations rather than by thermal fluctuations, is the consequence of the competition between the delocalization effects of the kinetic term, proportional to t, which reduce the phase fluctuations, and the localization effects of the interaction term, proportional to U, which reduce the on-site particle-number fluctuations.

The phase diagram of this model is qualitatively similar in all spatial dimensions. In 1D, it can be calculated by bosonization techniques (Haldane,, 1981a), which will be introduced in Secs. V and VI.A. Its general properties in any dimension can be easily understood in terms of perturbative arguments starting from the atomic limit and scaling arguments (Fisher *et al.*, 1989). For $t = 0$, $\hat{n}_i$ commutes with the Hamiltonian and each site is occupied by an integer number of bosons n (we drop the site index because of the translational invariance). The site occupation can be computed minimizing the on-site energy $E = -\mu n + Un(n-1)/2$. One finds that for $n - 1 \leq \mu/U < n$ (where $n > 0$) the occupation per site is n and for $\mu < 0$ is zero. Now we analyze what happens if one takes $\mu/U = n - 1/2 + \delta$, where $-1/2 < \delta < 1/2$ so that the site occupation is n, and adds some small hopping t. If t is smaller than the smallest of the energies required to add a particle $E_p \sim (1/2 - \delta)U$ or a hole $E_h \sim (1/2 + \delta)U$, then one immediately realizes that n will not change. This is because the kinetic energy ($\sim t$) gained by the hopping of the added particle (hole) will be smaller that the interaction energy that is needed to be overcome to add it. Hence, there are finite regions in the plane μ/U-t/U in which n is fixed at their values in the atomic limit. Hopping in energetically unfavorable in those regions and the bosons remain localized, i.e., the system is insulating. This insulating state, known as a Mott insulator, is characterized by an energy gap (the energy required to add or remove a particle), which leads to a vanishing compressibility $\kappa = \partial n/\partial \mu = 0$. The lowest lying particle conserving excitations in the Mott insulator are particle-hole excitations.

By changing μ for any finite value of t within the Mott-insulating phase, one realizes at some point $\mu_+(U,t)$ [$\mu_-(U,t)$] the kinetic energy gained by the added particle (hole) balances the interaction energy required to add it. At that point, the added particle (hole) will be free to hop and a finite density of those particles (holes) will led to BEC (in dimensions higher than 1) and superfluidity. Following the perturbative arguments given before, one can also realize that the gap [$\Delta(U,t) = \mu_+(U,t) - \mu_-(U,t)$] in the Mott insulator should decrease as the hopping amplitude increases, and this leads to a phase diagram with a lobelike structure (see, e.g., Fig. 6).

As discussed in Sec. VI.A, two different universality classes exist for the Mott transition. (i) A transition that occurs by changing the chemical potential (density), which is driven by density fluctuations and belongs to the mean-field universality class. (This transition has $d_u = 2$ as the upper critical dimension.) (ii) A transition that occurs by changing t/U at fixed density, which is driven by phase fluctuations and belongs to the $(d+1)$-dimensional XY universality class. (This transition has $d_u = 3$ as the upper critical dimension and $d_l = 1$ as the lower critical dimension.)

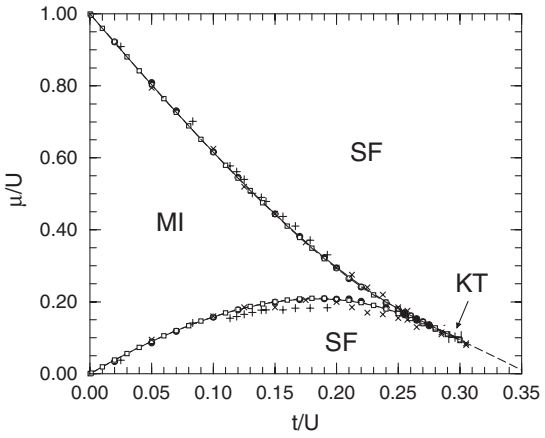

FIG. 6. Phase diagram for the 1D Bose-Hubbard model obtained by means of two different sets of quantum Monte Carlo results [+] (Batrouni *et al.*, 1990) and [×] (Kashurnikov *et al.*, 1996), a Padé analysis of 12th order strong-coupling expansions [solid line] (Elstner and Monien, 1999), earlier DMRG results [filled circles] (Kühner and Monien, 1998), and the DMRG results [empty boxes] from Kühner *et al.* (2000). The dashed lines indicate the area with integer density. The error bars in the μ/U direction are smaller than the circles, the error bar in the t/U direction is the error of $(t/U)_c$ for the BKT transition. The Mott-insulating phase is denoted by MI and the superfluid phase by SF. From Kühner *et al.*, 2000.

Several analytical and computational approaches have been used to study the phase diagram of the Bose-Hubbard model in one, two, three, and infinite dimensions. Among the most commonly used ones are mean-field theory, which is exact in infinite dimensions but qualitatively correct in dimensions higher than 1 (Fisher *et al.*, 1989; Rokhsar and Kotliar, 1991), quantum Monte Carlo simulations (Batrouni *et al.*, 1990; Batrouni and Scalettar, 1992; Capogrosso-Sansone *et al.*, 2007; 2008), strong-coupling expansions (Freericks and Monien, 1996; Elstner and Monien, 1999; Freericks *et al.*, 2009), and density-matrix renormalization group (Pai *et al.*, 1996; Kühner and Monien, 1998).

In what follows, we restrict our discussion to the 1D case. It is interesting to note that despite the close relation of the Bose-Hubbard model in 1D to the Lieb-Liniger model, the former is not Bethe-ansatz solvable (Haldane,, 1980; Choy and Haldane, 1982). The phase diagram for this model was first computed by Batrouni *et al.* (1990) by means of the worldline quantum Monte Carlo approach. In that work, the transition driven by changing the chemical potential was confirmed to have Gaussian exponents as proposed by Fisher *et al.* (1989).

Studying the transition at constant density turned out to be a more challenging task. This transition, as shown by Haldane (1981a) (see also Sec. VI.A and references therein), is in the same universality class as the two-dimensional Berezinskii-Kosterlitz-Thouless (BKT) transition. As a consequence, the gap vanishes as $\Delta \propto \exp[-\text{const}/\sqrt{(t/U)_{\text{crit}} - t/U}]$. This behavior makes the determination of $(t/U)_{\text{crit}}$ in 1D much more

difficult than in higher dimensions. Early attempts for $n = 1$ led to a wide range of values, such as $(t/U)_{\rm crit} = 0.215 \pm 0.01$ from worldline quantum Monte Carlo simulations (Batrouni *et al.*, 1990), $(t/U)_{\rm crit} = 1/(2\sqrt{3}) = 0.289$ from a Bethe-ansatz approximation (Krauth, 1991), $(t/U)_{\rm crit} = 0.304 \pm 0.002$ from a combination of exact diagonalization and renormalization-group theory (Kashurnikov and Svistunov, 1996), $(t/U)_{\rm crit} = 0.300 \pm 0.005$ from worldline QMC simulations (Kashurnikov *et al.*, 1996) and $(t/U)_{\rm crit} = 0.298$ from DMRG (Pai *et al.*, 1996) after fitting the gap to the exponential form given before, and $(t/U)_{\rm crit} = 0.265$ from a third order strong-coupling expansion after a constrained extrapolation method was used (Freericks and Monien, 1996).

A remarkable feature about the superfluid to Mott insulator transition that is unique to the phase diagram in 1D, and which was found in some of the previous studies, is that the Mott lobe exhibits a reentrant behavior with increasing t. Later studies using DMRG (Kühner and Monien, 1998; Kühner *et al.*, 2000), and higher order strong-coupling expansions combined with Padé approximants (Elstner and Monien, 1999), provided some of the most accurate results for the phase diagram. Those are depicted in Fig. 6 and compared with the results of quantum Monte Carlo simulations. The ratio $(t/U)_{\rm crit} = 0.297 \pm 0.010$ at the tip of the Mott lobe was determined using DMRG (Kühner *et al.*, 2000) by finding the value of t/U at which the Luttinger parameter $K = 2$ (see Sec. VI.A). Using directed loop Quantum Monte Carlo method, the spectral functions and the dynamical structure factor of the Bose-Hubbard model in the superfluid as well as in the Mott insulator phase have been obtained (Pippan *et al.*, 2009).

3. The Bose-Hubbard model in a trap

In relation to the experiments with ultracold bosons in optical lattices, a problem that has been extensively studied recently is that of the Bose-Hubbard model (BHM) in the presence of a confining potential. The Hamiltonian in this case is $\hat{H}_{\rm trap} = \hat{H}_{\rm BHM} + \sum_i V_i \hat{n}_i$, where V_i is usually taken to represent the nearly harmonic trap present in the experiments $V_i = V(i - L/2)^2$.

The effect of the trapping potential can be qualitatively, and in most instances quantitatively, understood in terms of the LDA. Within the LDA, one approximates local quantities in the inhomogeneous system by the corresponding quantities in a homogeneous (HOM) system with a local chemical potential equal to

$$\mu_{\rm HOM} = \mu_i \equiv \mu_0 - V(i - L/2)^2. \tag{103}$$

Hence, density profiles in the trap can be constructed from vertical cuts across the homogeneous phase diagram, which in 1D is depicted in Fig. 6, by starting at a point with $\mu = \mu_0$ and moving towards the point μ where the density vanishes. This leads to a wedding cake structure in which superfluid and Mott-insulating domains coexist space separated. Such a structure was originally predicted by means of mean-field theory by Jaksch *et al.* (1998) and, for 1D systems, obtained by means of worldline QMC simulations by Batrouni *et al.* (2002).

A consequence of the coexistence of superfluid and Mott-insulating domains is that the total compressibility in a trap never vanishes (Batrouni *et al.*, 2002). This has motivated the definition and use of various local quantities such as the local density fluctuations $\Delta_i = \langle n_i^2 \rangle - \langle n_i \rangle^2$ and local compressibility (Batrouni *et al.*, 2002; Wessel *et al.*, 2004; Rigol *et al.*, 2009)

$$\kappa_i^{[1]} = \frac{\partial n_i}{\partial \mu_i} = \frac{1}{\beta}\left[\left\langle\left(\int_0^\beta d\tau \hat{n}_i(\tau)\right)^2\right\rangle - \left\langle\int_0^\beta d\tau \hat{n}_i(\tau)\right\rangle^2\right] \tag{104}$$

and

$$\kappa_i^{[2]} = \frac{\partial N}{\partial \mu_i} = \int_0^\beta d\tau [\langle \hat{n}_i(\tau)\hat{N}\rangle - \langle \hat{n}_i(\tau)\rangle\langle \hat{N}\rangle], \tag{105}$$

to characterize trapped systems. We note that $\kappa_i^{[2]} \equiv \partial n_i/\partial\mu$, i.e., it can also be computed as the numerical derivative of experimentally measured density profiles. This quantity vanishes in the Mott-insulating domains and as such it can be taken as a local order parameter (Wessel *et al.*, 2004).

In Sec. III.A.2, we used a dimensional argument to introduce the characteristic density $\tilde{\rho} = Na/\zeta$ as the appropriate quantity to define the thermodynamic limit in a trapped system. Hence, for each value of U/t, this quantity uniquely determines the local phases that are present in the trap. A more rigorous derivation follows from the local density approximation (Batrouni *et al.*, 2008; Roscilde, 2010). Within the LDA $\langle n_i \rangle = n(\mu_i/t, U/t)$, where $n(\mu_i/t, U/t)$ is the density in a homogeneous system with a chemical potential μ_i as defined in Eq. (103), and μ_0 is determined by the normalization condition $N = \sum_i \langle n_i \rangle = \sum_i n(\mu_i/t, U/t)$. Approximating the sum by an integral, and taking into account the reflection symmetry of the trapped system, $N = 2\int_0^\infty dx n((\mu_0 - V(x/a)^2)/t, U/t)$. Finally, by making a change of variables $\mu_x = \mu_0 - V(x/a)^2$, one gets[4]

$$\tilde{\rho} \equiv Na\sqrt{V/t} = \int_{-\infty}^{\mu_0} d\mu_x \frac{n(\mu_x/t, U/t)}{\sqrt{t(\mu_0 - \mu_x)}}. \tag{106}$$

As discussed, within the LDA μ_0 uniquely determines the density profiles, and Eq. (106) shows that μ_0 is uniquely determined by $\tilde{\rho}$, so that indeed, $\tilde{\rho}$ uniquely determines the local phases in the trap. This fact has been recently used to construct state diagrams for trapped systems in 1D and 2D (Rigol *et al.*, 2009), which are useful in order to compare experimental and theoretical results in which different trap curvatures and system sizes are considered. Those state diagrams can be seen as the equivalent to phase diagrams for homogeneous systems.

A word of caution is needed when using the LDA. For example, for a homogeneous noninteracting bosonic gas in 2D there is no finite temperature transition to a BEC, from which, within the LDA, one could wrongly conclude that condensation cannot take place in the two-dimensional trapped case. This is incorrect because condensation does occur in the latter case (Dalfovo *et al.*, 1999). Equally, as the system is driven through the superfluid to Mott insulator transition in a homogeneous system in any dimension, or

[4]This result can be easily generalized to higher dimensions where $\tilde{\rho} \equiv Na(V/t)^{d/2}$ (Batrouni *et al.*, 2008).

any other second order transition for that matter, the system becomes critical and long-range correlation will preclude the local density approximation from being valid in the finite-size region where such a transition occurs in a trap. A finite-size scaling approach is required in those cases (Campostrini and Vicari, 2010a; 2010b). Finally, of particular relevance to the 1D case, the superfluid phase in 1D is already a critical phase with power-law decaying correlations, so that one needs to be particularly careful when using the LDA in 1D (Bergkvist *et al.*, 2004; Wessel *et al.*, 2004).

With that in mind, theoretical studies have addressed how correlations behave in the 1D trapped Bose-Hubbard model. Kollath *et al.* (2004) found that the same power-law decay of the one-particle correlations that is known from homogeneous systems can still be observed in the trap, in the regime of weak and intermediate interaction strength, after a proper rescaling $\tilde{g}_1(i,j) = \langle \hat{b}_i^\dagger \hat{b}_j \rangle / \sqrt{n_i n_j}$ is considered. In the infinite repulsive limit (Sec. III.A.2), on the other hand, Rigol and Muramatsu (2005c) concluded that a different rescaling is required, and $\tilde{g}_1(i,j) = \langle \hat{b}_i^\dagger \hat{b}_j \rangle / [n_i(1-n_i)n_j(1-n_j)]^{1/4}$ was proposed. The latter rescaling is consistent with the results in the continuum (equivalent to the low-density limit in the lattice) presented in Sec. III.A.1, where analytical expressions for the one-particle density matrix in the trap are available.

In the early experiments, the momentum distribution function $n(k)$ of the trapped gas (measured after time of flight) was one of the few probes available to extract information about those systems (see Sec. VIII). Hence, various numerical studies were devoted to identify how (i) the peak height and half width of $n(k)$ (Kollath *et al.*, 2004; Wessel *et al.*, 2004), (ii) the visibility $\mathcal{V} = [n^{\max}(k) - n^{\min}(k)]/[n^{\max}(k) + n^{\min}(k)]$ (Sengupta *et al.*, 2005), and (iii) other observables such as the total energy measured after time of flight (Rigol *et al.*, 2006), can be used to detect the formation of the Mott-insulating domains in 1D. More recently, local measurements have become available in trapped systems (Bakr *et al.*, 2009; 2010; Gemelke *et al.*, 2009) so that the local compressibility in Eq. (105) can be determined from the experiments and the local phases and transitions identified (Kato *et al.*, 2008; Zhou *et al.*, 2009). However, it has been argued (Pollet *et al.*, 2010) that $n(k)$ is nevertheless the best quantity to determine the parameters for the onset of critical correlations in the trap.

V. LOW-ENERGY UNIVERSAL DESCRIPTION

At low temperatures, the models discussed in the previous sections exhibit a liquid phase in which no continuous or discrete symmetry is broken. This phase has two salient features: (i) The low-energy excitations are collective modes with linear dispersion. (ii) At zero temperature, the correlation functions exhibit an algebraic decay characterized by exponents that depend on the model parameters. These two properties are intimately related to the MWH theorem, which rules broken continuous symmetry in 1D.[5] Haldane (1981b) noticed that these features are quite ubiquitous in 1D and thus defined a *universality class* of 1D systems that encompasses a large number of models of interacting bosons (both integrable and nonintegrable) in 1D (Gogolin *et al.*, 1999; Giamarchi, 2004). This universality class, known as TLLs, is a line of fixed points of the renormalization group (RG) characterized by a single parameter called the Tomonaga-Luttinger parameter.

A. Bosonization method

The collective nature of the low-energy excitations in 1D can be understood as follows: In the presence of interactions, a particle must push its neighbors away in order to propagate. Thus, when confinement forces particles to move on a line, any individual motion is quickly converted into a collective one. This collective character motivates a field-theoretic description in terms of collective fields, which is known as the "harmonic fluid approach" [also called "bosonization" (Mattis and Lieb, 1965; Luther and Peschel, 1974; Haldane, 1981a; 1981b; Giamarchi, 2004) for historical reasons]. For bosons, the collective fields are the density $\hat{\rho}(x,\tau)$ and the phase $\hat{\theta}(x,\tau)$ out of which the boson field operator $\hat{\Psi}^\dagger(x,\tau)$ is written in polar form

$$\hat{\Psi}^\dagger(x,\tau) = [\hat{\rho}(x,\tau)]^{1/2} e^{-i\hat{\theta}(x,\tau)}. \tag{107}$$

The above equation is the continuum version of Eq. (24). The quantum mechanical nature of harmonic fluid description requires that we also specify the commutation relations of the fields $\hat{\rho}(x,\tau)$ and $\hat{\theta}(x,\tau)$:

$$[\hat{\rho}(x), \hat{\theta}(x')] = i\delta(x-x'). \tag{108}$$

Equation (108) is consistent with $[\hat{\rho}(x), e^{-i\hat{\theta}(x')}] = \delta(x-x')e^{-i\hat{\theta}(x')}$, which is required by the canonical commutation relations of the field operator (Haldane, 1981a; Giamarchi, 2004). It expresses the well-known fact in the theory of superfluids that phase and density are canonically conjugated fields. Equation (107) can be derived from the commutation relation between the momentum current $\hat{j}_P(x) = \frac{1}{2}\sum_{j=1}^N [\hat{p}_j \delta(x-\hat{x}_j) + \delta(x-\hat{x}_j)\hat{p}_j]$ and the density operators

$$[\hat{\rho}(x), \hat{j}_P(x')] = i\hbar\hat{\rho}(x')\partial_{x'}\delta(x-x'), \tag{109}$$

which follows directly from $[\hat{x}_i, \hat{p}_j] = i\hbar\delta_{ij}$. Using Eqs. (112) and (113), and retaining only the slowly varying terms, this equation leads to $\hat{j}_P(x) = \hbar\sqrt{\hat{\rho}(x)}\partial_x\hat{\theta}\sqrt{\hat{\rho}(x)}$. Using Eq. (109), Eq. (108) is recovered.

In a translationally invariant system, the ground-state density is a constant, $\langle\hat{\rho}(x,\tau)\rangle = \rho_0 = N/L$. At small excitation energies, we expect that $\hat{\rho}(x,\tau)$ does not deviate much from ρ_0. In a simple-minded approach, these small deviations would be described by writing the density operator as

$$\hat{\rho}(x,\tau) \simeq \rho_0 - \frac{1}{\pi}\partial_x\hat{\phi}(x,\tau), \tag{110}$$

where $\hat{\phi}(x,\tau)$ is a slowly varying quantum field, which means that its Fourier components are predominantly around $q \simeq 0$. Such description is, however, insufficient, especially when the interactions are strong. For example, in the case of the TG

[5] Actually, the Calogero-Sutherland models (see Sec. III.E) escape one of the conditions of the theorem, which require the interactions to be short ranged. However, as the exact solution demonstrates, they also exhibit these properties.

gas (cf. Sec. III.A) the pair-correlation function, Eq. (30), is such that $D_2(x) - 1 = [1 - \cos(2\pi\rho_0 x)]/(2x^2)$. The first term in the right-hand side of this expression stems from the $q \approx 0$ density fluctuations and it can be recovered using the method of Popov (1972), Andersen *et al.* (2002), and Mora and Castin (2003), which is valid for weakly interacting bosons. However, the second oscillating term stems from density fluctuations of wave number $q_0 \approx 2\pi\rho_0$ and cannot be recovered from Eq. (110). The oscillating contribution reflects the discreteness of the constituent particles, which locally (but not globally) tend to develop a crystal-like ordering with a lattice spacing of order ρ_0^{-1}. Similar oscillating terms involving harmonics of $2\pi\rho_0$ also appear in other correlation functions of the TG gas such as the one-particle density matrix, cf. Eq. (33), as well as in the correlations of other models of interacting bosons in general. Efetov and Larkin (1975) argued that the density operator must contain, besides the $\partial_x\hat{\phi}$ term, a term proportional to $\cos 2\pi \int^x dx'\hat{\rho}(x') = \cos[2\pi\rho_0 x - 2\hat{\phi}(x)]$ in order to reproduce the oscillating contribution in $D_2(x)$.

A more complete derivation of the oscillating terms, which also automatically includes all higher harmonics of $2\pi\rho_0 x$, was given by Haldane (1981a), and is reviewed here. One enumerates the particles on the line by assigning them an index $j = 1, \ldots, N$, such that two consecutive values of j correspond to two neighboring particles. Next, a labeling field $\hat{\phi}_l(x, \tau)$ is introduced. This field is smooth on the scale of ρ_0^{-1} and such that $\hat{\phi}_l(x, \tau) = \pi j$ for $x = x_j(\tau)$, where $x_j(\tau)$ is the position of the jth particle. Hence,

$$\begin{aligned}\hat{\rho}(x, \tau) &= \sum_{j=1}^{N} \delta[x - \hat{x}_j(\tau)] \\ &\simeq \partial_x\hat{\phi}_l(x, \tau)\sum_j \delta[\hat{\phi}_l(x, \tau) - j\pi] \\ &= \frac{1}{\pi}\partial_x\hat{\phi}_l(x, \tau)\sum_{m=-\infty}^{+\infty} e^{2im\pi\hat{\phi}_l(x,\tau)}.\end{aligned} \tag{111}$$

The last expression follows from Poisson's summation formula. If we imagine that the particle positions $x_j(t)$ fluctuate about the 1D lattice defined by $x_j^0 = j\rho_0^{-1}$, it is possible to reintroduce $\hat{\phi}(x, \tau)$ as $\hat{\phi}_l(x, \tau) = \pi\rho_0 x - \hat{\phi}(x, \tau)$. In terms of $\hat{\phi}(x, \tau)$,

$$\hat{\rho}(x, \tau) \simeq \left(\rho_0 - \frac{1}{\pi}\partial_x\hat{\phi}(x, \tau)\right)\sum_{m=-\infty}^{+\infty} \alpha_m e^{2im[\pi\rho_0 x - \hat{\phi}(x,\tau)]}, \tag{112}$$

which reduces to Eq. (110) only when the $m = 0$ term of the series is retained.

The harmonic fluid approach also provides a representation for the boson field operator (Haldane, 1981a; Didier *et al.*, 2009) in terms of $\hat{\phi}(x, \tau)$ and $\hat{\theta}(x, \tau)$. From Eq. (107) it can be seen that this relies on finding a representation for the operator $[\hat{\rho}(x, \tau)]^{1/2}$. This can be achieved by noting that (by virtue of Fermi's trick) the square root of the sum of Dirac delta functions in Eq. (111) is also proportional to a sum of delta functions. Thus, $[\hat{\rho}(x, \tau)]^{1/2}$ in Eq. (107) lends itself to the same treatment as $\hat{\rho}(x, \tau)$, which leads to the following result (Haldane, 1981a; Cazalilla, 2004b; Giamarchi, 2004):

$$\begin{aligned}\hat{\Psi}^\dagger(x, \tau) \simeq &\left(\rho_0 - \frac{1}{\pi}\partial_x\hat{\phi}(x, \tau)\right)^{1/2} \\ &\times\left[\sum_{m=-\infty}^{+\infty} \beta_m e^{2im(\pi\rho_0 x - \hat{\phi}(x,\tau))}\right]e^{-i\hat{\theta}(x,\tau)}.\end{aligned} \tag{113}$$

Equations (112) and (113) must be understood as low-energy representations of the density and field operators as an infinite series of harmonics of $2[\pi\rho_0 x - \hat{\phi}(x)]$. They can be used, for instance, to compute the asymptotic behavior of correlation functions in 1D systems. However, it must also be emphasized that the coefficients α_m, β_m of each term in these series are not determined by the harmonic fluid approach and, in general, depend on the microscopic details of the model (i.e., they are *nonuniversal*). In some integrable models, such as the t-V model, it is possible to obtain these coefficients analytically (Lukyanov, 1998; 1999; Shashi *et al.*, 2010). In the case of the TG gas, they can be deduced from Eqs. (33) and (30). Similarly, for the Calogero-Sutherland models, Eqs. (89) and (87) can be used to derive the coefficients α_m and β_m. However, in the general case, one must resort to seminumerical (Caux and Calabrese, 2006) or fully numerical (Hikihara and Furusaki, 2004; Bouillot *et al.*, 2011) methods to compute them.

Finally, we provide a representation of the Hamiltonian and total momentum operators describing the (low-energy part of the) spectrum. For a system of bosons of mass m interacting via a two-body potential $V(x)$, such as (1) (with V_{ext}) one can substitute Eqs. (112) and (113) to obtain the following effective Hamiltonian:

$$\hat{H} = \frac{\hbar}{2\pi}\int dx\left[v K[\partial_x\hat{\theta}(x)]^2 + \frac{v}{K}[\partial_x\hat{\phi}(x)]^2\right] + \cdots \tag{114}$$

The ellipsis stands for an infinite series of *irrelevant* operators in the renormalization-group sense, which yield subleading corrections to the system properties. Similarly, applying the same identities, the momentum operator $[\hat{P} = \int dx\hat{j}_P(x)]$ becomes

$$\hat{P} = \frac{\hbar}{\pi}\int dx\left(\rho_0 - \frac{1}{\pi}\partial_x\hat{\phi}(x)\right)\partial_x\hat{\theta}(x) + \cdots \tag{115}$$

The Hamiltonian (114) and Eqs. (112) and (113) thus allow one to compute the low-energy behavior of all correlation functions of the initial problem. Since Eq. (114) is a simple quadratic Hamiltonian, with $[\hat{\theta}(x), \partial_{x'}\hat{\phi}(x')] = i\pi\delta(x - x')$, this is a remarkable simplification. The parameters $v_J = vK$ and $v_N = v/K$ in Eq. (114) are model dependent but can be related to the ground-state properties. All interaction effects are then encoded into the two effective parameters v and K. Moreover, it can be shown that the Hamiltonian (114) leads to ground-state wave functions of the Bijl-Jastrow form (Fradkin *et al.*, 1993; Cazalilla, 2004b). As we will see in Sec. V.B, K controls the behavior of correlation functions at long distance. As to v, one can immediately see that Eq. (114) leads to a linear dispersion $\omega = v|k|$ so that v is the velocity of propagation of density disturbances. The bosonization technique can reproduce the Bogoliubov spectrum simply by approximating the kinetic energy term as

$$\int dx \frac{\hbar^2}{2m}(\partial_x \hat{\Psi}^\dagger)(\partial_x \hat{\Psi}) \simeq \int dx \frac{\hbar^2}{2m}\left[\rho_0(\partial_x\hat{\theta})^2 + \left(\frac{\partial_x\hat{\rho}}{2\sqrt{\rho_0}}\right)^2\right], \tag{116}$$

leading to the Hamiltonian

$$\hat{H} \simeq \frac{\hbar}{2\pi}\int dx\left[\frac{\pi\hbar\rho_0}{m}[\partial_x\hat{\theta}(x)]^2 + \frac{g}{\pi\hbar}[\partial_x\hat{\phi}(x)]^2 + \frac{\hbar}{4m\pi\rho_0}[\partial_x^2\hat{\phi}(x)]^2\right] + \cdots \tag{117}$$

and yielding a spectrum $\epsilon(k) = \sqrt{g\rho_0(\hbar^2k^2/m) + (\hbar^2k^2/2m)^2}$, which is identical to the Bogoliubov spectrum discussed in Sec. II.A. Note, however, that here no condensate fraction assumption was made. We return to this point in Sec. V.E.

Since all of the low-energy properties only depend on v and K, it is enough to determine these two nonuniversal parameters to fully describe the system. There are very efficient ways to do such a calculation, based on either analytical or computational approaches. First, in a Galilean invariant system such as Eq. (10), the value of v_J (Haldane, 1981a) is independent of interaction as shown by the following argument. From Galilean invariance, the center of mass position $\hat{X} = (1/\hat{N})\int dx x\hat{\rho}(x)$ obeys the equation of motion

$$\frac{d\hat{X}}{dt} = \frac{1}{i\hbar}[\hat{X}, \hat{H}] = \frac{\hat{P}}{\hat{N}m}. \tag{118}$$

Using (112), $\hat{X} = -(1/\hat{N}\pi)\int dx x\partial_x\hat{\phi}(x) + \cdots$, along with Eq. (108)), in order to compute $[\hat{X}, \hat{H}]/i\hbar$, and comparing the result with $\hat{P}/\hat{N}m$, where $\hat{P}$ is given by Eq. (115), yields $v_J = \hbar\pi\rho_0/m$. Furthermore, this argument shows that Galilean invariance also requires the existence of an irrelevant operator [included in the ellipsis of Eq. (114)] of the form $-(\hbar^2/2\pi m)\int dx\partial_x\hat{\phi}(x)[\partial_x\hat{\theta}(x)]^2$, which describes the curvature of the quadratic free-particle dispersion. Various works (Pereira *et al.*, 2006; Khodas *et al.*, 2007) have emphasized that such irrelevant operators lead to a damping rate $\gamma_q \sim q^2/m$ for the collective excitations in 1D.

If Galilean invariance is absent, as in lattice models such as the Bose-Hubbard or the t-V models, then v_J can be renormalized by the interactions. Yet, v_J can be still related to the zero-temperature response of the system to an infinitesimal phase twist $\Delta\chi$ in the boundary conditions (Schulz, 1990; Shastry and Sutherland, 1990; Giamarchi, 1991; Maslov *et al.*, 1996; Prokof'ev and Svistunov, 2000; Cazalilla, 2004b; Giamarchi, 2004). Physically, this corresponds to the existence of a persistent current flowing through the system at zero temperature upon connecting it to two large phase-coherent reservoirs, whose phase differs by $\Delta\chi$. Thus, it is tempting to think that v_J is related to the superfluid fraction at zero temperature, $\rho_s(T=0) = \rho_s^0$ by means of the relation $v_J = \hbar\pi\rho_s^0/m$. However, this can be misleading. To clarify this point, we define

$$\rho_{\rm twist}(T, L) = \frac{\pi L}{\hbar}\frac{\partial^2 F(T, L, \Delta\chi)}{\partial\Delta\chi^2}\bigg|_{\Delta\chi=0}, \tag{119}$$

where $F(T, \Delta\chi)$ is the free energy of a system of length L computed assuming twisted boundary conditions, that is $\hat{\Psi}(L) = e^{i\Delta\chi}\hat{\Psi}(0)$. The superfluid fraction is a thermodynamic property obtained in the limit $\lim_{L\to+\infty}\rho_{\rm twist}(T, L) = \rho_s(T)$. However, it is important to stress that the limits $L \to +\infty$ and $T \to 0$ of $\rho_{\rm twist}(T, L)$ do not commute (Giamarchi and Shastry, 1995; Prokof'ev and Svistunov, 2000). For example, for the TG gas, whose thermodynamics is equivalent the 1D free Fermi gas thermodynamics, $\lim_{T\to0}\lim_{L\to+\infty}\rho_s(T) = \rho_s(T=0) = 0$ because the free Fermi gas is not superfluid. However, when the limits of the free Fermi gas $\rho_{\rm twist}(T, L)$ are taken in the reverse order, $\lim_{L\to+\infty}\lim_{T\to0}\rho_{\rm twist}(T, L) = \rho_0$. This corresponds to the result $v_J = v_F$, which follows from Galilean invariance. The product vK is thus related to Kohn's stiffness (Kohn, 1964) which is the weight of the $\delta(\omega)$ in the conductivity, and is related to the capability of the system to sustain persistent currents.

As to the other stiffness parameter, $v_N = v/K$, it can be related to the inverse of the macroscopic compressibility at $T = 0$ (Haldane, 1981a; Cazalilla, 2004b; Giamarchi, 2004), which is defined as

$$\kappa_s^{-1} = \rho_0^2 L\left[\frac{\partial^2 E_0(N)}{\partial N^2}\right], \tag{120}$$

where $E_0(N)$ is the ground-state energy with N particles. To relate κ_s^{-1} and v_N, first note that the operator $\delta\hat{N} = \hat{N} - N = -\int(dx/\pi)\partial_x\hat{\phi}(x)$, which means that, by shifting $\hat{\phi}(x) \to \hat{\phi}(x) - \pi x\delta\hat{N}/L$ in Eq. (114), and taking the expectation value over the ground state, it is possible to obtain $\partial^2E_0(N)/\partial N^2$ as the coefficient of the $O(\delta N_0^2)$ term. Hence, $\kappa_s^{-1} = \hbar\pi v_N\rho_0^2 = \hbar\pi\rho_0^2 v/K$. For Galilean invariant systems, this relationship can be written as $\kappa_s = mK^2/\hbar^2\pi^2\rho_0^3$, which means that as K increases, the system becomes more and more compressible. In particular, for a noninteracting boson system $\kappa_s = +\infty$, as the energy cost of adding new particles in the ground state vanishes and therefore $K = +\infty$. Repulsive interactions reduce the value of K. For instance, in the Lieb-Liniger and Bose-Hubbard models $K \geq 1$ (cf. Fig. 8), and $K = 1$ for TG gas, which stems from its equivalence to a free Fermi gas. In 1D boson systems with longer range interactions [such as dipolar interactions (Arkhipov *et al.*, 2005; Citro *et al.*, 2008)] and the t-V model, a regime where $K < 1$ is also possible.

B. Correlation functions: Temperature, boundaries, and finite-size effects

Realization of 1D ultracold atomic systems (see Sec. VIII), where the number of bosons confined to 1D typically ranges from a few tens to a few hundred, has renewed the interest in understanding finite-size systems (Cazalilla, 2004b; Batchelor *et al.*, 2005c). In a finite-size system, the low-energy excitation spectrum as well as the asymptotic behavior of correlation functions depend on the boundary conditions (BCs) obeyed by the field operator. These can be either periodic (PBCs) or open (OBCs). In physical realizations, PBCs are more convenient to describe systems near the thermodynamic limit, as they include translational invariance from the start, whereas OBCs are more realistic for finite or semi-infinite systems. Moreover, numerical methods such as the DMRG described in Sec. IV.B.1 work better with OBCs

than with PBCs. The effects of temperature can also be treated in the framework of finite-size effects. Indeed, in the Matsubara formalism, a finite temperature $\beta = 1/k_B T$ corresponds to PBCs on the imaginary time of size $\hbar\beta$. The harmonic fluid approach introduced in the previous section can be extended to deal with both finite-size and boundary effects. The conformal invariance of the theory (114) greatly simplifies that extension (Giamarchi, 2004) by enabling the use of conformal transformations (Cardy, 1996) to compute the finite-size effects. Finite-size, boundary, and finite temperature correlations can be also obtained by relying on this method (Eggert *et al.*, 2002).

1. Infinite systems and periodic boundary conditions

Since the effects of temperature are already discussed elsewhere (Giamarchi, 2004), we focus here on the spatial boundary conditions. We begin our discussion with the case where the field operator obeys twisted periodic BCs, that is, $\hat{\Psi}^\dagger(x+L) = e^{-i\Delta\chi}\hat{\Psi}^\dagger(x)$. Without the twist ($\Delta\chi = 0$), these are simply the usual periodic boundary conditions used to describe many thermodynamic systems. One physical realization of such PBCs, corresponds to loading an ultracold Bose gas in a tight toroidal trap, which can be created by, e.g., combining a Gaussian laser beam with a magnetic harmonic trap (Ryu *et al.*, 2007).

In order to determine the appropriate boundary conditions for the fields $\hat{\phi}(x)$ and $\hat{\theta}(x)$, we note that Eq. (113) implies that the boson field operator obeys (twisted) periodic BCs provided

$$\hat{\phi}(x+L) = \hat{\phi}(x) - \pi(\hat{N} - N), \tag{121}$$

$$\hat{\theta}(x+L) = \hat{\theta}(x) + \pi\left(\hat{J} + \frac{\Delta\chi}{\pi}\right), \tag{122}$$

where the operator $\hat{N}$ has integer eigenvalues whereas the eigenvalues of $\hat{J}$ obey the selection rule $(-1)^{\hat{J}} = 1$ (Haldane, 1981a). The conditions (121) and (122) must be taken into account when expanding $\hat{\theta}(x)$ and $\hat{\phi}(x)$ in Fourier series, which for the present system read

$$\begin{aligned}\hat{\phi}(x) &= \hat{\phi}_0 - \delta\hat{N}\frac{x\pi}{L} - \frac{i}{2}\sum_{q\neq 0}\left(\frac{2\pi K}{L|q|}\right)^{1/2}\mathrm{sgn}(q)e^{-iqx}[\hat{a}_q^\dagger + \hat{a}_{-q}],\\ \hat{\theta}(x) &= \hat{\theta}_0 + \hat{J}\frac{x\pi}{L} + \frac{i}{2}\sum_{q\neq 0}\left(\frac{2\pi}{L|q|K}\right)^{1/2}e^{-iqx}[\hat{a}_q^\dagger - \hat{a}_{-q}],\end{aligned} \tag{123}$$

where $q = 2\pi m/L$ (m being an integer), $[\hat{a}_q, \hat{a}_{q'}^\dagger] = \delta_{q,q'}$, commuting otherwise, $[\hat{N}, e^{-i\hat{\theta}_0}] = e^{-i\hat{\theta}_0}$ and $[\hat{J}, e^{-i\hat{\phi}_0}] = e^{-i\hat{\phi}_0}$. The operator $\hat{\phi}_0$ is related to the center of mass position of the liquid [and therefore $\pi^{-1}d\hat{\phi}_0/dt$ is the mean current operator (Haldane,, 1981a)], while $\hat{\theta}_0$ is related to the global phase.

Introducing these expressions into Eqs. (114) and (115) leads to

$$\hat{H} = \sum_{q\neq 0}\hbar v|q|\hat{a}_q^\dagger\hat{a}_q + \frac{\hbar\pi}{2LK}(\hat{N}-N)^2 + \frac{\hbar\pi vK}{2L}\left(\hat{J} + \frac{\Delta\chi}{\pi}\right)^2, \tag{124}$$

$$\hat{P} = \frac{\hbar\pi\hat{N}\hat{J}}{L} + \sum_{q\neq 0}\hbar q\hat{a}_q^\dagger\hat{a}_q. \tag{125}$$

Thus, the elementary excitations of the system are running waves carrying momentum $\hbar q$ and energy $\hbar v|q|$ (v is the sound velocity). The system can also sustain persistent currents, quantized in values proportional to the eigenvalues of $\hat{J}$, which for bosons must be *even* integers.

Furthermore, from Eqs. (121) and (122) the asymptotic behavior of correlation functions obeying PBCs can be obtained. For the one-particle density matrix and the pair-correlation function, it was obtained by Haldane (1981a)

$$\begin{aligned}g_1(x) &= \langle\hat{\Psi}^\dagger(x)\hat{\Psi}(0)\rangle\\ &= \rho_0\left[\frac{1}{\rho_0 d(x|L)}\right]^{1/2K}\left\{A_0 + \sum_{m=1}^{+\infty}A_m\left[\frac{1}{\rho_0 d(x|L)}\right]^{2m^2K}\right.\\ &\quad\left.\times\cos(2\pi m\rho_0 x)\right\},\end{aligned} \tag{126}$$

$$\begin{aligned}D_2(x) &= \rho_0^{-2}\langle\hat{\rho}(x)\hat{\rho}(0)\rangle\\ &= \left\{1 - \frac{K}{2\pi^2}\left[\frac{1}{\rho_0 d(x|L)}\right]^2 + \sum_{m>0}B_m\left[\frac{1}{\rho_0 d(x|L)}\right]^{2m^2K}\right.\\ &\quad\left.\times\cos(2\pi m\rho_0 x)\right\}.\end{aligned} \tag{127}$$

A more detailed treatment of the operator $(\rho_0 - \partial_x\hat{\phi}/\pi)^{1/2}$ in Eq. (113), showing how to obtain also the subleading corrections to Eq. (126), was presented by Didier *et al.* (2009). As mentioned, the coefficients $A_m = |\alpha_m|^2$ and $B_m = |\beta_m|^2$ are nonuniversal; $d(x|L) = L|\sin(\pi x/L)|/\pi$ is the *chord* function.

We first examine these expressions for an infinite system. In the thermodynamic limit ($L \to \infty$) $d(x|L) \to |x|$, and thus we retrieve the well-known power-law correlations controlled by the single parameter K. Furthermore, conformal invariance of the theory ensures that a similar power-law occurs in Matsubara time. We thus see that the system is in a critical state, exhibiting quasi-long-range order both in the phase and in the density correlations. Whereas, the latter measures the tendency of the system to form a charge-density wave of bosons, the former measures the tendency towards BEC. Thus, although there is no long-range order in 1D, one can still define a ''phase diagram'' depending on the dominant correlations (i.e., ''fluctuating'' type of orders) in the system, i.e., the one showing the slowest decay. Indeed, such fluctuating order is realized as true long-range order whenever identical 1D systems are coupled, as discussed in Sec. VII.B. Such a phase diagram is shown in Fig. 7.

Upon comparison with, e.g., Eqs. (33) and (30), it can be seen that the above series contains only the leading (i.e., the slowest decaying) term for each harmonic. The remaining subleading corrections stem from less relevant operators, which have been neglected in the derivation of Eqs. (126) and (127).

2. Open boundary conditions

In the case of a system of bosons trapped in a box with sufficiently high walls, OBCs of Dirichlet type must be used,

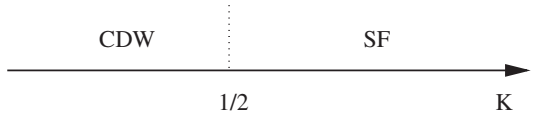

FIG. 7. "Phase diagram" indicating the slowest decaying fluctuation for 1D interacting bosons. The correlations are totally controlled by the Tomonaga-Luttinger liquid parameter K. For $K > 1/2$ the dominant order is superfluid (SF), while for $K < 1/2$ the system exhibits dominant charge-density wave (CDW) fluctuations. Note that for a model with purely local interactions, one has $1 < K < \infty$ so the system is always dominated by superfluid order. Nearest-neighbor repulsion on a lattice can allow one to reach the point $K = 1/2$.

i.e., the field operator must obey $\hat{\Psi}(x) = 0$ and hence $\hat{\rho}(x) = 0$ for $x = 0, L$. Thus, Eq. (111) implies that, for $x = 0, L$, the labeling field $\hat{\phi}_l(x) \neq \pi j$, where j is an integer. This is the minimum requirement to ensure that no particle exists at $x = 0, L$. Hence, $\hat{\phi}(x) = \pi\rho_0 x - \hat{\phi}_l(x) = \phi_0 \neq \pi j$ at $x = 0$. If the number of particles (that is the eigenvalue of $\hat{N}$) is fixed (as corresponds to a system of trapped ultracold atoms), then it follows from $\delta\hat{N} = \hat{N} - N = -\int_0^L (dx/\pi)\partial_x\hat{\phi}(x) = \hat{\phi}(0) - \hat{\phi}(L)$ that $\hat{\phi}(x = L) = \hat{\phi}(0) - \pi\hat{N}$.

When expanded in a Fourier series of modes that obey the open BC's,

$$\hat{\phi}(x) = \hat{\phi}_0 - \delta\hat{N}\frac{\pi x}{L} - \sum_{q>0}\left(\frac{\pi K}{qL}\right)^{1/2}\sin(qx)[\hat{a}_q^\dagger + \hat{a}_q],$$
$$\hat{\theta}(x) = \hat{\theta}_0 - i\sum_{q>0}\left(\frac{\pi K}{qL}\right)^{1/2}\cos(qx)[\hat{a}_q^\dagger - \hat{a}_q], \tag{128}$$

where $[\delta\hat{N}, e^{-i\hat{\theta}_0}] = e^{-i\hat{\theta}_0}$, but $\hat{\phi}_0$ is a real (noninteger) number, i.e., it is not an operator. The Hamiltonian operator becomes

$$\hat{H} = \sum_{q>0}\hbar v q\hat{a}_q^\dagger\hat{a}_q + \frac{\hbar\pi v}{2LK}(\hat{N} - N)^2. \tag{129}$$

Thus, the low-energy elementary excitations are standing waves characterized by a wave number $q > 0$ and an energy $\hbar v q$. However, the total momentum operator $\hat{P}$ vanishes identically as the center of mass position of the system is fixed (e.g., $\langle\hat{X}\rangle \propto \phi_0 = \text{const}$) by the confinement. This means that the operator $\hat{J}$ undergoes large fluctuations and therefore its canonical conjugate operator ϕ_0 acquires a constant expectation value.

The existence of boundaries leads to a dramatic change in the nature of the correlations as translational invariance is lost. Thus, for example, to leading order

$$\rho_0(x) = \rho_0 + C_1\left[\frac{1}{\rho_0 d(2x|2L)}\right]^K\cos(2\pi\rho_0 x + \delta_1), \tag{130}$$

$$g_1(x, y) = \rho_0 B_0\left[\frac{\rho_0^{-1}\sqrt{d(2x|2L)d(2y|2L)}}{d(x + y|2L)d(x - y|2L)}\right]^{1/2K}, \tag{131}$$

where C_1, δ_1, and B_0 are nonuniversal coefficients. For the full asymptotic series in harmonics of $2\pi\rho_0$ of these and other correlation functions, see the literature for zero temperature (Cazalilla, 2002; Cazalilla, 2004b) and positive temperature (Eggert *et al.*, 2002) cases. Thus, because the system has boundaries, the ground-state density $\rho_0(x) = \langle\hat{\rho}(x)\rangle$ is no longer uniform, and two-point correlation functions such as $g_1(x, y) = \langle\hat{\Psi}^\dagger(x)\hat{\Psi}(y)\rangle$ depend on both x and y (Eggert and Affleck, 1992; Hikihara and Furusaki, 2001; Cazalilla, 2002; 2004b; Giamarchi, 2004). It is also important to note that the boundaries do modify the asymptotic behavior of the correlation functions. This can be seen in the previous expressions if we consider, for instance, the behavior of $g_1(x, y)$. Away from the boundaries, in the bulk of the system, the leading behavior is the same as for PBCs, that is $|x|^{-1/2K}$. However, for $y \approx 0$ and $\rho_0^{-1} \ll x \ll L$, the decay of the asymptotic behavior is, $|x|^{-3/4K}$ controlled by the (*boundary*) exponent $3/4K$. The same remarks apply to the behavior of other correlation functions near the boundaries at $x = 0, L$.

Another type of OBCs (Neumann) corresponds to $\hat{\Psi}^\dagger(x = 0) = \Psi_0^*$ and $\hat{\Psi}^\dagger(x = L) = \Psi_L^*$, where $\Psi_{0,L} = |\Psi_{0,L}|e^{-i\chi_{0,L}} \neq 0$ (Maslov *et al.*, 1996). This amounts to enforcing that $\hat{\theta}(x = 0, L) = \chi_{0,L}$. In this case, the results obtained for open BCs of Dirichlet type can used upon interchanging the roles of θ and ϕ and making the replacement $K \to K^{-1}$.

The form of the effective Hamiltonian, however, is different,

$$\hat{H} = \sum_{q>0}\hbar v q\hat{a}_q^\dagger\hat{a}_q + \frac{\hbar\pi v K}{2L}\left(\hat{J} + \frac{\Delta\chi}{\pi}\right)^2, \tag{132}$$

where $\Delta\chi = \chi_L - \chi_0$ the phase difference across the system. Note that, in this case, the global phase $\langle\hat{\theta}_0\rangle = \Delta\chi$ is well defined, which means that the canonically conjugate operator, $\hat{N}$, undergoes large fluctuations about the ground-state value $N = \langle\hat{N}\rangle$ that fixes the zero-temperature chemical potential.

3. The t-V, Lieb-Liniger, and Bose-Hubbard models as Tomonaga-Luttinger liquids

Let us now establish a relation between some of the microscopic models that were examined in Sec. II and the TLL liquids. We examine, in particular, the t-V, Lieb-Liniger, and Bose-Hubbard models. Indeed these three models display TLL behavior at low energies, as can be seen from the exact results in Sec. III or the numerical ones in Sec. IV.B.1.

The phase diagram of the Lieb-Liniger model is the simplest, being described by the TLL fixed point for *all* values of the single dimensionless parameter that characterizes the model, namely $\gamma = mg/\hbar^2\rho_0$. The existence of the Bethe-ansatz solution allows us to compute the ground-state energy as described in Sec. III.B. From that result, the compressibility and hence the Tomonaga-Luttinger parameter, $K = K(\gamma)$ are obtained. The sound velocity then follows from the Galilean invariance of the model (Haldane, 1981a): $v(\gamma) = \hbar\pi\rho_0/[mK(\gamma)]$. These two functions are plotted in Fig. 8. In general, analytical expressions are not available for arbitrary values of γ. However, in the limit large and small γ, the following asymptotic formulas are known (Büchler *et al.*, 2003; Cazalilla, 2004b):

$$K(\gamma) = \begin{cases} 1 + \frac{4}{\gamma^2} + O(\gamma^{-3}) & \text{for } \gamma \gg 1 \\ \frac{\pi}{\sqrt{\gamma}}\left(1 - \frac{\sqrt{\gamma}}{2\pi}\right) & \text{for } \gamma \ll 1 \end{cases}. \tag{133}$$

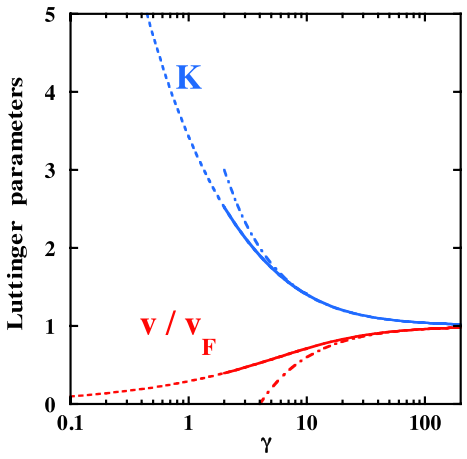

FIG. 8 (color online). Tomonaga-Luttinger liquid parameters for the Lieb-Liniger model (cf. Sec. III.B) as a function of $\gamma = Mg/\hbar^2\rho_0$. $v_F = \hbar v_F = \hbar\pi\rho_0/m$ is the Fermi velocity of a Fermi gas of the same density ρ_0. The dashed lines correspond to the asymptotic results following from Eq. (133). From Cazalilla, 2004b.

The asymptotic formulas for the sound velocity $v(\gamma)$ follow from Galilean invariance.

The t-V model is also integrable by the Bethe ansatz and thus it is found to be a TLL when the lattice filling n_0 is away from 0, $\frac{1}{2}$, and 1. In the half-filled case ($n_0 = \frac{1}{2}$), for $2t < V$ the system also belongs to the TLL universality class, and it is possible to obtain an analytic expression for the Tomonaga-Luttinger parameter and the sound velocity

$$K(\Delta) = \frac{1}{2 - (2/\pi)\cos^{-1}(\Delta)}, \qquad v(\Delta) = \frac{\pi v_F}{2}\frac{\sqrt{1-\Delta^2}}{\cos^{-1}(\Delta)}, \tag{134}$$

where $\Delta = V/2t$ and $v_F = 2ta/\hbar$, a being the lattice parameter. Away from half-filling, one has to resort in general to solving numerically the Bethe-ansatz equations to obtain K and v (Giamarchi, 2004).

Finally, the Bose-Hubbard model is a TLL for noninteger filling and also for sufficiently weak interactions at integer filling [$U/t < 0.297 \pm 0.001$ for lattice filling $n_0 = 1$ (Kühner *et al.*, 2000)]. Being a nonintegrable model, no analytic expressions are available for the Tomonaga-Luttinger parameter and the sound velocity. These parameters must be therefore obtained from numerical calculations. Nevertheless, for $n_0 \leq 1$ and $U/t \gg 1$, the following results have been obtained, to leading order in U/t from a strong-coupling expansion (Cazalilla, 2004a)

$$K \simeq 1 + \frac{4t}{\pi U}\sin\pi n_0, \qquad v \simeq v_B\left(1 - \frac{4t}{U}n_0\cos\pi n_0\right), \tag{135}$$

where $v_B = ta\sin(\pi n_0)/\hbar$.

The Tomonaga-Luttinger liquid parameters can be computed numerically for more complicated models [see, e.g., the case of spin ladders (Hikihara and Furusaki, 2001; Bouillot *et al.*, 2011)]. Typically one determines numerically the compressibility. For DMRG, it is convenient to determine K directly from the static correlation functions, but methods based on twisted boundary conditions, finite-size effects, or direct computation of the spectrum (Giamarchi, 2004) are also possible. Proceeding in such a way, one efficiently combines numerical and analytical insights since thermodynamic quantities are less sensitive to finite-size effects and can thus be accurately obtained numerically. It is then possible to plug the obtained values of v and K in the analytic expressions of the asymptotics of the correlation functions, which are more sensitive to finite-size effects and thus harder to calculate purely numerically. Such a combination has allowed for *quantitative* tests (Klanjšek *et al.*, 2008; Thielemann *et al.*, 2009a) of the Tomonaga-Luttinger liquid as we will see in Sec. VIII.

C. The Thomas-Fermi approximation in 1D

In the presence of harmonic trapping along the longitudinal direction, 1D Bose gases become inhomogeneous, finite-size systems. As a result of the finite size, a crossover between the noninteracting BEC regime and the quasi-long-range ordered regime becomes observable. Meanwhile, inhomogeneity makes the excitation spectrum different from the uniform case previously discussed. The equilibrium properties have been discussed theoretically (Dunjko *et al.*, 2001; Petrov *et al.*, 2004), while the consequences of harmonic trapping on the collective excitations were analyzed by an hydrodynamic approach (Ma and Ho, 1999; Petrov *et al.*, 2000; Menotti and Stringari, 2002; Gangardt and Shlyapnikov, 2006).

As we saw in Sec. III.B the dimensionless parameter $\gamma = c/\rho_0 = mg/\hbar^2\rho_0$ distinguishes the weakly ($\gamma \ll 1$) and strongly ($\gamma \gg 1$) interacting regimes. In the presence of the axial harmonic potential $V(x) = m\omega^2x^2/2$, one can introduce another dimensionless quantity,

$$\alpha = c\ell_{\mathrm{HO}} = \frac{mg\ell_{\mathrm{HO}}}{\hbar^2}, \tag{136}$$

where $\ell_{\mathrm{HO}} = \sqrt{\hbar/m\omega}$ is oscillator length. This parameter can be regarded as the ratio between the oscillator length and the interaction length $r_s = \hbar^2/mg$. The weakly interacting regime is characterized by $\alpha \ll 1$, which means that the relative motion of two particles approaching each other is governed by the harmonic trapping rather than the interparticle distance.

In the weakly interacting limit ($\gamma \ll 1$), we expect the system to behave almost like a BEC, and thus the GP equation (2) introduced in Sec. II.A can be used to estimate the (ground-state) density profile as $\rho_0(x) = |\Psi_0(x)|^2$, where we write the order parameter as $\Psi_0(\mathbf{r}) = \Psi_0(x)\phi_0(\mathbf{r}_\perp)$ [cf. Eq. (8)]. For $N \gg 1$ and $\gamma \ll 1$, the Thomas-Fermi (TF) approximation becomes accurate (see discussion in Sec. II.A and references therein). Hence,

$$\rho_0(x) = \frac{\mu}{g}\left(1 - \frac{x^2}{R_{\mathrm{TF}}^2}\right), \tag{137}$$

where $R_{\mathrm{TF}} = \sqrt{2\mu/m\omega^2}$ is the Thomas-Fermi radius. Imposing the normalization condition $\int_{-R_{\mathrm{TF}}}^{R_{\mathrm{TF}}} dx\rho(x) = N$, one obtains the expression of the chemical potential μ as a function of the number of particles N,

$$\mu = \hbar\omega\left(\frac{3N\alpha}{4\sqrt{2}}\right)^{2/3}, \tag{138}$$

where the parameter $\alpha = \sqrt{mg^2/\hbar^3\omega}$. The condition for the validity of the approximation $\gamma \ll 1$ then takes the form $(\alpha^2/N)^{2/3} \ll 1$, i.e., either $\alpha \ll 1$ and any N or $\alpha \gg 1$, but $N \gg \alpha^2$. The latter condition reflects the fact that the weakly interacting regime requires a sufficiently large number of particles. Since $\rho_0(0)\xi = \sqrt{\hbar^2\mu/(2mg^2)}$, the regime of a weakly interacting gas also is characterized by the healing length ξ being much larger than the interparticle distance $1/\rho_0(0)$.

The limit $\alpha \gg 1$ and $N \ll \alpha^2$ corresponds to the case of the TG gas. In this case, the mapping to a free-fermion Hamiltonian gives a chemical potential $\mu = N\hbar\omega$ and the density distribution (Mehta, 2004)

$$\rho_0(x) = \frac{m\omega R_{\rm TF}}{\pi\hbar}\left(1 - \frac{x^2}{R_{\rm TF}^2}\right)^{1/2}. \tag{139}$$

Note that a similar density profile was also obtained in the case of the Calogero-Sutherland model, as discussed in Sec. III.E. Finally, when the healing length $\xi = \sqrt{\hbar^2/m\mu} \gg R_{\rm TF}$, i.e., $\mu \ll \hbar\omega$, we can neglect the nonlinear term in the GP equation and find the density profile of the ground state in the form of a Gaussian $\Psi_0(x) = \sqrt{\mu/g}e^{-x^2/(2\ell_{\rm HO}^2)}$. The chemical potential is then $\mu = N\alpha\hbar\omega/\sqrt{\pi}$, and this regime is obtained for $\alpha \ll 1/N$. This regime corresponds to interactions so weak that the system is forming a true BEC at zero temperature. The resulting zero temperature crossover diagram is represented on Fig. 9.

A more general approach to the interacting Bose gas in a trap can be developed (Dunjko *et al.*, 2001). If the trapping potential is sufficiently shallow, one can assume, in the spirit of the Thomas-Fermi approximation, that the ground-state energy for a given density profile $\rho_0(x)$ can be written as the integral $P[\rho_0] = \int dx e[\rho_0(x)]$, where $e(\rho_0)$ is the energy per unit length of a uniform interacting Bose gas of mean density ρ_0. The ground-state energy in the presence of the trapping potential $V_{\rm ext}$ and chemical potential μ can be approximated as

$$P[\rho_0(x)] + \int (V_{\rm ext}(x) - \mu)\rho_0(x)dx. \tag{140}$$

Varying the functional (140) with respect to the particle density $\rho_0(x)$, one obtains

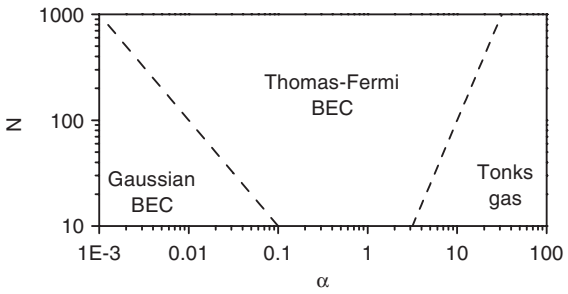

FIG. 9. Zero-temperature crossover diagram for a 1D Bose gas in a harmonic potential. For $\alpha \ll 1/N$, the ground state is a BEC. For $\alpha \gg \sqrt{N}$, the ground state is a TG gas. In between, the ground state is in the Thomas-Fermi regime. From Petrov *et al.*, 2004.

$$\left(\frac{\partial e(\rho_0)}{\partial\rho_0}\right)_{\rho_0=\rho_0(x)} + V_{\rm ext}(x) = \mu. \tag{141}$$

In the weakly interacting ("mean-field") limit $e(\rho_0) = g\rho_0^2/2$, and for a harmonic trap, Eq. (141) reduces to Eq. (137). In the opposite TG limit, Eq. (139) is recovered. Density profiles in the intermediate regime can be computed using $e(\rho_0)$ derived from the numerical solution of the Bethe-ansatz equation (Dunjko *et al.*, 2001).

D. Trapped bosons at finite temperature

We now turn to the properties of trapped 1D Bose gases at finite temperature and, in particular, the different regimes of quantum degeneracy (Petrov *et al.*, 2000; Petrov *et al.*, 2004). In a noninteracting 1D Bose gas in a harmonic trap, a sharp crossover from the classical regime to the trapped BEC is obtained (Ketterle and van Druten, 1996). The origin of the sharp crossover is related to the discrete nature of the levels in the trap. Interactions can suppress this sharp crossover by smearing out the discreteness of the levels. The criterion for the persistence of the sharp crossover is that the average interaction between particles is much smaller than the level spacing $\hbar\omega$. With a Gaussian profile for the density, the average interaction per particle is $\sim gN(m\omega/\hbar)^{1/2}$. The criterion for persistence of the sharp crossover is then $\alpha \ll 1/N$.

In the Thomas-Fermi regime, it is convenient to expand the Hamiltonian to second order in terms of phase and amplitude as was done in Eqs. (4) and (5),

$$\hat{H} = \int dx\left[\frac{\hbar^2\rho_0(x)}{2m}(\partial_x\hat{\theta}(x))^2 + \frac{\hbar^2[\partial_x\delta\hat{\rho}(x)]^2}{8m\rho_0(x)} + \frac{g}{2}[\delta\hat{\rho}(x)]^2\right]. \tag{142}$$

In the limit of high temperature, we can treat the fluctuations of $\delta\hat{\rho} = \hat{\rho}(x) - \rho_0(x)$ and $\hat{\theta}$ as purely classical. We consider first the fluctuations of the operator $\delta\hat{\rho}$. Since the Hamiltonian equation (142) is quadratic, we can easily compute the correlation functions $\langle[\delta\hat{\rho}(x) - \delta\hat{\rho}(x')]^2\rangle$. In order to simplify further the calculation, we make $\rho_0(x) = \rho_0(0)$ in Eq. (142). We then find that $\langle[\delta\hat{\rho}(x) - \delta\hat{\rho}(x')]^2\rangle = k_BT\sqrt{8m\rho_0(0)/\hbar^2 g}(1 - e^{-\sqrt{8mg\rho_0(0)}|x-x'|/\hbar})$. The relative density fluctuation (Petrov *et al.*, 2000), $\langle[\delta\hat{\rho}(x) - \delta\hat{\rho}(x')]^2\rangle/\rho_0(0)^2 \sim k_BT\sqrt{8mg^2/\hbar^2\mu^3}$, and is negligible provided $T < T_d = \sqrt{\hbar^2\mu^3/8mg^2}$. With Eq. (138), we have $T_d = \frac{3}{16}N\hbar\omega$, and T_d is just the degeneracy temperature. Below T_d, the density profile of the gas is given by Eq. (137) and above T_d it reduces to the one of a classical gas. We now turn to the phase fluctuations, using this time the Hamiltonian $H_{\rm phase} = \int dx\hbar^2\rho_0(x)(\partial_x\hat{\theta})^2/(2m)$. By the change of variable $\rho_0(0)s = \int_0^x \rho_0(x')dx'$, we obtain the phase fluctuations as $\langle[\hat{\theta}(x) - \hat{\theta}(x')]^2\rangle = [\pi k_BTm/2\hbar^2\rho_0(0)]|s(x) - s(x')|$. With the density profile (137), $s(x) = R_{\rm TF}\ln[(R_{\rm TF} + x)/(R_{\rm TF} - x)]/2$ and (Petrov *et al.*, 2000) $\langle[\hat{\theta}(x) - \hat{\theta}(x')]^2\rangle = [\pi k_BTm/4\hbar^2\rho_0(0)]R_{\rm TF}\ln\{(R_{\rm TF} + x)(R_{\rm TF} - x')/[(R_{\rm TF} - x)(R_{\rm TF} + x')]\}$. This time, the overall amplitude of the fluctuation is controlled by the parameter T/T_{ph}, where $T_{ph} = (\hbar\omega/\mu)T_d \ll T_d$ since

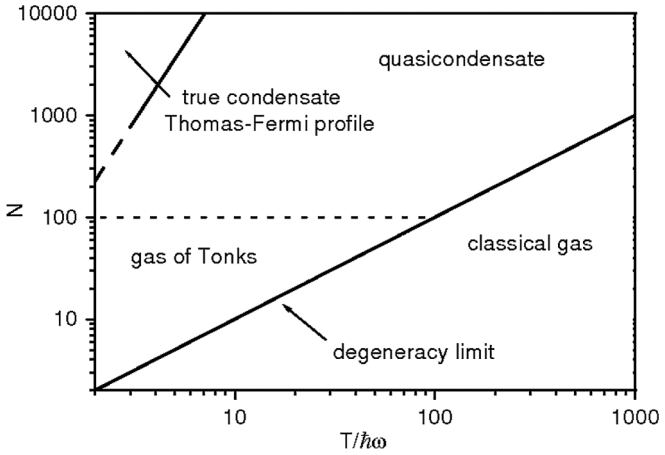

FIG. 10. Crossover diagram for a trapped 1D gas at finite temperature for $\alpha = 10$. For $N \ll \alpha^2$, the system is forming a TG gas below the degeneracy temperature $T_d \sim N\hbar\omega$. For $N \gg \alpha^2$, the system is a quasicondensate when $T_{ph} \ll T \ll T_d$. For $T \ll T_{ph} \sim N^{1/3}$, phase fluctuations are suppressed and the system is a true BEC. From Petrov *et al.*, 2000.

we are in the Thomas-Fermi regime. For $T < T_{ph}$, both phase and density fluctuations are negligible, and the system behaves as a true BEC when $T_{ph} < T < T_d$, there are no density fluctuations, but phase fluctuations are present. Such a regime is called *quasicondensate*. For $T > T_d$, we have a classical gas. We note that $T_{ph} \sim \hbar\omega(N/\alpha^2)^{1/3}$, so as N is increased, the width of the quasicondensate regime broadens.

The resulting crossover diagram at finite temperature, as computed by Petrov *et al.* (2000), is shown in Fig. 10. It can be summarized as follows: For $N \gg \alpha^2$, the decrease of the temperature to below T_d leads to the appearance of a quasicondensate that becomes a true condensate below T_{ph}. For $N < \alpha^2$, the system lies in the Tonks regime.

E. Collective excitations

We now turn to the collective excitations of the trapped gas. We generalize the Tomonaga-Luttinger liquid Hamiltonian and bosonization method to an inhomogeneous system (Petrov *et al.*, 2004; Citro *et al.*, 2008). The inhomogeneous Tomonaga-Luttinger liquid Hamiltonian is

$$\hat{H} = \int_{-R}^{R} dx \frac{\hbar v(x)}{2\pi}\left[K(x)[\partial_x\hat{\theta}(x)]^2 + \frac{[\partial_x\hat{\phi}(x)]^2}{K(x)}\right], \quad (143)$$

where the Tomonaga-Luttinger parameters are given by

$$v(x)K(x) = \frac{\hbar\pi\rho_0(x)}{m}, \qquad \frac{v(x)}{K(x)} = \frac{1}{\pi}\partial_{\rho_0}\mu[\rho_0(x)]. \quad (144)$$

The field $\hat{\phi}(x,\tau)$ obeys the boundary conditions

$$\hat{\phi}(R,\tau) = \phi_1 \quad \text{and} \quad \hat{\phi}(-R,\tau) = \phi_0, \quad (145)$$

which amount to require that no current is going in or out at the edges of the system. The fields satisfy the following equations of motion (Safi and Schulz, 1995):

$$\begin{aligned}\partial_\tau\hat{\phi}(x,\tau) &= v(x)K(x)\partial_x\hat{\theta}(x,\tau),\\ \partial_\tau\hat{\theta}(x,\tau) &= \partial_x\left(\frac{v(x)}{K(x)}\partial_x\hat{\phi}(x,\tau)\right).\end{aligned} \quad (146)$$

Noting that density operator $\delta\hat{\rho} = -\partial_x\hat{\phi}/\pi$ and $\hat{v} = \hbar\partial_x\hat{\theta}/m$, the above equations are the operator 1D equivalent of the linearized hydrodynamic equations discussed in Sec. II.A and employed by Menotti and Stringari (2002).

Combining the two equations (146), using the boundary condition (145), and Fourier transforming one obtains the eigenvalue equation for the normal modes of the operator $\hat{\phi}(x)$:

$$-\omega_n^2\varphi_n(x) = v(x)K(x)\partial_x\left(\frac{v(x)}{K(x)}\partial_x\varphi_n(x)\right), \quad (147)$$

with boundary conditions $\varphi_n(\pm R) = 0$. The eigenfunctions φ_n are normalized as

$$\int dx \frac{\varphi_n(x)\varphi_m(x)}{v(x)K(x)} = \delta_{n,m}. \quad (148)$$

The solution of the eigenvalue equation (147) gives access to the eigenmodes of the trapped gas. The zero frequency solution is immediately obtained by substituting $\partial_x\varphi = K(x)/u(x)$ into Eq. (147). With $\varphi(x) = \lambda\rho_0(x)$, a solution with $\omega_n = \omega$, that describes that the harmonic oscillations of the center of mass of the cloud (the Kohn mode) is obtained. For the particular case (Petrov *et al.*, 2004; Citro *et al.*, 2008)

$$v(x) = v_0\sqrt{1 - \frac{x^2}{R^2}}, \qquad K(x) = K_0\left(1 - \frac{x^2}{R^2}\right)^{\alpha}, \quad (149)$$

the solutions $\varphi_n(x)$ of Eq. (147) are obtained in terms of Gegenbauer (or ultraspherical) polynomials (Abramowitz and Stegun, 1972):

$$\varphi_n(x) = A_n\left(1 - \frac{x^2}{R^2}\right)^{\alpha+1/2} C_n^{(\alpha+1)}\left(\frac{x}{R}\right), \quad (150)$$

$$\omega_n^2 = \frac{v_0^2}{R^2}(n+1)(n+2\alpha+1), \quad (151)$$

where A_n is a normalization factor. The frequencies in Eq. (151) are in agreement with the results of Menotti and Stringari (2002). In the case of $\alpha = 1/2$, the dependence of $v(x)$ and $K(x)$ is the one predicted by the mean-field approach of Sec. V.C [Eq. (5)]. The Gegenbauer polynomials in Eq. (151) can then be expressed in terms of the simpler Legendre polynomials (Petrov *et al.*, 2000). Another interesting limit is $\alpha = 0$, which corresponds to the case of the Tonks-Girardeau gas, where the Gegenbauer polynomials reduce to Chebyshev polynomials. Then, $\omega_n = (n+1)\omega$, as expected for fermions in a harmonic potential.

VI. PERTURBATIONS ON 1D SUPERFLUIDS

Since the Tomonaga-Luttinger liquid theory reviewed in Sec. V incorporates the interaction effects into a relatively simple quadratic Hamiltonian, it provides a convenient starting point to study the effects of various external potentials on 1D superfluid systems. In this section, we consider the effect

that three different kinds of external potentials have on 1D superfluids. First, we discuss the effect of a periodic potential, i.e., a lattice. As mentioned in Sec. IV.B, this can lead to interaction driven insulating phases (Mott insulators). Then we introduce the random potential and disorder driven insulating phases (Anderson insulators). We conclude with the intermediate case of a quasiperiodic potential, for which recent cold atomic experiments have provided an experimental realization (Roati *et al.*, 2008).

A. Mott transition

1. Periodic potentials and the sine-Gordon model

In this section, we consider the effect of a periodic potential on an interacting boson system. Its effect can be described in two complementary ways. If the potential is weak, it can be added as a perturbation on the interacting bosons in the continuum. However, if the potential is strong, as described in Sec. II.C, it is better to start from a lattice model such as the extended Bose-Hubbard model (14), or its descendants. As we show below, both approaches lead to the same low-energy field theory.

We begin by considering a weak periodic potential $V_{\rm ext}(x) = V_0 \cos(Gx)$. The addition of this term to the Hamiltonian (9) reduces its invariance under continuous space translations to the discrete group of lattice translations $x \to x + 2\pi m/G$, with integer m. As noted by Haldane, (1981a), using Eq. (112) for the density leads to an additional term $\hat{H}_V$ [see, e.g., Giamarchi (2004) for a detailed derivation] in the TLL Hamiltonian, $\hat{H}$ [cf. Eq. (114)]

$$\hat{H}_V = \frac{\tilde{g}_u}{\pi} \int dx \cos[2p\hat{\phi}(x) + x\delta]. \tag{152}$$

For a weak potential, $\tilde{g}_u \approx \pi\rho_0 V_0 (V_0/\mu)^{n-1}$ is the bare coupling. In Eq. (152), we have retained the term with the smallest value of $\delta = nG - 2p\pi\rho_0$ (n, p being integers), which measures the degree of incommensurability of the potential; $\delta = 0$ corresponds to a commensurate number of bosons per site. For $p = 1$, there is an integer number of bosons per site since $\rho_0 = nG/(2\pi)$, while higher values of p, such as $p = 2$, correspond (modulo an integer) to one boson every two sites, etc. δ is thus a measure of the doping of the system away from this commensurate value. There are some subtle issues depending on whether one works at constant density or at constant chemical potential, and we refer the reader to Giamarchi (2004) for more details on that point.

Remarkably, the *same* effective model is obtained if one starts directly from a lattice model, such as the Hubbard model. In that case, the perturbation (152) arises because, in a lattice system, the quasimomentum is only conserved modulo a reciprocal lattice vector. Terms in which the quasimomentum of the final state differ from the one of the initial state by a nonzero multiple of G, called umklapp terms, can be obtained by using Eq. (112) and the condition that on a lattice (e.g., for one particle per site) one has $2\pi\rho_0 r_n = 2\pi n$ and thus $e^{i2\pi\rho_0 r_n} = 1$. For one particle per site the role of umklapp processes is to create a Mott insulator. The role of higher order umklapps, allowing an interaction process to transfer several times a vector of the reciprocal lattice, and its role in leading to Mott-insulating phases was pointed out by Giamarchi (1997), Giamarchi and Millis (1992). The final result is exactly Eq. (152) with the same condition for δ. The main difference is in the amplitude of this term which now is proportional to the interaction itself.

Hence, the model (114), and $\hat{H}_{\rm sG} = \hat{H} + \hat{H}_V$ [after Eq. (152)], is thus able to give a complete description of the effects of periodic potential or lattice in a 1D interacting bosonic system. This description depends on the value of the Tomonaga-Luttinger parameter, which is a measure of the interactions, the lattice potential, and the doping δ away from commensurability. One immediately sees that two different types of transition can be expected. In one case, one remains commensurate $\delta = 0$. The term $\hat{H}_V$ is a simple cosine. The corresponding model is known as the ''sine-Gordon'' (sG) model for historical reasons (Coleman, 1988). The transition can then occur as a function of the strength of the interactions, or in our low-energy model, as a function of the change of the Tomonaga-Luttinger parameter K. Alternatively, we can fix the interactions and change the degree of incommensurability δ inside the term $\hat{H}_V$. Next we examine these two type of transitions.

2. Commensurate transition

The first type of transition, which we denote Mott-U transition, corresponds to keeping the density fixed, and commensurate $\delta = 0$ and varying the Luttinger parameter. The physics of such a transition can be easily understood by looking at the term $\hat{H}_V$ to the Hamiltonian. When $\hat{H}_V$ (rather than $\hat{H}$) dominates the low-temperature properties of the system, the fluctuations of the field $\hat{\phi}(x)$ are strongly suppressed, and $\hat{\phi}$ can order. Since ordering $\hat{\phi}(x)$ means ordering the density, it follows that the bosons are localized at the potential minima and the system becomes a Mott insulator (MI). To see this, consider the limit $\tilde{g}_u \to -\infty$ for $\delta = 0$. In this limit, $\langle \cos 2p\hat{\phi}(x)\rangle \to 1$ and the ground-state density following from Eq. (112) is $\langle \hat{\rho}(x)\rangle \simeq \rho_0 + \rho_0 \sum_{m>0} A_m \times \cos m(nGx/p)$. This function is periodic for $x \to x + \frac{2\pi p}{nG} l$ (l being an integer). The insulating state is thus a system where, on average, $n_0 = n/p$ bosons are localized per potential minimum. Note that there is no violation of the Mermin-Wagner-Hohenberg theorem since, in the presence of the potential, the symmetry that is being broken is the discrete invariance under lattice translations, which is possible at $T = 0$ even in 1D.

To quantitatively study the effects of Eq. (152) on the low-temperature properties of the system, first consider a commensurate potential, and write renormalization-group equations. The RG flow maps one effective Hamiltonian $\hat{H}_{sG} = \hat{H} + \hat{H}_V$ characterized by a set of parameters (v, K, g_u) and a short-distance cutoff a_0 onto a new $\hat{H}'_{\rm sG}$ characterized by (v', K', g'_u) and a new cutoff scale $a'_0 > a_0$ by progressively integrating out high-energy degrees of freedom. This method is well documented (see, e.g., Giamarchi, 2004) so we only quote the results. To lowest order in g_u, the RG flow is described by the following set of differential equations for $[v(\ell), K(\ell), g_u(\ell)]$ as functions of $\ell = \ln(a'_0/a_0)$,

$$\frac{dg_u}{d\ell} = (2 - p^2 K) g_u, \qquad \frac{dK}{d\ell} = -g_u^2 K^2, \tag{153}$$

where $g_u = \tilde{g}_u a_0^2/\hbar v \ll 1$ is a dimensionless coupling. In addition to these equations, $dv(\ell)/d\ell = 0$ to all orders due to the Lorentz invariance of the theory. Equations (153) describe a BKT flow (Kosterlitz and Thouless, 1973; Kosterlitz, 1974). This flow has two different regimes, which asymptotically correspond to two different phases. For weak coupling, the separatrix between them is given by $K = 2/p^2 + 2g_u/p^3$. It delimits two phases. (i) A phase in which $g_u(l) \to 0$: This corresponds to a Tomonaga-Luttinger liquid phase, in which the decay of the correlations is algebraic, and the lattice plays asymptotically no role beyond a renormalization of the parameters entering in the Tomonaga-Luttinger Hamiltonian. (ii) A phase in which $g_u(l)$ scales up: This phase corresponds to ordering of $\hat{\phi}$. As discussed, this means that the particles are localized and correspond to a Mott insulator. It follows from the RG, or a variational treatment of the Hamiltonian (Giamarchi, 2004), that a gap G opens in the spectrum. Perturbative values are $G/\mu \sim g_u^{1/(2-K)}$ for $2 - K \gg 1$, but since the sine-Gordon model is integrable, exact values are also available (Gogolin *et al.*, 1999; Lukyanov and Zamolodchikov, 2001; Giamarchi, 2004).

Hence, generically for any commensurate filling, the system can undergo a transition between a TLL and a MI. At the transition point, the Luttinger parameter K takes a universal value that depends only on the lattice filling: $K^* = 2/p^2$. Since K/v is proportional to the compressibility and vK to the Kohn stiffness (cf. Sec. V.A), both compressibility and Kohn stiffness jump discontinuously to zero when entering the MI phase. The exponents of the various correlations have a *universal* algebraic decay at the transition. In the MI phase, the spectrum is gapped and the correlation functions decay exponentially.

We next examine some simple cases of the above transition. For $p = 1$, which corresponds to an integer number of particles per site, relevant the Bose-Hubbard model or the Lieb-Liniger gas in a periodic potential, the critical value is $K_1^* = 2$. The TLL phase is thus dominated by superfluid fluctuations since $K > 2$. One has a superfluid-MI transition. At the transition the one-particle correlation function is thus $g_1(x) \sim |x|^{-1/4}$. For one particle every two sites, one has $p = 2$ and thus $K_2^* = 1/2$. Note that this critical value is beyond the reach of a model with only local interactions such as the Lieb-Liniger or the Bose-Hubbard (BH) models, as for such models $1 < K < \infty$. A MI phase with one particle every two sites can thus never occur in those models. This is quite natural since it would correspond to an ordered phase of the form 1010101010 and a purely local interaction cannot hold the particles one site apart. In order to stabilize such MI phases, one needs longer range interactions, for example, nearest neighbor ones as in the $t - V$ or extended BH models, or dipolar interactions (Citro *et al.*, 2008; Burnell *et al.*, 2009). In those cases, $K_2^* = 1/2$ can be reached, and the MI phase appears. Note that the critical behavior of such a transition is also BKT-like but with different values for the universal jump and for the correlation functions. For the transition with one particle every two sites $g_1(x) \sim |x|^{-1}$. Moreover, logarithmic corrections to this scaling results exist in some cases (Giamarchi and Schulz, 1989; Giamarchi, 2004). The transport properties can be also computed near these phase transitions and we refer the reader to the literature

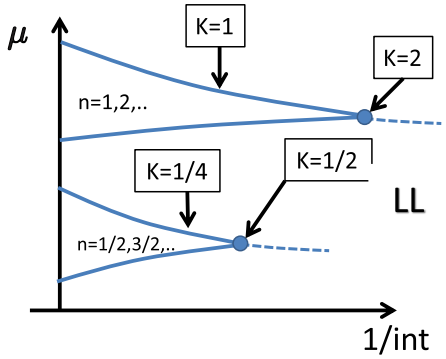

FIG. 11 (color online). Phase diagram for commensurate bosons as a function of the chemical potential μ and the interactions. Only the commensurabilities of one boson per site and one boson every two sites have been shown. The Mott phase for the bosons occurs for a commensurate filling and depends on the strength of the interactions. The Tomonaga-Luttinger liquid (TLL) parameters take a universal value both for the Mott-U and Mott-δ transitions. The value depends on the order of commensurability. From Giamarchi, 2004.

(Giamarchi, 1991; 1992; 2004; Rosch and Andrei, 2000; Controzzi *et al.*, 2001) for an extended discussion. Finally, in systems with nearest-neighbor interactions such as the extended BH model at unit lattice filling, other interesting phases, besides the MI, can also appear (Dalla Torre *et al.*, 2006; Lee, Lee, and Yang, 2007; Berg *et al.*, 2008).

The properties discussed above and summarized in Fig. 11 agree very well with the numerical results for the BH model of Sec. IV.B.2 and with results on the extended BH model (Kühner *et al.*, 2000), in which a value $K^* = 1/2$ was numerically found for the transition from the TLL and the MI with one boson every two sites.

As a final remark, we note that although for the BH model, which corresponds to the strong lattice case, the phase diagram is more or less independent on the dimension, 1D systems in presence of a weak periodic potential present a very interesting feature. Indeed from the scaling properties above, we see that in 1D one can realize a MI phase even for a very weak periodic potential provided that the interactions are strong enough (e.g., $K < 2$ for one boson per site). This is a true quantum effect coming from the interferences of the particles on the periodic potential that can lead to localization even if the periodic potential is much weaker than the kinetic energy. In the TG limit ($K = 1$) this would simply correspond to free fermions moving in a periodic potential with exactly $2k_F$ periodicity, where k_F is the Fermi wave vector. In that case, an arbitrarily weak potential will open a gap. Such a feature would not be present in higher dimensions where a strong lattice potential is needed to stabilize the Mott insulator phase, at least for the case of local interactions.

3. Incommensurate transition

The situation is drastically different when the system is incommensurate. Consider the case for which the commensurate system $\delta = 0$ is a MI, i.e., $K < K^*$ and consider the effect of increasing δ on the physics of the system. Naively, the presence of a $x\delta$ term in the argument of the cosine means

that this operator oscillates in space and thus at long length scales it will be wiped out, its sole effect being a renormalization of the TLL parameters. This would lead us back to the purely quadratic TLL Hamiltonian. This is a reflection of how the *doped* system at low energies always behaves as a TLL with algebraically decaying correlations. In order to have finite doping, since the MI phase is gapped, one needs to apply a chemical potential that exceeds the gap G. Therefore, there is the possibility of having another kind of MI-SF transition, this time driven by a change of the system density. This transition is sometimes referred to as a Mott-δ transition. Although it is not obvious in terms of the original boson degrees of freedom, the bosonization representation allows us to relate the Mott-δ transition to a two-dimensional classical phase transition, known as the commensurate-incommensurate (C-IC) phase transition (Japaridze and Nersesyan, 1978; Pokrovsky and Talapov, 1979; Schulz, 1980). The latter describes absorption of classical particles on a periodic substrate. The particle density is tuned from a value that is commensurate to one that is incommensurate with the substrate periodicity. It is thus possible to use the previous knowledge on the critical exponents of the C-IC transition to obtain the Mott-δ transition critical exponents. In other words, the universality class of the Mott-δ and C-IC transitions is the same.

In order to obtain the critical properties of the Mott-δ transition, two approaches are possible. One is to use the standard renormalization-group procedure and establish equations involving the doping δ (Giamarchi, 1991; 2004). Although these equations are very useful in deriving some of the physical quantities, especially away from the transition itself, they flow to strong coupling when one approaches the transition line, making it difficult to extract the critical exponents. It is thus especially useful to use a technique known as fermionization (Luther and Emery, 1974; Schulz, 1980; Giamarchi, 2004) to deal with this issue. The idea is simply to use the fact that, in a similar way, one can represent bosonic single-particle operators by collective variables as described by Sec. V, one also represent fermionic particles. It is thus possible to map the sine-Gordon Hamiltonian to a fictitious Hamiltonian of interacting "fermions." We will not detail here the relation between fermions and collective variables (the density operator is the same than for bosons, but a single-particle operator is slightly different) since it has been well described (Giamarchi, 2004) and simply quote the following final result (Schulz, 1980):

$$\hat{H} = \sum_k \hbar v k (\hat{\psi}^\dagger_{k,R}\hat{\psi}_{k,R} - \hat{\psi}^\dagger_{k,L}\hat{\psi}_{k,L}) + \hat{H}_{\rm int} + g_u \sum_k (\hat{\psi}^\dagger_{k,R}\hat{\psi}_{k,L} + \text{H.c.}) - \delta \sum_k (\hat{\psi}^\dagger_{k,R}\hat{\psi}_{k,R} + \hat{\psi}^\dagger_{k,L}\hat{\psi}_{k,L}), \tag{154}$$

where $\hat{H}_{\rm int}$ is an interaction term between the fermions. The above Hamiltonian describes right and left moving fermions (R and L) indices, with a Dirac-like linear dispersion controlled by the velocity v. The fermions represent the soliton excitations of the density field $\hat{\phi}(x)$, i.e., configurations in which $\hat{\phi}(x)$ goes from one of the minima of the cosine to the next, thereby changing by $\pm\pi/p^2$. The interaction term depends on the commensurability of the system and is proportional to $Kp^2 - 1/(Kp^2)$. So while in general the fermions interact making the fermionic theory as difficult to solve as the original sine-Gordon one, for a special value K_0 of the Luttinger parameter, this interaction disappears leading to a free fermionic theory. For $p = 1$, one has $K_0 = 1$ that corresponds to the TG limit, in which case the fermions in Eq. (154) are nothing but the spinless fermions of Eq. (28). This technique, introduced by Luther and Emery (1974), has been used in several contexts for 1D systems (Giamarchi, 2004). It provides a useful solution when the nonlinear excitations of the sine-Gordon model are important to keep and when a simple quadratic approximation of the cosine would be insufficient.

The former Mott term is now hybridizing the right and left movers and thus opens a gap in the initially gapless spectrum. The energy spectrum is $\epsilon_\pm(k) = \pm\sqrt{(vk)^2 + g_u^2}$. Fermionization also allows us to make quite rigorous in this context the concept of the upper and lower Hubbard bands, which now correspond to the two possible signs of $\epsilon_\pm(k)$. The corresponding "free" particles are the solitons of $\hat{\phi}(x)$, which correspond to the defects in the perfect arrangement existing in the MI phase. For example, starting from 10101010101010, configurations such as 10110101010010 would contain one soliton and one antisoliton. Thus, δ corresponds to the average density of fermions. If δ is nonzero, the chemical potential lies in either the upper or lower Hubbard band, and one thus recovers that there are gapless excitations described by the fermions. Therefore, in this language the Mott-δ transition can be understood (Giamarchi, 1997) as the *doping* of a *band* insulator.

Using the fermionization approach, one can also extract the critical behavior, which is markedly different from the commensurate case. Right at the transition $\delta \to 0_+$, the dynamical exponent relating space and time $\omega \sim k^z$ is $z = 2$ contrary to the commensurate case for which $z = 1$ because of Lorentz invariance. The effective velocity of excitations is for $0 < \delta \ll g_u/v$

$$v^* = \left(\frac{d\epsilon(k)}{dk}\right)_{k=\pi\delta} \simeq \frac{\pi v^2 \delta}{g_u}, \tag{155}$$

and goes to zero at the transition. The compressibility, which can be computed by $dN/d\mu$, *diverges* at the transition, before going to zero in the Mott phase. The Kohn stiffness $D \propto v^* K^*$ vanishes continuously with the doping δ since the Tomonaga-Luttinger parameter is a constant. Interestingly, the exponents of the various correlation functions at the transition are universal and can be determined by using the free-fermion value. For example, the density correlator of the fermions decays as $|x|^{-2}$. Since before the mapping the correlation would have corresponded to an exponent $2/K$, this means that at the Mott-δ transition the Tomonaga-Luttinger parameter takes the universal value $K_0 = 1$. For a generic commensurability p, it is easy to check that $K_0 = 1/p^2$. This is exactly half of the universal value of the commensurate Mott-U transition. A summary of is shown in Fig. 11. Interestingly, several of these scalings for both the commensurate and incommensurate case are also valid and extendable to higher dimensions (Fisher *et al.*, 1989).

These considerations also directly apply to the case of spin chains and ladders with a gapped phase and we refer the

reader to the literature (Chitra and Giamarchi, 1997; Furusaki and Zhang, 1999; Giamarchi and Tsvelik, 1999) and to Sec. VIII for more details on this point.

B. Disorder

Another type of perturbation is provided by a disordered potential. For noninteracting particles, disorder can give rise to Anderson localization: the single-particle eigenfunctions of the Hamiltonian decay exponentially over a characteristic length ξ_l, called the *localization* length (Anderson, 1958). Indeed, the effect of disorder depends on dimensionality. In 1D, all eigenstates are localized for any nonzero disorder strength (Mott and Twose, 1961). Exact solutions (Berezinskii, 1974; Abrikosov and Rhyzkin, 1978; Gogolin, 1982; Efetov, 1983) can be devised. For noninteracting particles, the localization length is of the order of the mean-free path in 1D. Higher dimensions (Abrahams *et al.*, 1979; Efetov *et al.*, 1980; Efetov, 1983) lead either to a full localization, albeit with a potentially exponentially large localization length in 2D, or to the existence of a mobility edge separating localized states (near band edges) from diffusive states (at band center) in 3D. Recently, cold atomic gases have allowed one to directly observe the localization of noninteracting 1D particles (Billy *et al.*, 2008; Roati *et al.*, 2008).

Although the noninteracting case is conceptually well understood, taking into account the combined effects of disorder and interactions is a formidable problem. For fermions, the noninteracting case is a good starting point and the effects of interactions can be at least tackled in a perturbative fashion (Altshuler and Aronov, 1985; Lee and Ramakhrishnan, 1985) or using renormalization-group techniques (Finkelstein, 1984).

Such an approach is impossible with bosons since the noninteracting disordered bosonic case is pathological. The ground state in the noninteracting case is a highly inhomogeneous Bose condensate in which all particles are in the lowest eigenstate of the Hamiltonian (which is necessarily localized). In the absence of repulsion, a *macroscopic* number of particles are thus trapped in a *finite* region of space. Such a state is clearly unstable to the introduction of even the weakest interaction. The interactions should thus be included from the start. Alternatively, the limit of very strong interactions can be considered starting from a crystal phase of particles (fermions or bosons since statistics in that case does not matter) (Giamarchi, 2003).

1. Incommensurate filling

We next consider the Hamiltonian of disordered interacting bosons. For convenience and generality, we deal with the case of bosons on a lattice. Similar results and methods are of course applicable in the continuum. The Hamiltonian reads

$$\hat{H} = \sum_{i=1}^{L}\left[-t_i(\hat{b}_i^\dagger \hat{b}_{i+1} + \text{H.c.}) - \epsilon_i \hat{n}_i + \frac{U}{2}\hat{b}_i^\dagger \hat{b}_i^\dagger \hat{b}_i \hat{b}_i\right]. \quad (156)$$

The t_i describe random hopping from site to site. This type of disorder is particularly pertinent for spin chains (see Sec. II.D) since in that case it corresponds to the case of random spin exchange (Hong *et al.*, 2010). ϵ_i is a random chemical potential. Note that in the case of cold atomic gases ϵ_i also contains in general the confining potential. Other types of disorder (random interactions, etc.) can of course also be treated, but we confine our discussion to the above two cases. Note that for the case of hard-core bosons (or spins) these two types of disorder have an important difference. The first one respects the particle-hole symmetry of the problem (for soft-core bosons no such particle-hole symmetry exists), while the second, being a random chemical potential, breaks it for each realization of the disorder, even if it is still respected in average.

Just as for the case of a periodic potential, we use the bosonization method introduced in Sec. V. We start with the on-site disorder. Similar results and equations can be derived for the random hopping. Microscopic disorder is in general rarely Gaussian. For example, impurities scattered in random positions represent a Poissonian disorder. It might be important for practical cases to carefully take into account the precise form of such correlations (see, e.g., Lugan *et al.*, 2009). However, the Gaussian limit is generic if the length scales over when the properties of the system vary (e.g., the localization length) and are large compared to the microscopic scale of the disorder. In that case, the central limit theorem applies. We thus for simplicity discuss the case of $\overline{\epsilon_i \epsilon_{i'}} = D\delta_{ii'}$, where D is the disorder strength.

For the case of incommensurate filling, or for bosons in the continuum, one can rewrite the coupling to a weak disorder potential as

$$\hat{H}_{\text{dis}} = \int dx V(x)\hat{\rho}(x), \quad (157)$$

where $\overline{V(x)V^\star(x')} = D\delta(x-x')$. Using the boson representation for the density of Sec. V and keeping only the most relevant harmonics, one has (Giamarchi and Schulz, 1988)

$$\hat{H}_{\text{dis}} = \int dx V(x)\left[-\frac{1}{\pi}\partial_x \hat{\phi}(x) + \rho_0(e^{i2[\pi\rho_0 x - \hat{\phi}(x)]} + \text{H.c.})\right]. \quad (158)$$

The term proportional to $\partial_x\hat{\phi}$ describes "forward" scattering by the random potential. It corresponds to a slowly (compared to the interparticle spacing ρ_0^{-1}) varying chemical potential. This term can be absorbed, for incommensurate cases, in the quadratic part of the Hamiltonian. It is straightforward to check that although it leads to exponential decay of density correlations, it cannot affect the superfluid ones nor change the conductivity.

The main disorder effects are thus coming from the "backscattering" term, i.e., the term for which the momentum exchanged with the impurities is of the order of $2\pi\rho_0$. This term can be treated by an RG procedure (Giamarchi and Schulz, 1988). The RG equations read

$$\frac{dK}{dl} = -\frac{K^2}{2}\tilde{D}, \qquad \frac{d\tilde{D}}{dl} = (3-2K)\tilde{D}, \quad (159)$$

where $\tilde{D} = D/\pi^2 u^2 \rho_0$. There is also an additional equation for the velocity showing that the compressibility is not renormalized at this order of the flow. These equations indicate that both disorder and interactions are renormalized when disorder (and interactions) is present. The equations for $\tilde{D}$ and

K have a BKT form like those of the Mott transition. There is a separatrix, depending on both K and $\tilde{D}$, which terminates at $K^* = 3/2$ and separates a phase in which $\tilde{D}$ scales to zero and a phase in which $\tilde{D}$ is relevant. The former clearly corresponds to a superfluid one. In the latter, $\tilde{D}$ scales to strong coupling, and the above equations, which are obtained perturbatively, cannot be trusted beyond a certain scale l^* such that $\tilde{D}(l^*) \sim 1$. One can nevertheless infer the properties of such a strong-coupling phase using various approaches. The simplest is to note that this phase contains the TG line $K = 1$ for which the bosons behave as noninteracting fermions, which in a disordered potential undergo Anderson localization. This line has same long-distance properties as a 1D Anderson insulator, in which all particles are localized for arbitrary disorder strength. This Anderson localized phase has been discussed for the Tonks gas by Radić *et al.* (2010).

The critical properties of the transition can be extracted from the flow. Since the transition is of the BKT type, K jumps discontinuously at the transition. Note that contrary to what happens for the periodic case, the system remains *compressible* in the localized phase, as one can see from the free-fermion limit, or the RG flow. The jump of K indicates that the Kohn stiffness, which is finite in the superfluid, goes to zero in the localized phase. The localization length, which can be extracted from the flow, diverges at the transition, in the usual stretched exponential way characteristic of BKT transition. Note that if one defines a critical exponent ν for the divergence of the localization length, one has $\nu = \infty$ in 1D. Disordered bosons in 1D provided the first derivation of a superfluid-localized transition and the existence of a localized bosonic phase (Giamarchi and Schulz, 1988). This phase, called Bose glass (BG), was surmised to exist in higher dimensions as well, and the critical properties of the SF-BG transition were obtained by general scaling arguments (Fisher *et al.*, 1989). In addition to 1D bosons, the same RG methodology has been applied to several systems using the mapping of Sec. II.D, such as spin chains and ladders or bosonic ladders. We refer the reader to the literature for details on those points (Doty and Fisher, 1992; Orignac and Giamarchi, 1998a; 1998b; Giamarchi, 2004).

If the value of K becomes too large (i.e., the interactions between the bosons become too weak), then the bosonization description becomes inadequate to describe the system since the chemical potential becomes smaller than the disorder strength. Since the noninteracting line is localized irrespective of the strength of the disorder, it was suggested that the separatrix bend down to the point $K = \infty$, $\tilde{D} = 0$, to lead to the reentrant phase diagram of Fig. 12.

These predictions were confirmed by different methods. On the analytic side, after bosonization the Hamiltonian bears resemblance to the one describing the pinning of charge-density waves (Fukuyama and Lee, 1978). This leads to a physical interpretation of the Bose-glass phase as a pinned density wave of bosons. The phase ϕ adjusts in Eq. (158) to the random phase $2\pi\rho_0 x_i$, where x_i would be the position of the impurities. For small disorder, the boundary between the superfluid and the localized phase has recently been reinvestigated (Lugan *et al.*, 2007; Falco *et al.*, 2009; Aleiner *et al.*, 2010), confirming the general shape of Fig. 12, and giving the precise position of the boundary.

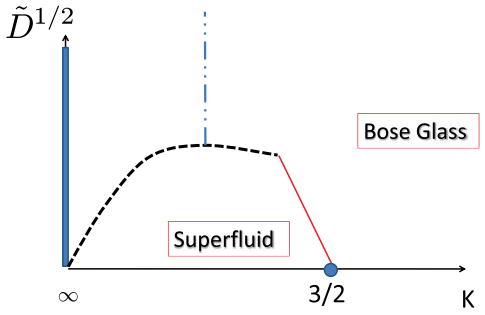

FIG. 12 (color online). Phase diagram of interacting disordered bosons (Giamarchi and Schulz, 1987), for incommensurate filling, in 1D. K is the Tomonaga-Luttinger parameter ($K = \infty$ for noninteracting bosons, and K decreases for increasing repulsion). $\tilde{D}$ is the strength of the disorder. Noninteracting bosons are localized in a finite region of space and have thus no thermodynamic limit. The solid line is the separatrix computed from the RG (see text). The limit of the superfluid region must bend down (dashed line) for small interactions to be compatible with the noninteracting limit, leading to a reentrant superconducting phase. The Bose-glass phase is a localized, compressible bosonic phase (see text). The question on whether distinct localized phases could exist (dash-dotted line) or whether there is only one single localized phase is still open.

The transition itself can be studied by two methods, slightly more approximate than the RG, since they amount to neglecting the first RG equation and consider that the interactions are not renormalized by the disorder. The first method is a self-consistent harmonic approximation, developed for the pinning of charge-density waves (Suzumura and Fukuyama, 1983). The second method is a variational approach based on the replica trick (Giamarchi and Le Doussal, 1996). Although they do not give the correct critical properties for the reasons just stated, they predict the transition at $K = 3/2$. The later method also allows the calculation of the correlation functions in the localized phase. It, in particular, shows that a second localization length corresponding to the localization of the particles in time exists. It also gives access to the frequency dependence of the conductivity at zero temperature.

The TG limit allows one to also obtain some of the properties in the localized phase. The density correlations can directly be extracted and the single-particle Green's function, which can be represented as a Pfaffian (Klein and Perez, 1990) as discussed in Sec. III.A. This allows one to show rigorously that for large distance the single-particle Green's function of the bosons decays exponentially, and thus that there is no off-diagonal quasi-long-range order. For a fixed disorder realization h_i, one can compute numerically the Pfaffian and then average over the different disorder realizations (Young and Rieger, 1996; Henelius and Girvin, 1998). A similar numerical study of the effect of disorder has also been done for a discrete binary probability distribution of random on-site energies (Krutitsky *et al.*, 2008). The probability distribution of on-site energies ϵ_i is given by $p(\epsilon) = p_0\delta(\epsilon) + (1 - p_0)\delta(\epsilon - U')$, where $1 - p_0$ is the concentration of impurities U' is the boson-impurity interaction term. This type of disorder can be obtained in experiments by the interaction of the bosons with impurity atoms having a large effective mass (Gavish and Castin, 2005). Hard-core bosons

also allow for an exact calculation of the superfluid fraction defined by Fisher *et al.* (1973) and Pollock and Ceperley (1987).

The numerical results show that for small t/U' the binary disorder destroys the superfluidity in the thermodynamic limit in a similar manner as for Gaussian disorder. A study of binary disorder in case of finite but large U has been performed with strong-coupling expansions and exact diagonalization by Krutitsky *et al.* (2008).

Although the bosonization approach is very efficient to describe the moderately and strongly interacting bosons, it is, as mentioned, not applicable when the interactions become weak or alternatively if the disorder become strong. If the disorder is very strong, one has *a priori* even to take into account broad distributions for the various parameters. An efficient real space renormalization-group technique (Fisher, 1994) has been developed to renormalize distribution of coupling constants. If the distributions are broad to start with, they become even broader, making the RG controlled. This RG has been applied with success to the study of strongly disordered bosons (Altman *et al.*, 2004b; 2010). This technique gives a transition between a Bose glass and the SF phase. It is interesting that in the limit of strong disorder, the transition is also of the BKT type but with some divergences of the distributions. Whether this indicates the presence of two different localized phases, one for weak interaction and one for strong interactions (see Fig. 12), or whether the two can be smoothly connected is an interesting and still open question. A proper order parameter separating the two phases would have to be defined. Note that the computational studies give conflicting results on that point (Batrouni and Scalettar, 1992; Rapsch *et al.*, 1999).

At finite temperature, the question of the conductivity of the Bose-glass phase is a very interesting and still open problem. If the system is in contact with a bath, an instanton calculation (Nattermann *et al.*, 2003) leads back to Mott's variable range hopping (Mott, 1990) $\sigma(T) \sim e^{-(T_0/T)^{1/2}}$. This technique can also be used to compute the ac conductivity (Rosenow and Nattermann, 2006). In the absence of such a bath, the situation is more subtle (Gornyi *et al.*, 2005; Basko *et al.*, 2006; Gornyi *et al.*, 2007; Aleiner *et al.*, 2010). In particular, it has been suggested that the conductivity could be zero below a certain temperature, and finite above, signaling a finite-temperature many-body localization transition. Consequences for bosonic systems have been investigated by Aleiner *et al.*, 2010.

2. Commensurate filling

We now turn to the case for which the system is at a commensurate filling. If the interactions is such that the commensurate potential could open a Mott gap, then there will be a competition between Mott and Anderson localization. To describe such a competition one must add to the Hamiltonian a term such as Eq. (152) at $\delta = 0$, where p describes the order of commensurability and is defined by $p = 1/\rho_0 a$. In the case of a commensurability $p > 1$, i.e., of an atom density wave competing with disorder, it can be shown (Shankar, 1990) that even a weak disorder turns the atom density wave into an Anderson insulator, by breaking it into domains. Indeed, a density wave has a ground-state degeneracy p, which allows the formation of domain walls. Since the energy cost of a domain wall is a constant proportional to the excitation gap of the pure atom density-wave phase, while the typical energy gained by forming a domain of length L can be estimated to be of order $\propto -\sqrt{DL}$ by a random walk argument (Imry and Ma, 1975), it is always energetically advantageous to break the density-wave phase into domains as soon as $D > 0$. The resulting ground state is gapless and thus a Bose glass.

In contrast, a Mott phase with each site occupied by an integer number of atoms has no ground-state degeneracy, and thus is stable in the presence of a weak (bounded) disorder. There will thus be several additional effects in that case that have to be taken into account. First, at variance with the incommensurate case, it is not possible anymore to eliminate the forward scattering by a simple shift of ϕ. Indeed, the forward scattering which is acting as a slowly varying chemical potential is in competition with the commensurate term $\cos(2\phi)$ just as was the case for the doping in the Mott transition in Sec. VI.A. The disorder will thus reduce the gap and ultimately above a certain threshold destroy the commensurability. Generally, it will reduce the stability of the Mott region compared to Fig. 11. The forward scattering part of the disorder thus leads to a *delocalization* by a reduction of the Mott effects. This is quite general and extends to higher dimensions as well. On the other hand, the effect of the backward potential will be to induce the Anderson localization and leads to the Bose-glass phase, as discussed in the previous section. It is easy to see that even if such a backward scattering was not present to start with, the combination of the forward scattering and the commensurate potential would always generate it. One can thus expect naively, when the disorder is increased, a transition between a Mott insulator, which is *incompressible* and localized to a Bose glass, which is *compressible* and also localized due to the backward scattering.

One interesting question (Fisher *et al.*, 1989) is whether the Bose-glass phase totally surrounds the shrunk Mott lobes in Fig. 11, or whether at commensurate filling, a direct MI-SF transition would be possible. In 1D, this question can be easily answered by looking at the combined renormalization of the commensurate potential, and the one of the backward scattering. For small forward scattering, the commensurate flow (153) is essentially unperturbed. It reaches strong coupling before the forward disorder can cut the RG, which signals the existence of the Mott gap. If the disorder is increased, the flow will now be cut before the scale at which the Mott gap develops. The Mott phase is thus destroyed by the disorder, which corresponds to the shrinking of the Mott lobe. On the other hand, as seen in Eq. (153), K has now being renormalized to small values K^*. Since when the commensurate potential flow is cut, backward scattering is present (or generated) one should then start with the flow for the backward scatting disorder (159). Just at the destruction of the Mott lobe $K \sim 0$ one has $K < 3/2$ and the system is always in the Bose-glass phase. As the *forward* scattering is increased (or alternatively as the initial value of K would be increased), the flow can be cut early enough such that $K^* > 3/2$ and one can be in the superfluid phase where the backward scattering is irrelevant. One thus sees that in 1D the RG

always predicts a sliver of Bose glass between the Mott and superfluid phase. Further analysis confirms these arguments (Svistunov, 1996; Herbut, 1998) and the topology of the phase diagram where the Mott lobes are surrounded by a Bose-glass phase applies to higher dimension as well (Pollet *et al.*, 2009). The Mott insulator Bose-glass phase transition has been understood to be of the Griffiths type (Gurarie *et al.*, 2009). This is to be contrasted with the transition between the Bose glass and the superfluid phase, which is a second order phase transition. The dynamical critical exponent of the latter transition has been suggested to be $z = d$, with no upper critical dimension $d_c = \infty$ (Fisher *et al.*, 1989). This relation is in agreement with the 1D result where the Lorentz invariance of the bosonized theory implies indeed $z = 1$ at the transition.

On the numerical side, the combined effects of disorder and commensurability have been intensively studied. One of the first studies of the effect of bounded disorder on the Mott lobes in 1D (Scalettar *et al.*, 1991; Batrouni and Scalettar, 1992) confirmed the shrinking of the Mott lobes, and the generation of a compressible Bose-glass phase in the weakly and strongly interacting regimes. The phase boundary between the Mott insulator and the Bose glass was further studied by means of strong-coupling expansions, both for finite systems and in the thermodynamic limit (Freericks and Monien, 1996). While for finite systems the results agreed with the ones obtained in Scalettar *et al.* (1991), Batrouni and Scalettar (1992), and Freericks and Monien (1996) pointed out the difficulty in obtaining the thermodynamic limit result from extrapolations of finite-system calculations because of the effect of rare regions imposed by the tails of the bounded disorder distribution.

In the thermodynamic limit, the effect of a bounded and symmetric distribution with $|\epsilon_i| \leq \Delta$ in the grand-canonical phase diagram (depicted in Fig. 6) is to shift the Mott-insulating boundaries inward by Δ. Later studies, using QMC simulations (Prokof'ev and Svistunov, 1998) and DMRG (Rapsch *et al.*, 1999), mapped out the full phase diagram for the Bose-Hubbard model in the presence of disorder [see also Pai *et al.*(1996)]. The phase diagram at fixed density $n = 1$ is shown in Fig. 13. It exhibits, when starting from the Mott-insulating phase, a reentrant behavior into the Bose-glass phase with increasing disorder strength. It also fully confirms the reentrance of the localized phase at small repulsion in agreement with Fig. 12.

Another interesting class of effects occur when the filling is commensurate and the disorder respects particle-hole symmetry. This is not the case of the random on-site potential, and is traduced by the presence of the forward scattering term. On the contrary, for hard-core bosons this would be the case of the random hopping term. This is a rather natural situation for spin chains, for which random exchange can be realized. In that case, there is an important difference with the case (158). Because of the commensurability $e^{i2\pi\rho_0 x} = 1$, the disorder term is

$$\hat{H}_{\rm dis} = \int dx V(x)\rho_0 \cos[2\hat{\phi}(x)]. \tag{160}$$

Although the two terms look superficially similar, there is thus no random phase on which $\phi(x)$ must pin. $\phi(x)$ is thus oscillating between the two minima $\phi = 0$ and $\phi = \pi/2$,

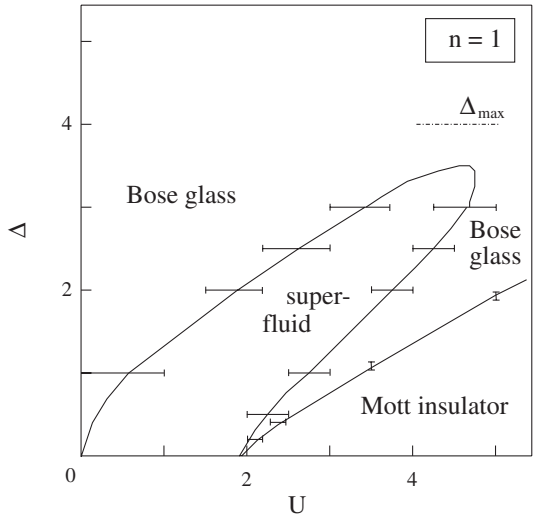

FIG. 13. Phase diagram of the Bose-Hubbard model, for commensurate filling $n = 1$, with an additional uniformly distributed disorder in the interval $[-\Delta, \Delta]$. Notice the presence of the Bose-glass phase between the Mott insulator and the superfluid, and the reentrant behavior in the Bose-glass phase when increasing the disorder amplitude for $2 \lesssim U \lesssim 5$. From Rapsch *et al.*, 1999.

and the physics of the problem is totally controlled by the kink between these two minima. Thus, although the initial steps of the flow (159) are identical for the two problems, the strong-coupling fixed points are different. In the particle-hole symmetric case, a delocalized state exists in the center of the band, leading to various singularities. This is a situation which is well adapted to the above mentioned real space RG (Fisher, 1994), and the system is dominated by broad distributions (so-called random singlet phase).

3. Superlattices and quasiperiodic potentials

As seen in the previous sections, the periodic and disordered potentials albeit leading to very different physical phases, seem to share some common features. In particular, disorder can be viewed as a potential for which all Fourier harmonics would be present. It is thus a natural question on whether one could generalize the case of a simple periodic potential to potentials with several periodicities or even to quasiperiodic potentials. In addition to the pure theoretical interest of this problem, it has become, thanks to optical lattices in cold atomic gases, an extremely relevant question experimentally. Consider first the case of a superlattice, i.e., of a potential with two commensurate periods Q_1 and Q_2. For simplicity, we assume in what follows that the first periodic potential is very large and thus defines the model on a lattice, and that the second potential is superimposed on this lattice. This defines a variant of the Bose-Hubbard Hamiltonian

$$\hat{H} = \sum_{i=1}^{L}\left[-t_i(\hat{b}_i^\dagger \hat{b}_{i+1} + \text{H.c.}) + \epsilon_i \hat{n}_i + \frac{U}{2}\hat{b}_i^\dagger \hat{b}_i^\dagger \hat{b}_i \hat{b}_i \right], \tag{161}$$

where $t_{i+l} = t_i$ and $\epsilon_i = \epsilon_{i+l}$ with $l \geq 2$.

The case of a commensurate superlattice (i.e., when Q_1 and Q_2 are commensurate) falls in the problems already described in Sec. VI.A. This situation allows one to obtain Mott-insulating states with fractional filling (Buonsante

et al., 2004; Buonsante and Vezzani, 2004; 2005; Rousseau *et al.*, 2006). The physics can be easily understood in the TG limit. In that case, one has free fermions in a periodic potential. The eigenstates of the noninteracting fermion Hamiltonian form l distinct bands separated by energy gaps. Within a given band, the eigenstates are indexed by a quasimomentum defined modulo $2\pi/l$, so that quasimomenta can be taken in the interval $[-\pi/l, \pi/l]$ (called the first Brillouin zone in solid state physics). The filling is determined by the condition $n_0 = N/L = \sum_{n=1}^{l} \int_{-k_{F,n}}^{k_{F,n}} dk/2\pi$, where n is the band index and $k_{F,n}$ is the Fermi wave vector in the nth band. As the density is increased, bands get progressively filled. From this picture, it is clear that when the highest nonempty band is partially filled, the system will be in a gapless state, which as we saw previously can be described as a Tomonaga-Luttinger liquid with exponent $K = 1$. However, when the highest nonempty band is completely filled, there is a gap to all excitations above the ground state and one obtains a Mott insulator. This situation is obtained every time the filling is an integer multiple of $1/l$, thus allowing the observation of a Mott-insulating state for a filling with less than one boson per site. In some cases, two energy bands may cross and, since there will be no gap, the system may not be insulating for some integer multiples of $1/l$ (Rousseau *et al.*, 2006).

For finite U, one can use bosonization and is back to the situation described in Sec. VI.A where one has added a periodic potential leading to an operator with $p > 1$. These terms will be relevant for $K < 2/p^2$, so that they can only contribute in the case of systems with long-range interaction, as discussed in Sec. VI.A.

An instructive way to understand the effect of the competition between U and the superlattice potential is to consider the atomic limit. For concreteness, assume that $\epsilon_i = A\cos(2\pi i/l)$ with $l = 2$. In this case, we have to deal with a two-site problem and $n = N/2$ (N is the number of bosons). In order to minimize the energy, the first particle should be added to the site with $\epsilon = -A$, i.e., the boundary between $n = 0$ and $n = 1/2$ occurs at $\mu \equiv E(n=1/2) - E(n=0) = -A$, and for $\mu < -A$ the system is empty. The fate of the second particle added will depend on the relation between A and U. If $A < U$, the energy is minimized by adding it to the site with $\epsilon = A$, i.e., the energy increases in A, while if $A > U$ then the second particle should be added to the site with $\epsilon_i = -A$, i.e., the energy increases in $U - A$. As a result, the boundary between $n = 1/2$ and $n = 1$ occurs at $\mu = \min(A, U - A)$, so that for $-A < \mu < \min(A, U - A)$ the density in the system is $n = 1/2$ (this phase is also referred to in the literature as a charge-density wave), and so on (see left panel in Fig. 14). As in the Bose-Hubbard model (Sec. IV.B.2), starting from the atomic limit result, one can perturbatively realize that the effect of a very small hopping amplitude will be to generate compressible superfluid phases between the boundaries of the insulating phases. An exact phase diagram for finite hopping from Rousseau *et al.* (2006), obtained using QMC simulations, is presented in the right panel in Fig. 14.

Incommensurate superlattices exhibit quite a different behavior. The case of two incommensurate periodicities is known as the Harper model (Hiramoto and Kohmoto, 1992), and constitutes one of the cases of quasiperiodic potentials. How such quasiperiodic potentials lead to properties similar or different from disordered ones is a long standing question. For noninteracting particles, the question can be addressed analytically. In a lattice, the model is known as the Aubry-André model (Hofstadter, 1976; Aubry and Andre, 1980; Jitomirskaya, 1999)

$$\hat{H} = \sum_{i=1}^{L} [-t(\hat{b}_i^\dagger \hat{b}_{i+1} + \text{H.c.}) + V_2 \cos(2\pi\beta i)\hat{n}_i]. \quad (162)$$

Here t is the tunneling rate and V_2 is the amplitude of the quasiperiodic modulation of the potential energy, while β is an irrational number. Such a model exhibits a localization transition even in 1D with a critical value $V_2/t = 2$. A duality transformation maps the Aubry-André model at $V_2/t > 2$ on the same model at $V_2/t < 2$ (Aubry and Andre, 1980). Below criticality, all states are extended Bloch-like states characteristic of a periodic potential. Above criticality, all states are exponentially localized and the spectrum is pointlike. At criticality, the spectrum is a Cantor set, and the gaps form a

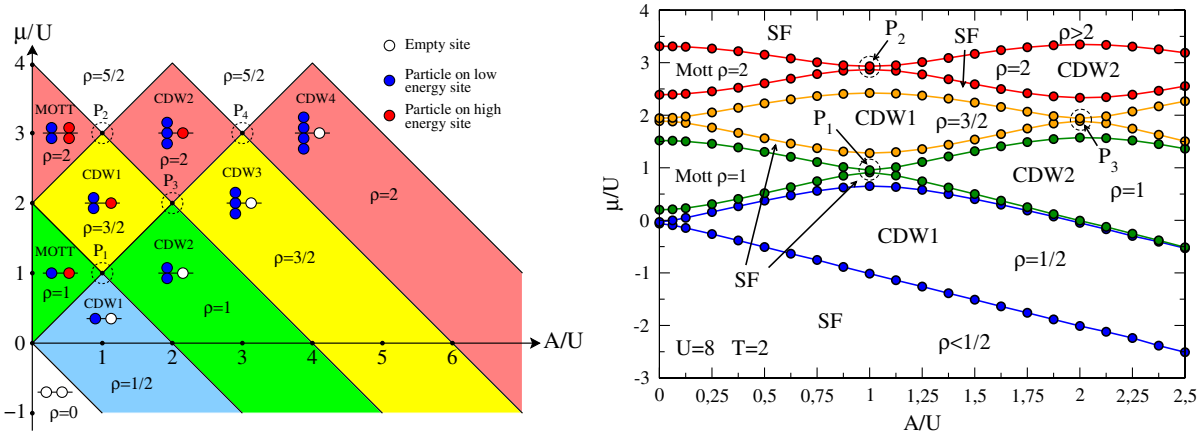

FIG. 14 (color online). (Left panel) Phase diagram of soft-core bosons in the atomic limit ($t = 0$) in a superlattice with $l = 2$. A is the amplitude of the periodic potential, T is its period, μ is the chemical potential, and ρ is the number of particle per site. (Right panel) Phase diagram computed with QMC simulations for $U = 8t$. In the latter, notice the appearance of superfluid phases (SF in the figure) in between the insulating ones. From Rousseau *et al.*, 2006.

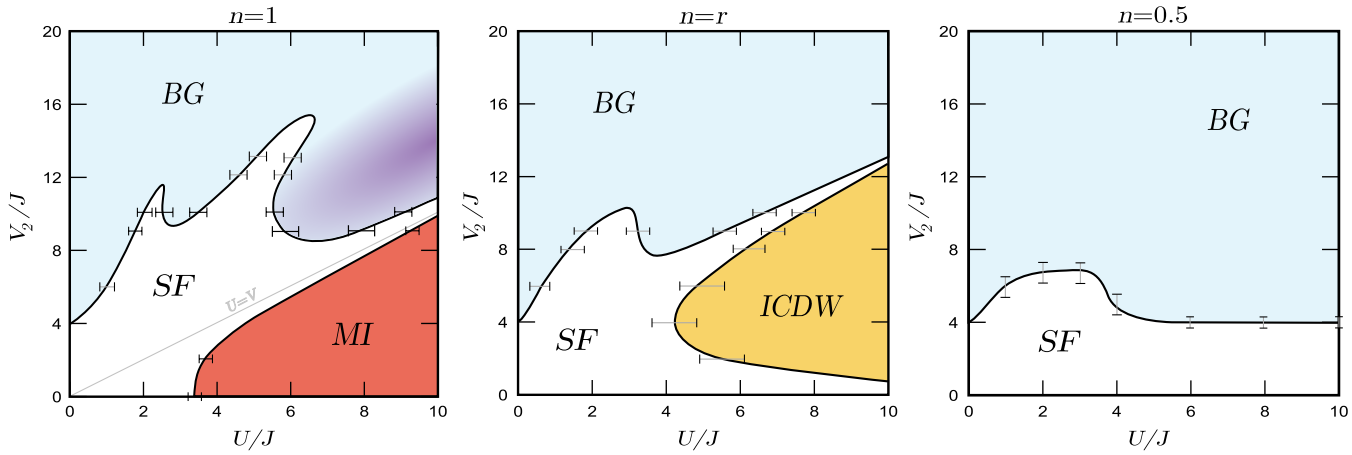

FIG. 15 (color online). Phase diagrams of the bichromatic Bose-Hubbard model for densities $n = 1$, r (the ratio of the potential wave lengths), and $n = 0.5$. SF stands for the superfluid phase, MI for the Mott-insulating phase, BG for the "Bose-glass" phase (meaning localized but with zero one-particle gap), and ICDW for incommensurate charge-density wave phase. The $U = V_2$ line on the phase diagram with $n = 1$ indicates the $J = 0$ limit for which the gap of the one-particle excitation vanishes. In the phase diagram with density $n = 1$, the darker region in the BG phase is localized but could have a small gap which cannot be resolved numerically. From Roux *et al.*, 2008.

devil's staircase (Harper, 1955). Some differences at the semiclassical level between this type of potential and localization by disorder were pointed out (Albert and Leboeuf, 2010). A generalization of the Aubry-André model to the presence of a nonlinear term in the dynamics was discussed by Flach *et al.* (2009). The crossover between extended to localized states in incommensurate superlattices has been experimentally observed for a noninteracting ^{39}K BEC where the effect of interactions has been canceled by tuning a static magnetic field in proximity of a Feshbach resonance to set the scattering length to zero (Roati *et al.*, 2008).

What remains of such a transition in the presence of interactions is of course a very challenging question. Here the effects of interactions can be taken into account within a mean-field type of approach (Larcher *et al.*, 2009) or by a bosonization technique. A unifying description of all types of potentials including periodic, disordered, and quasiperiodic (QP) was proposed by Vidal *et al.* (1999, 2001), by generalizing Eqs. (153) and (159) to a potential with arbitrary Fourier components $V(q)$. For quasiperiodic potentials, such as the Fibonacci sequence, the transition between a superfluid phase and a phase dominated by the QP potential was found. The critical point K_c depends on an exponent characteristic of the QP potential itself. These conclusions were confirmed by DMRG calculations on quasiperiodic spin and Hubbard chains (Hida, 1999; 2000; 2001). The case of the Aubry-André potential was studied by exact diagonalization (Roth and Burnett, 2003a; 2003b) on 8 and 12 site systems and also for the case of a specific choice of the height of the secondary lattice (Roscilde, 2008).

DMRG approaches (Deng *et al.*, 2008; Roux *et al.*, 2008), combined with the above analytical considerations, allowed for a rather complete description of the physics of such quasiperiodic systems. As discussed, for fillings commensurate with either the primary or the secondary lattice, the periodic potential changes the simple quadratic Hamiltonian of the Tomonaga-Luttinger liquid into a sine-Gordon Hamiltonian, which describes the physics of the Mott transition (Giamarchi, 2004). A Mott insulator is obtained in a case of filling commensurate with the primary lattice, and a pinned incommensurate density wave (ICDW) for filling commensurate with the secondary lattice. For fillings incommensurate with both lattices, the potential is irrelevant under RG flow and one expects from perturbative analysis a superfluid phase for all values of the interaction strength. As a consequence, when one of the potentials is commensurate, no Bose-glass phase can be created by the other potential in the vicinity of the Mott insulator superfluid transition in the regime where bosonization is applicable. In agreement with the limiting cases of free and hard-core bosons described by an Aubry-André problem, the transition towards the Bose-glass phase is found at $V_2/t \geq 2$, the critical value of V_2 being higher for bosons with finite interaction strength. Another feature of an interacting Bose gas in quasiperiodic potential is the shrinking of the Mott lobes as a function of V_2. The computed phase diagram in the $(V_2/J, U/J)$ plane for both commensurate and incommensurate fillings is reported in Fig. 15.

The Bose-glass phase has been shown to be localized by computing the expansion of the 1D cloud (Roux *et al.*, 2008), as is relevant for the experimental situation. Although from the point of view of the phase diagram, the localized nature of the phase in interacting quasiperiodic and disordered systems are found to be very similar, some experimental probes have been found to show some marked differences between the two cases (Orso *et al.*, 2009). Interacting quasiperiodic potentials are a problem deserving more experimental and theoretical investigations. We should add that the influence of a third harmonic as well as confining potentials in such systems have already been investigated by Roscilde (2008).

VII. MIXTURES, COUPLED SYSTEMS, AND NONEQUILIBRIUM

In this section, we briefly examine several developments going beyond the simple case of 1D bosons in the presence of an external potential. We present three main directions where new physics is obtained by either (i) mixing bosonic systems,

or bosonic and fermionic systems; (ii) going away from the 1D situation by coupling chains or structures. This leads to quasi-1D systems which links the 1D world with its higher dimensional counterpart; and (iii) setting systems out of equilibrium.

A. Multicomponent systems and mixtures

Compared to the case of a single component bosonic system, described in the previous sections, novel physics can be obtained by mixing several components in a 1D situation or giving to the bosons an internal degree of freedom.

1. Bose-Bose mixtures

Internal degrees of freedom for bosons lead to a wider range of physical phenomena. We focus here on the case of two internal degrees of freedom and refer the reader to the literature for the higher symmetry cases (Cao *et al.*, 2007; Essler *et al.*, 2009; Lee *et al.*, 2009; Nonne *et al.*, 2010). For two components, this is similar to giving a "spin" $1/2$ to the bosons. The corresponding case for fermions is well understood (Giamarchi, 2004). Because of the Pauli principle, a contact interaction in such a system can only exist between opposite spins $U = U_{\uparrow,\downarrow}$. The ground state of the two-component fermionic systems is in the TLL universality class, with dominant antiferromagnetic correlations. Quite remarkably, because in the TLL's everything depends on collective excitations, the Hilbert space separates into two independent sectors, one for the collective charge excitations, one for the spins. This phenomenon, known as spin-charge separation, is one of the hallmarks of the 1D properties.

For the case of two-component bosons, the situation is much richer. First, even in the case of contact interactions, interactions between the same species must be considered. The properties of the system thus depend on three interaction constants $U_{\uparrow,\uparrow}$, $U_{\downarrow,\downarrow}$, and $U_{\uparrow,\downarrow}$. The dominant magnetic exchange will be crucially dependent on those interactions (Duan, *et al.*, 2003), and can go for dominantly antiferromagnetic if $U_{\uparrow,\uparrow}$, $U_{\downarrow,\downarrow} \gg U_{\uparrow,\downarrow}$ while they are dominantly *ferromagnetic* in the opposite case. In particular, the isotropic case corresponds to a ferromagnetic ground state (Eisenberg and Lieb, 2002). The phase diagram of such systems can be obtained by using either a TLL description or numerical approaches such as DMRG or time evolving block decimation (Kleine *et al.*, 2008a; 2008b; Mathey, Danshita, and Clark, 2009; Takayoshi, Sato, and Furukawa, 2010). Probes such as noise correlations, as will be discussed in the next section, can be used to study the phases of such binary bosonic mixtures (Mathey, Vishwanath, Altman, 2009). When the exchange is dominantly antiferromagnetic, the physics is very similar to the fermionic counterpart, with two collective modes for the charge and spin excitations, and can be described in the TLL framework. Such bosonic systems thus provide an alternative to probe for spin-charge separation (Kleine *et al.*, 2008a; 2008b) compared to the electronic case for which this property could only be probed for quantum wires (Auslaender *et al.*, 2002; Tserkovnyak *et al.*, 2002). Depending on the interactions, one of the velocities can vanish, signaling an instability of the two-component TLL. This signals a phase separation that corresponds to entering into the ferromagnetic regime which we now examine.

When the ground state of the system is ferromagnetic, a phenomenon unusual to 1D takes place. Indeed, the system has now spin excitations that have a dispersion behaving as k^2 (Sutherland, 1968; Li, *et al.*, 2003; Fuchs *et al.*, 2005; Guan *et al.*, 2007), which cannot be described by a TLL framework. This leads to the interesting question of the interplay between charge and spin excitations, and it has been proposed (Zvonarev *et al.*, 2007) that such a system belongs to a new universality class, called "ferromagnetic liquid." This field is currently very active (Akhanjee and Tserkovnyak, 2007; Guan *et al.*, 2007; Matveev and Furusaki, 2008; Kamenev and Glazman, 2009; Caux *et al.*, 2009; Zvonarev *et al.*, 2009a; 2009b), and we refer the reader to the literature for further discussions on this subject and references.

2. Bose-Fermi mixtures

Cold atomic systems have allowed for the interesting possibility to realize Bose-Fermi mixtures. Such systems can be described by the techniques described in the previous sections, both in the continuum case and on a lattice. In the continuum, a Bose-Fermi mixture can be mapped, in the limit when the boson-boson interaction becomes hard core, to an integrable Gaudin-Yang model (Gaudin, 1967; Yang, 1967). For special symmetries between the masses and couplings, a mapping to an integrable model exists (Lai and Yang, 1971; Lai, 1974; Batchelor *et al.*, 2005b; Frahm and Palacios, 2005; Imambekov and Demler, 2006, 2006; Guan, *et al.*, 2008). In the case of a lattice, the system can be described by a generalized Bose-Hubbard description in which the parameters can be obtained from the continuum description (Albus *et al.*, 2003). Similar to the continuum case, if the boson-boson repulsion becomes infinite, the hard-core bosons can be mapped onto fermions either by using the boson-fermion mapping (Girardeau and Minguzzi, 2007) or by using the Jordan-Wigner transformation of Sec. II.D leading (Sengupta and Pryadko, 2007) to a 1D Fermi-Hubbard model that can be described by Bethe ansatz (Lieb and Wu, 1968) or by the various low energy or numerical methods appropriate for fermionic systems (Giamarchi, 2004).

Quite generally, the low energy of Bose-Fermi mixtures can be described by the TLL description (Cazalilla and Ho, 2003; Mathey *et al.*, 2004). As for Bose-Bose mixtures, the resulting low-energy Hamiltonian has a quadratic form and can be diagonalized by a linear change of variables (Muttalib and Emery, 1986; Loss and Martin, 1994; Cazalilla and Ho, 2003), which leads to two collective modes with two different velocities. The elementary excitations are polaronic modes (Mathey *et al.*, 2004; Mathey and Wang, 2007). In a similar way, the exponents of the correlation functions are given by the resulting TLL Hamiltonian (Mathey and Wang, 2007; Orignac *et al.*, 2010). Also, similar to the Bose-Bose mixtures, when the velocity of one of the mode vanishes, the two-component Tomonaga-Luttinger liquid shows an instability. This instability can be, depending on the coupling constants, either a phase separation or a collapse of the system. This is the analog of the Wentzel-Bardeen instability (Bardeen, 1951; Wentzel, 1951) obtained in 1D electron-phonon systems (Loss and Martin, 1994).

Several interesting extensions to this physics exist when the components of the mixture are close in density (Cazalilla and Ho, 2003; Mathey *et al.*, 2004). In particular, bound states of bosons and fermions can form leading to a TLL of composite particles (Burovski *et al.*, 2009). In the presence of a lattice, commensurability with the lattice can give rise to partially gapped phases, in a similar way to the Mott physics described in the previous section (Mathey and Wang, 2007; Mathey, Danshita, and Clark, 2009), and, in general, to very rich phase diagrams (Sengupta and Pryadko, 2007; Pollet *et al.*, 2006, 2008; Hébert *et al.*, 2007, 2008; Rizzi and Imambekov, 2008; Zujev *et al.*, 2008). Similarly, disorder effects can be investigated for Bose-Fermi mixtures (Crépin *et al.*, 2010).

The lattice Bose-Fermi Hubbard model has also been studied by worldline quantum Monte Carlo simulations (Takeuchi and Mori, 2005a; 2005b) and phase separation was found as a function both of the interparticle interaction and of the fermion density. The mixed phase was instead studied using stochastic series expansions by Sengupta and Pryadko (2007). For weak coupling, two-component TLL behavior was found, whereas, at strong coupling and commensurate filling, a phase with total gapped density mode was identified. Doping the gapped phase $n_F + n_B = 1$ with fermions was shown to lead to supersolid order (Hébert *et al.*, 2008). The ground-state phase diagram was obtained using the canonical worm algorithm for $n_F = n_B = 1/2$ by Pollet *et al.* (2006) and for other commensurate as well as incommensurate fillings by Zujev *et al.* (2008). The effect of a harmonic trapping potential was considered using both DMRG and quantum Monte Carlo calculations by Pollet *et al.* (2008) and a complete analysis of the boson visibility appeared in Varney *et al.* (2008).

B. Coupled systems

Although the extended Bose-Hubbard model [Eq. (14)], describes a single chain system, its bosonization description requires doubling the number of degrees of freedom, which means that it effectively becomes two coupled (hard-core boson or spin-$\frac{1}{2}$) systems. Here, we pursue further this issue and consider the rich physics that arises when coupling many such 1D systems. Reasons for studying coupled 1D boson systems are manifold. The main motivation is, of course, an experimental one, since many experimental realizations of 1D systems are typically not created in isolation but in arrays containing many of them. Considering the possible ways they can be coupled such as via quantum tunneling and/or interactions leads to many interesting theoretical questions. These include the understanding of the way in which the properties and excitations of the system evolve, as a function of the temperature or the energy scale at which the system is probed, from the fairly peculiar properties of 1D to the more familiar ones of higher dimensional systems (Giamarchi, 2010). Other important questions concern the competition between different ordered phases, which are stabilized by either interactions or tunneling between the different 1D systems. We next review the work done on some of these questions.

One of the simplest situations allowing one to transition from a low-dimensional to a high-dimensional system is provided by coupling zero dimensional objects. This is, for example, the case in spin systems where pairs of spins can form dimers. Such dimers form zero dimensional objects that can then be coupled into a higher dimensional structure by additional magnetic exchanges. Since the dimers are normally in a singlet state, separated by a gap from the triplet, a weak coupling between them is irrelevant and the ground state still consists in a collection of uncoupled singlets. A quantum phase transition can thus be obtained in two ways: (i) one can increase the coupling up to a point at which the ground state changes and becomes an antiferromagnetic one (Sachdev, 2008) or (ii) one can apply a magnetic field leading to transitions between the singlet and triplet states. As can be seen from the mappings of Sec. II.D, this model corresponds then to hard-core bosons (representing the triplet states) on a lattice and can lead to Bose-Einstein condensation and various interesting phases (Giamarchi *et al.*, 2008), which will be further described in the next section on experiments.

For bosonic chains, a typical coupling between the 1D systems is provided by a Josephson coupling

$$\hat{H}_J = -t_\perp \int \sum_{\langle \mathbf{R},\mathbf{R}'\rangle} [\hat{\Psi}^\dagger_{\mathbf{R}}(x)\hat{\Psi}_{\mathbf{R}'}(x) + \text{H.c.}]. \tag{163}$$

Such a term will combine with the 1D physics and lead to novel phases. In the case for which the physics of the 1D systems is described by a Tomonaga-Luttinger liquid, the interchain coupling is strongly renormalized by the 1D fluctuations (Efetov and Larkin, 1975; Ho *et al.*, 2004; Cazalilla *et al.*, 2006). Using the various mappings of Sec. II.D, such physics is relevant in various context ranging from spin chains (Schulz, 1996) to classically coupled XY planes (Benfatto *et al.*, 2007; Cazalilla *et al.*, 2007; Mathey, Polkovnikov, and Neto, 2008). Although the system becomes essentially an anisotropic 3D ordered system (superfluid or magnetically ordered), new modes (Higgs modes) appear (Schulz, 1996; Cazalilla *et al.*, 2006; Huber *et al.*, 2007; Huber *et al.*, 2008; Menotti and Trivedi, 2008) due to the quasi-1D nature of the system. Such modes have also been observed in strongly correlated anisotropic 3D systems.

When the 1D physics is gapped, such as in a Mott insulator, an interesting competition occurs between the 1D gap and the Josephson coupling. This leads to a quantum phase transition for which the system goes from a 1D Mott insulator to a higher dimensional superfluid. Such a deconfinement (Giamarchi, 2010) is relevant for a variety of systems ranging from spins to fermions. In the case of coupled bosonic systems, it can be studied (Ho *et al.*, 2004; Cazalilla *et al.*, 2006) by the low-energy methods described in the previous sections. Interesting results are also found in the case of a finite number of coupled chains [so-called ladder systems (Dagotto and Rice, 1996)] or planes. We refer the reader to the literature (Donohue and Giamarchi, 2001; Luthra *et al.*, 2008) for more on this subject.

C. Nonequilibrium dynamics

Another topic of much current interest is the nonequilibrium dynamics of 1D quantum systems (Dziaramga, 2010; Cazalilla and Rigol, 2010; Polkovnikov *et al.*, 2011). Research on this topic is mainly motivated by ultracold gases

experiments, where the unique degree of tunability, isolation, and long coherent times have enabled the exploration of phenomena not previously accessible in condensed matter experiments. In the latter, a strong coupling to the environment, combined with the short time scales associated to their microscopic properties, usually lead to rapid decoherence.

As discussed in Sec. VIII.D, driving cold gases with time-dependent potentials can be used to probe several properties of interest, such as the excitation spectra. However, the physics out of equilibrium is far richer than that. Optical lattices and Feshbach resonances can be used to transition between weakly and strongly interacting regimes in controllable time scales, and to generate exotic out of equilibrium states (Greiner *et al.*, 2002b; Winkler *et al.*, 2006; Strohmaier *et al.*, 2010; Will *et al.*, 2010). Those could lead to new phenomena and phases not present in systems in thermal equilibrium. Studying the dynamics of cold gases can also help us gain a better understanding of the inner working of statistical mechanics in isolated quantum systems (Rigol *et al.*, 2008). Furthermore, now that nearly integrable systems can be realized in experiments (Kinoshita *et al.*, 2004; Paredes *et al.*, 2004), one can study their dynamics and address questions previously considered purely academic, such as the effect of integrability in the properties of the gas after relaxation (Kinoshita *et al.*, 2006).

Some of the early studies of the nonequilibrium dynamics in 1D geometries addressed the effect of a lattice potential and the onset of the superfluid to Mott insulator transition on the transport properties of a bosonic gas (Stöferle *et al.*, 2004b; Fertig *et al.*, 2005b). In those experiments, the systems were loaded in deep two-dimensional optical lattices with a weaker lattice along the 1D tubes (see Sec. VIII.D). The harmonic trap along the 1D tubes was then suddenly displaced by a few lattice sites and the dynamics of the center of mass studied by time-of flight (TOF) expansion. Surprisingly, it was found that even very weak optical lattices could produce large damping rates,[6] and that, in some regimes, overdamping took place with the center of mass staying away from the center of the trap. The former effect was related to the large population of high momenta resulting from the strong transverse confinement (Ruostekoski and Isella, 2005), while the latter was related to the appearance of a Mott insulator in the trap (Rey *et al.*, 2005; Rigol *et al.*, 2005; Pupillo *et al.*, 2006). More recently, time-dependent DMRG studies have accurately reproduced the experimental findings in the regime where the one-band Bose-Hubbard model is a valid representation of the experiments (Danshita and Clark, 2009; Montangero *et al.*, 2009).

Correlations in 1D systems can manifest themselves in surprising ways out of equilibrium. As noted by Sutherland (1998), if a gas of interacting bosons is allowed to expand under a 1D geometry, the resulting momentum distribution after long expansion times can be very different from the initial momentum distribution of the trapped system, as opposed to what will happen in the usual TOF expansion in three dimensions. In fact, it has been shown both for the lattice (Rigol and Muramatsu, 2005a; 2005b) and continuum (Minguzzi and Gangardt, 2005; del Campo and Muga, 2006; del Campo, 2008) TG gas that free expansion results in the ''dynamical fermionization'' of the bosonic momentum distribution function. This is something that only occurs out of equilibrium and leads to a bosonic momentum distribution with a Fermi edge. The expansion of the more generic Lieb-Liniger gas has been studied by Jukić *et al.* (2008) using a Fermi-Bose transformation for time-dependent states (Buljan *et al.*, 2008). They found that, asymptotically, the wave functions acquire a Tonks-Girardeau structure but the properties of the gas are still very different from those of a TG gas in equilibrium. Gritsev, Barmettler, and Demler (2010) used a scaling transformation that mapped the time-dependent many-body Schroedinger equation on a time-independent model. A similar fermionization was observed for the momentum distribution function, even though the effective interaction parameter remained constant throughout, ruling out dilution as a cause of the fermionization. An analysis of the Lieb Liniger gas based on integrability was pioneered in Gritsev, Rostunov, and Demler, 2010.

The ultimate effect of one dimensionality in the dynamics of isolated systems may be the lack of thermalization associated to integrability. In a remarkable experiment, Kinoshita *et al.* (2006) studied the relaxation dynamics of an array of 1D bosonic gases created by a deep 2D optical lattice. They found that, as long as the system remained 1D, no relaxation occurred towards the expected thermal result. In the TG limit, in which the 1D system is integrable, the lack of thermalization can be understood to be a result of the constraints imposed by conserved quantities that make the TG gas integrable. Interestingly, in that regime, few-body observables after relaxation can still be described by a generalization of the Gibbs ensemble (GGE) (Rigol *et al.*, 2007). The GGE density matrix can be constructed following Jaynes (1957a, 1957b) principle of maximization of the many-body entropy subject to constraints, which in this case are a complete set of integrals of motion. The relevance of the GGE to different 1D integrable systems and few-body observables, as well as its limits of applicability, have been the subject of several studies during the last years (Cazalilla, 2006; Rigol, Muramatsu, Olshanii, 2006; Calabrese and Cardy, 2007; Rigol *et al.*, 2007; Barthel and Schollwöck, 2008; Cramer *et al.*, 2008; Kollar and Eckstein, 2008; Iucci and Cazalilla, 2009; Rossini *et al.*, 2009; Cassidy *et al.*, 2011; Fioretto and Mussardo, 2010; Iucci and Cazalilla, 2010).

In the opposite limit of nonintegrable systems, i.e., far from any integrable point, thermalization has been found to occur in general, despite the fact that the dynamics is unitary. Early studies in 1D lattice models resulted in mixed results in which thermalization was reported in some regimes and not in others (Kollath *et al.*, 2007; Manmana *et al.*, 2007; Roux, 2009). In 2D lattices, thermalization was observed in rather small systems (Rigol *et al.*, 2008) and was understood in terms of the eigenstate thermalization hypothesis (ETH) (Deutsch, 1991; Srednicki, 1994). Later systematic studies in 1D lattices have shown that, in general, thermalization occurs in nonintegrable 1D systems as it does in higher dimensions. However, the eigenstate thermalization hypothesis, and thermalization, break down as one approaches

[6]In a harmonic trap, in the absence of a lattice, no damping should occur as the center of mass follows the classical equation of motion of a harmonic oscillator.

integrable points (Rigol, 2009a, 2009b; Roux, 2010). This may be the reason behind the lack of thermalization observed by Kinoshita *et al.* (2006) for all 1D regimes, while relaxation to thermal equilibrium was inferred to occur in 1D experiments on atom chips (Hofferberth *et al.*, 2007). While the former were not sufficiently away from integrability, the latter were (Mazets *et al.*, 2008; Mazets and Schmiedmayer, 2010).

Many questions remain open in this exciting area of research. We mention some of them in the Outlook section at the end.

VIII. EXPERIMENTAL SYSTEMS

Experimentally, 1D quantum liquids have been created in various forms. We review several of them in this section. In the first three subsections, we examine condensed matter realizations, whereas the last subsection is devoted to ultracold atom realizations. Some of the former, such as spin ladder compounds subject to strong magnetic fields, have yielded a wealth of experimental evidence for exotic behavior related to the Tomonaga-Luttinger liquid. Ultracold atomic systems have properties that are largely tunable and therefore hold many promises for reaching regimes that are hardly accessible in condensed matter systems. However, their properties can only be tested by a still rather limited number of probes. Hence, the discussion of these systems is intimately linked to the developments related to the probes used to investigate their properties.

A. Josephson junctions

a. Theory: In a superconductor, electrons with opposite spins form Cooper pairs. The pairs have bosonic statistics so that a superconductor can be seen as a system of interacting bosons. In a Josephson junction, two grains (μm sized) of superconducting metal are separated by a barrier of insulating or nonsuperconducting material. Each grain is small enough to have a well-defined superconducting phase θ_j. The operator measuring the number of Cooper pairs transferred to the jth grain is $\hat{N}_j = \hat{Q}_j/(2e)$, where $\hat{Q}_j$ measures the charge imbalance of the grain and $2e$ is the Cooper-pair charge. The electrostatic energy of the charged grain is $E_C\hat{N}_j^2/2 - \delta\mu\hat{N}_j$, where $E_C = 4e^2/C$ and $\delta\mu = V_g/2e$, C being the capacity of the grain and V_g the gate potential. The phase rigidity of the superconductor leads to a contribution $-E_J\sum_j \cos[\hat{\theta}_j - \hat{\theta}_{j+1} - (2e/\hbar)\int_{\mathbf{r}_j}^{\mathbf{r}_{j+1}} d\mathbf{r}\cdot\mathbf{A}(\mathbf{r})]$ in the case of a chain, where $\mathbf{A}$ is the electromagnetic vector potential. Since $[\hat{N}_i, \hat{\theta}_j] = i\delta_{ij}$, the Josephson junction chain is a realization of the model (25), where V_g controls the chemical potential $\delta\mu$ of the Cooper pairs (Bradley and Doniach, 1984; Fazio and van der Zant, 2001).

The model defined by the Hamiltonian (25), the so-called phase model, was shown (Bradley and Doniach, 1984) to exhibit a zero-temperature superconductor-insulator phase transition for $V_g = 0$ (i.e., the particle-hole symmetric case) driven by the ratio of Josephson to charging energy, analogous to the transition between superfluid order and the bosonic Mott insulator discussed in Sec. VI. The insulating regime is called the Coulomb blockade of Cooper-pair tunneling (CBPCT). Using an approximate mapping of the Hamiltonian (25) onto the t-V model (Glazman and Larkin, 1997), the nonparticle-hole symmetric case ($V_g \neq 0$) can be analyzed. A CBPCT phase is predicted for integer filling, recovering the result of Bradley and Doniach (1984) while for fillings close to a half-integer number of particles per site a density-wave phase is obtained. For incommensurate filling or half-filling and weak or short-ranged electrostatic repulsion, a fluid phase is predicted. This model has also been studied with quantum Monte Carlo simulations (Baltin and Wagenblast, 1997).

b. Experiments: As we have seen previously, Josephson junction arrays provide an experimental realization of interacting boson systems. Experiments to probe the phase transition between the bosonic Mott insulator and the Tomonaga-Luttinger liquid have been reported. Chains of Josephson junctions are prepared by lithography. The capacities and influence coefficients are determined by the geometry. Because of the finite dimension of the grains, the application of a magnetic field can be used to create a dephasing that reduces the tunneling amplitude of the Cooper pairs $\tilde{E}_J = E_J|\cos(\pi\Phi/\Phi_0)|$, where Φ is the magnetic flux applied between the grains and $\Phi_0 = h/(2e)$ is the flux quantum for a Cooper pair. Since the repulsion between Cooper pairs is not affected, this allows one to vary the ratio of Coulomb to Josephson energy and induce the superconductor-insulator transition by increasing the applied magnetic field.

Experiments with $Al/Al_2O_3/Al$ junctions of 200 nm size show, as a function of magnetic field, a transition from a regime of high electrical conductance to a regime with a voltage threshold for electrical conduction (Chow *et al.*, 1998; Haviland *et al.*, 2000; Watanabe and Haviland, 2002), in qualitative agreement with the theoretical predictions (Bradley and Doniach, 1984). However, a study of scaling near the quantum phase transition (Kuo and Chen, 2001) showed disagreement between the measured critical exponent ν and the theoretical expectations (Fisher *et al.*, 1989). A possible explanation is the presence of random offset charges on the junctions (which in the boson language correspond to a random potential) which might turn the transition into an Anderson localization transition as discussed in Sec. VI.B. Another explanation could be related to the dissipation which has been neglected in Sec. II.C.

Dissipation can be included by adding to the Matsubara action a term proportional to $(1/\hbar\beta)(R_Q/R)\sum_n|\omega_n||\hat{\theta}(\omega_n)^2|$, where $R_Q = h/(4e^2)$ is the quantum of resistance, R is the resistance of the junction, and θ is the phase *difference* across the junction (Korshunov, 1989a, 1989b; Bobbert *et al.*, 1990, 1992). In the presence of such terms, a richer phase diagram is obtained with new superconducting phases. However, in the vicinity of the superconductor-insulator critical point, the dissipative contribution to the action could become relevant, and change the universality class of the phase transition.

Although the problem of quantum phase transitions in dissipative systems is interesting in its own right, this change of universality class would make Josephson junctions arrays unsuitable as an experimental realizations of the phase model (25). Another more direct realization of interacting bosons

using Josephson junctions is provided by the vortices in the Josephson junction arrays (van Oudenaarden and Mooij, 1996; van Oudenaarden *et al.*, 1998). In such systems, the vortices introduced by an applied magnetic field behave as bosonic quantum particles. The array acts on the vortices as a periodic potential, and a Mott-insulating state of the vortices is observable when the number of vortices per site is commensurate. The advantage of this type of experiment is that the vortices are insensitive to the random offset charges. The main inconvenience is that the quantum effects are weak (Bruder *et al.*, 1999).

B. Superfluid helium in porous media

Mesoporous materials with pores of diameter of nanometer scale have been available since the 1990s. Folded sheet mesoporous materials (FSM-16) synthesized from layered silicate kanemite possess pore forming long straight channels arranged in a honeycomb lattice. The diameter of the pores can be controlled between 1 and 5 nm using appropriate surfactants during the synthesis process. ^{4}He atoms adsorbed in these pores are confined in the transverse direction, and the pores can only interact with each other via the free surface of the materials. For temperatures that are low compared to the transverse confinement energy scale, the ^{4}He adatoms are thus expected to exhibit the properties of a 1D Bose fluid (Wada *et al.*, 2001). With a typical phonon velocity u of the order of 200 m/s, and pores of diameter $d = 18 \pm 2$ Å the temperature scale below which the 1D physics should appear is $T \sim \hbar u/\pi k_B d \sim 1$ K. With pores of a larger diameter, one dimensionalization occurs at lower temperatures. Experiments have shown that the first layer of ^{4}He adatoms on the surface of nanopore was inert. For coverages $n < n_1 = 2.4$ mmol, the ^{4}He atoms occupy only the inert layer, and heat capacity measurements gave $C/T \to 0$ as $T \to 0$ for these low coverages. For coverage $n > 1.15n_1 \sim 2.7$ mmol, the specific heat behaves as $C/T \sim \alpha(n) + bT$, for $T \to 0$, with $b = 1.4$ mJ K^{-3} independent of n. The bT contribution is attributed to the inert layer, and the contribution $\alpha(n)$ to the fluid layer.

As shown in Fig. 16, the T-linear behavior of the specific heat is the one expected in a 1D Tomonaga-Luttinger liquid. By fitting α to the Tomonaga-Luttinger liquid expression, it was possible to measure u as a function of coverage. Since the density of the 1D ^{4}He fluid can be obtained from the coverage knowing the pore diameters, the adsorption area S, and the first layer coverage, by assuming a Lieb-Liniger interaction, one can obtain the Lieb-Liniger interaction constant. For $n \sim 2.75$ mmol, Wada *et al.* (2001) obtained an interaction $c \sim 0.7$ Å^{-1}. For higher densities, $n > n_f \sim 1.4n_1$, the phonon velocity u is found to diverge. This corresponds to the hard-core repulsion between the ^{4}He atoms turning the second layer into a 1D Mott insulator. The hard-core area was estimated to be $A_0 = (4.24$ Å$)^2$.

Recently, the superfluid properties of narrow ^{4}He filled nanopores have been probed by means of the torsional oscillator by Taniguchi, Aoki, and Suzuki (2010). It was found that these systems exhibit a superfluid onset at temperatures $\sim$1 K, which can be strongly suppressed by pressurization. It was argued by Eggel, Cazalilla, and Oshikawa (2011) that this superfluid onset cannot be understood in terms of finite size effects of the helicity modulus and must have a dynamical origin.

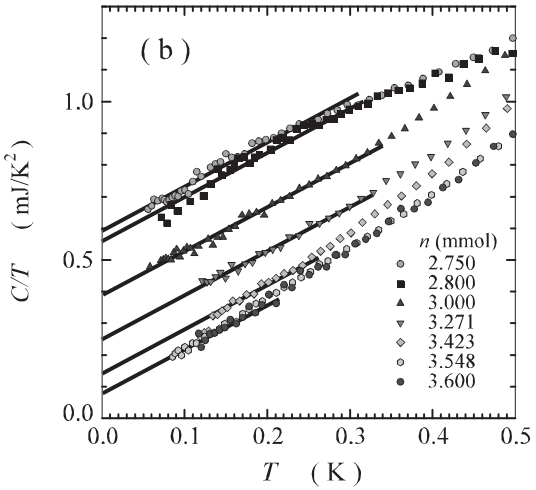

FIG. 16. Specific heat over temperature C_v/T of helium 4 in nanopores of 18 Å diameter. The T-linear contribution comes from the inert layer, and the constant contribution from the quasi-1D fluid. From Wada *et al.*, 2001.

C. Two-leg ladders in a magnetic field

Recently, quantum dimer spin systems in magnetic fields became of great interest because the experimental data on ladder geometries showed the possibility of a quantum phase transition (QPT) driven by the magnetic field (Sachdev, 2000; Giamarchi *et al.*, 2008). In such systems, the application of a magnetic field induces a zero-temperature QPT between a spin-gap phase with all dimers in the singlet state and zero magnetization and a phase where a nonzero density of spin dimers are the triplet state giving a nonzero magnetization. By increasing H, the spin gap between the singlet ground state and the lowest triplet ($S_z = -1$) excited states of the coupled dimers system decreases. It closes at hc_1, where the dimer system enters the gapless phase corresponding to the partially magnetized state. At $h > hc_2$, the system becomes fully polarized and the gap reopens. This transition has been shown (Giamarchi and Tsvelik, 1999) to fall in the universality class of BEC, where the dimers in the triplet state behave as hard-core bosons, the magnetization is proportional to the density of hard-core bosons, and the staggered magnetization in the plane orthogonal to the applied field plays the role of the BEC order parameter. Basic experimental evidence was recently obtained by magnetization (Nikuni *et al.*, 2000) and neutron (Ruegg *et al.*, 2003) measurements on the 3D material class $X\mathrm{CuCl}_3$ (X = Tl, K, NH_4). We refer the reader to Giamarchi *et al.* (2008) for more details and references.

As discussed in Sec. III, BEC cannot occur in 1D, but quasi-long range order is expected in the magnetized phase. In 1D systems, the continuous phase transition from the commensurate spin gapped (C) zero uniform magnetization phase to an incommensurate phase (IC) with nonzero magnetization has been studied theoretically by mapping the spin-1/2 antiferromagnetic (AF) ladder in an external magnetic field H onto a 1D system of interacting hard-core bosons (Chitra and Giamarchi, 1997; Hikihara and

Furusaki, 1998; Furusaki and Zhang, 1999; Giamarchi and Tsvelik, 1999), where H acts as a chemical potential. The interaction term in the hard-core boson picture is determined by the exchange coupling constants, which can be experimentally extracted, $J_\perp$ on the ladder rungs and $J_\parallel$ on the ladder legs, and by H, which controls the density of hard-core bosons. Thus the Hamiltonian is very well controlled, allowing for a precise determination of the Tomonaga-Luttinger parameters through the measurements of the magnetization and transverse staggered spin-spin correlation function $\langle \hat{S}^+(x)\hat{S}^-(x')\rangle$. By combining DMRG calculations with bosonization, the Luttinger parameters can be obtained numerically for arbitrary H (Hikihara and Furusaki, 1998; Bouillot *et al.*, 2011).

These studies are relevant for several experimental compounds. One of the first material studied was $Cu_2(C_5H_{12}N_2)_2Cl_4$ (Chaboussant *et al.*, 1997), but questions on whether its magnetic structure actually consists of coupled spin ladders have been raised (Stone *et al.*, 2002). Recently, $CuBr_4(C_5H_{12}N)_2$ [(bis(piperidinium)tetrabromocuprate(II) (BPCB)] (Patyal *et al.*, 1990) was shown to be an excellent realization of a ladder system. Namely, the low-temperature magnetization data was well described by the XXZ chain model (Watson *et al.*, 2001) in the strong-coupling limit ($J_\perp \gg J_\parallel$) of a ladder (Tachiki and Yamada, 1970; Chaboussant *et al.*, 1997; Mila, 1998; Giamarchi and Tsvelik, 1999).

In connection with the magnon BEC, another important question is the dimensional crossover, between the 1D and the 3D character in a system made of weakly coupled ladders as discussed in Sec. VII.B. At temperatures much larger than the interladder coupling, the system can be viewed as a collection of 1D ladders (Sachdev *et al.*, 1994; Chitra and Giamarchi, 1997; Furusaki and Zhang, 1999; Giamarchi and Tsvelik, 1999) in the universality class of Tomonaga-Luttinger liquids at high field. At lower temperature, interladder coupling

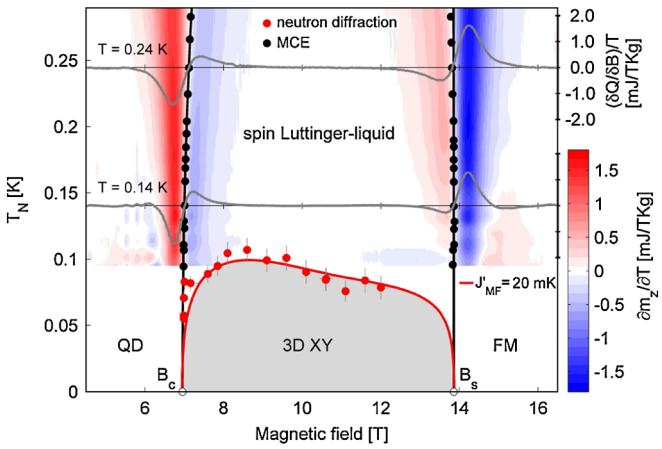

FIG. 17 (color online). Low T phase diagram of $(Hpip)_2CuBr4$. The top two gray lines represent field scans of the magnetocaloric effect (MCE) for two different temperatures. The contour plot is based on the MCE scans. The black solid lines represent crossover temperatures from quantum disordered (QD) and fully magnetized (FM) regimes to the spin Luttinger liquid regime deduced from the MCE measurements. The bottom solid gray (online red) line is a theoretical fit to the neutron scattering data. From Thielemann *et al.*, 2009a.

cannot be ignored, and the system falls into the universality class of magnon BEC condensates. From the experimental point of view, such a change of regime between the 1D and 3D limits is relevant for the above mentioned compound BPCB. Experimentally, to probe these different regimes and TLL behavior characterized by power laws, nuclear magnetic resonance Knight shift, and relaxation time T^{-1} measurements have been performed and compared with the theoretical predictions from bosonization and DMRG (Giamarchi and Tsvelik, 1999; Klanjšek *et al.*, 2008; Rüegg *et al.*, 2008; Thielemann *et al.*, 2009a, 2009b).

The above comparison allows for a quantitative check of the TLL theory (Klanjšek *et al.*, 2008). More generally, the phase diagram and order parameter have been found in good agreement with the theoretical predictions (Fig. 17). The neutron scattering spectrum has been measured and compared with exact solutions as described in Sec. III.D (Thielemann *et al.*, 2009b) or DMRG calculations (Bouillot *et al.*, 2011). Since they lead to a good realization of interacting bosons, these ladder systems open interesting possibilities such as the study of disordered bosons and the Bose-glass phase (see Sec. VI.B) (Hong *et al.*, 2010).

D. Trapped atoms

Atom trapping techniques allow for the realization of ultracold vapors of bosonic atoms, thus offering another route for the experimental study of low-dimensional interacting bosons. In experiments, Bose-Einstein condensates are usually created in 3D geometries. However, by making the trap very anisotropic (Dettmer *et al.*, 2001; Görlitz *et al.*, 2001; Schreck *et al.*, 2001), or by loading the condensate in 2D optical lattices (Greiner *et al.*, 2001; Moritz *et al.*, 2003) or by means of atom chips (Folman *et al.*, 2000; van Amerongen *et al.*, 2008), the quasi-1D regime can be accessed. In this section, we first review the basic principles of atom trapping techniques and the particular techniques developed for probing the atomic clouds. Then, we review the experiments done on quasi-1D bosonic systems.

1. Atom trapping techniques

a. Optical trapping: In this method, ultracold atoms are trapped in standing light patterns created by laser interference. The atoms respond to the electric field of the laser light by acquiring a small dipole moment, which in turn yields a force on the atom proportional to the gradient of the electric field. The optical potential thus created is proportional to the square of the electric field, that is, to the laser intensity. The proportionality factor is the atom polarizability. The latter, for a two-level atom (a cartoon model of alkali atoms such as ^{87}Rb or ^{133}Cs), is positive when the laser is *blue detuned* from a characteristic atomic transition and negative when it is *red detuned*. Therefore, atoms accumulate in regions of high light intensity when the laser is red detuned, whereas they are attracted towards regions of low light intensity when the laser is blue detuned. The two types of optical potentials are indeed used in the experiments described below (Bloch *et al.*, 2008).

The simplest type of optical potential is created by a retroreflected laser beam (propagating, say, along the z direction), which produces a standing wave potential of the form

$V_{\rm opt}(x) = V_{0z}\sin^2(kz)$, where V_{0z} is proportional to the laser intensity and $k = 2\pi/\lambda$, λ being the laser wavelength. The strength of the optical potential V_{0z} is conventionally measured in units of the recoil energy of the atom $E_R = \hbar^2k^2/2M$, where M is the atom mass. Combining three such mutually incoherent standing waves perpendicular to each other yields the following three-dimensional optical potential:

$$V_{\rm opt}(x, y, z) = \sum_{i=1}^{3} V_{0i}\sin^2(kx_i). \tag{164}$$

The minima of this potential occur at a cubic Bravais lattice. In addition, in the experiments a (harmonic) potential is needed in order to confine the gas. The latter may or may not be generated by the same lasers that create the lattice.

b. Magnetic trapping and atoms on chip: Another technique for trapping atoms relies on magnetic fields. The advantage of this technique is that the magnetic field can be created by wires deposited on a surface (the so-called atom chip trap) by microfabrication techniques. Atoms of total spin $\mathbf{F}$ interact with a magnetic field $\mathbf{B}$(r) by the Zeeman coupling $H_{\rm Zeeman} = -g\mu_B\mathbf{F}\cdot\mathbf{B}$. When the magnetic field is slowly varying in space, the spin follows adiabatically the direction of the magnetic field resulting in a potential proportional to $||\mathbf{B}||(r)$ (Folman *et al.*, 2002). When the magnetic moment $g\mu_B\mathbf{F}$ is parallel to the magnetic field, this potential is minimum where the strength of the magnetic field is maximum. The atom is then said to be in a strong field seeking state. Since Earnshaw's theorem (Ketterle and Pritchard, 1992) prohibits maxima of the magnetic field in vacuum, in such a situation trapping is possible only if a source of magnetic field is located inside the trap. With a magnetic moment antiparallel to the magnetic field, the potential is minimum when the magnetic field intensity is minimum. The atom is then said to be in a weak field seeking state, which is metastable. Since Earnshaw's theorem does not prohibit minima of the magnetic field in vacuum, no source of magnetic field is needed to be present inside that trap.

Hence, most atom chip traps operate in the metastable weak field seeking state. By superimposing the magnetic field created by a wire and a uniform field $\mathbf{B}_{\rm bias}$ orthogonal to the wire, one obtains a line of vanishing magnetic field which traps the weak field seeking atoms called a *side guide* trap. However, in this setup the adiabaticity condition $g\mu_B B/\hbar \gg (dB/d\tau)/B$ is not satisfied and Majorana spin flips switch atoms to the strong field seeking state causing losses from the trap. Thus, a second uniform offset magnetic field $\mathbf{B}_{\rm o}$ parallel to the wire is superimposed to the trapping field to ensure that the adiabaticity condition remains satisfied in the trap. The trapping in the transverse direction is then harmonic (Folman *et al.*, 2002; Fortagh *et al.*, 2004). With a Z-shaped wire, the atoms can also be confined along the central part of the wire by a shallow harmonic confining potential. Since magnetic trapping depends on the atoms remaining in the weak field seeking state, Feshbach resonances cannot be used to reach a regime of strong interactions. As a result, atom on chip trapping can only be used to study the regime of weak interaction.

2. Probes

A usual probe in condensed matter physics is the measurement of the structure factor,

$$S(q, \omega) = \int dx d\tau e^{-i(qx-\omega\tau)}\langle\hat{\rho}(x, \tau)\hat{\rho}(0, 0)\rangle, \tag{165}$$

a quantity which can be predicted via either computational techniques or analytical approaches. Using linear response theory, Brunello *et al.* (2001) showed that the structure factor of a trapped gas could be measured with Bragg spectroscopy. In Bragg spectroscopy measurements (Stenger *et al.*, 1999) two laser beams of different wavelengths are shone on an atomic clouds. This creates a time-dependent potential acting on the atoms,

$$\hat{H}_J = V_0\int dx\cos(qx - \omega\tau)\hat{\rho}(x, \tau). \tag{166}$$

After the perturbation has been applied, the total energy E or the total momentum P of the system is measured. Brunello *et al.* (2001) showed that both quantities are proportional to the structure factor. The effect of the trapping potential was considered by Golovach *et al.* (2009). Clément *et al.* (2009) used Bragg spectroscopy techniques to monitor the evolution of a trapped bosonic gas in a 1D lattice from the superfluid to the Mott insulator as the potential is ramped up.

a. Time-of-flight measurements

In a TOF measurement, the trapping potential containing the atomic gas is suddenly switched off and, after expansion, the density of the atomic cloud is measured using absorption imaging techniques. Assuming that interactions between atoms can be neglected and applying the stationary phase approximation to the solution of the time-dependent Schrödinger equation, the annihilation operator of a boson at position $\mathbf{r}$ and time $\tau \gg mL^2/\hbar$ [where L is the original (linear) size of the cloud] is found to be $\hat{\Psi}(\mathbf{r}, \tau)\sim \hat{\Psi}(\mathbf{k}(\mathbf{r}))/\tau^{d/2}$, with $\mathbf{k}(\mathbf{r}) = m\mathbf{r}/\hbar\tau$. That is, TOF provides a correspondence between the position of a boson after expansion and its initial momentum in the trap (the factor $\tau^{d/2}$ stems from the free propagation in d dimensions). After some straightforward manipulations, the density distribution measured after a TOF τ at the position $\mathbf{r}$ is then found to be proportional to the initial momentum distribution function

$$\langle\hat{\rho}(\mathbf{r}, \tau)\rangle \propto \frac{1}{\tau}\langle\hat{\rho}[\mathbf{k}(\mathbf{r})]\rangle. \tag{167}$$

Equation (167) implies that a BEC will show up as a prominent peak in $\langle\hat{\rho}(\mathbf{r} = 0, \tau)\rangle$ after TOF (Anderson *et al.*, 1995; Bradley *et al.*, 1995; Davis *et al.*, 1995). If a BEC is loaded in the lowest band of an optical lattice, one needs to relate the momentum distribution function $\hat{\rho}(\mathbf{k})$ to the quasimomentum distribution function $\hat{n}_{\mathbf{k}}$ in the lattice. The latter satisfies $\hat{n}_{\mathbf{k}} = \hat{n}_{\mathbf{k}+\mathbf{Q}}$, where $\mathbf{Q}$ is an arbitrary reciprocal lattice vector. Using the 3D version of Eq. (12), one finds that $\hat{\rho}(\mathbf{k}) = |w_0(\mathbf{k})|^2\hat{n}_{\mathbf{k}}$, where $w_0(\mathbf{k})$ is the Fourier transform of the Wannier orbitals. This relation implies that after TOF expansion, a BEC released from an optical lattice will exhibit Bragg peaks at $\mathbf{k}(\mathbf{r}) = \mathbf{Q}$ corresponding to reciprocal lattice vectors (Greiner *et al.*, 2002a).

We stress, however, that the density distribution after a TOF can be different from the in-trap momentum distribution

if interactions are nonnegligible during the expansion or when the TOF is not sufficiently long to neglect the initial size of the cloud (Pedri *et al.*, 2001; Gerbier *et al.*, 2008). For optical lattice experiments with small filling factors, the ballistic expansion is typically a good approximation. Moreover, by applying the Feshbach resonance technique, one can also always tune the collision interaction to a negligible value at the beginning of the expansion to satisfy the condition of ballistic expansion. Another deviation from the true BEC behavior occurs when the temperature is increased from zero, $T > T_\phi$, T_ϕ being the temperature at which the phase fluctuations become of order unity. In this quasi-BEC regime, the detection signal decreases and Bragg peaks becomes less visible. If instead, the interaction is increased while the temperature is still very low, i.e., in the Mott state, coherence is destroyed and there is no interference pattern in $\langle\hat{\rho}(\mathbf{r}, \tau)\rangle$.

For a Tomonaga-Luttinger liquid, the boson creation operator is represented by $\hat{\Psi}^\dagger(x) \sim e^{-i\hat{\theta}(x)}$, thus $\langle\hat{\rho}(k)\rangle \propto k^{1/2K-1}$ displaying a characteristic power-law divergence at zero momentum for $K > 1/2$. In particular, in the Tonks-Girardeau limit, the Tomonaga-Luttinger parameter $K = 1$ and the momentum distribution presents a square-root divergence at $k = 0$. During the past years, experimental groups were able to increase the interactions to reach this regime (Kinoshita *et al.*, 2004; Paredes *et al.*, 2004).

b. Noise correlations

Since atomic clouds are mesoscopic, the density fluctuates between different time-of-flight experiments. Altman, Demler, and Lukin (2004) thus proposed to use time-of-flight spectroscopy to measure correlations between occupation numbers for different momenta,

$$\mathcal{G}_{\mathbf{k},\mathbf{k}'} = \langle\hat{n}_\mathbf{k}\hat{n}_{\mathbf{k}'}\rangle - \langle\hat{n}_\mathbf{k}\rangle\langle\hat{n}_{\mathbf{k}'}\rangle, \tag{168}$$

where $\hat{n}_\mathbf{k}$ is the occupation number for momentum $\mathbf{k}$, and the average is taken over the initial state. Altman, Demler, and Lukin (2004) considered Fermi superfluids and bosonic Mott insulators.

For 1D boson systems, the correlations (168) were studied by Mathey, Vishwanath, Altman, 2009. For the Luttinger parameter $K \gg 1$, the correlation function $\mathcal{G}_{k,k'}$ shows a large peak for $k = k' = 0$, sharp power-law peaklike features for $k = \pm k'$, and power-law diplike features for $k = 0$ or $k' = 0$. The peak at $k = k'$ is the result of boson bunching familiar from quantum optics. The location of the other features is predicted (Mathey, Vishwanath, Altman, 2009) by the Bogoliubov approximation. However, their power-law character is a signature of the Tomonaga-Luttinger liquid physics unique to one dimension (Mathey, Vishwanath, Altman, 2009). For lattice hard-core bosons, noise correlations have been computed in the presence of commensurate and incommensurate superlattices, and in the presence of a trap, by Rey *et al.* (2006a, 2006b, 2006c) and their scaling has been studied by He and Rigol (2011) using the methods described in Sec. III.A.

A different approach to probe static quantum correlations with noise measurement has been proposed by Polkovnikov *et al.* (2006). The idea is to start from two independent 1D condensates parallel to the x axis and separated by a distance d, both tightly confined in the radial direction z. At time zero, both condensates are allowed to expand in the radial direction. Because the condensates were tightly confined, expansion is much faster in the radial direction z, and one can neglect expansion along the direction x. Under this assumption, the total annihilation operator of the bosons reads

$$\hat{\Psi}(z, x, \tau) \simeq \frac{-im}{2\pi\hbar\tau}\sum_{p=1,2}\hat{\Psi}_p(x)e^{[im/(2\hbar\tau)](z+s_p d/2)^2}, \tag{169}$$

where $s_{p=1} = -1$ and $s_{p=2} = +1$ and $\hat{\Psi}_{1,2}(x)$ is the annihilation operator of bosons initially trapped in the condensate 1 or 2. Absorption imaging techniques can then be used to measure the density profile integrated along the beam axis

$$\hat{\rho}(z, \tau) = \int_0^L dx\hat{\Psi}^\dagger(x, z, \tau)\hat{\Psi}(x, z, \tau). \tag{170}$$

Using Eq. (169), one can express $\hat{\rho}(z, \tau)$ as a function of the annihilation operators of condensate 1 or 2, which has an oscillatory contribution (that accounts for the interference fringes in the optical absorption images) proportional to $\hat{A}_Q e^{iQz}$, where we have introduced $Q = md/\hbar\tau$ and

$$\hat{A}_Q = \left(\frac{m}{2\pi\hbar\tau}\right)^2\int_0^L dx\hat{\Psi}_1^\dagger(x)\hat{\Psi}_2(x). \tag{171}$$

From one experimental realization to another, the quantity A_Q varies randomly. As a result, the amplitude of the fringes varies from experiment to experiment, and one needs the moments of the correlation function $\langle(\hat{A}_Q^\dagger)^n\hat{A}_Q^n\rangle$ to characterize the full probability distribution of $\hat{A}_Q$ (Glauber, 1963; Mandel and Wolf, 1965). As we will see, the probability distribution of $\hat{A}_Q$ is non-Gaussian, and depends on the Luttinger parameter, thus permitting its experimental determination. The higher moments are given by

$$\langle(\hat{A}_Q^\dagger)^n\hat{A}_Q^n\rangle = \int_0^L dx_1\cdots dx_n dx_1'\cdots dx_n' \times|\langle\hat{\Psi}^\dagger(x_1)\cdots\hat{\Psi}^\dagger(x_n)\hat{\Psi}^\dagger(x_1')\cdots\hat{\Psi}^\dagger(x_n')\rangle|^2. \tag{172}$$

Using bosonization, this integral can be rewritten as

$$\langle(\hat{A}_Q^\dagger)^n\hat{A}_Q^n\rangle \sim L^{n(2-1/K)}\int_0^1 d\omega_1\cdots d\omega_n d\omega_1'\cdots d\omega_n' \times\left|\frac{\prod_{1\le k<\ell\le n}|\omega_k-\omega_\ell||\omega_k'-\omega_\ell'|}{\prod_{1\le k,\ell\le n}|\omega_k-\omega_\ell'|}\right|^{1/K}, \tag{173}$$

where the change of variables $x_i = L\omega_i$, $x_i' = L\omega_i'$ has been used. Equation (173) shows that the higher moments are of the form $\langle(\hat{A}_Q^\dagger)^n\hat{A}_Q^n\rangle \sim (\langle(\hat{A}_Q^\dagger)\hat{A}_Q\rangle)^n Z_{2n}(K)$, where $Z_{2n}(K)$ is a dimensionless factor given by the multidimensional integral in Eq. (173) that depends only on n and K. The quantities $Z_{2n}(K)$ are the moments of the distribution function of the normalized fringe interference contrast. The integrals in Eq. (172) can be expressed using Jack polynomials (Fendley *et al.*, 1995), contour integration (Konik and LeClair, 1996), or Baxter's Q operator (Gritsev *et al.*, 2006) methods. Imambekov *et al.* (2008) related the distribution function to the statistics of random surfaces, allowing

for Monte Carlo computation. With periodic boundary conditions, the normalized distribution $\tilde{W}(\alpha)$ such that $Z_{2n}(K)/Z_2(K)^n = \int d\alpha \alpha^n \tilde{W}(\alpha)$ goes to a Gumbell distribution $W_G(\alpha) = K \exp[K(\alpha-1) - \gamma - e^{K(\alpha-1)-\gamma}]$ in the limit $K \to \infty$. This is the result of the rare events (Imambekov *et al.*, 2007) in the fluctuations of the equivalent random surface model. The prediction of a Gumbel distribution of interference fringe contrasts was checked experimentally (Hofferberth *et al.*, 2008) using ^{87}Rb atoms in radio frequency microtraps on atom chips.

3. One-dimensional bosons with cold atoms

On a chip, atoms can be trapped in a quasi-1D geometry, allowing one to access the weakly interacting regime. A study of the density profile of atoms on chip (Trebbia, *et al.*, 2006) showed that the Hartree-Fock approximation breaks down already in the weakly interaction regime for quasi-1D trapping. Later experiments (van Amerongen *et al.*, 2008) showed that the density profiles could be well fitted using the Yang-Yang thermodynamics (Yang and Yang, 1969) of the Lieb-Liniger gas (Lieb and Liniger, 1963). To access the regime of strong interaction, optical lattices are more suitable.

In what follows, we consider ultracold quantum gases in strongly anisotropic lattices. By "strongly anisotropic," we mean that the optical potential is of the form of Eq. (163) but such that $|V_{0z}| \ll |V_{0x}| = |V_{0y}|$. Under this condition, it is possible to confine atoms to 1D (Greiner *et al.*, 2001; Moritz *et al.*, 2003; Kinoshita *et al.*, 2004, 2005; Paredes *et al.*, 2004; Tolra *et al.*, 2004; Stöferle *et al.*, 2004a; Fertig *et al.*, 2005a; Haller *et al.*, 2010). Indeed, this requires that the chemical potential of the 1D gas μ is much smaller than the trap frequency, which for a deep lattice $\simeq k|V_{0z}/M|^{1/2}$. Thus, the atoms are strongly localized about the minima of the potential in the transverse directions (i.e., y and z in the previous example), forming elongated clouds (referred to as "tubes"). Since the potential along the longitudinal (x) direction is much weaker, all the dynamics will occur in that direction. The resulting system is an ensemble of a few thousand (finite-size) 1D ultracold gas tubes, which is sometimes called a 2D optical lattice (in the case where $V_{0x} = 0$, see Fig. 18), or, as we do in what follows, a quasi-1D lattice.

Nevertheless, once the condition for one dimensionality of the tubes is achieved, two quasi-1D regimes are possible. This

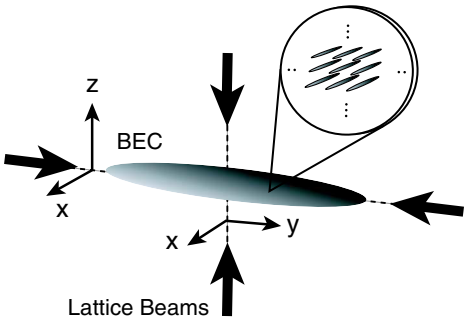

FIG. 18 (color online). Experimental setup for the creation of a 2D optical lattice. The optical potential resulting form the interference of a pair of retroreflected, mutually perpendicular, lasers splits a BEC into an array of several thousand 1D gas tubes. From Greiner *et al.*, 2001.

is because, even if the atoms only undergo zero-point motion transversally, the hopping amplitude between tubes $t_\perp$ is in general nonvanishing. Regime (i): if over typical duration of a experiment, $\tau_{\rm exp} \lesssim 10^2$ s, the characteristic hopping time $\tau_{\rm hop} \sim \hbar/t_\perp \gtrsim \tau_{\rm exp}$, then hoping events will rarely occur and therefore phase coherence between different tubes cannot be established. In the RG language used in Sec. VII.B, the energy scale associated with the observation time $\sim h/\tau_{\rm exp}$ behaves as an infrared cutoff of the RG flow preventing the renormalized Josephson coupling g_J from becoming of order 1. Regime (ii): if $\tau_{\rm hop} \ll \tau_{\rm exp}$, then the establishment of long-range phase coherence will be possible (but it may be prevented by other terms of the Hamiltonian, see below and Sec. VII.B). Indeed, experimental groups have explored the two regimes, as we review in more detail below.

The regime of a phase-coherent ensemble of tubes and the transition to the phase-incoherent regime was explored in the early experiments by Greiner *et al.* (2001), where the 1D regime was first reached in a quasi-1D lattice, and later more thoroughly by Moritz *et al.* (2003) and Stöferle *et al.* (2004a). However, other groups have focused directly in the 1D (phase-incoherent) regime (Kinoshita *et al.*, 2004, 2005; Paredes *et al.*, 2004; Haller *et al.*, 2010). In what follows, these experiments are reviewed and the theoretical background for the probes used in some of them will also be discussed. We begin with the experiments that explored the phase-incoherent 1D regime, and near the end of this section, discuss the experiments where intertube hoping may become a relevant perturbation on the system.

a. Strongly Interacting 1D bosons in optical lattices: For alkali atoms, which at ultracold temperatures (from $\sim$10 nK to ~ 1 μK) interact dominantly via the s-wave channel (see Sec. II), the interaction is short ranged. When ultracold atoms are loaded into an anisotropic optical lattice, they occupy the lowest available (Bloch) band. This system is thus amenable to a lattice description in terms of the (anisotropic) Bose-Hubbard model. Furthermore, if the experimental conditions are such that the hopping between tubes can be neglected (see discussion above), the system can be described as an array of independent tubes. Each tube is described by a 1D Bose-Hubbard model Eq. (15). The particle number within each tube is largest at the center and decreases towards the edges of the lattice in response to the existence of the harmonic trap, which makes the system inhomogeneous.

Tuning the longitudinal potential ($\propto V_{0x}$) effectively changes the ratio t/U of the 1D Bose-Hubbard model. For deep potentials, it is thus possible to access the strongly interacting regime of the model and to observe the transition from the superfluid (i.e., Tomonaga-Luttinger liquid) phase to the Mott insulator. Indeed, shortly after this transition was observed in a 3D optical lattice (Greiner *et al.*, 2002a), the 1D transition was observed by Stöferle *et al.* (2004a). More recently, the Mott transition in a weak lattice, as discussed in Sec. VI.A, was also observed (Haller *et al.*, 2010). In order to probe the excitation spectra of the phases realized by tuning V_{0x} in the quasi-1D optical lattice, Stöferle *et al.* (2004a) followed a novel spectroscopic method, which relied on modulating in time the amplitude of the longitudinal potential. In equations, this amounts to replacing $V_{0x} \to V_{0x} + \delta V_{0x} \cos\omega\tau$ in Eq. (164). The time-dependent

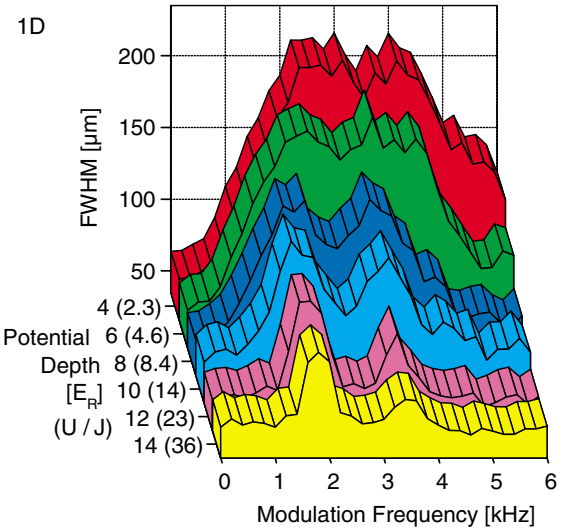

FIG. 19 (color online). Energy absorption of a strongly interacting 1D Bose system measured as a function of the longitudinal potential V_{0x}/E_R (E_R is the atom recoil energy). Notice the broad spectrum of the superfluid (small V_{0x}/E_R) and the double peak structure characterizing the Mott insulator (large V_{0x}/E_R). From Stöferle *et al.*, 2004a.

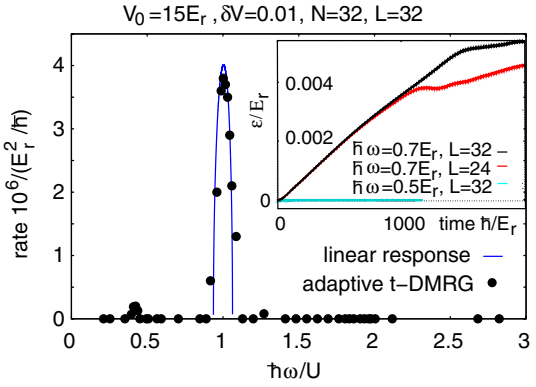

FIG. 20 (color online). Comparison of the analytical results of Iucci *et al.* (2006) (continuous curve) the time-dependent DMRG calculations of Kollath *et al.* (2006) (black dots) for the energy absorption rate due to a periodic modulation of the lattice. The inset shows the behavior of the energy absorption with time and how it deviates from the linear response for different system sizes.

potential heats up the system, and the transferred energy can be estimated in a time-of-flight experiment from the enhancement of the width at half maximum of the peak around zero momentum. The measured spectra for different values of the lattice depth (V_{0x}/E_R) are displayed in Fig. 19. The superfluid phase is characterized by a broad spectrum, whereas the emergence of the 1D Mott insulator is characterized by the appearance of two peaks: A prominent one at $\hbar\omega \simeq U$ and a smaller one at $\hbar\omega \simeq 2U$.

In order to qualitatively understand these spectra, Iucci *et al.* (2006) employed linear response theory, and considered the limit of both small and large potential V_{0x}. When V_{0x} is smaller than μ, the lattice modulation couples to the density operator. Using the bosonization formula (112), the $q \approx 0$ term $\propto \partial_x \hat{\phi}$ gives a vanishing contribution to the energy absorption within linear response and, to leading order, the modulation of the amplitude of the optical potential is described by the perturbation $\hat{H}_1(\tau) = B\rho_0 \delta V_{0x} \cos\omega\tau \times \int dx \cos[2\hat{\phi}(x,\tau) + x\delta]$, where $\delta = 2G - 2\pi\rho_0$, that is, the modulation couples to the density operator for $q \approx 2\pi\rho_0$. In the limit of large V_{0x}, it is most convenient to begin with the Bose-Hubbard model. Within this framework, it can be shown that the lattice modulation can be expressed as a modulation of the hopping amplitude $\hat{H}_1(\tau) = -\delta t \cos\omega\tau \sum_m [\hat{b}^\dagger_{m+1}\hat{b}_m + \text{H.c.}]$, where $\delta t = (dt/dV_{0x})\delta V_{0x}$. Hence, the (time-averaged) energy absorption rate per particle reads

$$\dot{\epsilon}(\omega) = \frac{\delta V_{0x}^2}{N}\,\omega\,\mathrm{Im}[-\chi_{\mathcal{O}}(\omega)], \tag{174}$$

where $\chi_{\mathcal{O}}(\omega)$ is the Fourier transform of $\chi(\tau) = -i/\hbar\langle[\hat{\mathcal{O}}(\tau), \hat{\mathcal{O}}(0)]\rangle$. The operator $\hat{\mathcal{O}} = \int dx \cos(2\hat{\phi}(x) + x\delta)$ in the weak lattice regime, and $\hat{\mathcal{O}} = -\delta J \sum_m [\hat{b}^\dagger_{m+1}\hat{b}_m + \text{H.c.}]$ in the strong lattice regime.

For a weak commensurate lattice, in the superfluid (Tomonaga-Luttinger liquid) phase, $\dot{\epsilon}(\omega) \sim \hbar\omega(\hbar\omega/\mu)^{2K-2}$, where K is the Tomonaga-Luttinger liquid parameter and μ is the chemical potential. Since for the superfluid phase ($K \gtrsim 2$), the calculated low frequency part contains very little spectral weight, using the f-sum rule, Iucci *et al.* (2006) argued that the absorption spectrum of the superfluid phase should be broad, in agreement with the experiment and the calculations of Caux and Calabrese (2006) based on the Bethe ansatz. For the Mott insulator phase, in the weak coupling limit, a threshold behavior of the form $\dot{\epsilon}(\omega) \sim \hbar\omega F(\hbar\omega)\theta(\hbar\omega - \Delta)$ exists, where Δ is the Mott gap and $F(x)$ is a smooth function. This threshold behavior was observed in the experiments of Haller *et al.* (2010), which recently explored the phase diagram of the 1D Bose gas in a weak periodic potential.

In the strong-coupling regime, the perturbation reads, in an expansion to $O(t^2/U)$, in the subspace of particle-hole states

$$\dot{\epsilon}(\omega) = \frac{(\delta t)^2}{2t}\hbar\omega\left(\frac{n_0+1}{2n_0+1}\right)\sqrt{1-\left[\frac{\hbar\omega - U}{(2n_0+1)t}\right]^2}, \tag{175}$$

and zero otherwise. The accuracy of this expression was tested using time-dependent DMRG by Kollath *et al.* (2006), and the results are shown in Fig. 20. The latter numerical technique allows one to go beyond linear response and to incorporate the effects of the trap and thus to deal with the experiments of Stöferle *et al.* (2004a) for which $\delta V_{0x}/V_{0x} \sim 10\%$. Numerically investigating the inhomogeneity brought about by the trap, it was shown by Kollath *et al.* (2006) that the smaller peak near $\hbar\omega = 2U$ is indeed a measurement of the incommensurability in the 1D tubes.

An alternative interpretation of the broad resonance observed in the superfluid phase was given in terms of a parametric instability of Bogoliubov modes and their nonlinear dynamics (Krämer *et al.*, 2005). This interpretation assumes that the Bogoliugov approximation is also applicable for strongly interacting bosons in 1D.

Approaching the Tonks-Girardeau limit: For bosonic atoms, there are essentially two routes into the strongly interacting regime, which asymptotically approaches the Tonks-Girardeau limit where fermionization occurs. The two routes were explored simultaneously by Kinoshita *et al.* (2004) and Paredes *et al.* (2004). One of them (Paredes *et al.*, 2004) relies on reaching the strong interacting limit of the 1D Bose-Hubbard model while ensuring that the system remains incommensurate with the lattice potential (e.g., at average filling $n_0 < 1$). In the presence of a longitudinal harmonic confinement, this is by no means straightforward, because, as discussed in Sec. IV.B.3, the center of the cloud easily becomes Mott insulating as the ratio t/U decreases. Thus, carefully controlling the trapping potential, Paredes *et al.* (2004) entered the strongly-interacting regime where the bosons undergo fermionization. The signatures of the latter were observed in the momentum distribution as measured in time-of-flight experiments (cf. Sec. VIII.D.2.a). After averaging over the distribution of tubes resulting from the inhomogeneous density profile, Paredes *et al.* (2004) were able to reproduce the experimentally measured momentum distribution of the strongest interacting systems. Computational studies of the approach to the Tonks-Girardeau regime were done by Pollet *et al.* (2004) and Wessel *et al.* (2005).

The other route into the strongly correlated regime for bosons in 1D is to first load the atoms in a deep 2D optical lattice [$V_{0x} = 0$ and $V_{0y} = V_{0z} \gtrsim 30E_R$ in Eq. (164)]. The resulting system is described by the Lieb-Liniger model in a harmonic trap. The strongly interacting regime of this model is reached by making $\gamma = Mg/\hbar\rho_0$ large. This can be achieved either by decreasing the mean density ρ_0, which for small atom numbers $\lesssim 10$ per tube ultimately poses detection problems, or by increasing the coupling constant g [cf. Eq. (92)]. As predicted by Olshanii (1998), this is possible either by making the transverse confinement tighter (Kinoshita *et al.*, 2004, 2005) or by increasing the scattering length using Feshbach resonance (Haller *et al.*, 2010). Kinoshita *et al.* (2004 and 2005) used a blue-detuned 2D optical lattice potential (cf. Fig. 18) to confine an ultracold ^{87}Rb gas into an array of 1D traps ($\sim 10^3$ tubes). In addition, the atoms were confined longitudinally by an optical (red-detuned) dipole trap. The blue-detuned lattice potential makes it possible to reach a tighter transverse confinement without increasing the probability of spontaneous emission, which due to the atom recoil may result in the latter being lost from the trap. In addition, as mentioned, by virtue of Eq. (92), a tighter confinement allows for the increase of the interaction coupling g.

By measuring the mean atom energy after the expansion in 1D (turning off the optical dipole trap only), Kinoshita *et al.* (2004) were able to detect the incipient signatures of fermionization of the 1D gases. However, the most dramatic signatures of strong interactions were observed in a later experiment (Kinoshita *et al.*, 2005), in which local pair correlations $g_2(x)$ were measured.

For the Lieb-Liniger model, g_2 (note that we drop x assuming translational invariance) is a thermodynamic quantity that can be obtained from the free energy by using the Hellman-Feynman theorem

$$g_2(\gamma,\vartheta) = \rho_0^{-2}\langle[\hat{\Psi}^\dagger(x)]^2[\hat{\Psi}(x)]^2\rangle = -2\frac{T}{L}\frac{\partial F(T)}{\partial g}, \quad (176)$$

where $F = -T\ln \mathrm{Tr} e^{-H/T}$ is the free energy for the Lieb-Liniger model [H is given by Eq. (10)], $\vartheta = T/T_d$, T is the absolute temperature, and $T_d = \hbar^2\rho_0/2M$ is the characteristic temperature for quantum degeneracy. Gangardt and Shlyapnikov (2003) first obtained $g_2(\gamma,\vartheta)$ for $\tau = 0$ for all γ values using the Bethe-ansatz result for the ground-state energy. Kheruntsyan *et al.* (2005) extended these results to finite temperatures. For large and small γ values, the following asymptotic limits have been derived (Gangardt and Shlyapnikov, 2003; Kheruntsyan *et al.*, 2005):

$$g_2(\gamma,\vartheta) \simeq \begin{cases} \frac{4}{3}\left(\frac{\pi}{\gamma}\right)^2\left[1+\frac{\vartheta^2}{4\pi^2}\right] & \gamma \gg 1 \quad \text{and} \quad \vartheta \ll 1, \\ \frac{2\vartheta}{\gamma^2} & 1 \ll \vartheta \ll \gamma^2, \\ 1-\frac{2}{\pi}\sqrt{\gamma}+\frac{\pi\vartheta^2}{24\gamma^{3/2}} & \vartheta \ll \gamma \ll 1, \\ 1+\frac{\vartheta}{2\sqrt{\gamma}} & \gamma \ll \vartheta \ll \sqrt{\gamma}, \\ 2-\frac{4\gamma}{\vartheta^2} & \sqrt{\gamma} \ll \vartheta \ll 1, \\ 2-\gamma\sqrt{\frac{2\pi}{\vartheta}} & \vartheta \gg \max\{1,\gamma^2\} \end{cases} . \quad (177)$$

The results for large γ can also be reproduced from the low-density limit of a strong-coupling expansion for the Bose-Hubbard model (Cazalilla, 2004a).

The asymptotic expressions (177) show that for $T \to 0$, $g_2 \to 0$ as $\gamma \to +\infty$. The latter reflects the fermionization that becomes complete in the Tonks-Girardeau limit, where $g_2 = 0$ at all temperatures. The dramatic decrease in g_2 (Kinoshita *et al.*, 2005) as it crosses over from the behavior for weakly interacting bosons (i.e., $g_2 \approx 1$ for $\gamma \sim 0.1$) to strongly interacting bosons (i.e., $g_2 \approx 0.1$ for $\gamma \simeq 10$) was observed by tuning the interaction coupling g, as described above. The measurements are depicted in Fig. 21, which also show the excellent agreement with theory.

In order to measure g_2, atoms in the optical lattice were photo associated into molecules using a broad laser beam resonant with a well-defined molecular state of the Rb-Rb dimer. The molecule formation was subsequently detected as a loss of atoms from the trap. One important issue that must be addressed in order to compare theory and experiment is the inhomogeneity of the 1D systems due to the harmonic trap. Fortunately, the LDA allows one to obtain $g_2(x)$ for the trapped system from the $g_2(\gamma)$ calculated for the uniform system.

Another experimentally accessible local correlation is $g_3 = \rho_0^{-3}\langle[\hat{\Psi}^\dagger(x)]^3[\hat{\Psi}(x)]^3\rangle$. This local correlation function is related to the rate of three-body recombination processes where molecules form out of three-atom encounters. The calculation of g_3 is less straightforward. Gangardt and Shlyapnikov (2003) obtained the following asymptotic expressions for the Lieb-Liniger model at large and small γ and $T = 0$:

$$g_3(\gamma) = \begin{cases} \frac{4\pi^2}{3\gamma^2} & \gamma \gg 1, \\ 1-\frac{6}{\pi}\sqrt{\gamma} & \gamma \ll 1. \end{cases} \quad (178)$$

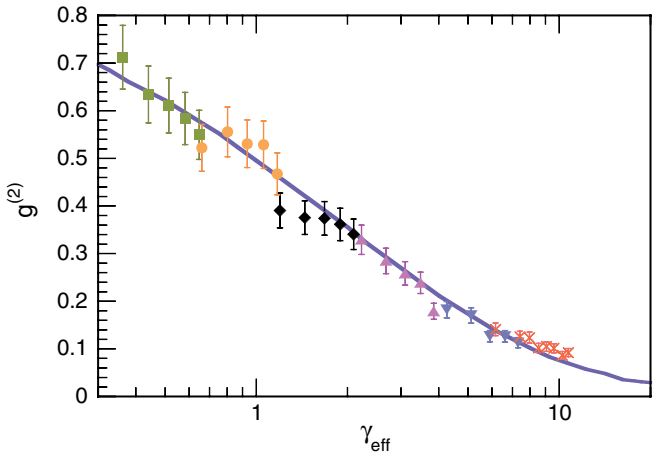

FIG. 21 (color online). Pair-correlation function as determined from photo association by Kinoshita *et al.* (2005) vs dimensionless parameter γ. The solid line is from the 1D interacting bosons theory of Gangardt and Shlyapnikov (2003). The different symbols correspond to different dipole trap power intensities P_{cd}, and thus different one-dimensional densities: squares, $P_{cd} = 3.1$ W; circles, $P_{cd} = 1$ W; diamonds, $P_{cd} = 320$ mW; up triangles, $P_{cd} = 110$ mW; and down triangles, $P_{cd} = 36$ mW.

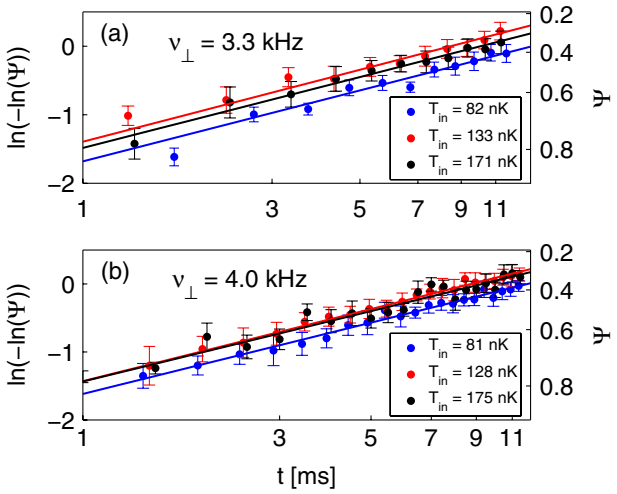

FIG. 22 (color online). Double logarithmic plot of the coherence factor vs time for decoupled 1D condensates. Each point is the average of 15 measurements, and error bars indicate the standard error. The slopes of the linear fits are in good agreement with a 2/3 exponent. From Hofferberth *et al.*, 2007.

Subsequently, in a mathematical *tour de force*, Cheianov *et al.* (2006) computed the behavior of $g_3(\gamma)$ at $T = 0$ for the entire crossover from weakly to strongly interacting gas. More generally, at any finite T and for intermediate of γ, one has to rely on the general expressions recently obtained by Kormos *et al.* (2009). These results predict a strong reduction in $g_3(\gamma)$ at low T as the 1D gas enters the strongly interacting regime. This behavior should manifest itself in a strong reduction of the atom losses due to three-body recombination. Indeed, this is consistent with the experiments in optical lattices in the 1D regime (Tolra *et al.*, 2004).

Finally, in a recent experiment, Haller *et al.* (2009) have been able to access the super-Tonks-Girardeau regime in a 2D optical lattice by starting with a low-energy initial state in the Tonks-Girardeau regime (with a large and positive value of g) and quickly changing g across the confinement-induced resonance (see Sec. IV.A) to a negative final value. In this experiment, g was changed by means of a Feshbach resonance. The ratio between the lowest compressional and dipole modes of oscillation in the highly excited state (with $g < 0$) created in such a way was found to be larger than the one in the Tonks-Girardeau regime, a hallmark of the super-Tonks-Girardeau regime (Astrakharchik *et al.*, 2005).

c. Coupled condensates The behavior of the Bose gas in the quasi-1D optical lattice as the transverse potential is tuned and phase coherence between the tubes emerges has been explored by Moritz *et al.* (2003) and Stöferle *et al.* (2004a). A theoretical discussion of these experiments has been given by Cazalilla *et al.* (2006) and we thus refer the interested reader to this work.

Using atom chips, a 1D Bose gas with a few thousand atoms can be trapped in the 1D quasicondensate regime $k_B T$, $\mu \ll \hbar\nu_\perp$ (Hofferberth *et al.*, 2007). Applying a radio frequency (rf) induced adiabatic potential, the 1D gas can be split into two 1D quasicondensates. The height of the barrier between the two condensates can be adjusted by controlling the amplitude of the applied rf field. This allows one to achieve both Josephson coupled and fully decoupled quasicondensates. The fluctuations of the relative phase of the two condensates are measured by the quantity

$$\hat{\mathcal{A}}(\tau) = \frac{1}{L}\left|\int dx e^{i[\hat{\theta}_1(x,\tau)-\hat{\theta}_2(x,\tau)]}\right|, \tag{179}$$

where $\hat{\theta}_1$, $\hat{\theta}_2$ are the respective phases of the two condensates obtained after the splitting. From the theoretical point of view, split condensates can be analyzed within the Tomonaga-Luttinger liquid framework (Bistritzer and Altman, 2007; Burkov *et al.*, 2007). One introduces $\hat{\theta}_+ = (\hat{\theta}_1 + \hat{\theta}_2)/2$ and $\hat{\theta}_- = \hat{\theta}_1 - \hat{\theta}_2$. The Hamiltonian $\hat{H} = \hat{H}[\hat{\theta}_1] + \hat{H}[\hat{\theta}_2]$ can be rewritten as $\hat{H}[\hat{\theta}_+] + \hat{H}[\hat{\theta}_-]$. In the initial state, the wave function factorizes $\Psi[\hat{\theta}_1, \hat{\theta}_2] = \Psi_+[\hat{\theta}_+] \times \Psi_-[\hat{\theta}_-]$, where Ψ_+ is determined by the initial state of the condensate and Ψ_- is initially localized near $\hat{\theta}_-(x) = 0$. Assuming an initial state with $\langle\hat{\theta}_-(x)\hat{\theta}_-(x')\rangle = \delta(x - x')/2\rho$, the quantum dynamics of the phase $\hat{\theta}_-$ under the Hamiltonian (114) gives $\langle\hat{\mathcal{A}}\rangle = \mathcal{A}_0 e^{-\tau/\tau_Q}$ with $\tau_Q = 2K^2/\pi^2 v\rho$ (Bistritzer and Altman, 2007). For long times, $\tau \gg \hbar/k_B T$, the symmetric and antisymmetric modes interact with each other. The symmetric modes remain in thermal equilibrium, and generate friction $1/\tau_f(k) \propto k^{3/2}$ and noise $\zeta(x, \tau)$ (satisfying the fluctuation dissipation relation) for the dynamics of the antisymmetric mode. The field $\hat{\theta}_-$ can then be treated as a classical variable, satisfying the Langevin equation

$$\partial_\tau^2\hat{\theta}_-(k,\tau) + \frac{\partial_\tau\hat{\theta}_-(k,\tau)}{\tau_f(k)} + (vk)^2\hat{\theta}_-(k,\tau) = \zeta(k,\tau). \tag{180}$$

Solving this second order differential equation by the variation of the constant method with initial conditions $\hat{\theta}(k, \tau) = \partial_\tau\hat{\theta}(k, \tau)$, one finds that $\langle\hat{\theta}_-(x, \tau)^2\rangle = 2(\tau/\tau_C)^{2/3}$, and thus

$\mathcal{A} \propto e^{-(\tau/\tau_C)^{2/3}}$. This behavior was indeed observed in experiments in the case of a large potential barrier (Hofferberth *et al.*, 2007), as shown in Fig. 22.

IX. OUTLOOK

Quantum interacting bosons in 1D provide an exciting research arena where solid state, low-temperature, and atomic physics converge. In previous sections, we have seen that the properties of these systems can be captured by a variety of theoretical techniques ranging from exact solutions and computational methods to low-energy effective theories such as Tomonaga-Luttinger liquids. Although we now have a firm understanding of several of these properties, many challenges still remain. This is, in particular, prompted by many remarkable experiments, some of which were discussed in Sec. VIII. In the present section, we discuss some of the open problems and recent developments in the field and provide an outlook for future research. Our list is of course nonexhaustive and many unexpected developments will certainly take place in the future. These are all the ingredients of a very lively field that will surely continue to provide exciting results in the years to come.

a. Beyond Tomonaga-Luttinger liquid theory: The low-energy, long wave length description based on the bosonization technique introduces a particle-hole symmetry that is not present in the original models that it intends to describe. In the recent years, there has been intensive theoretical efforts to improve bosonization by including nonlinear terms (Bettelheim *et al.*, 2006; Pereira *et al.*, 2006; Khodas *et al.*, 2007; Imambekov and Glazman, 2009). In particular, damping rates and universal crossover functions for the spectral functions have been derived. A related problem is the existence of a quantum critical regime at sufficiently large temperature which does not obey Luttinger liquid scaling (Guan and Batchelor, 2011). The search for experimental signatures of these effects going beyond the simplest Tomonaga-Luttinger liquid theory is one possible future development of interacting bosons in 1D. In a similar way, as discussed in Sec. VII.A, systems which do not obey the paradigm of Tomonaga-Luttinger liquids (Zvonarev *et al.*, 2007) have been found and will lead to interesting further developments.

b. Disorder and many-body localization: As discussed in Sec. VI.B, important developments have occurred in the understanding of the interplay between disorder and interactions. However, many questions still remain open, in particular, the understanding of the finite temperature transport properties of disordered quantum systems, a topic that should lead to a wealth of future developments (Oganesyan and Huse, 2007; Aleiner *et al.*, 2010; Monthus and Garel, 2010; Pal and Huse, 2010).

Another interesting open problem is the far-from-equilibrium dynamics of interacting bosons in the presence of a random potential. This problem is relevant for the expansion of condensates in experiments in which either a quasiperiodic or speckle potential is present (Roati *et al.*, 2008). More generally, understanding how those systems respond to quenches, and the steady states in the presence of time-dependent (Dalla Torre *et al.*, 2010) or time-independent noise, are of very much interest. A related question is the one of aging in disordered and glassy quantum systems. It is well known that in disordered systems, below a certain temperature, the relaxation may become extremely slow so that the system never equilibrates on any reasonable time scale. In such a regime, both correlation $C(\tau, \tau')$ and response $R(\tau, \tau')$ functions depend on both τ and τ' and not just $\tau - \tau'$ as in equilibrium. Some of these properties were understood for classical glasses (Cugliandolo, 2003) but remain largely to be understood for quantum glassy systems.

c. Dimensional crossover: In Sec. VII.B, we discussed briefly the issue of the dimensional crossover. A particularly interesting case is the one of coupled chains in a single plane. In that case, the system possesses long-range order in the ground state but, for any strictly positive temperature, long-range order is replaced by quasi-long-range order with a temperature-dependent exponent. At higher temperature, the system undergoes a BKT transition and is fully disordered above the transition. By contrast, a single chain has no long-range order at any strictly positive temperature, with a correlation length that diverges with temperature. There is thus an important issue of understanding the crossover from between the 1D decoupled chain regime and the 2D regime. Since both regimes are strongly fluctuating, this crossover cannot be tackled within a mean-field approximation, in contrast to the 1D–3D crossover.

Another important problem is the magnon BEC in coupled two-leg ladders when the interladder coupling is frustrated. In that case, one has to understand whether the formation of the magnon BEC is suppressed leaving the system in a critical state (Emery *et al.*, 2000; Vishwanath and Carpentier, 2001), or whether a more exotic broken symmetry develops, making the system off critical albeit with an unconventional spin ordering. A related problem exists in arrays of Josephson junctions (Tewari *et al.*, 2005; Tewari *et al.*, 2006) where dissipative effects can also come into play.

d. Ergodicity, quantum chaos, and thermalization: In Sec. VII.C, we briefly touched upon some of the recent experimental and theoretical studies that have dealt with the nonequilibrium dynamics of isolated quantum systems in 1D. This field is in its infancy and many important questions are currently being addressed by both experimentalists and theorists.

Most of the computational works so far have considered either small systems (with less than 10 particles), for which all time scales are accessible by means of full exact diagonalization techniques, or systems with up to $\sim$100 particles, for which only the short time scales ($\sim 10\hbar/t$) can be addressed with time-dependent DMRG and related techniques. It is becoming apparent that in order to gain further understanding of the long-time limit in large systems (or in the thermodynamic limit) a close collaboration will be needed between cold gases experiments, with their "quantum analog simulators," and theory. Among the things we would like to learn from those studies is what kind of memory of the initial conditions few-body observables retain in isolated quantum systems after relaxation (Olshanii and Yurovsky, 2011), the relevance of typicality arguments (Tasaki, 1998; Goldstein *et al.*, 2006; Popescu *et al.*, 2006; Reimann, 2008) to

experimental systems, the relation between thermalization and quantum chaos (Santos and Rigol, 2010a, 2010b), the time scales for thermalization (Moeckel and Kehrein, 2008; Barmettler *et al.*, 2009; Eckstein *et al.*, 2009), and the proper definition of thermodynamic quantities (Polkovnikov, 2008, 2011; Santos, Polkovnikov, and Rigol, 2011).

ACKNOWLEDGMENTS

We thank G. Astrakarchik, G. G. Batrouni, M. Batchelor, A. del Campo, E. G. Dalla Torre, F. Dalfovo, S. Giorgini, X.-W. Guan, A. Imambekov, A. Muramatsu, G. Mussardo, A. Minguzzi, H.-C. Nägerl, G. Orso, L. Pollet, N. Prokof'ev, R. T. Scalettar, B. Svistunov, and M. Troyer for valuable comments on the manuscript. M. A. C. thanks the hospitality of M. Ueda (Ueda ERATO Macroscopic Quantum Control Project of JST, Japan) and M. Oshikawa (ISSP) at the University of Tokyo, and D.-W. Wang at NCTS (Taiwan), where parts of this review were written, and the support of the Spanish MEC Grant No. FIS2007-066711-C02-02. M. R. was supported by the US Office of Naval Research under Grant No. N000140910966 and by the National Science Foundation under Grant No. OCI-0904597. This work was supported in part by the Swiss National Science Foundation under MaNEP and Division II.

REFERENCES

Abrahams, E., P. W. Anderson, D. Licciardello, and T. V. Ramakhrishnan, 1979, Phys. Rev. Lett. **42**, 673.
Abramowitz, M., and I. Stegun, 1972, *Handbook of Mathematical Functions* (Dover, New York).
Abrikosov, A., and J. Rhyzkin, 1978, Adv. Phys. **27**, 147.
Akhanjee, S., and Y. Tserkovnyak, 2007, Phys. Rev. B **76**, 140408.
Albert, M., and P. Leboeuf, 2010, Phys. Rev. A **81**, 013614.
Albus, A., F. Illuminati, and J. Eisert, 2003, Phys. Rev. A **68**, 023606.
Aleiner, I. L., B. L. Altshuler, and G. V. Shlyapnikov, 2010, Nature Phys. **6**, 900.
Alet, F., S. Wessel, and M. Troyer, 2005, Phys. Rev. E **71**, 036706.
Altman, E., E. Demler, and M. D. Lukin, 2004, Phys. Rev. A **70**, 013603.
Altman, E., Y. Kafri, Y. Polkovnikov, and G. Refael, 2004, Phys. Rev. Lett. **93**, 150402.
Altman, E., Y. Kafri, Y. Polkovnikov, and G. Refael, 2010, Phys. Rev. B **81**, 174528.
Altshuler, B. L., and A. G. Aronov, 1985, in *Electron–Electron Interactions in Disordered Systems*, edited by A. L. Efros, and M. Pollak (North-Holland, Amsterdam).
Amico, L., and V. Korepin, 2004, Ann. Phys. (N.Y.) **314**, 496.
Andersen, J. O., U. Al Khawaja, and H. T. C. Stoof, 2002, Phys. Rev. Lett. **88**, 070407.
Anderson, M. H., J. R. Ensher, M. R. Matthews, C. E. Wieman, and E. A. Cornell, 1995, Science **269**, 198.
Anderson, P. W., 1958, Phys. Rev. **109**, 1492.
Arkhipov, A. S., A. V. Belikov, G. E. Astrakharchik, and Y. E. Lozovik, 2005, JETP Lett. **82**, 39.
Assaad, F. F., 2002, in *Quantum Simulations of Complex Many-Body Systems: From Theory to Algorithms*, edited by J. Grotendorst, D. Marx, and A. Muramatsu, John von Neumann Institute for Computing (NIC) Series No. 10 (FZ-Jülich, Jülich, Germany), pp. 99–155.
Astrakharchik, G. E., D. Blume, S. Giorgini, and B. E. Granger, 2004a, J. Phys. B **37**, S205.
Astrakharchik, G. E., D. Blume, S. Giorgini, and B. E. Granger, 2004b, Phys. Rev. Lett. **92**, 030402.
Astrakharchik, G. E., J. Boronat, J. Casulleras, and S. Giorgini, 2005, Phys. Rev. Lett. **95**, 190407.
Astrakharchik, G. E., and S. Giorgini, 2002, Phys. Rev. A **66**, 053614.
Astrakharchik, G. E., and S. Giorgini, 2003, Phys. Rev. A **68**, 031602.
Astrakharchik, G. E., D. M. Gangardt, Yu. E. Lozovik, and I. Sorokin, 2006, Phys. Rev. E **74**, 021105.
Astrakharchik, G. E., and S. Giorgini, 2006, J. Phys. B **39**, S1.
Aubry, S., and G. André, 1980, Ann. Isr. Phys. Soc. **3**, 133.
Auslaender, O. M., A. Yacoby, R. de Picciotto, K. W. Baldwin, L. N. Pfeiffer, and K. W. West, 2002, Science **295**, 825.
Bakr, W. S., J. I. Gillen, A. Peng, S. Fölling, and M. Greiner, 2009, Nature (London) **462**, 74.
Bakr, W. S., A. Peng, M. E. Tai, R. Ma, J. Simon, J. I. Gillen, S. Folling, L. Pollet, and M. Greiner, 2010, Science **329**, 547.
Baltin, R., and K.-H. Wagenblast, 1997, Europhys. Lett. **39**, 7.
Bardeen, J., 1951, Rev. Mod. Phys. **23**, 261.
Barmettler, P., M. Punk, V. Gritsev, E. Demler, and E. Altman, 2009, Phys. Rev. Lett. **102**, 130603.
Barouch, E., and B. M. McCoy, 1971a, Phys. Rev. A **3**, 786.
Barouch, E., and B. M. McCoy, 1971b, Phys. Rev. A **3**, 2137.
Barouch, E., B. M. McCoy, and M. Dresden, 1970, Phys. Rev. A **2**, 1075.
Barthel, T., and U. Schollwöck, 2008, Phys. Rev. Lett. **100**, 100601.
Basko, D. M., I. L. Aleiner, and B. L. Altshuler, 2006, Ann. Phys. (N.Y.) **321**, 1126.
Batchelor, M., M. Bortz, X. W. Guan, and N. Oelkers, 2005a, J. Stat. Mech. L10001.
Batchelor, M. T., M. Bortz, X. W. Guan, and N. Oelkers, 2005b, Phys. Rev. A **72**, 061603.
Batchelor, M. T., X. W. Guan, N. Oelkers, and C. Lee, 2005c, J. Phys. A **38**, 7787.
Batrouni, G. G., H. R. Krishnamurthy, K. W. Mahmud, V. G. Rousseau, and R. T. Scalettar, 2008, Phys. Rev. A **78**, 023627.
Batrouni, G. G., V. Rousseau, R. T. Scalettar, M. Rigol, A. Muramatsu, P. J. H. Denteneer, and M. Troyer, 2002, Phys. Rev. Lett. **89**, 117203.
Batrouni, G. G., and R. T. Scalettar, 1992, Phys. Rev. B **46**, 9051.
Batrouni, G. G., R. T. Scalettar, and G. T. Zimanyi, 1990, Phys. Rev. Lett. **65**, 1765.
Beard, B. B., and U.-J. Wiese, 1996, Phys. Rev. Lett. **77**, 5130.
Benfatto, L., C. Castellani, and T. Giamarchi, 2007, Phys. Rev. Lett. **98**, 117008.
Berezinskii, V., 1974, Zh. Eksp. Teor. Fiz. **65**, 1251 [Sov. Phys. JETP **38**, 620 (1974)].
Berg, E., E. G. Dalla Torre, T. Giamarchi, and E. Altman, 2008, Phys. Rev. B **77**, 245119.
Bergkvist, S., P. Henelius, and A. Rosengren, 2004, Phys. Rev. A **70**, 053601.
Bethe, H. A., 1931, Z. Phys. **71**, 205.
Bettelheim, E., A. G. Abanov, and P. Wiegmann, 2006, Phys. Rev. Lett. **97**, 246401.
Bijl, A., 1937, Physica (Amsterdam) **4**, 329.
Bijl, A., 1940, Physica (Amsterdam) **7**, 869.
Billy, J., V. Josse, Z. Zuo, A. Bernard, B. Hambrecht, P. Lugan, D. Clément, L. Sanchez-Palencia, P. Bouyer, and A. Aspect, 2008, Nature (London) **453**, 891.

Bistritzer, R., and E. Altman, 2007, Proc. Natl. Acad. Sci. U.S.A. **104**, 9955.
Bloch, I., J. Dalibard, and W. Zwerger, 2008, Rev. Mod. Phys. **80**, 885.
Blume, D., 2002, Phys. Rev. A **66**, 053613.
Bobbert, P. A., R. Fazio, G. Schön, and A. D. Zaikin, 1992, Phys. Rev. B **45**, 2294.
Bobbert, P. A., R. Fazio, G. Schön, and G. T. Zimanyi, 1990, Phys. Rev. B **41**, 4009.
Bouillot, P., *et al.*, 2011, Phys. Rev. B **83**, 054407.
Brack, M., and B. P. van Zyl, 2001, Phys. Rev. Lett. **86**, 1574.
Bradley, C. C., C. A. Sackett, J. J. Tollett, and R. G. Hulet, 1995, Phys. Rev. Lett. **75**, 1687.
Bradley, R. M., and S. Doniach, 1984, Phys. Rev. B **30**, 1138.
Bruder, C., L. I. Glazman, A. I. Larkin, J. E. Mooij, and A. van Oudenaarden, 1999, Phys. Rev. B **59**, 1383.
Brunello, A., F. Dalfovo, L. Pitaevskii, S. Stringari, and F. Zambelli, 2001, Phys. Rev. A **64**, 063614.
Büchler, H., G. Blatter, and W. Zwerger, 2003, Phys. Rev. Lett. **90**, 130401.
Buljan, H., K. Lelas, R. Pezer, and M. Jablan, 2007, Phys. Rev. A **76**, 043609.
Buljan, H., R. Pezer, and T. Gasenzer, 2008, Phys. Rev. Lett. **100**, 080406.
Buonsante, P., V. Penna, and A. Vezzani, 2004, Phys. Rev. A **70**, 061603(R).
Buonsante, P., and A. Vezzani, 2004, Phys. Rev. A **70**, 033608.
Buonsante, P., and A. Vezzani, 2005, Phys. Rev. A **72**, 013614.
Burkov, A. A., M. D. Lukin, and E. Demler, 2007, Phys. Rev. Lett. **98**, 200404.
Burnell, F. J., M. M. Parish, N. R. Cooper, and S. L. Sondhi, 2009, Phys. Rev. B **80**, 174519.
Burovski, E., G. Orso, and T. Jolicoeur, 2009, Phys. Rev. Lett. **103**, 215301.
Caianiello, E., and S. Fubini, 1952, Nuovo Cimento **9**, 1218.
Calabrese, P., and J. Cardy, 2007, J. Stat. Mech., P06008.
Calogero, F., 1969, J. Math. Phys. (N.Y.) **10**, 2191.
Campostrini, M., and E. Vicari, 2010a, Phys. Rev. A **81**, 063614.
Campostrini, M., and E. Vicari, 2010b, Phys. Rev. A **81**, 023606.
Cao, J., Y. Jiang, and Y. Wang, 2007, Europhys. Lett. **79**, 30005.
Capogrosso-Sansone, B., N. V. Prokof'ev, and B. V. Svistunov, 2007, Phys. Rev. B **75**, 134302.
Capogrosso-Sansone, B., Ş. G. Söyler, N. Prokof'ev, and B. Svistunov, 2008, Phys. Rev. A **77**, 015602.
Cardy, J., 1996, *Scaling and Renormalization in Statistical Physics* (Cambridge University Press, Cambridge, England).
Cassidy, A. C., C. W. Clark, and M. Rigol, 2011, Phys. Rev. Lett. **106**, 140405.
Caux, J., A. Klauser, and J. van den Brink, 2009, Phys. Rev. A **80**, 061605.
Caux, J. S., and J. M. Maillet, 2005, Phys. Rev. Lett. **95**, 077201.
Caux, J.-S., and P. Calabrese, 2006, Phys. Rev. A **74**, 031605.
Caux, J.-S., P. Calabrese, and N. A. Slavnov, 2007, J. Stat. Mech., P01008.
Caux, J.-S., R. Hagemans, and J. M. Maillet, 2005, J. Stat. Mech., P09003.
Cazalilla, M. A., 2002, Europhys. Lett. **59**, 793.
Cazalilla, M. A., 2003, Phys. Rev. A **67**, 53606.
Cazalilla, M. A., 2004a, Phys. Rev. A **70**, 41604.
Cazalilla, M. A., 2004b, J. Phys. B **37**, S1.
Cazalilla, M. A., 2006, Phys. Rev. Lett. **97**, 156403.
Cazalilla, M. A., and A. F. Ho, 2003, Phys. Rev. Lett. **91**, 150403.
Cazalilla, M. A., A. F. Ho, and T. Giamarchi, 2006, New J. Phys. **8**, 158.
Cazalilla, M. A., A. Iucci, and T. Giamarchi, 2007, Phys. Rev. A **75**, 051603(R).
Cazalilla, M. A., and M. Rigol, 2010, New J. Phys. **12**, 055006.
Ceperley, D. M., and M. H. Kalos, 1979, in *Monte Carlo Methods in Statistical Physics*, edited by K. Binder (Springer Verlag, Berlin).
Chaboussant, G., P. Crowell, L. P. Lévy, O. Poivesana, A. Madouri, and D. Mailly, 1997, Phys. Rev. B **55**, 3046.
Cheianov, V., H. Smith, and M. B. Zvonarev, 2006, Phys. Rev. A **73**, 051604(R).
Cheon, T., and T. Shigehara, 1999, Phys. Rev. Lett. **82**, 2536.
Cherny, A. Y., and Brand J., 2009, Phys. Rev. A **79**, 043607
Chiara, G. D., M. Rizzi, D. Rossini, and S. Montangero, 2008, J. Comput. Theor. Nanosci. **5**, 1277.
Chitra, R., and T. Giamarchi, 1997, Phys. Rev. B **55**, 5816.
Chow, E., P. Delsing, and D. B. Haviland, 1998, Phys. Rev. Lett. **81**, 204.
Choy, T. C., and F. D. M. Haldane, 1982, Phys. Lett. A **90**, 83.
Citro, R., S. De Palo, E. Orignac, P. Pedri, and M.-L. Chiofalo, 2008, New J. Phys. **10**, 045011.
Clément, T., *et al.*, 2009, Phys. Rev. Lett. **102**, 155301.
Coleman, S., 1988, *Aspects of Symmetry* (Cambridge University Press, Cambridge, England).
Controzzi, D., F. H. Essler, and A. M. Tsvelik, 2001, Phys. Rev. Lett. **86**, 680.
Cramer, M., C. M. Dawson, J. Eisert, and T. J. Osborne, 2008, Phys. Rev. Lett. **100**, 030602.
Crépin, F., G. Zarand, and P. Simon, 2010, Phys. Rev. Lett. **105**, 115301.
Cugliandolo, L. F., 2003, in *Slow Relaxations and Nonequilibrium Dynamics in Condensed Matter*, edited by J.-L. Barrat, M. Feigelman, J. Kurchan, and J. Dalibard (Springer-Verlag, Heidelberg), p. 371.
Cullum, J. K., and R. A. Willoughby, 1985, in *Progress in Scientific Computing* (Birkhäuser Boston, Inc., Boston).
Dagotto, E., and T. Rice, 1996, Science **271**, 618.
Dalfovo, F., S. Giorgini, L. P. Pitaevskii, and S. Stringari, 1999, Rev. Mod. Phys. **71**, 463.
Dalla Torre, E. G., E. Berg, and E. Altman, 2006, Phys. Rev. Lett. **97**, 260401.
Dalla Torre, E. G., E. Demler, T. Giamarchi, and E. Altman, 2010, Nature Phys. **6**, 806.
Danshita, I., and C. W. Clark, 2009, Phys. Rev. Lett. **102**, 030407.
Davis, K. B., M. O. Mewes, M. R. Andrews, N. J. van Druten, D. S. Durfee, D. M. Kurn, and W. Ketterle, 1995, Phys. Rev. Lett. **75**, 3969.
del Campo, A., 2008, Phys. Rev. A **78**, 045602.
del Campo, A., and J. G. Muga, 2006, Europhys. Lett. **74**, 965.
Deng, X., R. Citro, A. Minguzzi, and E. Orignac, 2008, Phys. Rev. A **78**, 013625.
Dettmer, S., *et al.*, 2001, Phys. Rev. Lett. **87**, 160406.
Deuar, P., A. G. Sykes, D. M. Gangardt, M. J. Davis, P. D. Drummond, and K. V. Kheruntsyan, 2009, Phys. Rev. A **79**, 043619.
Deutsch, J. M., 1991, Phys. Rev. A **43**, 2046.
Didier, N., A. Minguzzi, and F. W. J. Hekking, 2009, Phys. Rev. A **80**, 033608.
Donohue, P., and T. Giamarchi, 2001, Phys. Rev. B **63**, 180508(R).
Dorneich, A., and M. Troyer, 2001, Phys. Rev. E **64**, 066701.
Doty, C., and D. S. Fisher, 1992, Phys. Rev. B **45**, 2167.
Drummond, P. D., P. Deuar, and K. V. Kheruntsyan, 2004, Phys. Rev. Lett. **92**, 040405.
Duan, L.-M., E. Demler, and M. D. Lukin, 2003, Phys. Rev. Lett. **91**, 090402.
DuBois, J. L., and H. R. Glyde, 2001, Phys. Rev. A **63**, 023602.

Dunjko, V., V. Lorent, and M. Olshanii, 2001, Phys. Rev. Lett. **86**, 5413.
Dziarmaga, J., 2010, Adv. Phys. **59**, 1063.
Eckstein, M., M. Kollar, and P. Werner, 2009, Phys. Rev. Lett. **103**, 056403.
Efetov, K. B., 1983, Adv. Phys. **32**, 53.
Efetov, K. B., A. Larkin, and D. Khmelnitskii, 1980, Zh. Eksp. Teor. Fiz. **79**, 1120, http://www.jetp.ac.ru/cgi-bin/e/index/e/52/3/p568?a=list [Sov. Phys. JETP **52**, 568 (1980)].
Efetov, K. B., and A. I. Larkin, 1975Zh. Eksp. Teor. Fiz. **69**, 764, http://www.jetp.ac.ru/cgi-bin/e/index/e/42/2/p390?a=list [Sov. Phys. JETP **42**, 390 (1975)].
Eggel, T., M. A. Cazalilla, and M. Oshikawa, 2011, arXiv:1104.0175.
Eggert, S., and I. Affleck, 1992, Phys. Rev. B **46**, 10866.
Eggert, S., I. Affleck, and M. D. P. Horton, 2002, Phys. Rev. Lett. **89**, 047202.
Eisenberg, E., and E. H. Lieb, 2002, Phys. Rev. Lett. **89**, 220403.
Elstner, N., and H. Monien, 1999, Phys. Rev. B **59**, 12184.
Emery, V. J., E. Fradkin, S. A. Kivelson, and T. C. Lubensky, 2000, Phys. Rev. Lett. **85**, 2160.
Essler, F., G. Shlyapnikov, and A. Tsvelik, 2009, J. Stat. Mech., P02027.
Evertz, H. G., 2003, Adv. Phys. **52**, 1.
Evertz, H. G., G. Lana, and M. Marcu, 1993, Phys. Rev. Lett. **70**, 875.
Falco, G. M., T. Nattermann, and V. L. Pokrovsky, 2009, Phys. Rev. B **80**, 104515.
Fazio, R., and H. van der Zant, 2001, Phys. Rep. **355**, 235.
Fendley, P., F. Lesage, and H. Saleur, 1995, J. Stat. Phys. **79**, 799.
Fertig, C. D., K. M. O'Hara, J. H. Huckans, S. L. Rolston, W. D. Phillips, and J. V. Porto, 2005a, Phys. Rev. Lett. **94**, 120403.
Fertig, C. D., K. M. O'Hara, J. H. Huckans, S. L. Rolston, W. D. Phillips, and J. V. Porto, 2005b, Phys. Rev. Lett. **94**, 120403.
Feynman, R. P., 1972, *Statistical Mechanics* (W. A. Benjamin, Reading, MA).
Finkelstein, A. M., 1984, Z. Phys. B **56**, 189.
Fioretto, D., and G. Mussardo, 2010, New J. Phys. **12**, 055015.
Fisher, D. S., 1994, Phys. Rev. B **50**, 3799.
Fisher, M. E., 1967, Rep. Prog. Phys. **30**, 615, and references therein.
Fisher, M. E., M. N. Barber, and D. Jasnow, 1973, Phys. Rev. A **8**, 1111.
Fisher, M. E., and R. E. Hartwig, 1968, Adv. Chem. Phys. **15**, 333.
Fisher, M. P. A., P. B. Weichman, G. Grinstein, and D. S. Fisher, 1989, Phys. Rev. B **40**, 546.
Flach, S., D. O. Krimer, and C. Skokos, 2009, Phys. Rev. Lett. **102**, 024101.
Folman, R., P. Krüger, J. Schmiedmayer, J. Denschlag, and C. Henkel, 2002, Adv. At. Mol. Opt. Phys. **48**, 263.
Folman, R., P. Krüger, D. Cassettari, B. Hessmo, T. Maier, and J. Schmiedmayer, 2000, Phys. Rev. Lett. **84**, 4749.
Forrester, P. J., N. E. Frankel, T. M. Garoni, and N. S. Witte, 2003a, Commun. Math. Phys. **238**, 257.
Forrester, P. J., N. E. Frankel, T. M. Garoni, and N. S. Witte, 2003b, Phys. Rev. A **67**, 043607.
Fortagh, J., *et al.*, 2004, Opt. Commun. **243**, 45.
Fradkin, E., E. Moreno, and F. A. Schaposnik, 1993, Nucl. Phys. **B392**, 667.
Frahm, H., and G. Palacios, 2005, Phys. Rev. A **72**, 061604(R).
Freericks, J. K., H. R. Krishnamurthy, Y. Kato, N. Kawashima, and N. Trivedi, 2009, Phys. Rev. A **79**, 053631.
Freericks, J. K., and H. Monien, 1996, Phys. Rev. B **53**, 2691.
Fuchs, J. N., D. M. Gangardt, T. Keilmann, and G. V. Shlyapnikov, 2005, Phys. Rev. Lett. **95**, 150402.
Fukuyama, H., and P. A. Lee, 1978, Phys. Rev. B **17**, 535.
Furusaki, A., and S.-C. Zhang, 1999, Phys. Rev. B **60**, 1175.
Fye, R. M., 1986, Phys. Rev. B **33**, 6271.
Gangardt, D. M., 2004, J. Phys. A **37**, 9335.
Gangardt, D. M., and A. Kamenev, 2001, Nucl. Phys. **B610**, 578.
Gangardt, D. M., and G. V. Shlyapnikov, 2003, Phys. Rev. Lett. **90**, 010401.
Gangardt, D. M., and G. V. Shlyapnikov, 2006, New J. Phys. **8**, 167.
Gaudin, M., 1967, Phys. Lett. A **24**, 55.
Gavish, U., and Y. Castin, 2005, Phys. Rev. Lett. **95**, 020401.
Gemelke, N., X. Zhang, C.-L. Hung, and C. Chin, 2009, Nature (London) **460**, 995.
Gerbier, F., *et al.*, 2008, Phys. Rev. Lett. **101**, 155303.
Giamarchi, T., 1991, Phys. Rev. B **44**, 2905.
Giamarchi, T., 1992, Phys. Rev. B **46**, 342.
Giamarchi, T., 1997, Physica B (Amsterdam) **230–232**, 975.
Giamarchi, T., 2003, in *Quantum Phenomena in Mesoscopic Systems, Volume 151 of International School of Physics Enrico Fermi*, edited by B. Altshuler, V. Tognetti, and A. Tagliacozzo (IOS Press, Amsterdam), p. 303.
Giamarchi, T., 2004, *Quantum Physics in One Dimension* (Oxford University Press, Oxford).
Giamarchi, T., 2010, in *Understanding Quantum Phase Transitions*, edited by L. D. Carr (CRC Press/Taylor & Francis, Boca Raton, FL), p. 291.
Giamarchi, T., and P. Le Doussal, 1996, Phys. Rev. B **53**, 15206.
Giamarchi, T., and A. J. Millis, 1992, Phys. Rev. B **46**, 9325.
Giamarchi, T., C. Rüegg, and O. Tchernyshyov, 2008, Nature Phys. **4**, 198.
Giamarchi, T., and H. J. Schulz, 1987, Europhys. Lett. **3**, 1287.
Giamarchi, T., and H. J. Schulz, 1988, Phys. Rev. B **37**, 325.
Giamarchi, T., and H. J. Schulz, 1989, Phys. Rev. B **39**, 4620.
Giamarchi, T., and B. S. Shastry, 1995, Phys. Rev. B **51**, 10915.
Giamarchi, T., and A. M. Tsvelik, 1999, Phys. Rev. B **59**, 11398.
Girardeau, M., 1960, J. Math. Phys. (N.Y.) **1**, 516.
Girardeau, M. D., and G. E. Astrakharchik, 2010, Phys. Rev. A **81**, 061601.
Girardeau, M. D., and A. Minguzzi, 2007, Phys. Rev. Lett. **99**, 230402.
Girardeau, M. D., E. M. Wright, and J. M. Triscari, 2001, Phys. Rev. A **63**, 033601.
Glauber, R. J., 1963, Phys. Rev. **130**, 2529.
Glazman, L. I., and A. I. Larkin, 1997, Phys. Rev. Lett. **79**, 3736.
Gogolin, A. A., 1982, Phys. Rep. **86**, 1.
Gogolin, A. O., A. A. Nersesyan, and A. M. Tsvelik, 1999, *Bosonization and Strongly Correlated Systems* (Cambridge University Press, Cambridge, England).
Goldstein, S., J. L. Lebowitz, R. Tumulka, and N. Zanghì, 2006, Phys. Rev. Lett. **96**, 050403.
Golovach, V. N., A. Minguzzi, and L. I. Glazman, 2009, Phys. Rev. A **80**, 043611.
Görlitz, A., *et al.*, 2001, Phys. Rev. Lett. **87**, 130402.
Gornyi, I. V., A. D. Mirlin, and D. G. Polyakov, 2005, Phys. Rev. Lett. **95**, 206603.
Gornyi, I. V., A. D. Mirlin, and D. G. Polyakov, 2007, Phys. Rev. B **75**, 085421.
Greiner, M., I. Bloch, O. Mandel, T. Hänsch, and T. Esslinger, 2001, Phys. Rev. Lett. **87**, 160405.
Greiner, M., O. Mandel, T. Esslinger, T. W. Hänsch, and I. Bloch, 2002a, Nature (London) **415**, 39.

Greiner, M., O. Mandel, T. W. Hänsch, and I. Bloch, 2002b, Nature (London) **419**, 51.
Griesmaier, A., J. Werner, S. Hensler, J. Stuhler, and T. Pfau, 2005, Phys. Rev. Lett. **94**, 160401.
Gritsev, V., E. Altman, E. Demler, and A. Polkovnikov, 2006, Nature Phys. **2**, 705.
Gritsev, V., P. Barmettler, and E. Demler, 2010, New J. Phys. **12**, 113005.
Gritsev, V., T. Rostunov, and E. Demler, 2010, J. Stat. Mech., P05012.
Gross, E. P., 1963, J. Math. Phys. (N.Y.) **4**, 195.
Guan, X., and M. T. Batchelor, 2011, J. Phys. A **44**, 102001.
Guan, X., M. T. Batchelor, and M. Takahashi, 2007, Phys. Rev. A **76**, 043617.
Guan, X.-W., M. T. Batchelor, and J.-Y. Lee, 2008, Phys. Rev. A **78**, 023621.
Gurarie, V., 2006, Phys. Rev. A **73**, 033612.
Gurarie, V., L. Pollet, N. V. Prokof'ev, B. V. Svistunov, and M. Troyer, 2009, Phys. Rev. B **80**, 214519.
Ha, Z. N. C., 1994, Phys. Rev. Lett. **73**, 1574.
Ha, Z. N. C., 1995, Nucl. Phys. **B435**, 604.
Haldane, F. D. M., 1980, Phys. Lett. A **80**, 281.
Haldane, F. D. M., 1981a, Phys. Rev. Lett. **47**, 1840.
Haldane, F. D. M., 1981b, J. Phys. C **14**, 2585.
Hallberg, K., 2003, in *CRM Series in Mathematical Physics*, edited by D. Sénéchal, A.-M. S. Tremblay, and C. Bourbonnais (Springer, New York).
Haller, E., M. Gustavsson, M. J. Mark, J. G. Danzl, R. Hart, G. Pupillo, and H.-C. Nägerl, 2009, Science **325**, 1224.
Haller, E., R. Hart, M. J. Mark, J. G. Danzl, L. Reichsöller, M. Gustavsson, M. Dalmonte, G. Pupillo, and H.-C. Nagerl, 2010, Nature (London) **466**, 597.
Hao, Y., Y. Zhang, and S. Chen, 2009, Phys. Rev. A **79**, 043633.
Harper, P., 1955, Proc. Phys. Soc. London Sect. A **68**, 874.
Haviland, D. B., K. Andersson, and P. Ägren, 2000, J. Low Temp. Phys. **118**, 733.
He, K., and M. Rigol, 2011, Phys. Rev. A **83**, 023611.
Hébert, F., G. G. Batrouni, X. Roy, and V. G. Rousseau, 2008, Phys. Rev. B **78**, 184505.
Hébert, F., F. Haudin, L. Pollet, and G. G. Batrouni, 2007, Phys. Rev. A **76**, 043619.
Henelius, P., and S. M. Girvin, 1998, Phys. Rev. B **57**, 11457.
Herbut, I. F., 1998, Phys. Rev. B **57**, 13729.
Hida, K., 1999, J. Phys. Soc. Jpn. **68**, 3177.
Hida, K., 2000, J. Phys. Soc. Jpn., Supp. A **69**, 311.
Hida, K., 2001, Phys. Rev. Lett. **86**, 1331.
Hikihara, T., and A. Furusaki, 1998, Phys. Rev. B **58**, R583.
Hikihara, T., and A. Furusaki, 2001, Phys. Rev. B **63**, 134438.
Hikihara, T., and A. Furusaki, 2004, Phys. Rev. B **69**, 064427.
Hiramoto, H., and M. Kohmoto, 1992, Int. J. Mod. Phys. B **6**, 281.
Hirsch, J. E., R. L. Sugar, D. J. Scalapino, and R. Blankenbecler, 1982, Phys. Rev. B **26**, 5033.
Ho, A. F., M. A. Cazalilla, and T. Giamarchi, 2004, Phys. Rev. Lett. **92**, 130405.
Hofferberth, S., I. Lesanovsky, B. Fischer, T. Schumm, and J. Schmiedmayer, 2007, Nature (London) **449**, 324.
Hofferberth, S., I. Lesanovsky, T. Schumm, A. Imambekov, V. Gritsev, E. Demler, and J. Schmiedmayer, 2008, Nature Phys. **4**, 489.
Hofstadter, D., 1976, Phys. Rev. B **14**, 2239.
Hohenberg, P. C., 1967, Phys. Rev. **158**, 383.
Holstein, T., and H. Primakoff, 1940, Phys. Rev. **58**, 1098.
Hong, T., A. Zheludev, H. Manaka, and L.-P. Regnault, 2010, Phys. Rev. B **81**, 060410.
Huang, K., and C. N. Yang, 1957, Phys. Rev. **105**, 767.
Huber, S. D., E. Altman, H. P. Büchler, and G. Blatter, 2007, Phys. Rev. Lett. **75**, 085106.
Huber, S. D., B. Theiler, E. Altman, and G. Blatter, 2008, Phys. Rev. Lett. **100**, 050404.
Iida, T., and M. Wadati, 2005, J. Phys. Soc. Jpn. **74**, 1724.
Imambekov, A., and E. Demler, 2006, Phys. Rev. A **73**, 021602(R).
Imambekov, A., and E. Demler, 2006, Ann. Phys. (N.Y.) **321**, 2390.
Imambekov, A., and L. I. Glazman, 2008, Phys. Rev. Lett. **100**, 206805.
Imambekov, A., and L. I. Glazman, 2009, Science **323**, 228.
Imambekov, A., V. Gritsev, and E. Demler, 2007, in *Proceedings of the International School of Physics "Enrico Fermi" (Varenna, Italy, June 2006)*, edited by M. Inguscio, W. Ketterle, and C. Salomon (IOS Press, Amsterdam), Vol. 164, p. 535.
Imambekov, A., V. Gritsev, and E. Demler, 2008, Phys. Rev. A **77**, 063606.
Imry, Y., and S. Ma, 1975, Phys. Rev. Lett. **35**, 1399.
Ince, E. L., 1956, *Ordinary Differential Equations* (Dover, Mineola, NY).
Its, A., A. Izergin, and V. Korepin, 1991, Physica D (Amsterdam) **53**, 187.
Its, A. R., A. G. Izergin, V. E. Korepin, and N. A. Slavnov, 1993, Phys. Rev. Lett. **70**, 1704.
Itzykson, C., and J. B. Zuber, 1980, *Quantum Field Theory* (McGraw Hill, New York).
Iucci, A., and M. A. Cazalilla, 2009, Phys. Rev. A **80**, 063619.
Iucci, A., and M. A. Cazalilla, 2010, New J. Phys. **12**, 055019.
Iucci, A., M. A. Cazalilla, A. F. Ho, and T. Giamarchi, 2006, Phys. Rev. A **73**, 41608.
Jaksch, D., C. Bruder, J. I. Cirac, C. W. Gardiner, and P. Zoller, 1998, Phys. Rev. Lett. **81**, 3108.
Japaridze, G. I., and A. A. Nersesyan, 1978, Pis'ma Zh. Eksp. Teor. Fiz. **27**, 356 [JETP Lett. **27**, 334 (1978)], http://www.jetpletters.ac.ru/ps/1549/article_23715.shtml.
Jastrow, R., 1955, Phys. Rev. **98**, 1479.
Jaynes, E. T., 1957a, Phys. Rev. **106**, 620.
Jaynes, E. T., 1957b, Phys. Rev. **108**, 171.
Jimbo, M., T. Miwa, Y. Môri, and M. Sato, 1980, Physica D (Amsterdam) **1**, 80.
Jitomirskaya, S. Y., 1999, Ann. Math. **150**, 1159.
Johnson, J. D., and B. M. McCoy, 1971, Phys. Rev. A **4**, 2314.
Jordan, P., and E. Wigner, 1928, Z. Phys. **47**, 631.
Jukić, D., R. Pezer, T. Gasenzer, and H. Buljan, 2008, Phys. Rev. A **78**, 053602.
Kalos, M. H., D. Levesque, and L. Verlet, 1974, Phys. Rev. A **9**, 2178.
Kamenev, A., and L. Glazman, 2009, Phys. Rev. A **80**, 011603(R).
Kashurnikov, V. A., A. V. Krasavin, and B. V. Svistunov, 1996, JETP Lett. **64**, 99.
Kashurnikov, V. A., and B. V. Svistunov, 1996, Phys. Rev. B **53**, 11776.
Kato, Y., Q. Zhou, N. Kawashima, and N. Trivedi, 2008, Nature Phys. **4**, 617.
Katsura, S., 1962, Phys. Rev. **127**, 1508.
Kawashima, N., J. E. Gubernatis, and H. G. Evertz, 1994, Phys. Rev. B **50**, 136.
Kennedy, T., E. H. Lieb, and B. S. Shastry, 1988, Phys. Rev. Lett. **61**, 2582.
Ketterle, W., and D. E. Pritchard, 1992, Appl. Phys. B **54**, 403.
Ketterle, W., and N. van Druten, 1996, Phys. Rev. A **54**, 656.
Kheruntsyan, K. V., D. M. Gangardt, P. D. Drummond, and G. V. Shlyapnikov, 2003, Phys. Rev. Lett. **91**, 040403.
Kheruntsyan, K. V., D. M. Gangardt, P. D. Drummond, and G. V. Shlyapnikov, 2005, Phys. Rev. A **71**, 053615.

Khodas, M., M. Pustilnik, A. Kamenev, and L. I. Glazman, 2007, Phys. Rev. Lett. **99**, 110405.
Kinoshita, T., T. Wenger, and D. S. Weiss, 2004, Science **305**, 1125.
Kinoshita, T., T. Wenger, and D. S. Weiss, 2005, Phys. Rev. Lett. **95**, 190406.
Kinoshita, T., T. Wenger, and D. S. Weiss, 2006, Nature (London) **440**, 900.
Klanjšek, M., *et al.*, 2008, Phys. Rev. Lett. **101**, 137207.
Klein, A., and J. F. Perez, 1990, Commun. Math. Phys. **128**, 99.
Kleine, A., C. Kollath, I. P. McCulloch, T. Giamarchi, and U. Schollwök, 2008a, Phys. Rev. A **77**, 013607.
Kleine, A., C. Kollath, I. P. McCulloch, T. Giamarchi, and U. Schollwöck, 2008b, New J. Phys. **10**, 045025.
Kohn, W., 1964, Phys. Rev. **133**, A171.
Kollar, M., and M. Eckstein, 2008, Phys. Rev. A **78**, 013626.
Kollath, C., A. Iucci, T. Giamarchi, W. Hofstetter, and U. Schollwöck, 2006, Phys. Rev. Lett. **97**, 050402.
Kollath, C., A. M. Läuchli, and E. Altman, 2007, Phys. Rev. Lett. **98**, 180601.
Kollath, C., U. Schollwöck, J. von Delft, and W. Zwerger, 2004, Phys. Rev. A **69**, 031601.
Konik, R. M., and A. LeClair, 1996, Nucl. Phys. **B479**, 619.
Korepin, V. E., N. M. Bogoliubov, and A. G. Izergin, 1993, *Quantum Inverse Scattering Method and Correlation Functions* (Cambridge University Press, Cambridge, England).
Kormos, M., G. Mussardo, and A. Trombettoni, 2009, Phys. Rev. Lett. **103**, 210404.
Kormos, M., G. Mussardo, and A. Trombettoni, 2010, Phys. Rev. A **81**, 043606.
Kormos, M., G. Mussardo, and V. Trombettoni, 2011, Phys. Rev. A **83**, 013617.
Korshunov, S. E., 1989a, Zh. Eksp. Teor. Fiz. **95**, 1058 [Sov. Phys. JETP **68**, 609 (1989), http://www.jetp.ac.ru/cgi-bin/e/index/e/68/3/p609?a=list].
Korshunov, S. E., 1989b, Europhys. Lett. **9**, 107.
Kosterlitz, J. M., 1974, J. Phys. C **7**, 1046.
Kosterlitz, J. M., and D. J. Thouless, 1973, J. Phys. C **6**, 1181.
Krämer, M., C. Tozzo, and F. Dalfovo, 2005, Phys. Rev. A **71**, 061602.
Krauth, W., 1991, Phys. Rev. B **44**, 9772.
Krutitsky, K. V., M. Thorwart, R. Egger, and R. Graham, 2008, Phys. Rev. A **77**, 053609.
Kühner, T. D., and H. Monien, 1998, Phys. Rev. B **58**, R14741.
Kühner, T. D., S. R. White, and H. Monien, 2000, Phys. Rev. B **61**, 12474.
Kuo, W., and C. D. Chen, 2001, Phys. Rev. Lett. **87**, 186804.
Lai, C. K., 1974, J. Math. Phys. (N.Y.) **15**, 954.
Lai, C. K., and C. N. Yang, 1971, Phys. Rev. A **3**, 393.
Lapeyre, G. J., M. D. Girardeau, and E. M. Wright, 2002, Phys. Rev. A **66**, 023606.
Larcher, M., F. Dalfovo, and M. Modugno, 2009, Phys. Rev. A **80**, 053606.
Lee, J. Y., X. W. Guan, M. T. Batchelor, and C. Lee, 2009, Phys. Rev. A **80**, 063625.
Lee, P., and T. V. Ramakhrishnan, 1985, Rev. Mod. Phys. **57**, 287.
Lee, T. D., K. Huang, and C. N. Yang, 1957, Phys. Rev. **106**, 1135.
Lee, T. D., and C. N. Yang, 1957, Phys. Rev. **105**, 1119.
Lee, Y.-W., Y.-L. Lee, and M.-F. Yang, 2007, Phys. Rev. B **76**, 075117.
Leggett, A., 1973, Phys. Fenn. **8**, 125.
Leggett, A. J., 2001, Rev. Mod. Phys. **73**, 307.
Leggett, A. J., 2006, *Quantum Liquids: Bose Condensation and Cooper Pairing in Condensed-Matter Systems* (Oxford University Press, New York).
Lenard, A., 1964, J. Math. Phys. (N.Y.) **5**, 930.
Lenard, A., 1966, J. Math. Phys. (N.Y.) **7**, 1268.
Li, Y.-Q., S.-J. Gu, Z.-J. Ying, and U. Eckern, 2003, Europhys. Lett. **61**, 368.
Lieb, E., T. Schultz, and D. Mattis, 1961, Ann. Phys. (N.Y.) **16**, 407.
Lieb, E. H., 1963, Phys. Rev. **130**, 1616.
Lieb, E. H., 1967, Phys. Rev. **162**, 162.
Lieb, E. H., and W. Liniger, 1963, Phys. Rev. **130**, 1605.
Lieb, E. H., and R. Seiringer, 2002, Phys. Rev. Lett. **88**, 170409.
Lieb, E. H., R. Seiringer, and J. Yngvason, 2000, Phys. Rev. A **61**, 043602.
Lieb, E. H., R. Seiringer, and J. Yngvason, 2002, Phys. Rev. B **66**, 134529.
Lieb, E. H., and F. Y. Wu, 1968, Phys. Rev. Lett. **20**, 1445.
Loh, E. Y., J. E. Gubernatis, R. T. Scalettar, S. R. White, D. J. Scalapino, and R. L. Sugar, 1990, Phys. Rev. B **41**, 9301.
Loss, D., and T. Martin, 1994, Phys. Rev. B **50**, 12160.
Lugan, P., A. Aspect, L. Sanchez-Palencia, D. Delande, B. Grémaud, C. A. Müller, and C. Miniatura, 2009, Phys. Rev. A **80**, 023605.
Lugan, P., D. Clément, P. Bouyer, A. Aspect, M. Lewenstein, and L. Sanchez-Palencia, 2007, Phys. Rev. Lett. **98**, 170403.
Lukyanov, S., 1998, Nucl. Phys. **B522**, 533.
Lukyanov, S., 1999, Phys. Rev. B **59**, 11163.
Lukyanov, S., and A. B. Zamolodchikov, 2001, Nucl. Phys. **B607**, 437.
Luther, A., and V. J. Emery, 1974, Phys. Rev. Lett. **33**, 589.
Luther, A., and I. Peschel, 1974, Phys. Rev. B **9**, 2911.
Luthra, M. S., T. Mishra, R. V. Pai, and B. P. Das, 2008, Phys. Rev. B **78**, 165104.
Ma, M., and T. L. Ho, 1999, J. Low Temp. Phys. **115**, 61.
Mandel, L., and E. Wolf, 1965, Rev. Mod. Phys. **37**, 231.
Manmana, S. R., A. Muramatsu, and R. M. Noack, 2005, AIP Conf. Proc. **789**, 269.
Manmana, S. R., S. Wessel, R. M. Noack, and A. Muramatsu, 2007, Phys. Rev. Lett. **98**, 210405.
Maslov, D. L., M. Stone, P. M. Goldbart, and D. Loss, 1996, Phys. Rev. B **53**, 1548.
Mathey, L., I. Danshita, and C. W. Clark, 2009, Phys. Rev. A **79**, 011602.
Mathey, L., A. Polkovnikov, and A. C. Neto, 2008, Europhys. Lett. **81**, 10008.
Mathey, L., A. Vishwanath, and E. Altman, 2009, Phys. Rev. A **79**, 013609.
Mathey, L., and D.-W. Wang, 2007, Phys. Rev. A **75**, 013602.
Mathey, L., D.-W. Wang, W. Hofstetter, M. D. Lukin, and E. Demler, 2004, Phys. Rev. Lett. **93**, 120404.
Matsubara, T., and H. Matsuda, 1956, Prog. Theor. Phys. **16**, 569.
Mattis, D. C., and E. H. Lieb, 1965, J. Math. Phys. (N.Y.) **6**, 304.
Matveev, A., and A. Furusaki, 2008, Phys. Rev. Lett. **101**, 170403.
Mazets, I. E., and J. Schmiedmayer, 2010, New J. Phys. **12**, 055023.
Mazets, I. E., T. Schumm, and J. Schmiedmayer, 2008, Phys. Rev. Lett. **100**, 210403.
Mazzanti, F., G. E. Astrakharchik, J. Boronat, and J. Casulleras, 2008, Phys. Rev. Lett. **100**, 020401.
McCoy, B. M., 1968, Phys. Rev. **173**, 531.
McCoy, B. M., E. Barouch, and D. B. Abraham, 1971, Phys. Rev. A **4**, 2331.
McCoy, B. M., J. H. Perk, and R. E. Schrock, 1983a, Nucl. Phys. **B220**, 35.

McCoy, B. M., J. H. Perk, and R. E. Schrock, 1983b, Nucl. Phys. **B220**, 269.
McGuire, J., 1964, J. Math. Phys. (N.Y.) **5**, 622.
Mehta, M. L., 2004, *Random Matrices* (Academic Press, New York).
Menotti, C., and S. Stringari, 2002, Phys. Rev. A **66**, 043610.
Menotti, C., and N. Trivedi, 2008, Phys. Rev. B **77**, 235120.
Mermin, N. D., 1968, Phys. Rev. **176**, 250.
Mermin, N. D., and H. Wagner, 1966, Phys. Rev. Lett. **17**, 1133.
Mila, F., 1998, Eur. Phys. J. B **6**, 201.
Minguzzi, A., and D. M. Gangardt, 2005, Phys. Rev. Lett. **94**, 240404.
Minguzzi, A., P. Vignolo, and M. P. Tosi, 2002, Phys. Lett. A **294**, 222.
Moeckel, M., and S. Kehrein, 2008, Phys. Rev. Lett. **100**, 175702.
Montangero, S., R. Fazio, P. Zoller, and G. Pupillo, 2009, Phys. Rev. A **79**, 041602.
Monthus, C., and T. Garel, 2010, Phys. Rev. B **81**, 134202.
Mora, C., and Y. Castin, 2003, Phys. Rev. A **67**, 053615.
Moritz, H., T. Stöferle, M. Köhl, and T. Esslinger, 2003, Phys. Rev. Lett. **91**, 250402.
Mott, N. F., 1990, *Metal-Insulator Transitions* (Taylor and Francis, London).
Mott, N. F., and W. D. Twose, 1961, Adv. Phys. **10**, 107.
Mucciolo, E. R., B. S. Shastry, B. D. Simons, and B. L. Altshuler, 1994, Phys. Rev. B **49**, 15197.
Mueller, E. J., T. L. Ho, M. Ueda, and G. Baym, 2006, Phys. Rev. A **74**, 033612.
Müller, G., and R. E. Shrock, 1983, Phys. Rev. Lett. **51**, 219.
Müller, G., and R. E. Shrock, 1984, Phys. Rev. B **29**, 288.
Muttalib, K. A., and V. J. Emery, 1986, Phys. Rev. Lett. **57**, 1370.
Nagamiya, T., 1940, Proc. Phys. Math. Soc. Japan **22**, 705, http://www.journalarchive.jst.go.jp/english/jnlabstract_en.php?cdjournal=ppmsj1919&cdvol=22&noissue=8-9&startpage=705.
Nattermann, T., T. Giamarchi, and P. Le Doussal, 2003, Phys. Rev. Lett. **91**, 56603.
Niemeijer, T., 1967, Physica (Amsterdam) **36**, 377.
Nikuni, T., M. Oshikawa, A. Oosawa, and H. Tanaka, 2000, Phys. Rev. Lett. **84**, 5868.
Noack, R. M., and S. R. Manmana, 2005, AIP Conf. Proc. **789**, 93.
Nonne, H., P. Lecheminant, S. Capponi, G. Roux, and E. Boulat, 2010, Phys. Rev. B **81**, 020408(R).
Oganesyan, V., and D. A. Huse, 2007, Phys. Rev. B **75**, 155111.
Olshanii, M., 1998, Phys. Rev. Lett. **81**, 938.
Olshanii, M., and V. Dunjko, 2003, Phys. Rev. Lett. **91**, 090401.
Olshanii, M., and V. Yurovsky, 2011, Phys. Rev. Lett. **106**, 025303.
Orbach, R., 1958, Phys. Rev. **112**, 309.
Orignac, E., and T. Giamarchi, 1998a, Phys. Rev. B **57**, 5812.
Orignac, E., and T. Giamarchi, 1998b, Phys. Rev. B **57**, 11713.
Orignac, E., M. Tsuchiizu, and Y. Suzumura, 2010, Phys. Rev. A **81**, 053626.
Orso, G., A. Iucci, M. A. Cazalilla, and T. Giamarchi, 2009, Phys. Rev. A **80**, 033625.
Ovchinnikov, A. A., 2002, J. Phys. Condens. Matter **14**, 10193.
Ovchinnikov, A. A., 2004, J. Phys. Condens. Matter **16**, 3147.
Ovchinnikov, A. A., 2009, Phys. Lett. A **373**, 305.
Pai, R. V., R. Pandit, H. R. Krishnamurthy, and S. Ramasesha, 1996, Phys. Rev. Lett. **76**, 2937.
Pal, A., and D. A. Huse, 2010, Phys. Rev. B **82**, 174411.
Papenbrock, T., 2003, Phys. Rev. A **67**, 041601(R).
Paredes, B., A. Widera, V. Murg, O. Mandel, S. Fölling, I. Cirac, G. V. Shlyapnikov, T. W. Hänsch, and I. Bloch, 2004, Nature (London) **429**, 277.
Patyal, B., B. Scott, and R. Willet, 1990, Phys. Rev. B **41**, 1657.
Pedri, P., *et al.*, 2001, Phys. Rev. Lett. **87**, 220401.
Penrose, O., and L. Onsager, 1956, Phys. Rev. **104**, 576.
Pereira, R. G., J. Sirker, J.-S. Caux, R. Hagemans, J. M. Maillet, S. R. White, and I. Affleck, 2006, Phys. Rev. Lett. **96**, 257202.
Petrov, D. S., D. M. Gangardt, and G. V. Shlyapnikov, 2004, J. Phys. IV (Colloque) **116**, 5.
Petrov, D. S., G. V. Shlyapnikov, and J. T. M. Walraven, 2000, Phys. Rev. Lett. **85**, 3745.
Pezer, R., and H. Buljan, 2007, Phys. Rev. Lett. **98**, 240403.
Pippan, P., H. G. Evertz, and M. Hohenadler, 2009, Phys. Rev. A **80**, 033612.
Pitaevskii, L., and S. Stringari, 1991, J. Low Temp. Phys. **85**, 377.
Pitaevskii, L., and S. Stringari, 2003, *Bose-Einstein Condensation* (Oxford University Press, New York).
Pitaevskii, L. P., 1961, Zh. Eksp. Teor. Fiz. **40**, 646 [Sov. Phys. JETP **13**, 451 (1963)].
Pokrovsky, V. L., and A. L. Talapov, 1979, Phys. Rev. Lett. **42**, 65.
Polkovnikov, A., 2008, Phys. Rev. Lett. **101**, 220402.
Polkovnikov, A., 2011, Ann. Phys. (N.Y.) **326**, 486.
Polkovnikov, A., E. Altman, and E. Demler, 2006, Proc. Natl. Acad. Sci. U.S.A. **103**, 6125.
Polkovnikov, A., K. Sengupta, A. Silva, and M. Vengalattore, 2011, Rev. Mod. Phys. **83**, 863.
Pollet, L., C. Kollath, U. Schollwöck, and M. Troyer, 2008, Phys. Rev. A **77**, 023608.
Pollet, L., N. V. Prokof'ev, and B. V. Svistunov, 2010, Phys. Rev. Lett. **104**, 245705.
Pollet, L., N. V. Prokof'ev, B. V. Svistunov, and M. Troyer, 2009, Phys. Rev. Lett. **103**, 140402.
Pollet, L., S. M. A. Rombouts, and P. J. H. Denteneer, 2004, Phys. Rev. Lett. **93**, 210401.
Pollet, L., M. Troyer, K. van Houcke, and S. M. A. Rombouts, 2006, Phys. Rev. Lett. **96**, 190402.
Pollock, E. L., and D. M. Ceperley, 1987, Phys. Rev. B **36**, 8343.
Ponomarev, A. V., S. Denisov, and P. Hänggi, 2010, Phys. Rev. A **81**, 043615.
Popescu, S., A. J. Short, and A. Winter, 2006, Nature Phys. **2**, 754.
Popov, V. N., 1972, Theor. Math. Phys. **11**, 565.
Popov, V. N., 1987, *Functional Integrals and collective excitations* (Cambridge University Press, Cambridge, England).
Press, W. H., B. P. Flannery, S. A. Teukolski, and W. T. Vetterling, 1988, *Numerical Recipes: The Art of Scientific Computing* (Cambridge University Press, Cambridge, England).
Prokof'ev, N., and B. Svistunov, 2009, arXiv:0910.1393.
Prokof'ev, N. V., and B. V. Svistunov, 1998, Phys. Rev. Lett. **80**, 4355.
Prokof'ev, N. V., and B. V. Svistunov, 2000, Phys. Rev. B **61**, 11282.
Prokof'ev, N. V., B. V. Svistunov, and I. S. Tupitsyn, 1996, JETP Lett. **64**, 911.
Pupillo, G., A. M. Rey, C. J. Williams, and C. W. Clark, 2006, New J. Phys. **8**, 161.
Pustilnik, M., 2006, Phys. Rev. Lett. **97**, 036404.
Radić, J., V. Bačić, D. Jukić, M. Segev, and H. Buljan, 2010, Phys. Rev. A **81**, 063639.
Rapsch, S., U. Schollwock, and W. Zwerger, 1999, Europhys. Lett. **46**, 559.
Reimann, P., 2008, Phys. Rev. Lett. **101**, 190403.
Rey, A. M., G. Pupillo, C. W. Clark, and C. J. Williams, 2005, Phys. Rev. A **72**, 033616.
Rey, A. M., I. I. Satija, and C. W. Clark, 2006a, New J. Phys. **8**, 155.
Rey, A. M., I. I. Satija, and C. W. Clark, 2006b, J. Phys. B **39**, S177.
Rey, A. M., I. I. Satija, and C. W. Clark, 2006c, Phys. Rev. A **73**, 063610.

Reynolds, P. J., D. M. Ceperley, B. J. Alder, and W. A. Lester, 1982, J. Chem. Phys. **77**, 5593.
Rigol, M., 2005, Phys. Rev. A **72**, 063607.
Rigol, M., 2009a, Phys. Rev. Lett. **103**, 100403.
Rigol, M., 2009b, Phys. Rev. A **80**, 053607.
Rigol, M., G. G. Batrouni, V. G. Rousseau, and R. T. Scalettar, 2009, Phys. Rev. A **79**, 053605.
Rigol, M., V. Dunjko, and M. Olshanii, 2008, Nature (London) **452**, 854.
Rigol, M., V. Dunjko, V. Yurovsky, and M. Olshanii, 2007, Phys. Rev. Lett. **98**, 050405.
Rigol, M., and A. Muramatsu, 2004, Phys. Rev. A **70**, 031603(R).
Rigol, M., and A. Muramatsu, 2005a, Phys. Rev. Lett. **94**, 240403.
Rigol, M., and A. Muramatsu, 2005b, Mod. Phys. Lett. B **19**, 861.
Rigol, M., and A. Muramatsu, 2005c, Phys. Rev. A **72**, 013604.
Rigol, M., A. Muramatsu, and M. Olshanii, 2006, Phys. Rev. A **74**, 053616.
Rigol, M., V. Rousseau, R. T. Scalettar, and R. R. P. Singh, 2005, Phys. Rev. Lett. **95**, 110402.
Rigol, M., R. T. Scalettar, P. Sengupta, and G. G. Batrouni, 2006, Phys. Rev. B **73**, 121103(R).
Rizzi, M., and A. Imambekov, 2008, Phys. Rev. A **77**, 023621.
Roati, G., C. D'Errico, L. Fallani, M. Fattori, C. Fort, M. Zaccanti, G. Modugno, M. Modugno, and M. Inguscio, 2008, Nature (London) **453**, 895.
Rokhsar, D. S., and B. G. Kotliar, 1991, Phys. Rev. B **44**, 10328.
Rosch, A., and N. Andrei, 2000, Phys. Rev. Lett. **85**, 1092.
Roscilde, T., 2008, Phys. Rev. A **77**, 063605.
Roscilde, T., 2010, Phys. Rev. A **82**, 023601.
Rosenow, B., and T. Nattermann, 2006, Phys. Rev. B **73**, 085103.
Rossini, D., A. Silva, G. Mussardo, and G. E. Santoro, 2009, Phys. Rev. Lett. **102**, 127204.
Roth, R., and K. Burnett, 2003a, Phys. Rev. A **68**, 023604.
Roth, R., and K. Burnett, 2003b, J. Opt. B **5**, S50.
Rousseau, V. G., D. P. Arovas, M. Rigol, F. Hébert, G. G. Batrouni, and R. T. Scalettar, 2006, Phys. Rev. B **73**, 174516.
Roux, G., 2009, Phys. Rev. A **79**, 021608.
Roux, G., 2010, Phys. Rev. A **81**, 053604.
Roux, G., T. Barthel, I. P. McCulloch, C. Kollath, U. Schollwöck, and T. Giamarchi, 2008, Phys. Rev. A **78**, 023628.
Ruegg, C., N. Cavadini, A. Furrer, and H. Gudel, 2003, Nature (London) **423**, 62.
Rüegg, C., *et al.*, 2008, Phys. Rev. Lett. **101**, 247202.
Ruostekoski, J., and L. Isella, 2005, Phys. Rev. Lett. **95**, 110403.
Ryu, C., M. F. Andersen, P. Cladé, V. Natarajan, K. Helmerson, and W. D. Phillips, 2007, Phys. Rev. Lett. **99**, 260401.
Sachdev, S., 2000, Science **288**, 475.
Sachdev, S., 2008, Nature Phys. **4**, 173.
Sachdev, S., T. Senthil, and R. Shankar, 1994, Phys. Rev. B **50**, 258.
Safi, I., and H. J. Schulz, 1995, Phys. Rev. B **52**, R17040.
Sandvik, A. W., 1992, J. Phys. A **25**, 3667.
Sandvik, A. W., 1999, Phys. Rev. B **59**, R14157.
Santos, L. F., A. Polkovnikov, and M. Rigol, 2011, Phys. Rev. Lett. **107**, 040601.
Santos, L. F., and M. Rigol, 2010a, Phys. Rev. E **82**, 031130.
Santos, L. F., and M. Rigol, 2010b, Phys. Rev. E **81**, 036206.
Scalettar, R. T., 1999, in *Quantum Monte Carlo Methods in Physics and Chemistry*, edited by M. P. Nightingale and C. J. Umrigar, NATO Science Series (Kluwer Academic Press, Dordrecht), pp. 65–100.
Scalettar, R. T., G. G. Batrouni, and G. T. Zimanyi, 1991, Phys. Rev. Lett. **66**, 3144.
Schmidt, E., 1907, Math. Ann. **63**, 433.
Schollwöck, U., 2005, Rev. Mod. Phys. **77**, 259.
Schreck, F., L. Khaykovich, K. L. Corwin, G. Ferrari, T. Bourdel, J. Cubizolles, and C. Salomon, 2001, Phys. Rev. Lett. **87**, 080403.
Schultz, T. D., 1963, J. Math. Phys. (N.Y.) **4**, 666.
Schulz, H. J., 1980, Phys. Rev. B **22**, 5274.
Schulz, H. J., 1990, Phys. Rev. Lett. **64**, 2831.
Schulz, H. J., 1996, Phys. Rev. Lett. **77**, 2790.
Sen, D., 1999, Int. J. Mod. Phys. A **14**, 1789.
Sen D., 2003, J. Phys. A **36**, 7517.
Sengupta, P., and L. P. Pryadko, 2007, Phys. Rev. B **75**, 132507.
Sengupta, P., M. Rigol, G. G. Batrouni, P. J. H. Denteneer, and R. T. Scalettar, 2005, Phys. Rev. Lett. **95**, 220402.
Shankar, R., 1990, Int. J. Mod. Phys. B **4**, 2371.
Shashi, A., L. I. Glazman, J.-S. Caux, and A. Imambekov, 2010, arXiv:1010.2268.
Shastry, B. S., and B. Sutherland, 1990, Phys. Rev. Lett. **65**, 243.
Srednicki, M., 1994, Phys. Rev. E **50**, 888.
Stenger, J., S. T. Inouye, D. Chikkatur, D. Stamper-Kurn, D. Pritchard, and W. Ketterle, 1999, Phys. Rev. Lett. **82**, 4569.
Stöferle, T., H. Moritz, C. Schori, M. Köhl, and T. Esslinger, 2004a, Phys. Rev. Lett. **92**, 130403.
Stöferle, T., H. Moritz, C. Schori, M. Köhl, and T. Esslinger, 2004b, Phys. Rev. Lett. **92**, 130403.
Stone, M. B., Y. Chen, J. Rittner, H. Yardimci, D. H. Reich, C. Broholm, D. V. Ferraris, and T. Lectka, 2002, Phys. Rev. B **65**, 64423.
Strohmaier, N., D. Greif, R. Jördens, L. Tarruell, H. Moritz, T. Esslinger, R. Sensarma, D. Pekker, E. Altman, and E. Demler, 2010, Phys. Rev. Lett. **104**, 080401.
Sur, A., D. Jasnow, and I. J. Lowe, 1975, Phys. Rev. B **12**, 3845.
Sutherland, B., 1968, Phys. Rev. Lett. **20**, 98.
Sutherland, B., 1971a, J. Math. Phys. (N.Y.) **12**, 246.
Sutherland, B., 1971b, Phys. Rev. A **4**, 2019.
Sutherland, B., 1998, Phys. Rev. Lett. **80**, 3678.
Suzuki, M., 1976, Commun. Math. Phys. **51**, 183.
Suzumura, Y., and H. Fukuyama, 1983, J. Phys. Soc. Jpn. **52**, 2870.
Svistunov, B. V., 1996, Phys. Rev. B **54**, 16131.
Swendsen, R. H., and J.-S. Wang, 1987, Phys. Rev. Lett. **58**, 86.
Sykes, A. G., D. M. Gangardt, M. J. Davis, K. Viering, M. G. Raizen, and K. V. Kheruntsyan, 2008, Phys. Rev. Lett. **100**, 160406.
Syljuåsen, O. F., and A. W. Sandvik, 2002, Phys. Rev. E **66**, 046701.
Szego, G., 1952, Commun. Seminair. Math. Univ. Lund **228**.
Tachiki, M., and T. Yamada, 1970, J. Phys. Soc. Jpn. **28**, 1413.
Takayoshi, S., M. Sato, and S. Furukawa, 2010, Phys. Rev. A **81**, 053606.
Takeuchi, Y., and H. Mori, 2005a, J. Phys. Soc. Jpn. **74**, 3391.
Takeuchi, Y., and H. Mori, 2005b, Phys. Rev. A **72**, 063617.
Taniguchi, J., Y. Aoki, and M. Suzuki, 2010, Phys. Rev. B **82**, 104509.
Tasaki, H., 1998, Phys. Rev. Lett. **80**, 1373.
Tewari, S., J. Toner, and S. Chakravarty, 2005, Phys. Rev. B **72**, 060505.
Tewari, S., J. Toner, and S. Chakravarty, 2006, Phys. Rev. B **73**, 064503.
Thielemann, B., *et al.*, 2009a, Phys. Rev. B **79**, 020408.
Thielemann, B., *et al.*, 2009b, Phys. Rev. Lett. **102**, 107204.
Tolra, B. L., K. M. O'Hara, J. H. Huckans, W. D. Phillips, S. L. Rolston, and J. V. Porto, 2004, Phys. Rev. Lett. **92**, 190401.
Trebbia, J.-B., J. Esteve, C. I. Westbrook, and I. Bouchoule, 2006, Phys. Rev. Lett. **97**, 250403.
Tricomi, F. G., 1985, *Integral Equations* (Dover, Mineola, New York).
Trotter, H. F., 1959, Proc. Am. Math. Soc. **10**, 545.
Troyer, M., and U.-J. Wiese, 2005, Phys. Rev. Lett. **94**, 170201.

Tserkovnyak, Y., B. I. Halperin, O. M. Auslaender, and A. Yacoby, 2002, Phys. Rev. Lett. **89**, 136805.
Umrigar, C. J., 1999, in *Quantum Monte Carlo Methods in Physics and Chemistry*, edited by M. P. Nightingale and C. J. Umrigar, NATO Science Series (Kluwer Academic Press, Dordrecht), pp. 129–160.
Vaidya, H. G., and C. A. Tracy, 1978, Phys. Lett. A **68**, 378.
Vaidya, H. G., and C. A. Tracy, 1979a, J. Math. Phys. (N.Y.) **20**, 2291.
Vaidya, H. G., and C. A. Tracy, 1979b, Phys. Rev. Lett. **42**, 3; **43**, 1540(E) (1979).
van Amerongen, A. H., J. J. P. van Es, P. Wicke, K. V. Kheruntsyan, and N. J. van Druten, 2008, Phys. Rev. Lett. **100**, 090402.
van Oudenaarden, A., and J. E. Mooij, 1996, Phys. Rev. Lett. **76**, 4947.
van Oudenaarden, A., B. van Leeuwen, M. P. M. Robbens, and J. E. Mooij, 1998, Phys. Rev. B **57**, 11684.
Varney, C. N., V. G. Rousseau, and R. T. Scalettar, 2008, Phys. Rev. A **77**, 041608.
Vidal, J., D. Mouhanna, and T. Giamarchi, 1999, Phys. Rev. Lett. **83**, 3908.
Vidal, J., D. Mouhanna, and T. Giamarchi, 2001, Phys. Rev. B **65**, 014201.
Vignolo, P., A. Minguzzi, and M. P. Tosi, 2000, Phys. Rev. Lett. **85**, 2850.
Vishwanath, A., and D. Carpentier, 2001, Phys. Rev. Lett. **86**, 676.
Wada, N., J. Taniguchi, H. Ikegami, S. Inagaki, and Y. Fukushima, 2001, Phys. Rev. Lett. **86**, 4322.
Walker, L. R., 1959, Phys. Rev. **116**, 1089.
Watanabe, M., and D. B. Haviland, 2002, J. Phys. Chem. Solids **63**, 1307.
Watson, B. C., *et al.*, 2001, Phys. Rev. Lett. **86**, 5168.
Wentzel, G., 1951, Phys. Rev. **83**, 168.
Wessel, S., F. Alet, S. Trebst, D. Leumann, M. Troyer, and G. G. Batrouni, 2005, J. Phys. Soc. Jpn. Suppl. **74**, 10, http://jpsj.ipap.jp/link?JPSJS/74S/10/.
Wessel, S., F. Alet, M. Troyer, and G. G. Batrouni, 2004, Phys. Rev. A **70**, 053615.
White, S. R., 1992, Phys. Rev. Lett. **69**, 2863.
White, S. R., 1993, Phys. Rev. B **48**, 10345.
White, S. R., and R. M. Noack, 1992, Phys. Rev. Lett. **68**, 3487.
Will, S., T. Best, U. Schneider, L. Hackermüller, D.-S. Lühmann, and I. Bloch, 2010, Nature (London) **465**, 197.
Wilson, K. G., 1975, Rev. Mod. Phys. **47**, 773.
Winkler, K., G. Thalhammer, F. Lang, R. Grimm, J. H. Denschlag, A. J. Daley, A. Kantian, H. P. Büchler, and P. Zoller, 2006, Nature (London) **441**, 853.
Wu, T., 1966, Phys. Rev. **149**, 380.
Yang, C. N., 1962, Rev. Mod. Phys. **34**, 694.
Yang, C. N., 1967, Phys. Rev. Lett. **19**, 1312.
Yang, C. N., and C. P. Yang, 1966a, Phys. Rev. **150**, 321.
Yang, C. N., and C. P. Yang, 1966b, Phys. Rev. **150**, 327.
Yang, C. N., and C. P. Yang, 1966c, Phys. Rev. **151**, 258.
Yang, C. N., and C. P. Yang, 1969, J. Math. Phys. (N.Y.) **10**, 1115.
Young, A. P., and H. Rieger, 1996, Phys. Rev. B **53**, 8486.
Zhou, Q., Y. Kato, N. Kawashima, and N. Trivedi, 2009, Phys. Rev. Lett. **103**, 085701.
Zujev, A., A. Baldwin, R. T. Scalettar, V. G. Rousseau, P. J. H. Denteneer, and M. Rigol, 2008, Phys. Rev. A **78**, 033619.
Zvonarev, M., V. V. Cheianov, and T. Giamarchi, 2007, Phys. Rev. Lett. **99**, 240404.
Zvonarev, M., V. V. Cheianov, and T. Giamarchi, 2009a, Phys. Rev. Lett. **103**, 110401.
Zvonarev, M., V. V. Cheianov, and T. Giamarchi, 2009b, Phys. Rev. B **80**, 201102(R).
Zvonarev, M. B., V. V. Cheianov, and T. Giamarchi, 2007, Phys. Rev. Lett. **99**, 240404.